Genetic Engineering of heavy metal sequestering / precipitating proteins for bioremediation

By

Chitra Seetharam Misra

LIFE01200904001

Bhabha Atomic Research Centre, Mumbai

A thesis submitted to the
Board of Studies in Life Sciences

In partial fulfilment of requirements
for the Degree of
DOCTOR OF PHILOSOPHY
of
HOMI BHABHA NATIONAL INSTITUTE

December, 2014

STATEMENT BY AUTHOR

This dissertation has been submitted in partial fulfillment of requirements for an advanced degree at Homi Bhabha National Institute (HBNI) and is deposited in the Library to be made available to borrowers under rules of the HBNI.

Brief quotations from this dissertation are allowable without special permission, provided that accurate acknowledgement of source is made. Requests for permission for extended quotation from or reproduction of this manuscript in whole or in part may be granted by the Competent Authority of HBNI when in his or her judgment the proposed use of the material is in the interests of scholarship. In all other instances, however, permission must be obtained from the author.

Chitra Seetharam Misra

DECLARATION

I, hereby declare that the investigation presented in the thesis has been carried out by me. The work is original and has not been submitted earlier as a whole or in part for a degree / diploma at this or any other Institution / University.

Chitra Seetharam Misra

List of Publications arising from the thesis

Journal

1. Lyophilized, non-viable, recombinant *E. coli* cells for cadmium bioprecipitation and recovery. Seetharam Chitra, Soundarajan Suvarna, Udas A. C., Rao A. S. and Apte S. K., Process *Biochemistry*, **2009**, 44, 24-250.

2. PhoN-expressing, lyophilized, recombinant *Deinococcus radiodurans* cells for uranium bioprecipitation. Appukuttan Deepti[1], Seetharam Chitra[1], N. Padma, Rao A. S. and Apte S. K. *Journal of Biotechnology*, **2011,** 154(4), 285-290.
[1]These authors contributed equally to the work.

3. Recombinant *D. radiodurans* cells for bioremediation of heavy metals from acidic/neutral aqueous wastes. Misra Chitra Seetharam[1], Appukuttan Deepti[1], Kantamreddi VSS, Rao A. S and Apte S. K., *Bioengineered Bugs*, **2012,** 3, 44-48.
[1]These authors contributed equally to the work.

Conferences

1. Natural and recombinant bacteria for bioremediation of uranium from acidic/alkaline aqueous solutions in high radiation environment. Appukuttan Deepti, Nilgiriwala Kayzad, Seetharam Chitra, and Apte S. K. In Abstracts of the 14th International Biotechnology Symposium and Exhibition "IBS2010" in September 2010 in Rimini, Italy.

2. Seetharam Chitra,, Soundarajan Suvarna, Udas A C, Basu Bhakti and Apte SK. The utility of Hpi, the Surface layer protein of *D. radiodurans* in metal removal from solutions. In Abstracts of the Life Sciences Symposium held in 2015 in BARC, Mumbai.

Chitra Seetharam Misra

Dedicated to my family

Acknowledgements

Pursuing Phd is not only an academic challenge; it is also an exercise in recognizing the importance of scientific and personal interactions with peers and non-peers in putting together a decent piece of work. In this regard, I have been lucky to be mostly surrounded by people from whom I received enormous help, constructive advice, bright ideas, technical help and moral support and I would like to acknowledge them here.

I would like to first thank my Guide, Dr. Shree Kumar Apte for guiding my work in spite of a very busy schedule, giving me a good and just hearing whenever I discussed my work with him and for honing my scientific writing skills. There is a lot I have learnt that will stand me in good stead throughout my life.

I thank my doctoral committee for their encouragement and valuable suggestions. I was fortunate to be able to discuss my work without any inhibitions with them on account of their friendly and cordial demeanour. Dr. Hema Rajaram, Dean, Life Sciences to whom I went very often for all Ph.D related paperwork and who was always obliging.

I sincerely thank Shri. A. S. Rao who was always supportive throughout my initial work and gave me constant encouragement to do my Ph.D. He provided the basic ideas which started this work and I will always be thankful to him.

I thank my collaborators, Dr. Ambuja C Udas and Dr. Suvarna Soundarajan, Dr. Padma N, for un-complainingly running my samples for analysis and giving valuable scientific inputs. I also thank Dr. Rita Mukhopadhyaya for sequencing a couple of my constructs, Dr. Bhakti Basu, for peptide mass fingerprinting using MALDI-TOF-MS, Mr. Anand Ballal and Mrs. Alka Gupta for electron microscopic studies, Dr. Hassan and Mrs. Suman for help with the zetameter. I must acknowledge Dr. Mary Lidstrom for very promptly sending me a strain which was used in this study. I also thank Dr. Celin Acharya for letting me use a plasmid she constructed in the lab, which was a starting point for some of the work reported in this thesis.

This work got a lot of help from my colleague, Mrs. Saraswathi Perumal who in spite of ill health helped me in carrying out many routine experiments to perfection. I must thank Dr. Deepti Appukuttan who taught me quite a few things during my initial years as a scientist and whose work served as a base for this study. I was fortunate to have very amicable colleagues, Mr. Shyam Sunder, a great sounding board for all my scientific and non-scientific gibberish, Ms. Sayali Kulkarni, for her unflinching help and for being another sounding board, Mrs. Pallavi Joshi and Mr. Pawan Nimje for all their help which came timely. Thanks to Nilesh and Divya for keeping the mood in the lab young and vibrant.

This would never have happened without enormous support from my family, my parents and husband. But I will surely fall short of words when it comes to thanking them. I therefore, dedicate this thesis to them.

ABBREVIATIONS

µg	microgram
µl	microlitre
µM	micromolar
AAS	Atomic Absorption Spectrophotometer
Ap	Ampicillin
bp	base pairs
Cm	Chloramphenicol
CBB	Coomassie Brilliant Blue
D/W	Distilled water
EDX	Energy Dispersive X-ray Spectroscopy
IPTG	Isopropyl-β-D-thiogalactopyranoside
Kan	Kanamycin
kb	kilo bases
kDa	kilo Dalton
LDS	Lithium dodecyl sulphate
MG	Methyl Green
MT	Metallothionein
NBT/BCIP	Nitro Blue Tetrazolium / 5'Bromo 4' Chloro 3-Indolyl Phosphate
ng	nanogram
nmoles	nano moles
OD	Optical Density
ORF	Open Reading Frame
PAGE	Polyacrylamide gel electrophoresis

PCR	Polymerase Chain Reaction
PDP	Phenolphthalein Di-Phosphate
pNP	para Nitro Phenol
pNPP	para Nitro Phenyl Phosphate
SCWP	Secondary Cell Wall Polymers
SDS	Sodium dodecyl sulphate
SEM	Scanning Electron Microscopy
S-layer	Surface layer
SLH	Surface Layer Homology Domain
TEM	Transmission Electron Microscopy
TEMED	N,N,N`,N`-Tetramethylenediamine
TGY	Tryptone, Glucose, Yeast Extract
Tris	Tris (hydroxymethyl)-aminomethane

CONTENTS PAGE

Homi Bhabha National Institute

Ph. D. PROGRAMME

1. Name of the Student: Chitra Seetharam Misra
2. Name of the Constituent Institution: Bhabha atomic Research Centre
3. Enrolment No.: LIFE01200904001
4. Title of the Thesis: Genetic Engineering of heavy metal sequestering / precipitating proteins for bioremediation
5. Board of Studies: Life Sciences

Synopsis

Environmental pollution, including that by metals, is on the rise. Metals such as cadmium (Cd) and uranium (U) are generally toxic to all life-forms (1). They form non-specific complex compounds with cellular components thereby exerting toxicity (1). Due to rapid industrialization, large amount of toxic effluents containing a cocktail of such metals is released into the environment, contaminating soil and water. Environmental pollution by Cd, arising mainly from mining, smelting, electronic waste and use of phosphate fertilizers is increasing alarmingly (2). U mining and re-processing of nuclear fuel has resulted in generation of U containing effluents which exert both chemical and radiological toxicity (3). While the uranium waste is managed by the nuclear industry, the ever increasing cadmium containing waste is a cause for concern.

The removal of metals from the environment is difficult and unlike many other pollutants, they cannot be chemically or biologically degraded. A number of physico-chemical

processes have been used for removing metals from waste solutions (2). However, such methods are expensive and may themselves contribute to secondary environmental pollution (4). The use of micro-organisms for decontamination of metals has attracted considerable attention. Owing to relatively low costs and high efficiency microbial remediation can be used to supplement conventional methods (2). Microbes have evolved measures to respond to metal stress via processes such as transport across cell membrane, biosorption to cell walls, extra or intracellular precipitation, and complexation and oxidation-reduction reactions (5). Among the biological mechanisms involved in metal remediation, intracellular metal complexation by metal binding peptides called metallothioneins and extracellular metal precipitation mediated by phosphatases have been extensively studied and hold promise for development of effective bioremediation technologies.

Metallothioneins (MT) are low molecular weight (6–7 kDa), cysteine-rich proteins found in animals, higher plants, eukaryotic microorganisms and some prokaryotes. The large number of cysteine residues in MTs bind a variety of metals such as cadmium, zinc, copper, mercury etc. by mercaptide bonds (6). In prokaryotes, 'MT-like' proteins have been defined only in *Synechococcus* sp. and *Pseudomonas putida* (7). The *smtA* gene codes for metallothionein in *Synechococcus elongatus* and has been cloned in *E. coli* for increased metal uptake and removal earlier (8). In addition to this, MTs from various sources have been expressed intracellularly in *Escherichia coli* including monkey MT, yeast MT, human MT-II, mouse MT-I, rainbow trout MT and plant MT (2). Bioprecipitation of metals as phosphates is mediated by phosphatases which cleave a phosphomonoester substrate to release the phosphate moiety, which in turn precipitates metals such as U and Cd from solutions (9). Earlier, *Citrobacter* strain harbouring an

acid phosphatase was shown to precipitate several metals such as uranium, cadmium, nickel, americium and plutonium from solution (10).

Genetic engineering has been modestly successful in endowing microbes, which occur and grow in waste, with ability to remediate metals, and in enhancing their bioremediation potential (5). For example, *E. coli*, has been genetically manipulated for such purpose and offers the advantage of convenient expression of foreign proteins (11-13), but is highly radiosensitive. Radioactive waste sites pose a unique problem since their remediation requires a radio-resistant system which must not only remove metals but also survive in such environment. The Gram positive bacterium, *Deinococcus radiodurans* can tolerate very high doses of ionizing radiation and exhibits remarkable resistance to DNA damage caused by ionizing radiation, desiccation and other stresses (14-15). These properties make *D. radiodurans* an attractive candidate for bioremediation of radioactive waste. The organism has been engineered earlier for degradation of toluene, and detoxification of Hg and Cr in radioactive environments (16-17). It has also been successfully manipulated to express acid and alkaline phosphatases from other bacteria to precipitate U from aqueous waste solutions over a wide pH range (9, 18).

In the past, *phoN* gene of *Salmonella enteric* serovar Typhi that encodes a non-specific acid phosphatase (NSAP) was over-expressed in *D. radiodurans* (9). Such recombinant *D. radiodurans* cells exhibited metal precipitation even after being subjected to 6 kGy gamma radiation, while *E. coli* cells carrying the same construct failed to do so. However, the phosphatase activity obtained in *D. radiodurans* was far less (10%) than that obtained in recombinant *E. coli* cells carrying the same construct. It was suggested that the seven layered cell wall in *D. radiodurans* might limit substrate accessibility to PhoN. Since, the thick complex cell wall of this organism could pose a major problem in engineering this organism for any kind of

extracellular metal remediation, the possibility of exploiting the membrane localized proteins on the cell surface, Surface (S) - layer proteins for display of proteins relevant to bioremediation has been explored in the present study.

S layer proteins are two dimensional protein layers found in a variety of prokaryotes as the outermost cell boundary (19). They have been employed for surface display of proteins such as major birch allergen, fluorescent proteins, core streptavidin etc. for specific applications (19). Whether the surface display of phosphatases and metallothionein by their fusion to S layer proteins can enhance their metal bioremediation potential is the question addressed by the present work. It is equally important to evaluate the biochemical attributes of engineered proteins *in vitro* and the biology of bioremediation by the recombinant bacterial strains expressing them. Converting the biomass into a formulation for easy application and storage was also explored. The present work addressed the aforesaid issues with the following objectives:

1. Construction of the S layer fusion proteins with bioremediation active phosphatase (PhoN) and metallothionein (SmtA) proteins for metal removal, using recombinant DNA technology.
2. Studies on the expression, localization and activity of the fusion proteins.
3. Evaluation of microbes expressing fusion proteins for removal of metals such as U and Cd from solution.
4. Assessment of the utility of purified S-layer proteins and S-layer fusion proteins in removing metals from solutions *in vitro*, and
5. Evaluation of lyophilized recombinant microbes for metal removal from solution.

The work is presented in a thesis comprising of the following chapters:

Chapter 1. General Introduction. This chapter provides a brief overview of the problem of metal pollution, its sources, nature of toxicity and remediation strategies used. The chapter also describes microbes capable of removing metals, the underlying mechanism and attempts made at genetic manipulation of microbes to enhance their ability to remove metals from aqueous waste. A number of organisms have also been genetically engineered to express phosphatases and metallothionein to enhance their potential to remove metals from waste solution. Engineering proteins for cell surface display on microbes endows intact cells with new functionalities and applications, and with respect to bioremediation, provides the protein with better metal accessibility. Such approaches using surface layer proteins are discussed.

As a radio-resistant organism, *D. radiodurans* is highly suited for remediation of radioactive waste solutions and has been used for over-expression of proteins relevant to bioremediation of metals likely to be present in such waste solutions. *Deinococcus* possesses two S layer proteins, Hpi and SlpA, which can be suitably exploited for fusion for surface display of relevant proteins like, phosphatase and metallothionein. Hpi is a well characterized layer which forms the outermost proteinaceous coat in deinococcal cell envelope, while SlpA protein is a very large protein which is poorly characterized. Deinococcal SlpA protein carries a surface layer homology (SLH) domain which, in other microbes have been shown to bind Secondary Cell Wall Polymers (SCWP) covalently attached to the peptidoglycan and has been employed for cell surface targeting (20). The chapter summarizes the available information on deinococcal S layer proteins. It also discusses possibilities of engineering them for surface display of PhoN and SmtA and delineates the specific objectives of this study.

Chapter 2. Materials & Methods.

The methods employed in the present work are detailed in Chapter 2.

E. coli JM109/*E. coli* (DE3) were grown in Luria Bertani broth at 37°C, while *D. radiodurans* strain R1 was grown in Tryptone Glucose Yeast extract medium at 32°C, under agitation. Standard protocols for plasmid isolation, restriction digestion, ligation, transformation etc. used in all the cloning work are described in this chapter. A binary shuttle vector for *E. coli* and *D. radiodurans,* pRAD1, was used for cloning. The deinococcal *PgroESL* promoter was employed for expression of all genes in *D. radiodurans*. The *hpi* gene and the sequence coding for the SLH domain were independently fused to *phoN* or the *smtA* ORF. The *SLH-phoN* fusion gene was also cloned for over-expression in *E. coli*. Expression of proteins was assessed using electrophoresis, Western blotting followed by immunodetection, zymograms and phosphatase activity assays. Matrix Assisted Laser Desorption Ionization-Time of Flight-Mass Spectrometer (MALDI-TOF) was also used to confirm identity of proteins. The chapter provides details of isolation of Hpi and peptidoglycan from *D. radiodurans*. Cd or U precipitation assays were performed, along with appropriate controls, to estimate Cd by Atomic Absorption Spectrophotometer while U was estimated spectrophotometrically using the Arsenazo III reagent. Protocols used for scanning and transmission electron microscopy are described. Details of lyophilisation of cells have been specified.

Chapter 3. Construction of deinococcal S layer fusion proteins with metallothionein (SmtA) and acid phosphatase (PhoN): cloning, expression and cellular localization.

Characterization of the two S layer proteins of *D. radiodurans* was carried out to gain insight into their localization in the seven layered deinococcal cell envelope. MALDI-TOF-MS identified bands obtained on electrophoretic separation of isolated Hpi layer on denaturing gel. The 123 kDa protein which is a contaminant in all Hpi preparations was found to be DR2577, the protein from *D. radiodurans* annotated as an S layer protein homologous to the S layer protein,

SlpA from *Thermus thermophilus*. The work showed, for the first time, that the two S layer proteins, Hpi and SlpA in *D. radiodurans* are intimately associated with each other as part of the architecture of the deinococcal cell envelope. Since Hpi is the better characterized S layer protein and the SLH domain in other S layer proteins have been used for surface display of proteins, the PhoN and SmtA proteins were independently fused to Hpi or the SLH domain of SlpA in *D. radiodurans.*

The *smtA* gene, from the cyanobacterium, *Synechococcus elongatus,* which encodes a metallothionein was cloned and expressed from *PgroESL* promoter in *D. radiodurans*. Recombinant strains carrying three different type of constructs were generated, one with *smtA* alone (pPS1), one with *hpi-smtA* fusion gene (pPHS1) and one with *SLH-smtA* fusion gene (pPSS1). Independent fusions with the Hpi protein or the SLH domain facilitated surface localization of the fusion protein, as determined by Western blotting and immunodetection with Anti-SmtA antibody. When SmtA protein was expressed without such fusions with S-layer protein, it was found to localize exclusively in the cytoplasm of recombinant *D. radiodurans*.

The *phoN* gene was also fused to *hpi* gene or the nucleotide sequence encoding SLH domain, to generate the plasmids pGDRF3 and pPSP1 respectively. Recombinant *D. radiodurans* strains carrying *hpi-phoN* fusion displayed whole cell PhoN phosphatase activity, as determined on histochemical plate and by cell-based enzyme assays, while those carrying *SLH-phoN* did not. PhoN activity bands of 127 kDa and 36 kDa, which are the expected sizes for the Hpi-PhoN and SLH-PhoN fusion protein, could be distinctly visualized in in-gel zymograms of electrophoretically resolved protein extracts from recombinants bearing *hpi-phoN* and *SLH-phoN* respectively. Localization studies in *D. radiodurnas* cells clearly showed that the Hpi-PhoN fusion protein was membrane bound, while the SLH-PhoN protein was present both in the

membrane and cytosolic fractions of recombinant cells. Absence of whole cell phosphatase activity in SLH-PhoN expressing recombinants may therefore be either due to the protein being lodged deep into the cell wall or because the protein was not folded appropriately and lodged in the cytosol.

To circumvent the lack of whole cell phosphatase activity in recombinants expressing SLH-PhoN, an alternate approach was attempted. SLH domains are known to bind SCWP on peptidoglycan and therefore, the possibility of using SLH-PhoN protein immobilized on deinococcal peptidoglycan was evaluated. The SLH-PhoN protein was over-expressed in *E. coli* BL21 cells and its identity confirmed by peptide mass fingerprinting using MALDI-TOF-MS. Peptidoglycan binding assays using SLH-PhoN fusion protein showed that while the SLH-PhoN protein bound peptidoglycan, PhoN alone did not bind the cell wall. The data demonstrate that the SLH domain indeed contributes to binding of SLH-PhoN to peptidoglycan. Peptidoglycan itself was used as an immobilization matrix for the SLH-PhoN protein in U precipitation assays, reported in Chapter 4.

Thus, except for SLH-PhoN, fusion of PhoN and SmtA to S layer proteins resulted in expression, membrane localization and expected activity in recombinant *D. radiodurans* cells. The fusion proteins and recombinants expressing them were evaluated for metal removal.

Chapter 4. Metal bioremediation using engineered proteins and recombinant bacteria. The native Hpi layer isolated from *D. radiodurans* could bind nearly 166 µg / mg protein at near neutral pH. *D. radiodurans* cells could bind more U than mutant cells (HMR202) lacking the Hpi protein. Zetameter measurements with whole cells revealed that the wild type cells carried much more surface negative charge than mutant cells. The results suggested that the Hpi protein

contributes to a net negative charge on the cell surface which in turn might have a bearing on metal interactions.

Metal binding experiments were carried out with *D. radiodurans* carrying the *hpi-smtA* or *SLH-smt* or *smtA* or pRAD1 plasmid alone. Recombinants expressing *hpi-smtA* bound 1.2 mg Cd/g dry weight biomass, while all other recombinants showed metal binding in the range of 0.5 mg/g dry weight biomass. Similarly, *D. radiodurans* recombinants carrying *hpi-smtA* could bind 225 µg Cu and 210 µg Zn/g dry weight biomass compared to around 100-125 µg Cu and Zn/g dry biomass bound by all other recombinants. Recombinants carrying the *SLH-smtA* fusion gene did not show enhanced metal binding compared to those carrying pRAD1 alone. The data suggested that while surface localization mediated by fusion to Hpi enhanced the metal removal ability of recombinants cells, fusion to SLH domain did not result in enhanced metal binding. This may be consequence of SLH domain localization proximal to the peptidoglycan but away from cell surface.

Among recombinants expressing the PhoN fusion protein, *D. radiodurans* cells carrying *hpi-phoN* fusion gene precipitated 119 µg U/mg cells in 6 h while *D. radiodurans* (PhoN) could precipitate 214 µg U/mg cells in the same time. However, when recombinant strains were used at equivalent PhoN specific activity, the U precipitation kinetics were similar. SLH-PhoN over-expressed in *E. coli* BL21 cells and immobilized on peptidoglycan (SPhoNP) could remove 95% U in 4 h from a 1 mM solution. Isolated Hpi layer from recombinant *D. radiodurans* cells expressing Hpi-PhoN could remove 90% uranium in 24 h as compared to that from control cells carrying pRAD1 which could remove 35% uranium from solution. SPhoNP was tested for its ability to precipitate U in multiple cycles. The interaction between peptidoglycan and SLH domain showed reasonable stability in U precipitation assays with only a 10 % drop in amount of

U precipitated in 4 h for upto three cycles. SLH-PhoN immobilized on peptidoglycan when stabilized by glutaraldehyde cross linking showed a marginal decrease in phosphatase activity, but showed excellent re-usability in U precipitation assays for upto five cycles.

In order to compare various biomass bearing PhoN for their metal precipitation ability, equal dry weights of *D. radiodurans* expressing Hpi-PhoN or PhoN alone and glutaraldehyde stabilized SPhoNP were used in a typical metal precipitation assay. While SPhoNP removed 317 µg U/mg biomass in 4h, recombinants carrying *phoN* alone and *hpi-phoN* precipitated 230 µg U/mg cells and 138 µg U/mg cells respectively, showing superiority of SPhoNP over other biomass in precipitating U.

Lyophilization of *E. coli* and *D. radiodurans* cells bearing *phoN* was carried out to reduce the bulk volume and convert the biomass into a dry powdered form, thereby increasing the ease of handling, storage, transport and application. Lyophilized recombinants retained PhoN activity as well as U precipitation ability, while also retaining cellular integrity and surface precipitation property. This facilitated easy recovery of precipitated metal with the biomass. Most importantly, lyophilisation significantly extended the shelf life of the product in terms of metal precipitation up to six months.

E. coli and *D. radiodurans* cells expressing PhoN alone could remove Cd much faster than U. Visualization of recombinant cells which had precipitated the metal showed cell surface association of the cadmium phosphate and uranyl phosphate precipitates. The presence of U/Cd and phosphate was confirmed in such cells by EDX. In both cases, the metal precipitate was firmly lodged onto the cell surface with no free precipitate seen in the fields observed. This observation is important since cell bound precipitate makes cells heavy and easy to settle down compared to free precipitate.

The purpose of making S layer fusions with PhoN and SmtA was to construct recombinant proteins which would display superior bioremediation ability through surface display. This was achieved best by Hpi-SmtA fusion protein in recombinant cells and by SLH-PhoN fusion protein immobilized on peptidoglycan, SPhoNP.

Chapter 5. Summary and Conclusions. The salient findings of this study are summarized in the last chapter. The study showed that the two S layer proteins of *D. radiodurans*, Hpi and SlpA are closely associated in the deinococcal cell envelope. The SLH domain of the SlpA protein was shown to bind peptidoglycan, forming continuity in the interactions between different layers of the deinococcal cell wall. The Hpi protein layer itself bound U, but not Cd, at near neutral pH. Further, Hpi was found to confer substantial negative charge to deinococcal cell surface, thereby enhancing its interaction and binding with metals.

The S-layer fusion proteins, Hpi-SmtA, SLH-SmtA and Hpi-PhoN localized exclusively to the deinococcal cell membrane, while SLH-PhoN was also present in the cytoplasmic fraction. Therefore, Hpi emerged as an efficient membrane targeting vehicle. Recombinants expressing Hpi-SmtA bound higher amounts of Cu, Zn and Cd, compared to those expressing SLH-SmtA or SmtA alone. The Hpi-PhoN carrying *D. radiodurans* cells when used at equivalent phosphatase activity, could remove around 214 µg U/mg cells in 6 h similar to PhoN expressing *D. radiodurans*. However, *D. radiodurans* expressing SLH-PhoN did not display any cell bound phosphatase activity. Use of peptidoglycan as an immobilization matrix by exploiting its interaction with the SLH domain is an important finding of this study. SLH-PhoN immobilized on peptidoglycan could efficiently remove U from solution and showed excellent stability and re-usability.

Lyophilization provided a good value addition to phosphatase mediated bioremediation by increasing the shelf life of recombinants and making their handling and storage easy. Cd could be precipitated more rapidly than U using *phoN* expressing *E. coli* and *D. radiodurans* cells. Both the uranyl phosphate and cadmium phosphate precipitates were shown to be cell surface associated leading to easy separation of metal laden cells and convenient downstream processing of effluent. Generation of S layers exclusively of fusion proteins, by expressing the protein at high levels in Hpi mutant cells, and evaluation of metal precipitation utility of SPhoNP in a flow-through process may hold promise for superior bioremediation in future.

References:

1. Nies DH. **1999**. *Applied Microbiology and Biotechnology* 51: 730-50
2. Mejare M, Bulow L. **2001**. *Trends Biotechnol* 19: 67-73
3. Merroun ML, Selenska-Pobell S. 2008. *Journal of Contaminant Hydrology* 102: 285-95
4. Malik A. **2004**. *Environment International* 30: 261-78
5. Gadd GM. **2000**. *Curr Opin Biotechnol* 11: 271-9
6. Cobbett C, Goldsbrough P. **2002**. *Annual Review of Plant Biology* 53: 159-82
7. Turner JS, Robinson NJ. 1995. *J Ind Microbiol* 14: 119-25
8. Shi J, Lindsay WP, Huckle JW, Morby AP, Robinson NJ. **1992**. *FEBS Lett* 303: 159-63
9. Appukuttan D, Rao AS, Apte SK. **2006**. *Appl Environ Microbiol* 72: 7873-8
10. Macaskie LE, Jeong BC, Tolley MR. **1994**. *FEMS Microbiol Rev* 14: 351-67
11. Yuan C, Lu X, Qin J, Rosen BP, Le XC. **2008**. *Environmental Science & Technology* 42: 3201-6
12. Deng X, Yi XE, Liu G. **2007.** *Journal of Hazardous Materials* 139: 340-4
13. Zhao XW, Zhou MH, Li QB, Lu YH, He N, et al. **2005**. *Process Biochemistry* 40: 1611-6
14. Battista JR. **1997**. *Annu Rev Microbiol* 51: 203-24
15. Venkateswaran A, McFarlan SC, Ghosal D, Minton KW, Vasilenko A, et al. **2000.** *Appl Environ Microbiol* 66: 2620-6
16. Brim H, McFarlan SC, Fredrickson JK, Minton KW, Zhai M, et al. **2000**. *Nat Biotechnol* 18: 85-90
17. Lange CC, Wackett LP, Minton KW, Daly MJ. **1998**. *Nat Biotechnol* 16: 929-33
18. Kulkarni S, Ballal A, Apte SK. **2013**. *J Hazard Mater* 262: 853-61
19. Sleytr UB, Schuster B, Egelseer EM, Pum D. **2014**. *FEMS Microbiol Rev*
20. Cava F, de Pedro MA, Schwarz H, Henne A, Berenguer J. **2004**. *Mol Microbiol* 52: 677-90

Journal **Publications:**

1. Seetharam Chitra, Soundarajan Suvarna, Udas A. C., Rao A. S. and Apte S. K. (2009) Lyophilized, non-viable, recombinant *E. coli* cells for cadmium bioprecipitation and recovery. **Process Biochemistry**; 44: 246-250.

2. Appukuttan Deepti**,** Seetharam Chitra**,** N. Padma**,** Rao A. S. and Apte S. K. (2011) PhoN-expressing, lyophilized, recombinant *Deinococcus radiodurans* cells for uranium bioprecipitation. **Journal of Biotechnology.** 154(4): 285-290.

3. Misra Chitra Seetharam, Appukuttan Deepti, Kantamreddi VSS, Rao A. S and Apte S. K (2012)**.** Recombinant *D. radiodurans* cells for bioremediation of heavy metals from acidic/neutral aqueous wastes; **Bioengineered**, 3,44-48

Conferences:

Appukuttan Deepti, Nilgiriwala Kayzad, Seetharam Chitra, and Apte S. K.Natural and recombinant bacteria for bioremediation of uranium from acidic/alkaline aqueous solutions in high radiation environment. In Abstracts of the 14th International Biotechnology Symposium and Exhibition "IBS2010" in September 2010 in Rimini, Italy.

S. No.	Name	Designation	Signature	Date
1.	Dr. J. S. Melo	Chairman		
2.	Dr. S. K. Apte	Convener		
3.	Dr. J. R. Bandekar	Member		
4.	Dr. H. S. Misra	Member		
5.	Dr. Gautam S.	Member		
6.				

List of Figures

List of Tables

Chapter 1

Introduction

Introduction

Man's increasing mastery of natural law has brought us increased life expectancy and a higher quality of life but has also resulted in sites contaminated with residuals of our industrial output, which are a threat to the environment and impair human health [1]. Tens of thousands of sites stand contaminated and waste management has become an international problem. Among the components of waste, heavy metals are the most problematic to remove due to their indestructible nature, unlike organic contaminants which can be degraded [2]. Waste from the nuclear industry, for example, predominantly consists of heavy metals, which being radioactive in nature, add a complication to nuclear waste management. The need to manage such waste has led to the development of new technologies. While conventional methods mostly include physico-chemical approaches, alternative approaches like bioremediation are gaining importance due to their eco-friendly nature and cost-effectivenes [3].

1.1 Metal Pollution

Metals are essential for life as trace elements but are toxic at higher concentrations [2]. Due to rapid industrialization, large amounts of toxic effluents, containing a cocktail of heavy metals are released into the environment, contaminating soil and water. The main sources of heavy metal pollution are mining, milling and surface finishing industries, discharging a variety of toxic metals such as Cd, Cu, Ni, Co, Zn and Pb into the environment [4]. Eventually, build up of dangerous concentrations in food crops grown in contaminated soil poses a much more serious hazard [2].

Heavy metals form complexes with cellular components which interfere with normal metabolism of the cell [5]. Apart from this chemical toxicity, heavy metals which exist as radioisotopes, also exert radiological toxicity. Mining of uranium and re-processing of

nuclear fuel has resulted in generation of large amount of effluents containing radioisotopes of uranium, plutonium, cesium, strontium etc. The release of radio nuclides, either as discharge of process effluents produced by industrial activities allied to nuclear power or through accidental release is a subject of intense public concern [6].

Heavy metals are difficult to remove from the environment and unlike many other pollutants cannot be chemically or biologically degraded. A number of physico-chemical processes such as oxidation and reduction, electrochemical treatment, evaporation, ion exchange and reverse osmosis have been used for removing heavy metals from waste solutions [2]. High reagent requirement and unpredictable metal ion removal are major disadvantages associated with such techniques. Further, contaminating reagents are used for desorption, resulting in toxic sludge and secondary environmental pollution. These disadvantages can become more pronounced and further aggravate the process cost in case of contaminated ground waters, mine tailings effluent and other industrial wastewaters due to voluminous effluents containing complexing organic matter [4]. Biotechnological approaches can succeed in these areas where physico-chemical methods are inefficient.

In the context of radiological contamination, in a few instances, containment of nuclear waste has been compromised leading to contamination of trillions of gallons of groundwater. Aggressive invasive chemical treatments on such large scale can have negative impacts on biodiversity and can even result in increased dispersion of radioactive materials. Thus, passive, *in situ* biological treatment processes are highly desirable [6].

1.2 Bioremediation of heavy metals

Micro-organisms have evolved measures to respond to heavy metal stress via numerous processes, some of which can be exploited for the remediation of heavy metal containing waste **(Fig. 1.1)**. Bacterial metal detoxification and removal can be an efficient strategy due

to its low cost, high efficiency and eco-friendly nature [7]. Besides this, microbes have proven capability to take up heavy metals from aqueous solutions, especially when the metal concentrations in the effluent range from less than 1 to about 20 mg/l. In addition, microbes also show selectivity in binding specific metals [4].

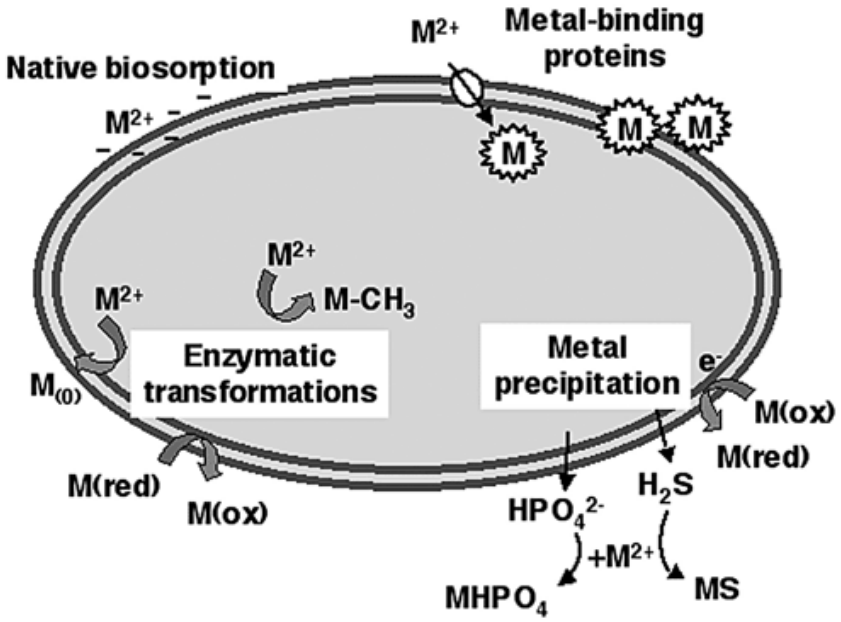

Fig. 1.1. How bacteria cope with toxic concentrations of heavy ions. The scheme summarises the various means by which bacteria react to the presence of metals (M^{2+}) in the medium, with reference to the cellular compartment that harbours the response. These mechanisms include the intra- or extracellular binding (and thus immobilisation) of the metal with a cognate protein (frequently a metallothionein) or a matching anion, the biotransformation of the toxic ion into a less noxious or more volatile form, metal precipitation by a enzymically generated ligand, and the dissimilatory reduction of the metal. (Source: Valls and Lorenzo, 2002).

The 'term' bioremediation when applied to heavy metals has a meaning that is very different from that applied for other organic pollutants such as pesticides, solvents, oil etc. While the clean-up of sites contaminated with the latter involves degradation into non-toxic

components, the only way to remediate sites contaminated by heavy metals is to convert them into relatively less toxic forms which mainly results in immobilization of the metal. Heavy metal de-contamination using biological means mainly involves the following steps [8]:

- Immobilization of the metal
- Concentration and volume reduction of contaminated matrix
- Compartmentalization of matrix or recovery of metals for re-use

Many microbial-metal interactions have been exploited to facilitate metal immobilization and these have been shown in **Fig. 1.1** and elaborated upon in the text that follows.

1.2.1 Biosorption

Biosorption refers to the passive, metabolically independent adsorption of heavy metals from aqueous solutions on biomass [9]. The biomass may be living or dead and the sequestration of metals may involve ion exchange, adsorption, micro-precipitation, and electrostatic and hydrophobic interactions. Biosorption is affected by molecular size, charge, solubility, hydrophobicity as well as waste water composition [10]. Several active groups on cell surface like acetamido group in chitin, the structural polysaccharides of fungi, amine, sulphydryl and carboxyl groups in protein, phosphodiester (teichoic acid), phosphate, hydroxyl groups in polysaccharides, participate in biosorption [11]. Ligand preferences of metal ions on microbial cell surfaces are governed by the hard-soft-acid principle. Hard acids like uranyl ion preferentially bind to oxygen containing ligands, while soft acids such as Cd^{2+} bind to –S and –N containing ligands [10]. Both bacterial as well as fungal biomass have been used either in batch bioreactors or in immobilized matrices to remove a host of heavy metals from waste waters [9].

To be able to compare metal uptake capacities of different types of biosorbents, the adsorption process can be expressed as a batch equilibrium isotherm curve. The biosorption

phenomenon can therefore be simulated and used for predicting changes in operational conditions and for process optimization [7]. It is, at present, the most practical and widely used approach for the bioremediation of metals and radionuclides due to its simplicity, ease of operation and availability of biomass and waste bio-products [8,10].

1.2.2 Metal binding molecules

A number of organisms respond to heavy metal stress by producing metal binding molecules which bind and sequester the heavy metal ion making it unavailable for exerting its toxicity. For example, Metallothioneins (MTs) are low molecular weight (6–7 kDa), cysteine-rich proteins found in animals, higher plants, eukaryotic microorganisms and some prokaryotes. The large number of cysteine residues in MTs bind a variety of metals such as cadmium, zinc, copper, mercury etc. by mercaptide bonds [12]. MT proteins are classified based on the arrangement of Cys residues. Class I MTs contain 20 highly conserved Cys residues based on mammalian MTs and are widespread in vertebrates. MTs without this strict arrangement of cysteines are referred to as Class II MTs and include all those from plants and fungi as well as non vertebrate animals. In this MT classification system, Phytochelatins are, somewhat confusingly, described as Class III MTs [2].

In prokaryotes, 'MT-like' proteins have been defined only in *Synechococcus sp.* and *Pseudomonas putida* [13]. MT in *Synechococcus sp.* was induced following exposure to elevated concentrations of Cd^{2+} or Zn^{2+}, but not Cu^{2+}. Cyanobacterial (*Synechococcus* PCC 7942) mutants, smt-, are sensitive (5-fold reduction in tolerance) to Zn^{2+}, and show some reduction in tolerance to Cd^{2+} [14].

While MTs are genetically coded, enzymically synthesized polypeptides which occur in plants, fungi, nematodes and all groups of algae including cyanobacteria called phytochelatins (PCs) are also known to bind heavy metals such as Cd, Hg, As and Pb [7].

PCs form a family of structures with increasing repetitions of the γ-Glu-Cys dipeptide followed by a terminal Gly; (γ-GluCys)*n*-Gly, where *n* is generally in the range of 2 to 5 [12]. The biosynthesis of PCs is induced by many metals including Cd, Hg, Ag, Cu, Ni, Au, Pb and Zn; however Cd is by far the strongest inducer. The metal binds to the constitutively expressed enzyme, PC synthase, thereby activating it to catalyse the conversion of glutathione (GSH) to phytochelatin [2].

Apart from metallothionein and phytochelatins, randomly generated synthetic polypeptides, synthetic phytochelatins and polyhistidines have also been engineered for enhanced accumulation of metals by recombinant microbes [8].

1.2.3 Biomineralization

Biomineralization is the formation of insoluble metal precipitates by interactions with microbial metabolic products. Metal precipitation as phosphates, sulfides and as a consequence of metal reduction are known to be mediated by microbes and have potential for bioremediation [9]. Sulfate-reducing bacteria (SRB) are anaerobic heterotrophs utilizing a range of organic substrates and SO_4^{2-} as a terminal electron acceptor. The sulfide produced from sulfate reduction not only plays a major role in metal sulfide immobilization in sediments but has also been applied to bioremediation of metals in waters and leachates [15]. While all metal sulphides are insoluble at neutral pH, several are also insoluble in moderately acidic anaerobic solutions. Metal sulphides exhibiting these properties include those of copper, mercury, cadmium, arsenic, selenium and lead. Other metal sulphides, such as cobalt, zinc, nickel and iron, require a more-alkaline environment to ensure complete precipitation and stability. It is possible, therefore, to separate some of the highly toxic metals from the less toxic ones based on sulphide chemistry [11]. However, even low concentrations of free

metals are toxic to SRB. A highly cadmium resistant *Kebsiella planticola* strain could precipitate 50 times more cadmium than that reported for isolated SRBs [16].

Reductive precipitation involves reducing the metal to a lower redox state which is less soluble. For example, U(VI) can be reduced to U(IV) by certain Fe(III) dissimilatory microbes, such as *Geobacter metallireducens,* in turn leading to precipitation of uranium metal from solution. Such processes can also accompany other indirect reductive metal precipitation mechanisms, for example, in sulfate-reducing bacterial systems where reduction of Cr(VI) can be a result of indirect reduction by Fe^{2+} and the sulfide produced [9].

A third mode of metal precipitation involves release of a phosphate ligand (Pi) by biological processes which in turn results in precipitation of heavy metals. One of the first reports on this involved a *Citrobacter* strain harboring an acid phosphatase which was efficiently used for precipitating several heavy metals such as uranium, cadmium, nickel, americium and plutonium from solution [17-21]. Another mechanism relevant to phosphate mediated metal precipitation involves degradation of polyphosphates under specific conditions which results in release of Pi for metal precipitation [9,22-23].

Phosphatase mediated metal precipitation occurs at even low concentrations of metal due to localized high concentration of the phosphate released, and downstream processing is easier due to the cell bound nature of the precipitate [24]. While biosorption and metal binding molecules are typically useful at very low metal concentrations in the micromolar range, bioprecipitation is more effective at higher metal concentrations [25]. Therefore, the mechanisms described here, together cover the spectrum of metal concentrations likely to be present in waste sites.

1.3 Genetic Engineering for heavy metal bioremediation

Genetic engineering for bioremediation of heavy metals has been modestly successful in endowing microbes, which occur and grow in waste, with ability to remediate metals, and in enhancing their bioremediation potential. *E. coli*, has been a favourite for genetic manipulation for such purpose and offers the advantage of convenient expression of foreign proteins [26-28]. But other microbes such as *Ralstonia eutropha, Pseudomonas fluorecens, Sphingomonas desiccabilis, Bacillus subtilis, Deinococcus radiodurans and Caulobacter crescentus* have also been genetically manipulated for metal bioremediation [7].

1.3.1 Genetic engineering for heterologous expression of metallothionein encoding genes

MTs from various sources, including monkey MT, yeast MT, human MT-II, mouse MT-I, rainbow trout MT and plant MT [2], have been expressed intracellularly in *Escherichia coli.* Recombinants expressing the engineered protein not only displayed superior metal binding but in many cases also showed higher tolerance to the metal. The *smtA* from *Synechococcus elongatus* was expressed as a Glutathione-S-transferase fusion protein in *E. coli* cells. Such recombinant protein showed enhanced accumulation of zinc but *E. coli* cells harboring the fusion protein did not show any detectable increase in tolerance towards cadmium, copper or zinc [14].

In certain cases, the genes involved in metal transport were co-engineered with the MT gene resulting in increased metal sequestration by recombinant cells compared to engineering MT alone. This has been done for several metals such as Hg, Cd and Ni [7]. *Ralstonia eutropha* CH34 strain, which is adapted to thrive in metal contaminated soils, was engineered to express the mouse metallothionein I protein on the cell surface. Inoculation of such recombinant cells into Cd contaminated soils significantly decreased the toxic effects of the metal on the growth of tobacco plants [29].

1.3.2 Genetic engineering for phosphate mediated bioprecipitation of metals

Genes encoding enzymes involved in phosphate metabolism have been cloned for phosphate mediated bioprecipitation. Gene *(phoN)* coding a non specific-acid phosphatase, PhoN from *Salmonella enterica* serovar Typhi was introduced into *E. coli* for removing uranium and nickel from solutions [19]. In another variation of exploitation of biologically generated phosphate for metal precipitation, *Pseudomonas aeruginosa* was engineered to over-express its native polyphosphate kinase which resulted in accumulation of large amount of polyphosphate. Under carbon starvation conditions, polyphosphate was degraded, in turn resulting in uranium precipitation from solution. Nearly 80% of uranium could be removed by such cells within 48 h from a 1 mM metal solution [23]. In *E. coli*, manipulation of polyphosphate metabolism by overexpression of the native genes for polyphosphate kinase (*ppk*) and polyphosphatase (*ppx*) resulted in lower intracellular polyphosphate, phosphate secretion and increased metal tolerance [22].

An alkaline phosphatase PhoK encoding gene, *phoK*, from *Sphingomonas* was introduced into *E. coli* and used for bioprecipitation of uranium from alkaline solutions [30]. Such recombinant cells could remove >90% of input uranium in less than 2 h from alkaline solutions containing 0.5 to 5 mM of uranyl carbonate. Specifically for uranium, the uranyl phosphate mineral is extremely stable providing a long-term sink for uranium contaminated sites. These attributes make this mechanism highly desirable for metal bioremediation.

1.3.3 Surface Expression of proteins for Bioremediation

The expression of recombinant protein of interest inside suitable hosts is fraught with problems of stability and short half-life of the expressed heterologous proteins. For eg., in the case of metallothionein, the high cysteine content might interfere with cellular redox pathways in the cytosol [2]. In, addition to this, the intracellular expression of proteins leads

to decreased contact between enzymes and target contaminant and low uptake of substrates resulting in poor bioremediation potential. Engineering proteins for cell surface display on microbes endows intact cells with new functionalities that have a vast sphere of new applications [31].

Among gram negative bacteria, *E. coli* has been extensively investigated for cell surface engineering. Metal binding peptides of sequences Gly-His-His-Pro-His-Gly (namely HP) and Gly-Cys-Gly-Cys-Pro-Cys-Gly-Cys-Gly (namely CP) were genetically engineered into the native LamB protein and expressed in *E. coli*. The potential of *E. coli* expressing CP to bind cadmium (Cd^{2+}) from the growth medium was increased fourfold compared to wild-type cells. Synthetic phytochelatin were fused to Outer membrane protein A and maltose binding protein for enhanced cadmium accumulation. Similarly genetically modified *E. coli* co-expressing a Hg^{2+} transport system with $(Glu\text{-}Cys)_{20}Gly$(EC20) or by directly expressing EC20 on the cell surface effectively removed $Hg^{2+}$from liquid medium [31].

Mouse metallothionein protein was targeted to the cell surface of *Ralstonia eutropha* by fusing it to the auto transporter β-domain of IgA protease of *Neisseria gonorrhoeae* which targeted the hybrid protein toward the bacterial outer membrane [32]. The genetically engineered strain *R. eutropha* MTB accumulated increased amounts of $Cd^{2+}$from liquid media.

In Gram positive bacteria, there are relatively fewer examples of surface display. The fungal cellulose-binding domain (CBD), derived from *Trichoderma reesei* cellulase Cel6A, has been expressed in its non-engineered form onto the surface of *Staphylococcus carnosus.* The cell surface expression of the CBD scaffold could prove helpful for enhanced bio-accumulation of Ni^{2+}[31].While all these techniques of surface engineering have been successful, a more recent tool for surface display of proteins in bacteria is by fusing to Surface Layer Proteins.

1.4 Surface layer proteins

Among the most commonly observed prokaryotic cell surface structures are two-dimensional arrays of proteinaceous subunits forming surface layers (termed S-layers) on cells **(Fig. 1.2)**. S-layers have now been identified in hundreds of different species of almost every taxonomic group of walled Bacteria and are an almost universal feature of Archaea. Because S-layer proteins account for approximately ten percent of cellular proteins in Archaea and Bacteria, they represent interesting model systems for studying the processes involved in the synthesis, secretion, and assembly of extracellular proteins. S-layers also represent the simplest biological protein or glycoprotein membranes developed during evolution [33].

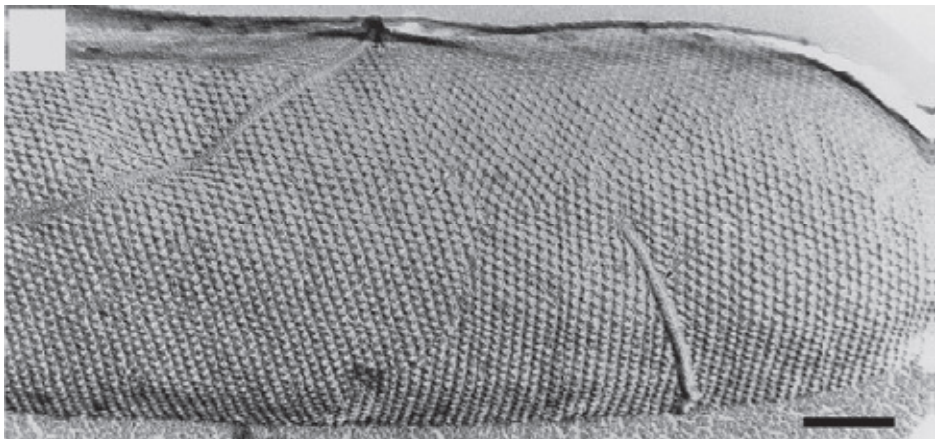

Fig. 1.2. S layer covering bacterial surface. (Source: Seytr et al. 2014.)

S layers are generally composed of a single molecular species endowed with the ability to assemble on the cell surface into closed regular arrays occupying a low free-energy arrangement. Although a considerable amount of knowledge has accumulated on the structure, assembly, chemistry, and genetics of S-layers, relatively little data are available about their specific biological functions [34]. It is now recognized that they can function as protective coats, molecular sieves, molecule and ion traps, promoters for cell adhesion,

immunomodulators, surface recognition, antifouling coatings, and as virulence factors in pathogenic organisms [35]. In those Archaea that possess S-layers as the exclusive envelope component external to the cytoplasmic membrane, the lattice is involved in the determination of cell shape and as a structure aiding in the cell division process [35].

On an ultrastructural level, S-layer proteins form regular crystalline lattices, which may have an oblique (p1, p2), square (p4), or hexagonal (p3, p6) symmetry. Lattice constants can vary from 5 to 30 nm and the S-layer thickness from 5 to 20 nm. Detailed atomic resolution structures of lattices are not available, but several low-resolution three-dimensional (3D) structures have been obtained by electron microscopy of negatively stained samples. A striking similarity even among quite unrelated species is the central core forming region, which is usually oriented toward the cell envelope, giving rise to an overall corrugated inner surface. By contrast, the outer surface appears smooth despite highly variable and species-specific ultrastructure. Between 30% and 70% of one unit cell is occupied by the protein, which leads to the formation of identical and well-defined pores with a diameter of 2–8 nm [36].

S-layer proteins exhibit mostly two separated morphological regions, responsible for cell wall binding and for self-assembly, as shown by mutagenesis studies. The position of the cell wall anchoring region within the protein, as well as its sequence composition, can vary among the bacterial species, similar to the molecular binding partner within the underlying cell wall [33]. In several Gram-positive and Gram-negative bacteria, S-layers bind via the N-terminal region to the underlying peptidoglycan sacculus by recognizing Secondary Cell Wall Polymers (SCWP). This specific molecular interaction with the polysaccharide is mediated by a recurring structural motif termed the ‘‘surface layer homology’’ (SLH) motif. S-layer proteins devoid of SLH motifs are anchored to different types of SCWPs through their N- or

C-terminal domains. In Gram-negative bacteria, the S-layer is attached with its N- or C-terminus to the component of the outer membrane [36].

1.5 Applications of S layer proteins

The wealth of information accumulated on the general principles of S-layers has led to a broad spectrum of applications. As S-layers are periodic structures, they exhibit repetitive identical physicochemical properties down to the subnanometer scale and possess pores identical in size and morphology. Most importantly, properties of S-layer proteins can be changed by chemical modifications and genetic engineering. It is now evident that S-layers also represent a unique structural basis and pattering element for generating complex supramolecular assemblies involving all relevant 'building blocks' such as proteins, lipids, glycans, and nucleic acids [33].

The regularly arranged pores in S layer proteins have been exploited for developing S layer isoporous ultrafiltration membranes, with sharp molecular weight cut-offs. S layers have also been used as an immobilization matrix for functional molecules and nano particles. Because S-layer lattices are composed of identical protein or glycoprotein species, functional sequences introduced either by chemical modification or genetic engineering must be aligned in exact positions and orientation down to the subnanometer scale. Enzymes like invertase, glucose oxidase, β-galactosidase were immobilized on the outer surface of surface layers [33]. Furthermore, a universal biospecific matrix for immunoassays and dipsticks could be generated by immobilizing monolayers of either protein A or streptavidin onto S layers. S layer supported lipid membranes have been developed to study characteristics of archaeal cell envelopes, as surfaces with new properties such as anti-fouling and as a matrix for re-constitution of transmembrane proteins [33]. Further, S layer coated liposomes demonstrated much higher mechanical and thermal stability than plain ones. S layers proteins being surface

components are likely to have an important role in virulene of pathogenic bacteria. They are prime candidates for vaccine development. They have been used as attenuated pathogens, as antigen/hapten carrier, as adjuvants or as part of vaccination vesicles [33].

Due to the promising results obtained with native S layer protein, as immobilization matrix, genetic engineering of S layer proteins was envisaged [37]. While earlier, the functional molecules were adsorbed and/ or cross-linked to the S layer protein, now construction of chimeric functional S layer protein has taken precedence. S layer are capable of tolerating fusions with foreign proteins that never participate in lattice formation while retaining the ability to assemble into geometrically highly defined layers. Fusions with the major birch allergen, fluorescent proteins, core streptavidin, a C-terminally fused cysteine residue for patterning of nanoparticles, or enzymes from extremophiles have been re-crystallized on various supports [33]. Significant advantages for enzyme immobilization by the S-layer self assembly system over processes based on random immobilization of sole enzymes include the requirement of only a simple, one-step incubation process for site-directed immobilization without preceding surface activation of the support. Moreover, the provision of a cushion for the enzyme through the S-layer moiety of the fusion protein prevents denaturation and consequently loss of enzyme activity upon immobilization [33].

Another current approach considers the use of bacterial S-layers as a potential alternative for bioremediation processes of heavy metals in field. The S-layer of *Bacillus sphaericus* JG-A12, an isolate from a uranium mining waste pile in Germany, was shown to bind high amounts of toxic metals such as U, Cu, Pd(II), Pt(II), and Au(III) [38]. Furthermore, Velasquez and coworkers in 2009 determined the tolerance of different Colombian *B. sphaericus* native strains to different heavy metals and came to the conclusion that their S-layer proteins might have the ability to entrap metallic ions, either on living or dead cells [39].

1.6 Chimeric Fusion proteins tagged to S layer for bioremediation

While S layer proteins have been fused to many proteins for various applications, very few examples for chimeric proteins for bioremediation exist in literature. A Hexa-histidine peptide was inserted to a permissive site of the surface layer (S-layer) protein RsaA of *Caulobacter crescentus*. The recombinant strain JS4022/p723–6H, expressing RsaA-6His fusion protein was examined for its ability to sequester Cd (II) from the bacterial growth medium. When mixed with 1 ppm $CdCl_2$, JS4022/p723–6H removed 94.3∼99.9% of the Cd(II), whereas the control strain removed only 11.4∼37.0% leading to a metal loading of 16 mg/g dry cell weight [40]. In another study, the S layer protein from *Bacillus spahericus* was overexpressed in *E. coli* with a 6X-histidine tag. The purified protein was re-assembled and tested for nickel binding ability. While the wild type protein could remove 13.8 mg Ni/g proteins, the recombinant protein could remove 31 mg Ni/g protein respectively [41].

1.7 *Deinococcus radiodurans*, an ideal candidate for bioremediation of radioactive waste

Deinococcus radiodurans is an ancient Gram positive bacterium that can tolerate extremely high doses of ionizing radiation. Members of the Deinococcaceae family are vegetative, non-pathogenic, ubiquitous, and show resistance to DNA damage caused by ionizing radiation, desiccation, ultraviolet radiation, oxidizing agents, and electrophilic mutagen [42-46]. The organism has been extensively studied for its highly proficient DNA damage repair mechanisms that are aided by proteins rapidly induced upon irradiation [47-48].

Radioactive waste sites typically contain organopollutants such as toluene, trichloroethylene; radionuclides such as uranium, plutonium, cesium etc. and heavy metals such as lead, mercury, chromium, arsenic etc. [49]. Numerous organisms have the ability to degrade, transform, detoxify and immobilize these pollutants as has been already described.

However, most of them are sensitive to the damaging effects of radiation. Choice of the appropriate organism depends on its ability to survive and efficiently express desired genes under the harsh conditions prevailing in waste sites. This necessitates use of radioresistant organism like *D. radiodurans* for bioremediation of radioactive waste.

Genes coding for Toluene dioxygenase were cloned from *Pseuodomonas putida F1* into the chromosome of *D. radiodurans* to produce a recombinant strain which could oxidize toluene, chlorobenzene, indole etc. Such cells could grow in the presence of chlorobenzene and at 60 Gy /min irradiation, while degrading the pollutant simultaneously [50]. In addition to the toluene genes, the mercury resistance gene, *merA* was also cloned from *E. coli* strain BL308 into *D. radiodurans*. Such cells could grow in the presence of both radiation and the metal while detoxifying mercury to its volatile form [49].

In another study, *phoN*, an acid phosphatase gene from *Salmonella enteric* serovar *Typhi* was cloned into *D. radiodurans* under a strong deinococcal promoter, *PgroESL.* The phosphatase activity of the recombinant strain was utilized for precipitation of uranium. Nearly 90% of 1 mM uranium could be precipitated in 6 h by recombinant *D. radiodurans* strain carrying *PgroESL-phoN* construct on plasmid pPN1. Further, they could bring about metal precipitation even after 6 kGy gamma radiation under non-growing conditions, while *E. coli* cells carrying the same construct failed to do so [51]. This organism has also been used for engineering an alkaline phosphatase, PhoK for removal of uranyl carbonate from alkaline waste solutions [52]. Taken together, *D. radiodurans* has emerged as an organism which is easy to genetically manipulate and is also radiation resistant making it an ideal candidate for genetic manipulation for radioactive waste management.

1.8 S layer proteins in *D. radiodurans*.

The structure of the *D. radiodurans* cell envelope has been studied since the 1960s. It consists of the inner membrane, the periplasmic space, a peptidoglycan layer, an interstitial layer, the lipid-rich backing-layer, the S-layer which is made of the Hpi protein [53], and a long-chain carbohydrate coat as the outermost layer (**Fig. 1.3**). The last four layers, together with carotenoids, form the so-called ‘‘pink envelope’’ [54]. Upon removal of the membrane-like backing-layer, the bacteria lose their typical shape, suggesting that this layer is responsible for the curvature of the bacteria.

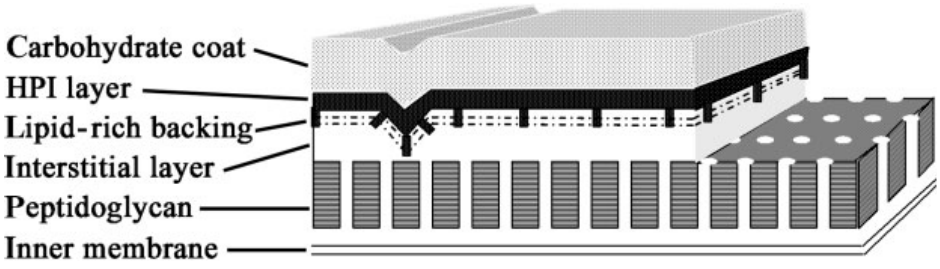

Fig. 1.3. A schematic representation of the deinococcal cell envelope. (Source: Rothfuss et al, 2006.)

The S layer protein from *D. radiodurans* R1 strain, Hpi is a hexagonally patterned macromolecular monolayer, intimately associated with outer backing layer [53]. The 100 kDa protein is 948 aa long with a pI of 4.8. The isolated HPI layer exhibits p6 symmetry. This lattice is consistent with the hexagonal array observed on the bacteria in their native state, unperturbed by sample preparation. The integrity of the Hpi layer is preserved in presence of sodium dodecyl sulfate and urea up to a temperature nearing 100°C. Likewise the secondary structure was found to be preserved between 25°C and 60°C even in the presence of detergents. Upon lowering the pH to 2.2, the secondary structure comprising beta sheets changed drastically, with disintegration of the Hpi layer. At this pH, the lattice structure is

destroyed as well, indicating that the β structures are important in maintaining the integrity of the HPI layer [36,53].

HPI layer exhibits a core concentrated around the six fold axis with a radius of 2.2 nm, a central pore of 2.5–3 nm in diameter, and fine spokes that connect adjacent units. The core is surrounded by six relatively large openings showing threefold symmetry; the spokes exhibit a two fold symmetry **(Fig. 1.4a)**.

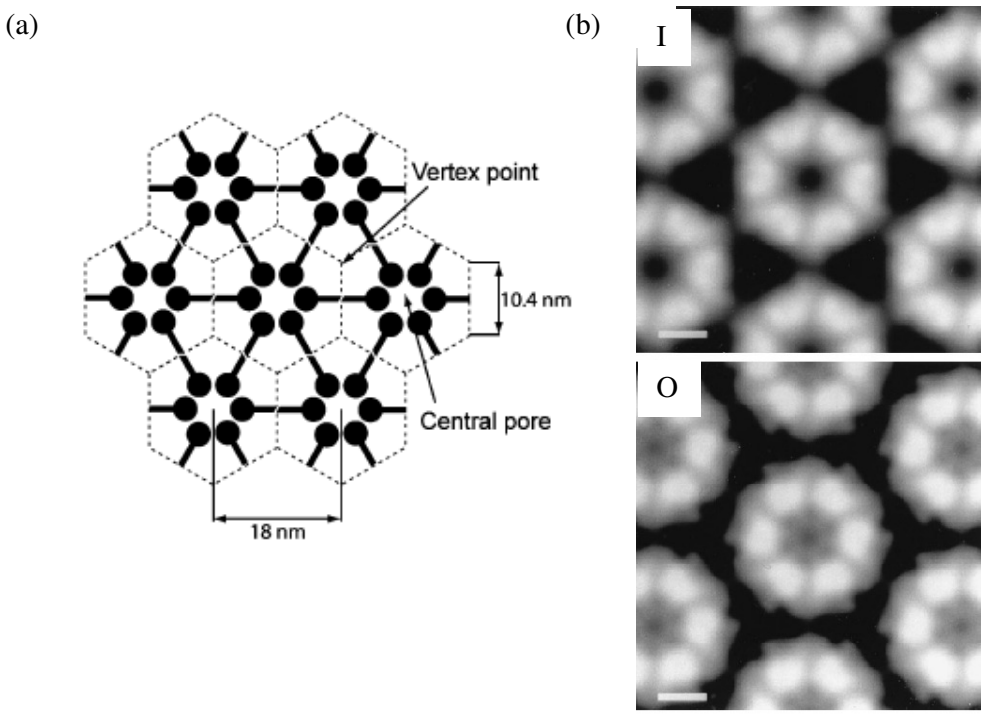

Fig. 1.4. The Hpi protein of *D. radiodurans*. (a) Schematic representation of the Hpi protein arrangement. Source: Pavkov Keller 2011 (b) AFM images of the inner (I) and outer surface (O) of the Hpi layer. Source: Muller et al. 1996.

The core encloses a pore and is surrounded by six relatively large openings centered about the three fold axis [55]. The hydrophobic inner surface of the S-layer lattice interacts with the outer membrane, while the outer surface is more hydrophilic [56] **(Fig. 1.4b)**. When the inner surface was analyzed using Atomic Force Microscopy, pores with and without a central plug

were found. By repeating the measurement after 5 min, switching from the open to the closed state was observed for individual pores. It is not known what induces the switching, although tip-induced conformational changes are ruled out. It was suggested that molecules up to 5 kDa could pass through the central 2.2 nm wide channel [57]. Further, serine and threonine are clustered in the N-terminal region of the sequence that faces the underlying outer membrane. Close to the C-terminus which faces the outer surface, there is a stretch that shows a significant elevated content of tyrosine as well as serine plus threonine, with hydroxylamine totaling almost 30% [58].

The existence of an additional protein involved in the maintenance and integrity of the S-layer in *D. radiodurans* was first reported by Cava et al [59]. SlpA (DR2577) is a proposed homolog of an S-layer protein from *T. thermophilus*, since both proteins contain one SLH motif at the N-terminus. Cava et al. 2004 proposed that most of the cell wall of *Thermus thermophilus* was covered by secondary cell wall polymers (SCWP) which was recognized by an antibody (αSAC) raised against S-layer attached cell wall fragments. Further, pyruvylation of the SCWP was essential for SLH-domain mediated binding by SlpA. The pyruvylation function was assigned to the *csaB* gene. Cell walls from *csaB* mutant bound SlpA with much lesser affinity. Immunological cross-reactivity was detected with αSAC on cell walls of *D. radiodurans*. Further a *csaB* homologue was found in *D. radiodurans* lending support to occurrence of similar interactions in this organism [59].

SlpA of *D. radiodurans* comprises 1167 amino acids, of which the first 19 amino acids most likely constitute a signaling peptide. The mature protein has a theoretical molecular mass of 121.8 kDa, a theoretical pI of 4.9 and contains two cysteines. Deletion of the *slpA* gene in this organism leads to a change in the structure of the cell envelope as well as in resistance to solvent and shear stress [54]. By comparison deleting the *hpi* gene caused little alternations in the structure of the cell envelope or its reaction to shear- or solvent-

induced stress. This indicates that the SlpA protein may play an important role in the preservation of the cell envelope structure. Since the Hpi protein does not contain any SLH motifs, it was proposed that the SlpA protein could be responsible for anchoring to the inner cell envelope [54].The structure of the SlpA lattice has not been analyzed so far.

1.9 Stabilization of biomass for bioremediation

While bioremediation shows promise, the application of microbial biomass to waste sites and its stability are issues which also need to be addressed. Often microbes are pre-treated to generate a formulation which can be readily used and is likely to retain metal removal potential for a longer period of time. Physical treatments such as heating, autoclaving, freeze drying and chemical pre-treatments such as using acids, alkali and organic chemicals showed enhancement in metal biosorption in a few cases [60]. For example pre-treatment of *Streptomyces rimosus* with NaOH resulted in increasing Cd biosorption capacity [61]. Some of these treatments render the biomass non-viable which offers a few advantages. For example, constant nutrient supply is not required for systems using dead cells and recovery of metals and regeneration of biosorbents is less complicated than for living cells [10,60].

Specifically freeze drying/lyophilization of biomass is a technique which preserves cell structure and functionalities better than other treatments and is therefore well suited for bioremediation. Lyophilized residual brewery yeast was used for removing uranium from aqueous solutions [62]. A *Pseudomonas* strain was lyophilized and used for remediation of uranium and thorium [63]. Freeze dried marine microalgae could adsorb cadmium more rapidly than fresh cells [64]. Similarly, use of 'reagent-like' freeze dried recombinant bacteria for measuring bioavailability of arsenic and antimony have been reported [65]. While a number of examples for lyophilization of biomass exist in literature for biosorption of heavy metals, there are very few examples for enzyme mediated metal immobilization. The only

examples that can be found are reports on chromium reductase and uranium reductase activity in *D. desulfuricans* which were stable after freeze drying and storing at room temperature [66].

1.10 This study

In the past, *phoN* gene of *Salmonella enterica* serovar Typhi that encodes a non-specific acid phosphatase (NSAP) was over-expressed in *D. radiodurans* [51]. However, the phosphatase activity obtained in *D. radiodurans* was far less (10%) than that obtained in recombinant *E. coli* cells carrying the same construct. It was suggested that this may be due to the multi layered complex cell wall in *D. radiodurans* [54] which might limit substrate accessibility to PhoN. Since, the thick complex cell wall of this organism could pose a major problem in engineering this organism for any kind of extracellular metal remediation, the possibility of exploiting membrane localized proteins on the cell surface for display of proteins relevant to bioremediation has been explored in the present study. Earlier work has shown that Surface (S) layer proteins are ideally suited for display of peptides and proteins. *D. radiodurans* is known to possess two S-layer proteins, Hpi and SlpA. The possibility of fusing such proteins to PhoN for enhanced metal precipitation ability was explored along with another protein relevant to bioremediation, the metallothionein SmtA from *Synechococcus elongatus*, which would be useful for sequestering metals such as cadmium, copper and zinc. The utility of the fusion proteins so generated as well as recombinant strains expressing them were studied. The specific objectives of the present work were as follows:

1. Construction of the S layer fusion proteins with bioremediation active phosphatase (PhoN) and metallothionein (SmtA) proteins for metal removal, using recombinant DNA technology.
2. Studies on the expression, localization and activity of the fusion proteins.

3. Evaluation of microbes expressing fusion proteins for removal of metals such as U and Cd from solution.
4. Assessment of the utility of purified S-layer proteins and S-layer fusion proteins in removing metals from solutions *in vitro*, and
5. Evaluation of lyophilized recombinant microbes for metal removal from solution.

The work carried out is presented in the following chapters:

Chapter 2 describes materials, methods and protocols followed in this study. The Chapters 3 and 4 describe the results from this work. Chapter 3 deals with the cloning and expression of S layer fusion proteins. The *hpi* gene and the nucleotide sequence encoding SLH domain of the SlpA protein of *D. radiodurans* were fused independently to *phoN* and *smtA* and their expression and localization was studied. Chapter 4 describes the potential of recombinants expressing the fusion protein as well as the purified S-layer proteins and S-layer fusion proteins for metal binding / precipitation. The utility of lyophilization in microbe based bioremediation has also been studied and elaborated in this chapter. Chapter 5 summarizes all the major findings of this study.

Chapter 2

Materials and Methods

2.1 Growth media & culture conditions

Different bacterial strains used in this study are described in **Table 2.1.**

Table 2.1. List of bacterial strains used in this study

Strain	Characteristics	Source/Reference
E. coli JM109	(endA1 glnV44 thi-1 relA1 gyrA96 recA1 mcrB$^+$ Δ(lac-proAB) e14- [F' traD36 proAB$^+$ lacI^q lacZΔM15] hsdR17($r_K^-m_K^+$)	Lab collection
E. coli (BL21) pLysS	(F^- ompT gal dcmlonhsdS_B(r_B^- m_B^-) λ(DE3) pLysS(cm^R)	Lab collection
D. radiodurans R1	Wild-type strain	Minton, K. W.
D. radiodurans HMR202	Hpi mutant	Rothfuss et al. 2006

E. coli cells were routinely grown aerobically in Luria–Bertani (LB) growth medium at 37°C with shaking (180 rpm) unless otherwise mentioned. *D. radiodurans* R1 was routinely grown aerobically in TGY (1% BactoTryptone, 0.1% glucose, and 0.5% yeast extract) liquid medium at 32°C under agitation (180 rpm).

Bacterial growth was assessed by measuring turbidity (OD_{600nm}) of liquid cultures or by determining colony forming units (CFUs) on appropriate agar plates (1.5% BactoAgar). The antibiotic concentration used for selection of *E. coli* transformants was 100 µg/ml of Ampicillin for recombinants carrying pRAD1 based constructs, or 50 µg/ml of Kanamycin and 33 µg/ml of Chloramphenicol for pET29b based constructs. In case of *D. radiodurans*,

recombinants were grown on 3 µg/ml chloramphenicol for pRAD1 based constructs. The *D. radiodurans* Hpi mutant, HMR202 was routinely grown in TGY containing 8 µg/ml of Kanamycin.

2.2 Histochemical screening of recombinants expressing PhoN

Histochemical screening of PhoN expressing *E. coli* clones was carried out by growing cells on LB plates containing phenolphthalein diphosphate (PDP) at 1 mg/ml and methyl green (MG) at 50 µg/ml [67]. For screening *D. radiodurans* cells, the MG concentration was reduced to 5 µg /ml due to its toxicity to growth of this organism. Recombinants which display cell based phosphatase activity give rise to dark green colored colonies on PDP-MG plates. Phosphoric acid released from PDP due to action of phosphatases causes local acidification of medium leading to pH indicator dye, MG stain turning dark green. Precipitation of the dark green MG on phosphatase producing colonies forms the basis for screening of phosphatase positive strains.

2.3 Recombinant DNA techniques

2.3.1 Isolation of chromosomal DNA from *D. radiodurans*

D. radiodurans cells from a 25 ml overnight grown culture was re-suspended in 250 µl ethanol and kept at 4°C for 5 min. The cells were re-suspended in 250 µl Tris-EDTA ($T_{10}E_1$) buffer (10 mM Tris and 1 mM EDTA), pH 8. Cells were lysed by addition of 50 µl lysozyme (2 mg/ml) and incubation at 37°C for 30 min, followed by addition of 6 units of Proteinase K (New England Biolabs) and 50 µl SDS incubated at 37°C for 3 h. To this, equal amount of phenol equilibrated with 100 mM Tris-HCl, pH 8.0 was added, mixed gently and subjected to centrifugation at 10,000 rpm for 15 min. The aqueous phase was removed and phenol extraction was repeated. This was followed by two rounds of chloroform extraction. To the

aqueous layer, 8 µl of RNAse (10 mg/ml) was added, followed by incubation at 37°C for 1.5 h. The aqueous layer was extracted twice with phenol:chloroform:isoamyl alchohol (25:24:1). Chromosomal DNA was spooled after gently mixing the aqueous layer with 1/10th volume of 150 mM NaCl, pH 7.5 and two volumes of chilled absolute ethanol. The spooled DNA was washed with 70% ethanol, air dried, dissolved in $T_{10}E_1$ buffer, pH 8.0 and stored at -20°C till further use.

2.3.2 Restriction endonuclease digestion and electrophoresis of DNA

Restriction endonuclease digestion of DNA was carried out according to the manufacturer's protocol (New England Biolabs). The digested DNA (with appropriate amount of 10X loading dye) was resolved on a 1 % agarose gel containing 0.5 µg/ml ethidium bromide prepared in 0.5 X TBE (4.45 mM Tris, 4.45 mM boric acid, 0.1 mM EDTA, pH 8.3) buffer. Electrophoresis was carried out at 8V/cm and DNA fragments were visualized using UV transilluminator. The 1 kb and 100 bp DNA ladder from New England Biolabs were used as markers to calculate the molecular mass of the various DNA fragments.

2.3.3 Amplification of DNA by Polymerase Chain Reaction

Primers for PCR amplification were designed on the basis of the published sequence of the genes for *D. radiodurans* (http://www.tigr.org) and *Salmonella enterica* serovar Typhi (http://www.ncbi.nlm.nih.gov). Primers used in this study are listed in **Table 2.2.** PCR amplification was generally carried out using 20 pmoles of each primer, 200 µM dNTPs, 1.5 U Taq DNA polymerase in 1X Taq buffer (Bangalore Genei Ltd.). For PCR of longer DNA fragments from deinococcal chromosome, the GC Rich PCR amplification kit from Roche was used. The template for PCR was either recombinant plasmid or chromosomal DNA or a colony. In case of *D. radiodurans*, colony PCR was carried out by making a suspension of

cells taken from the colony in 10 µl distilled water which was placed in a boiling water bath for 10 min. Five µl of this suspension was directly used as template in PCR reactions. The PCR products were purified by PCR purification kit supplied by Roche Diagnostics.

Table 2.2. List of primers used in this study.

Primer	Sequence	RE site
Smt-f	5'- GGAATTCCATATGACCTCAACAACCTTGGTC -3'	NdeI
Smt-r	5'-CGGGATCCTTAGCCGTGGCAGTTACAGCC-3'	BamHI
CD-gro	5'-CGGAGTCTAGATGAAGAAAAATATCG-3'	XbaI
CD-r	5'-ACTTCTTACATATGGACGGTTTCG-3'	NdeI
SlpA-f	5'-ATTGGGGGTTCTAGATGAAGAAAAG-3'	XbaI
SLH99-r	5'-GCGTTTTGCATATGGGTCATGTC-3'	NdeI
DG-f	5'-GTGGCCGCCAGATCTGTTCAGG-3'	BglII
Gro-r	5-GTTTCAGCATCTAGAGTCCTCCTG-3'	XbaI
Hpinx-r	5'-GGTGCATATGCTTCTTACTTCTG-3'	NdeI
Hpi5-f	5'-CAGTGGAACCGTATTCGTGAC-3'	-
P5	5'-GGAGCGGATAACAATTTCACACA-3'	-
P6	5'-AACGCGGCTGCAAGAATGGTA-3'	-
SLHo-f	5'-ACTCTACCATGGAGAAAAGTC-3'	NcoI
PetC-r	5'-CTTTCACCTCGAGTAATTAAG-3'	XhoI

The underlined nucleotide sequence relates to the restriction endonuclease site included in the primer

2.3.4 Ligation and transformation

Ligation of DNA insert to the vector was typically carried out in 3:1 to 5:1 molar ratio. The Rapid Ligation Kit from Roche was used for DNA ligation. Around 2.5 Units of T4 DNA

ligase was added to a 20 µl reaction containing the T4 ligase buffer, vector, insert and DNA dilution buffer according to the manufacturer's protocol (Roche Biochemicals, Germany). The ligated DNA (50 – 100 ng) was used to transform competent *E. coli* cells prepared using RbCl protocol and transformation of such cells was carried out as described [68]. *Deinococcus* transformations were carried out as described earlier with some modifications [69]. Briefly, exponentially grown cells were chilled on ice for 10 min and subjected to centrifugation. They were re-suspended in 3 ml TGY with 30 mM $CaCl_2$. To 100 µl cell aliquot, 1 µg plasmid was added and kept on ice for 45 min. Cells were then incubated at 32°C for 45 min. About 900 µl TGY was added to the cells and incubated at 32°C under agitation (180 rpm) overnight. The following day, the cells (100µl) were plated on TGY agar medium containing 3 µg/ml chloramphenicol.

2.3.5 Plasmid Isolation

Plasmid DNA was isolated from *E. coli* cells by alkaline lysis method using the High Pure Plasmid Isolation Kit, Roche Diagnostics as per the manufacturer's protocol. Various plasmids used or constructed in this study are listed in **Table 2.3.**

Table 2.3. List of plasmids used in this study.

Sl. no.	Plasmid	Description of construct	Source/Reference
1.	pRAD1	*E. coli-D. radiodurans* shuttle vector, Ap^r, Cm^r, 6.28kb	Meima R. and M. E. Lidstrom, 2000
2.	pS1	*E. coli* over-expression vector, pET16b containing *SmtA* gene from *S. elongatus;* Kan^r, 4.335kb	Unpublished data from this lab

3.	pPS1	pRAD1 containing ORF of *S. elongatus smtA* with deinococcal *groESL* promoter; Ap^r, Cm^r, 6.7kb	This study
4.	pPH1	pRAD1 containing the deinococcal *hpi* ORF with deinococcal *groESL* promoter; Ap^r, Cm^r, 9.28kb	This study
5.	pPHS1	pRAD1 containing the *hpi-smtA* fusion gene under deinococcal *groESL* promoter, Ap^r, Cm^r, 9.5kb	This study
6.	pPSS1	pRAD1 containing the *SLH-smtA* fusion gene with deinococcal *groESL* promoter, Ap^r, Cm^r, 7.55kb	This study
7.	pPN1	pRAD1 containing *phoN* ORF of *Salmonella typhi* with deinococcal *groESL* promoter, Ap^r, Cm^r, 7.35kb	Appukuttan et al. 2006
8.	pGRDF2	pRAD1 containing ORF of *S. typhi phoN* (without its signal peptide) tagged with sequence encoding deinococcal FliY signal peptide and deinococcal *groESL* promoter Ap^r, Cm^r, 7.35kb	Unpublished results. This lab.
9.	pGRDF3	pRAD1 containing the *hpi-phoN* fusion gene with deinococcal *groESL* promoter Ap^r, Cm^r, 10.8kb	This study
10.	pPSP1	pRAD1 containing the *SLH-phoN* fusion gene with deinococcal *groESL* promoter Ap^r, Cm^r, 8.175kb	This study
11.	pET16b	*E. coli* protein over-expression vector, Kan^r, 5.71kb	Novagen
12.	pPSP2	pET16b containing the *SLH-phoN* fusion gene, Kan^r, 7.085	This study

		kb	
13.	pET29b	*E. coli* protein over-expression vector, Kan^r,5.37kb	Novagen
14.	pPSP3	pET29b containing the *SLH-phoN* fusion gene, Kan^r, 6.45kb	This study
15.	pUC18	*E. coli* cloning vector, Ap^r, 2.68kb	NEB
16.	pASK1	pUC18 containing the *S. typhi phoN* gene with *phoN* promoter, Ap^r, 3.62kb	Work from this lab

2.4 Isolation of Hpi layer from *D. radiodurans* cells

Deinococcus radiodurans was grown in TGY to an OD_{600nm} ~ 1.5/ml and subsequently harvested by centrifugation at 5000 g for 5 min at 4°C. Cells were washed twice by resuspension in distilled water containing protease inhibitor, 1 mM phenylmethanesulfonyl fluoride (PMSF), followed by centrifugation as above. The cell pellet was resuspended in distilled water containing 1 mM PMSF and 2 % Lithium dodecyl sulphate in a volume 20 times the initial cell pellet volume. Extraction of Hpi S-layer sheet was carried out at 50 rpm agitation at 4 °C for 4 h. After extraction, cells were removed by centrifugation at 3500 g for 6 min and the Hpi layer was subsequently pelleted by centrifugation at 20,000 g for 40 min at 4°C. Hpi preparation was washed in distilled water by repeated resuspension-centrifugation at 20,000 g, as above. The isolated Hpi layer was stored (~2 mg/mL protein in distilled water) at 4°C, until further use.

2.5 Extraction, estimation and electrophoresis of cellular proteins

Cultures of *E. coli* or *D. radiodurans* were harvested by centrifugation, washed in

distilled water twice and re-suspended in chilled distilled water. Cell fractionation was carried out by sonication of cells (Branson Sonicator, 2 second On/Off pulse for 2 min), followed by centrifugation at 3500 g for 6 min to separate unbroken cells from rest of the suspension. The cytosolic and membrane bound fractions were separated by centrifugation at 15,000 g for 30 min. Protein concentration was estimated by using SIGMA Total Protein Kit (SIGMA-ALDRICH, Germany) based on Peterson's modification of micro Lowry modified method [70] . For zymogram analysis, the cells were lysed in non-reducing Laemmli's [71] cracking buffer (2% SDS, 4% glycerol, 40 mM Tris-HCl, pH 6.8 and 0.01% bromophenol blue) at 50°C for 15 min. The suspension was clarified by centrifugation at 15,000 g for 30 min. For all other applications, protein samples were boiled in Laemmli's buffer followed by centrifugation at 15,000 g for 30 min to remove insoluble cell debris. The protein samples were resolved electrophoretically using sodium dodecyl sulphate polyacrylamide gels (SDS-PAGE). SDS-PAGE was carried out using the Tarson's Electrophoresis apparatus. The gel was poured between a glass and ceramic plate separated by 1 mm spacers. The resolving gel and stacking of 5% were poured according to details given in Table 2.4.

Table 2.4. Composition of polyacrylamide gels.

SL. No.	Ingredient	10% resolving gel	5% stacking gel
1	30% acrylamide solution	2.5 ml	0.625 ml
2	Tris-Cl 1.5 M	1.875 ml, pH 8.8	1.25 ml, pH 6.8
3	10% SDS	75 µl	50 µl
4	10% Ammonium per sulfate	56.25 µl	37.5 µl
5	TEMED (Tetramethylethylenediamine)	3.75 µl	3.75 µl
6	D/W	2.99 ml	3.033 ml

After gelation, the protein extracts were loaded into the wells and electrophoresis was carried at 15 V/cm. Post-run, gels were washed in distilled water followed by processing for Western blotting or zymogram or staining by a 0.25% Coomassie brilliant blue solution.

2.6 Matrix Assisted Laser Desorption/ Ionization - Time of Flight - Mass Spectrometry (MALDI-TOF-MS)

Proteins resolved by SDS-PAGE, were excised as 1mm X 1mm gel plugs. The gel protein plug was subjected to destaining, reduction, alkylation, in-gel trypsin digestion and elution of oligopeptides as described earlier [72]. The eluted peptides were subjected to mass spectrometry (UltraFlex III MALDI-TOF/TOF mass spectrometer, Bruker Daltonics, Germany). The oligopeptides were co-crystallized with α-Cyano-4-hydroxycinnamic acid (CHCA) (5 mg/ml in 0.1% Trifluoro acetic acid and 30% Acetonitrile) on target plate (384-well stainless steel plate, Bruker Daltonics, Germany). The machine was externally calibrated using Peptide calibration mix I (Bruker Daltonics, Germany) or with the trypsin autodigest peptides. The mass spectra were generated in the mass range of 600-4500 Da using standard ToF-MS protocol in positive ion reflection mode. Laser was set to fire 150 times per spot. Peak list was generated using FlexAnalysis software 3.0 (Bruker Daltonics, Germany) and mass spectra were imported into the database search engine (BioTools v3.1 connected to Mascot, Version 2.2.04, Matrix Science). Mascot searches were conducted using the NCBI non redundant database (released in March 2013 or later with minimum of 14344429 entries actually searched) with the following settings: Number of miscleavages permitted was 1; fixed modifications such as Carbamidomethyl on cysteine, variable modification of oxidation on methionine residue; peptide tolerance as 100 ppm; enzyme used as trypsin and a peptide charge setting as +1. A match with *D. radiodurans / Salmonella enterica* as appropriate with

the best score in each Mascot search was accepted as successful identification. A Mascot score of >65 with a minimum of 6 peptide matches was considered to be a significant identification ($p < 0.05$) when sequence coverage was at least 25%.

2.7 Bioinformatic analysis

The sequence alignment of proteins was carried out using the web-based ClustalW software (http://www.ebi.ac.uk/Tools/msa/clustalw2/).

2.8 Determination of phosphatase activity

2.8.1 *In vitro* acid phosphatase activity by zymogram analysis

Equal amount of proteins in non-reducing Laemmli's buffer were electrophoretically resolved by 10% SDS-PAGE at 75 V for 30 min followed by 100 V. After electrophoresis, the gel was rinsed briefly with water to remove surface SDS and renatured using 1% Triton X-100 in 100 mM acetate buffer pH 5.0 (Two washes of 20 min each) followed by a wash in 100 mM acetate buffer pH 5.0. The gel was developed using 200 µl of nitroblue tetrazolium chloride/5-bromo-4-chloro-indolyl phosphate (NBT/BCIP) (Roche Diagnostics, 18.75 mg/ml NBT and 9.4 mg/ml BCIP in 67% Dimethyl sulfoxide) mix in 20 ml of 100 mM acetate buffer pH 5.0 for 16 h. The assay was terminated by rinsing the gel in distilled water.

2.8.2 *In vivo* cell-based acid phosphatase activity

Cell bound acid phosphatase activity was estimated by the liberation of *p*-nitophenol from di-sodium *p*-nitrophenyl phosphate as described earlier [73]. Recombinant cells were re-

suspended in 100 mM acetate buffer, pH 5.0 containing 8 mM *p*-nitrophenol and incubated at 37°C for 30 min. The reaction was stopped by addition of 2N NaOH and the amount of *p*-nitrophenol released was spectrophotometrically determined by measuring the OD at 405 nm. The cell-bound PhoN activity was expressed as nmoles of *p*-nitrophenol (pNP) liberated min^{-1} mg^{-1} bacterial protein.

2.9 Western Blotting and Immunodetection

Equal amount of whole cell protein extracts (50 µg-80 µg) prepared in Laemmli's cracking buffer (2% SDS, 2 mM dithiothreitol, 4% glycerol, 40 mM Tris-HCl, pH 6.8 and 0.01% bromophenol blue) were resolved by 10% SDS-PAGE. The gel was equilibrated in Transfer buffer (0.125 M Tris base, 0.192M Glycine, 20% methanol) for 20 min. The proteins were electroblotted on nitrocellulose membrane at 300 V for 2 h. The blot was processed for immunodetection. Briefly, the blot was placed in an appropriate dilution of the antibody serum in MaNa (0.1M Maleic acid and 0.15 M NaCl) buffer, containing 1% casein suspension, for interaction with primary antibody. After 1 h of incubation, the blot was washed in 100 mM MaNa buffer twice for 20 min each to remove antibody bound non-specifically to the blot. The blot was then incubated in blocking buffer containing the secondary antibody, alkaline phosphatase conjugated anti-rabbit IgG (SIGMA-ALDRICH) at 1:10,000 dilution for 1 h. The blot was rinsed in MaNa buffer for 20 min, twice. After equilibration in Tris-NaCl buffer pH 9.0, the blot was processed for colour development using NBT-BCIP (Roche Diagnostics) as substrate in the same buffer. The colour development reaction was stopped by adding distilled water.

2.10 Over-expression of SLH-PhoN

Recombinant *E. coli* BL21 pLysS cells carrying the *SLH-phoN* construct (pPSP3) were grown at 37°C in LB broth containing 50 µg/ml kanamycin and 33 µg/ml chloramphenicol till they attained a OD_{600nm} of 0.6-0.8/ml. SLH-PhoN expression was induced by addition of 1 mM isopropyl-β-D-thiogalactopyranoside (IPTG) followed by incubation at 30°C under shaking conditions (180 rpm). Cells were harvested after 5 h of growth and lysed for analysis by 10% SDS-PAGE or used in peptidoglycan binding assays.

2.11 Peptidoglycan isolation from *D. radiodurans*

Isolation of peptidoglycan from *D. radiodurans* cells was carried out by boiling cells in sodium dodecyl sulphate which dissolves all cellular components except the peptidoglycan which remains insoluble and can be separated by centrifugation. *D. radiodurans* cells grown to stationary phase were harvested by centrifugation and washed in distilled water. The pellet obtained was re-suspended in 10 times the volume of 2% sodium dodecyl sulphate solution. The suspension was refluxed under constant stirring conditions for 8 h continuously. This was followed by centrifugation of the suspension at 20,000 g for 40 min. The resultant pellet was re-suspended in 2% SDS and the entire process repeated two times. The final pellet obtained was washed in distilled water 6 times to remove SDS and stored at 4°C.

Peptidoglycan concentration was routinely calculated from their diamino acid, ornithine content as described [59]. Around 10 mg dry weight of peptidoglycan was resuspended in 2 ml of concentrated HCl and transferred to a round bottom flask. The flask was placed in an oil bath at 115°C for 6 h. The solution was vacuum dried. The residue was

re-suspended in 200 µl distilled water and clarified by centrifugation at 15,000 g for 30 min. This solution was diluted 1:10 and used for estimation of ornithine.

Ornithine estimation was carried out as described [74]. Appropriate volume of hydrolyzed peptidoglycan solution was taken in 50 µl distilled water. To this 50 µl acetic acid and 50 µl Ninhydrin reagent (250 mg in 6 ml acetc acid and 4 ml 0.6 M phosphoric acid) were added and kept in a boiling water bath for 7 min. The solution was cooled and the absorbance of the resulting red color was measured spectrophotometrically at 515 nm. A standard curve constructed by estimation of free ornithine amino acid similarly, was used to determine concentration of ornithine in peptidoglycan.

2.12 Peptidoglycan binding studies and glutaraldehyde stabilization

Peptidoglycan binding assay was carried out as shown in the schematic below, as described **(Fig. 2.1)** [75]. Briefly, 30 µl of peptidoglycan (corresponding to 43 µg of ornithine equivalent) was added to 60 µl of cell extract from *E. coli* cells expressing SLH-PhoN in 50 mM Tris-Cl, pH 8.0 and incubated at 4°C for 2 h. This was followed by centrifugation to obtain supernatant (soluble fraction, S) and a pellet. The pellet was washed and again fractionated into the supernatant, (W) and the pellet. The pellet was then incubated in non-reducing cracking buffer [71] at 50^{o}C for 15 min and again subjected to centrifugation to obtain the supernatant (insoluble fraction, I) and pellet. The insoluble fraction, I, represents the protein which bound to the peptidoglycan, while the soluble fraction, S represents protein which did not bind to the peptidoglycan. A zymogram was carried out with the soluble, wash and the insoluble fractions.

The interaction between peptidoglycan and SLH-PhoN protein was stabilized by treatment with glutaraldehyde. About 7 mg of SPhoNP (peptidoglycan on which SLH-PhoN was immobilized) was suspended in 0.2% glutaraldehyde in 100 mM acetate buffer pH 5.0 and kept on a rocker in ice for 1 h. The peptidoglycan to which the SLH-PhoN was cross-linked was subsequently washed in acetate buffer twice and finally re-suspended in acetate buffer and stored at 4°C until further use.

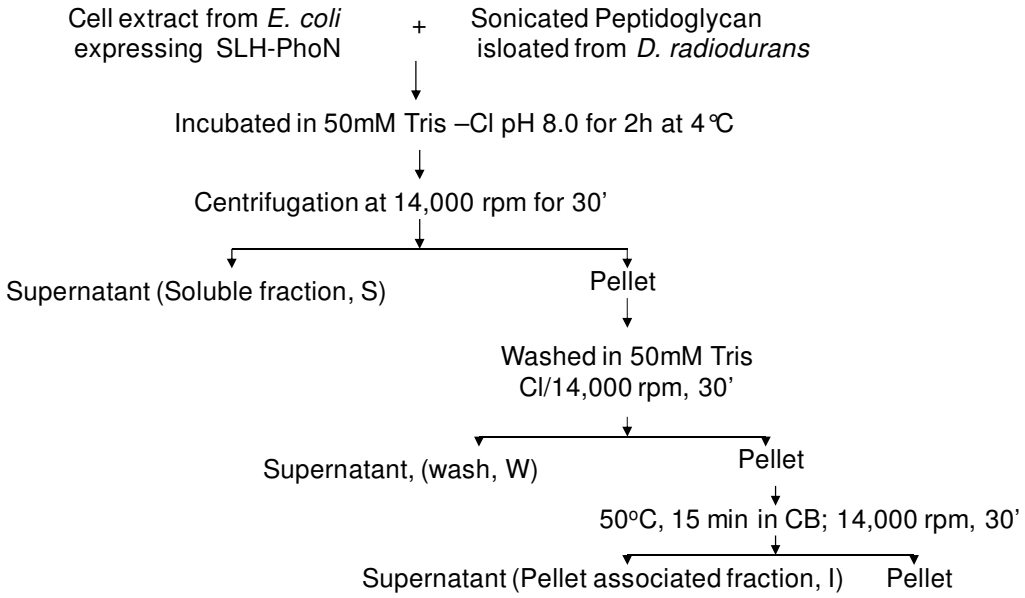

Fig. 2.1. Peptidoglycan binding Assay.

2.13 Determination of surface charge of cells

The surface charge on cells was determined by measuring their zeta potential. Cells were suspended in distilled water or MOPS buffer of specified pH at OD_{600nm} 1.0/ml and their zeta potential was determined in a electrophoretic cell using Zetasizer nano series (Malvern Instruments, UK).

2.14 Metal binding studies using recombinants expressing SmtA

Overnight grown cultures of recombinant cells were inoculated into fresh medium at a starting $OD_{600nm}$of 0.05/ml. After 5 h of growth under aerobic conditions, when OD_{600nm} reached 0.6/ml, the metal (Cd, Cu, Zn) was added at the specified concentrations. The culture was then grown in presence of the metal overnight. Cells were removed by centrifugation, washed in the growth medium once, and dried at 80°C for 4 h. The samples were weighed and digested in hot concentrated HNO_3. Acid digested samples were diluted and the metal estimated by Flame/Graphite Atomic Absorption Spectrophotometry (Model 906AA FAAS, GBC Scientific Equipment Pvt. Ltd., Australia). When the experiment was carried out with 40 µM cadmium for recombinant *D. radiodurans* cultures, the metal was added after a pre-culture of 16 h (OD_{600nm} of 3.0/ml), instead of 5 h to allow for more growth, because at this concentration the metal is known to be toxic to *D. radiodurans.*

2.15 Bioprecipitation of metals

Metal precipitation assays were performed as described, earlier [18] with certain modifications. In a typical experiment, overnight grown cultures of *D. radiodurans* and *E. coli* recombinants were harvested and washed in distilled water. Cell suspensions (OD_{600nm} of 0.3/ml of *E. coli* and 3.0/ml of *D. radiodurans* or 0.1 mg/ml of *E. coli* and 0.8 mg/ml of *D. radiodurans* lyophilized cells) were incubated in 1 mM uranyl nitrate or 1 mM cadmium nitrate in 2 mM acetate buffer (pH 5.0), supplemented with 5 mM β-glycerophosphate at 30 °C under shaking conditions (50 rpm). The final pH of this solution was 6.8. The cell density and concentrations of uranyl nitrate and β-glycerophosphate were varied in different experiments. Bioprecipitation studies using glutaraldehyde stabilized SPhoNP (peptidoglycan to which PhoN was immobilized) were carried out using 7 mg/ml of material in a typical assay as mentioned above. After complete precipitation of metal, SPhoNP was transferred to

a fresh solution of similar composition. This was repeated multiple times. Appropriate controls were included to ascertain (a) spontaneous chemical precipitation of the metal or sorption to the container surface by excluding cells in the reaction mix and (b) biosorption of metal on the cell surface by excluding the substrate, β-glycerophosphate.

In all metal precipitation assays, aliquots were removed at specified time intervals, and residual metal in the supernatant was estimated following removal of cells by centrifugation. Metal was estimated in the supernatant or in the cell lysate, obtained from acid (Conc. HNO3) digestion of cell pellet as described earlier (Section 2.13). Uranium was estimated using Arsenazo-III reagent by a modification of the method by Fritz and Bradford [76]. A 0.1% solution of Arsenazo-III was prepared by dissolving 0.2 of the reagent in 180 ml of 0.01N HCl and 20 ml of absolute ethanol (30 min, stirring) and filtered through Whatman No. 1 filter paper. Twenty µl of the supernatant was diluted to a total volume of 600 µl. The samples were acidified (200 µl of 0.01N HCl), followed by addition of 200 µl of Arsenazo-III. The resultant purple colored metal-Arsenazo-III complex was estimated spectrophotometrically at 655nm. Cadmium was estimated by Flame/Graphite Atomic Absorption Spectrophotometry (Model 906AA FAAS, GBC Scientific Equipment Pvt. Ltd., Australia).

2.16 Lyophilization

A thick saline-based suspension of recombinant cells, was placed in Petriplates, frozen in liquid nitrogen for 5 min and lyophilized without any lyo/cryoprotectant overnight in a Lyophilizer (Lyospeed, Genevac, United Kingdom) at 0.07 mbar for 18 h and stored in vials, at room temperature without applying vacuum, until further use. Equivalence between the OD_{600nm} of the suspension submitted for lyophilisation and the dry weight of the lyophilized powder obtained was determined to calculate the total number of viable cells in the

lyophilized powder and to equalize cell numbers used in metal precipitation studies. The lyophilized cells when re-suspended, rapidly formed a uniform suspension in 100 mM acetate buffer, pH 5.0 and were allowed to equilibrate for 5 min before the PhoN activity and uranium precipitation assays were carried out. For metal precipitation studies, ~ 80 mg/mL suspension of lyophilized cells was prepared in 100 mM MOPS buffer and used immediately.

2.17 Scanning Electron Microscopy

E. coli cell samples were washed in normal saline and fixed in 2.5% glutaraldehyde for 2 h while *Deinococcus* cells samples were washed in cacodylate buffer (100 mM, pH 7.4) and fixed in Karnovskys fixative [77] for 2 h at 4°C. Samples were washed in 100 mM cacodylate buffer. Fixed *E. coli* and *D. radiodurans* cells were dehydrated in a graded ethanol series ranging from 20%-100%. The samples were spotted on aluminium studs and dried at 37°C for 1 h. The dried samples were gold coated by thermal evaporation technique and analyzed by scanning electron microscopy (SEM) and energy dispersive X-ray spectroscopy (EDXS) using a Tescan VEGA 40 Microscope and INCA energy 250, Oxford Instrument EDXS system.

2.18 Transmission Electron Microscopy

E. coli or *D. radiodurans* cells were washed twice with 50 mM cacodylate buffer (pH 7.4) and fixed in 2.5 % glutaraldehyde and 0.5 % Para-formaldehyde overnight at 4°C. The fixed samples were washed with cacodylate buffer three times and embedded in 2 % noble agar. The samples were dehydrated in a graded series of ethanol (30, 60, 75, 90, and 100 %). Ethanol was removed by treatment with propylene oxide and the agar blocks were subsequently infiltrated with Spurr reagent on sequential incubation with 1:3, 3:1 and 1:1 (propylene oxide:Spurr reagent v/v) for 2 h each. The samples were finally infiltrated with

Spurr resin for 16 h and embedded in it by incubation at 60°C for 72 h. Thin sections of samples were prepared with a microtome (Leica, Germany), placed on 200 mesh formvar-coated copper grids and viewed with a Libra 120 plus Transmission electron Microscope (Carl Zeiss, Germany) without uranyl acetate staining. TEM of the Hpi layer was done by dropping 10µl of 2 µg/µl suspension of the Hpi protein layer on formvar coated copper grids followed by staining in 1 % uranyl acetate. The copper grids were air dried and analyzed as mentioned above.

Chapter 3

Construction of deinococcal S layer fusion proteins with metallothionein (SmtA) and acid phosphatase (PhoN): cloning and expression

Deinococcus radiodurans is known to possess two S layer proteins, Hpi and SlpA [54]. Of these, the Hpi has been studied extensively while the SlpA has been annotated as an S layer protein based on its homology with the S layer protein from *Thermus thermophilus* [54]. It is not known how Hpi and SlpA proteins are placed with respect to each other in the deinococcal cell envelope. The SlpA is a large protein whose location in the deinococcal cell envelope is not very clear. It contains a surface layer homology (SLH) motif which is known to bind secondary cell wall polymers present on peptidoglycan in a number of bacteria such as *Bacillus anthracis, Clostridium thermocellum, Paenibacillus alvei* and others [75,78-79]. Further, the SLH domain has been exploited for anchoring proteins to peptidoglycan for cell surface display [80]. In *Thermus thermophilus* also, the SLH domain binds secondary cell wall polymer which is covalently attached to the peptidoglycan [59]. As a result, instead of the entire SlpA protein, sequence coding only for the SLH domain have often been used for generating fusion proteins.

SmtA is a cyanobacterial metallothionein rich in cysteine residues and therefore relevant to metal bioremediation. SmtA has been over-expressed earlier in *E. coli* for enhanced metal binding [14]. The PhoN is a non-specific acid phosphatase from *Salmonella enterica* serovar Typhi. The corresponding gene was earlier cloned and over-expressed in *D. radiodurans* for bioremediation of heavy metals, especially uranium [51]. *phoN* was expressed under the control of the strong deinococcal *PgroESL* promoter on the binary *D. radiodurans/E. coli* shuttle vector, pRAD1 [81].

This chapter describes partial characterization of the S layer proteins of *D. radiodurans* and construction of fusion proteins involving Hpi protein and SLH domain with PhoN on one hand, and SmtA on the other. Further, the expression and localization of the various fusion proteins in the recombinant strain were also determined.

3.1 Isolation of Hpi protein from *Deinococcus* cells and its characterization by Peptide Mass Fingerprinting

A translucent pink membranous pellet was obtained on isolation of the Hpi protein by incubating *Deinococcus* cells in 2% lithium dodecyl sulphate at 4^{o}C under constant stirring followed by centrifugation. This preparation under an electron microscope appeared like a film **(Fig. 3.1)**. Attempts to further increase magnification for observing the hexagonal pattern of this film were not successful due to unavailability of an appropriate stain for enhancing contrast.

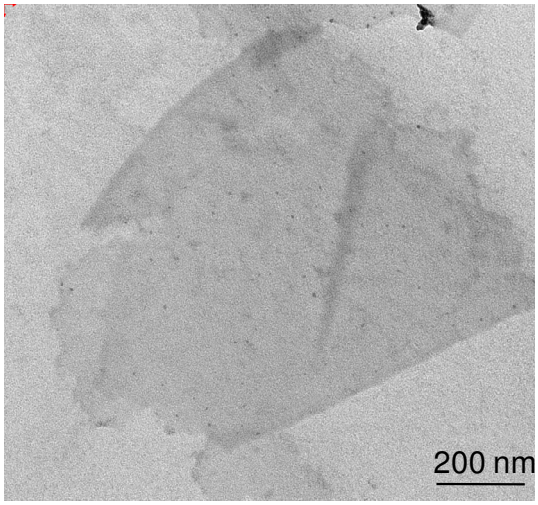

Fig. 3.1. TEM of the Hpi layer preparation from *D. radiodurans* cells.

On boiling this sample in Laemmli's cracking buffer [71], and subjecting the samples to electrophoresis by denaturing SDS-PAGE, around eight bands were visualized upon Coomassie Brilliant Blue (CBB) staining **(Fig. 3.2a)**. The Hpi protein is expected to be a 100 kDa protein but the preparation had one band of higher size of around 123 kDa and multiple bands of smaller sizes were also observed on the gel. This pattern has also been reported in previous literature **(Fig. 3.2b)** for the Hpi preparation [53,56] and the lower molecular weight

bands were said to be a result of *in vivo* proteolytic degradation of the Hpi layer by a membrane bound protease.

It has also been reported in literature that the higher molecular weight band corresponding to ~123 kDa is another protein associated with the Hpi layer which can be eliminated by treatment with 2% SDS at 60^{o}C [82]. When this treatment was carried out on the Hpi preparation, the 123 kDa band disappeared as shown in **Fig. 3.2c**. Therefore, this treatment was incorporated in the protocol to obtain a pure Hpi preparation.

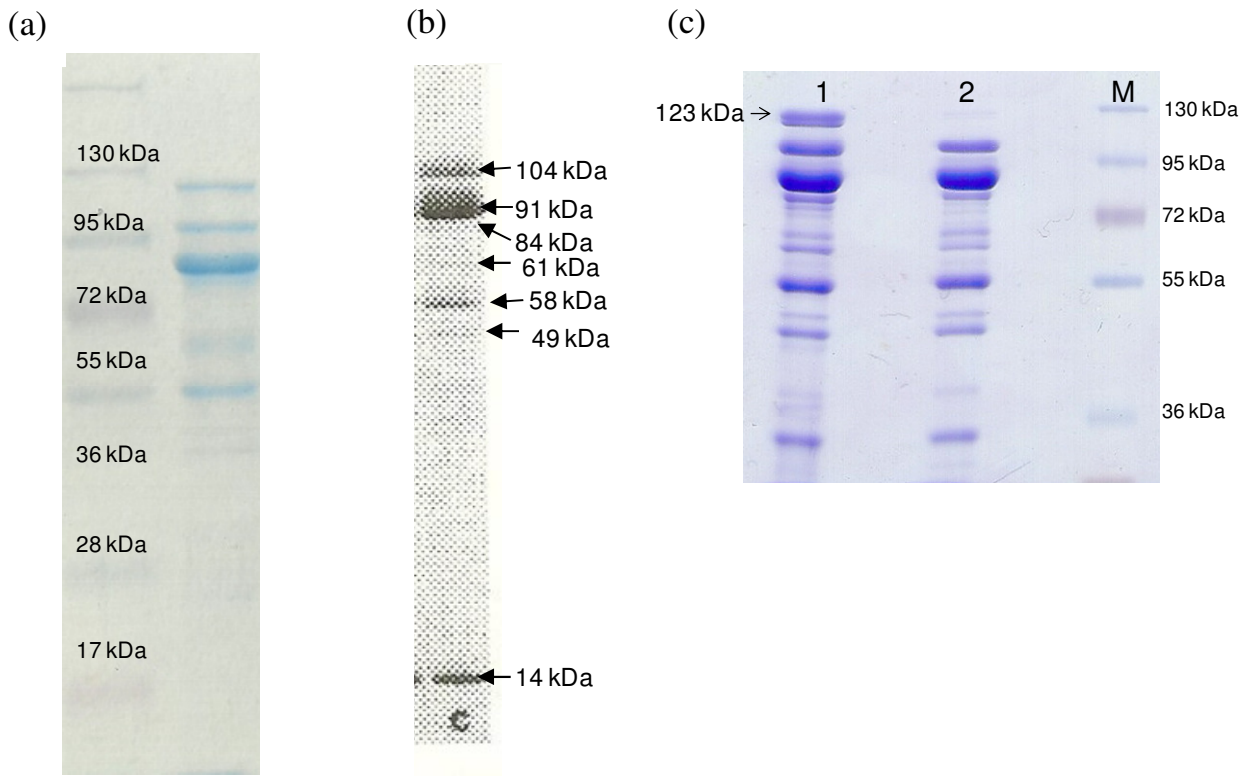

Fig. 3.2. Hpi protein of *D. radiodurans*. (a) Hpi protein was isolated from *Deinococcus radiodurans* cells, boiled in Laemmli's cracking buffer and 10 µg protein was resolved by 10% denaturing SDS-PAGE followed by staining with Coomassie Brilliant Blue (CBB). (b) Hpi degradation product bands and their masses as reported in literature [53]. (c) Hpi was treated with SDS at 60°C for 15 min and 30 µg of protein before (Lane 1) and after (Lane 2) treatment were resolved by 10% SDS-PAGE and stained with CBB. Protein extract were co-electrophoresed with molecular mass standards (Lane M).

(a)

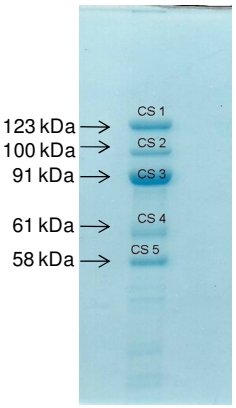

(b)

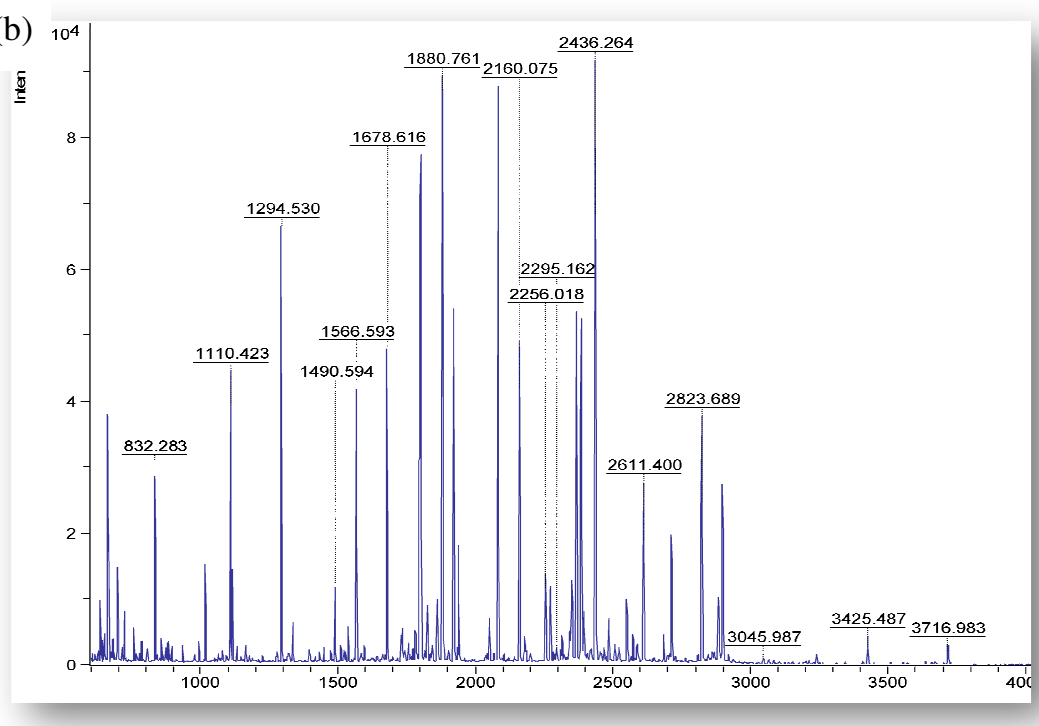

(c)

gi|15807560 **Mass:** 123769 **Score:** 158 **Expect:** 2.3e-09 **Matches:** 25

S-layer protein [Deinococcus radiodurans R1]

```
   1 MKKSLIALTT ALSFGLAAAQ TAAPVSAPQV PALTDVPAGH WAKDAIDRLV
  51 SRGVILGYPD GTFRGTQNLT RYEAAIIIAR LLDQMRDGET PAGMTAEDMT
 101 ALQNAIQELA ADLAALGVRV SDLEANAVSK DDFARLEARI EEVAAAGGEQ
 151 GATEALQGQI DDLTARVDEY DALRADVDDN ASSIAALNDL TVLLNQDILD
 201 LQDRVSAVEA AQADFVQRSD FDALGGRVTT VETRVETVNN SLTGRIAALE
 251 RNAFSVKPSL TIGYSVSRTS RNFDVDRLFP LNADGTVANN AFTSGGIDTD
 301 TGAQRRDFGD FGNASDPVVA GAAGLYGFAD GVSYTVYFTD GSTATFDGLN
 351 PADYKVPTGK VIDTTKGRNG FGFNNLARYK EGSTDIGISL GFDTSGQFSQ
 401 VTSGTGGSLF STAGRLQVNQ IDLNFGLVTG LPSDAYVDTN GNGKKDDGEA
 451 TGRGTYLGSG GTAAILRDPA GNVYRPVFFR FKNATTQFSV GNNPVIVTLG
 501 QQQKFYFSDY VFDNNYDGRG DGFTVTVDGS NVPVIGAWKP QIKGVYGSRS
 551 GLDGTAEAGY GVYYRGVRAQ ITPVGTLTAG IHYAQEGRDM FGAAQNTTST
 601 PSDVTTYGAD LHGKAFGVEL HSEYATSRVR PNTANAAVQT SNAFYARVAT
 651 RKDNLAFDLN TPAAKFGNDT FGVSLYDLNY RKIDAGYNNV AGISEYGYGS
 701 YSRTSAQNIA YNPDTGVTAP FANLDRQAYT DANNDGTSDR NADGTVVATN
 751 TKIGQMGFGV KAAANLGPVA IGGYYDTSTG ANGDNANRMT EAGGSAKVAY
 801 SIFSLRGTYN TLDSNRPQIY RDAAGTQIIG DAKVRRYAVQ ADVTPGLGLF
 851 VGAYYRDVNV NGVRSTTDRG LLGRGYLASS FEPGVGNNAY RTGLRCADNN
 901 FGTGTRDIDG VGGVLNPAVN LDQSRTATCF TSYGVEAGHA GDNANALVKD
 951 LFFRVGYSRV YVPTTATATT GDFSGSVTYG DARYDRKVGV ANVRLAGSFS
1001 TTNTQLDSRP AGTRGAVGLI VRTDPLENVP FRPQFNGQVG YYTADNRVAA
1051 GNYNANATKY GAGVVLNDFL LPQTKIGVRY DGYMAQNRQY TPFDGDGTQG
1101 YFSDANNNRR TNLNGVYVEG AYQDLIFSYG TYTLSQKDLN GVEYGSGINN
1151 GQPARGQTFK ISYKVNF
```

Fig. 3.3. Identififcation of 123 kDa CS1 band. (a) Coomassie Brilliant Blue stained gel showing bands obtained from a Hpi preparation which were processed for identification by MALDI-TOF-MS. (b) Peptide mass spectrum of protein of 123 kDa, marked CS1 and (c) corresponding MASCOT search results and peptide coverage.

Bands of apparent molecular mass, 123 kDa, 100 kDa, 90 kDa, 61 kDa and 58 kDa, seen after SDS-PAGE **(Fig. 3.3a)** were excised from the gel, subjected to trypsin digestion and processed for identification using Matrix Assisted Laser Desorption /Ionization – Time of Flight – Mass Spectrometer (MALDI-TOF-MS) based peptide mass fingerprinting. Results from the analysis showed that the band CS1 **(Fig. 3.3b & c)** was the protein encoded by DR2577, which is in fact annotated as SlpA, another S layer protein from *D. radiodurans* which typically always co-elutes with the Hpi layer. CS2 which appeared at 100 kDa was indeed identified as Hpi protein **(Fig. 3.4)**. The bands CS3, CS4 and CS5 were also identified as Hpi polypeptide, thereby confirming that these were all degradation products of the Hpi protein **(Fig. 3.5, 3.6 & 3.7)**. The degradation products of Hpi protein yielded low scores for identity as can be expected due to the molecular weight mis-match. The sequence coverage data were not sufficient to conclude if the degradation products were N-terminal or C-terminal fragments. The band CS5 however, showed peptide coverage mostly in the middle of the sequence away from the two termini **(Fig. 3.7)**.

(a)

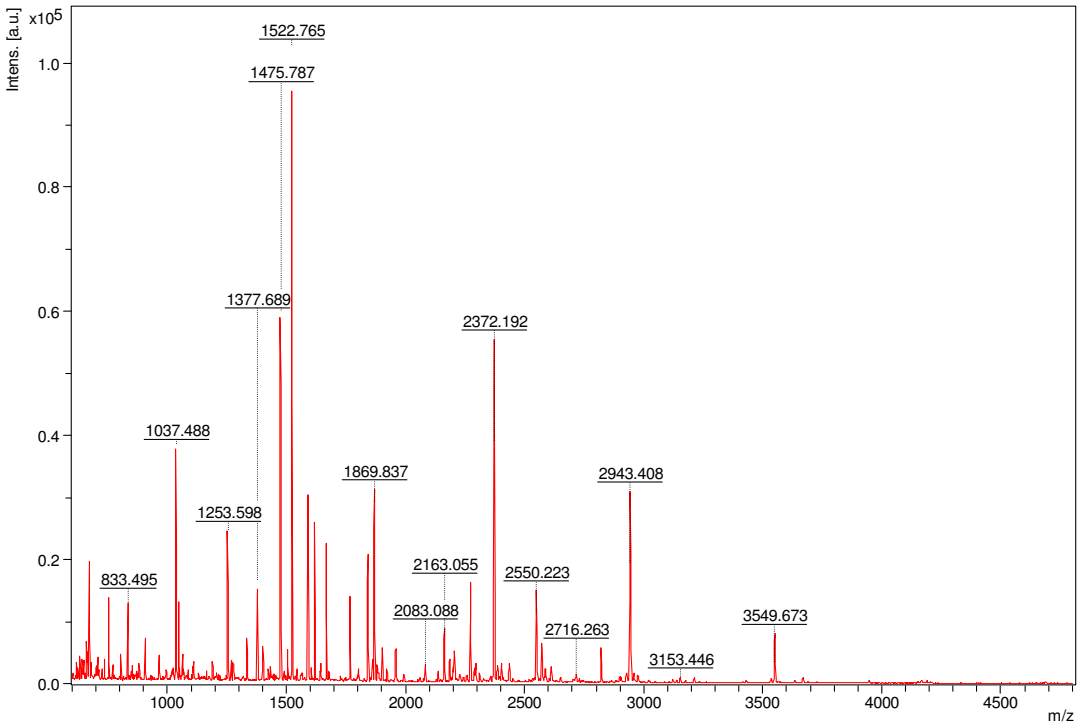

1. gi|15807493 **Mass:** 99694 **Score:** 185 **Expect:** 4.5e-12 **Matches:** 29
hexagonally packed intermediate-layer surface protein [Deinococcus radiodurans R1]

```
  1 MKKNIALMAL TGILTLASCG QNGTGTTPTA DACATANTCS VTVNISGVSS
 51 ADFDVTMDGK TTSMTLSNGQ KLPVAKTGTV TLTPKAKDGY TTPAAQSTTI
101 SSTNLTPSVN FAYTTVPSTG NGNGNGGTTP TQPFTLNITS PTNGAAATTG
151 TPIRVVFTSS VALSSATCKI GNSAAVNAQV SSTGGYCDVT PTTAGGGLIT
201 VTGTANGQTV SSTVTVDVKA PVVDNRYGTV TPAGDQELTL TNEGIVKDAD
251 NGWRRLGQGV STPSDPNGNV DIYVKGTVNF SVNAAAGSKV EVFLARTTGS
301 DVPTNDDVQA GDVLRSVAST SGTETFSLDS RRLAEFDGVR KWIVVRINGT
351 QVTYQPVIAD NKGPQQPDPE LNGVQNAYSN ILNNYNNSGL TYVRGDVNVF
401 TGNPSLQDRE FGQAPLGSSF VQRRPSGFES IRYYLVPETA FGNKALQESD
451 EMLRAKAIKS VATVVSAPVL EPGTVKATSF SRVIGSGATS TVTPKAQDNV
501 TYRVYAISRD QLGNETASAT YELVRFDNVG PTITGSVIRD TSDLPFASQE
551 PERCLSDIAT ITLGGITDNA GGVGLNPGQG LTFTLGGRQI QAGQFDTNQL
601 ADGEYTIGFN SLTDALGNPV VSAPTNAKVY IDNTDPTVNF NRAVMQGTFA
651 SGERVSVESD ASDGGCGVYE TRLFWDTDNG VVDDATTTPA IGHPVQFARQ
701 RVTDGAKADS LNAGWNALQL PNGAGAVYLR ALVVDRAGNA TISTTPIVVN
751 AKITNQARPL LGGFDAFKRN ASAQFMSNSN AISGVNGTAV TPNTTANSAL
801 DNILSLDSVG TLTTNAYLPR GATETAITEK IRNVGAYGRF DATQWNRIRD
851 YQLNTDPTLR SAYVNAGNLA NQRGNNWRIR TPWVELGSSD TANTQQKFDF
901 NSDLLNDFYF GRTFGNNDNV NLFSYDQFNG IVSGTAGAYS FYGETVQK
```

Fig. 3.4. Identification of 100 kDa CS2 band. (a) Peptide mass spectrum of 100 kDa band CS2 shown in Fig. 3.3a, (b) its corresponding MASCOT search result and peptide coverage.

gi|15807493 **Mass:** 99694 **Score:** 151 **Expect:** 1.1e-08 **Matches:** 27
hexagonally packed intermediate-layer surface protein [Deinococcus radiodurans R1]

```
  1 MKKNIALMAL TGILTLASCG QNGTGTTPTA DACATANTCS VTVNISGVSS
 51 ADFDVTMDGK TTSMTLSNGQ KLPVAKTGTV TLTPKAKDGY TTPAAQSTTI
101 SSTNLTPSVN FAYTTVPSTG NGNGNGGTTP TQPFTLNITS PTNGAAATTG
151 TPIRVVFTSS VALSSATCKI GNSAAVNAQV SSTGGYCDVT PTTAGGGLIT
201 VTGTANGQTV SSTVTVDVKA PVVDNRYGTV TPAGDQELTL TNEGIVKDAD
251 NGWRRLGQGV STPSDPNGNV DIYVKGTVNF SVNAAAGSKV EVFLARTTGS
301 DVPTNDDVQA GDVLRSVAST SGTETFSLDS RRLAEFDGVR KWIVVRINGT
351 QVTYQPVIAD NKGPQQPDPE LNGVQNAYSN ILNNYNNSGL TYVRGDVNVF
401 TGNPSLQDRE FGQAPLGSSF VQRRPSGFES IRYYLVPETA FGNKALQESD
451 EMLRAKAIKS VATVVSAPVL EPGTVKATSF SRVIGSGATS TVTPKAQDNV
501 TYRVYAISRD QLGNETASAT YELVRFDNVG PTITGSVIRD TSDLPFASQE
551 PERCLSDIAT ITLGGITDNA GGVGLNPGQG LTFTLGGRQI QAGQFDTNQL
601 ADGEYTIGFN SLTDALGNPV VSAPTNAKVY IDNTDPTVNF NRAVMQGTFA
651 SGERVSVESD ASDGGCGVYE TRLFWDTDNG VVDDATTTPA IGHPVQFARQ
701 RVTDGAKADS LNAGWNALQL PNGAGAVYLR ALVVDRAGNA TISTTPIVVN
751 AKITNQARPL LGGFDAFKRN ASAQFMSNSN AISGVNGTAV TPNTTANSAL
801 DNILSLDSVG TLTTNAYLPR GATETAITEK IRNVGAYGRF DATQWNRIRD
851 YQLNTDPTLR SAYVNAGNLA NQRGNNWRIR TPWVELGSSD TANTQQKFDF
901 NSDLLNDFYF GRTFGNNDNV NLFSYDQFNG IVSGTAGAYS FYGETVQK
```

Fig. 3.5. MASCOT search results for mass spectra of 91 kDa band, CS3 shown in Fig. 3.3a and its peptide coverage.

2. gi|15807493 **Mass:** 99694 **Score:** 81 **Expect:** 0.11 **Matches:** 22

hexagonally packed intermediate-layer surface protein [Deinococcus radiodurans R1]

```
  1 MKKNIALMAL TGILTLASCG QNGTGTTPTA DACATANTCS VTVNISGVSS
 51 ADFDVTMDGK TTSMTLSNGQ KLPVAKTGTV TLTPKAKDGY TTPAAQSTTI
101 SSTNLTPSVN FAYTTVPSTG NGNGNGGTTP TQPFTLNITS PTNGAAATTG
151 TPIRVVFTSS VALSSATCKI GNSAAVNAQV SSTGGYCDVT PTTAGGGLIT
201 VTGTANGQTV SSTVTVDVKA PVVDNRYGTV TPAGDQELTL TNEGIVKDAD
251 NGWRRLGQGV STPSDPNGNV DIYVKGTVNF SVNAAAGSKV EVFLARTTGS
301 DVPTNDDVQA GDVLRSVAST SGTETFSLDS RRLAEFDGVR KWIVVRINGT
351 QVTYQPVIAD NKGPQQPDPE LNGVQNAYSN ILNNYNNSGL TYVRGDVNVF
401 TGNPSLQDRE FGQAPLGSSF VQRRPSGFES IRYYLVPETA FGNKALQESD
451 EMLRAKAIKS VATVVSAPVL EPGTVKATSF SRVIGSGATS TVTPKAQDNV
501 TYRVYAISRD QLGNETASAT YELVRFDNVG PTITGSVIRD TSDLPFASQE
551 PERCLSDIAT ITLGGITDNA GGVGLNPGQG LTFTLGGRQI QAGQFDTNQL
601 ADGEYTIGFN SLTDALGNPV VSAPTNAKVY IDNTDPTVNF NRAVMQGTFA
651 SGERVSVESD ASDGGCGVYE TRLFWDTDNG VVDDATTTPA IGHPVQFARQ
701 RVTDGAKADS LNAGWNALQL PNGAGAVYLR ALVVDRAGNA TISTTPIVVN
751 AKITNQARPL LGGFDAFKRN ASAQFMSNSN AISGVNGTAV TPNTTANSAL
801 DNILSLDSVG TLTTNAYLPR GATETAITEK IRNVGAYGRF DATQWNRIRD
851 YQLNTDPTLR SAYVNAGNLA NQRGNNWRIR TPWVELGSSD TANTQQKFDF
901 NSDLLNDFYF GRTFGNNDNV NLFSYDQFNG IVSGTAGAYS FYGETVQK
```

Fig. 3.6. MASCOT search results for mass spectra of 61 kDa band CS4 shown in Fig. 3.3a and its peptide coverage.

1. gi|15807493 **Mass:** 99694 **Score:** 113 **Expect:** 7.2e-05 **Matches:** 18
hexagonally packed intermediate-layer surface protein [Deinococcus radiodurans R1]

```
  1 MKKNIALMAL TGILTLASCG QNGTGTTPTA DACATANTCS VTVNISGVSS
 51 ADFDVTMDGK TTSMTLSNGQ KLPVAKTGTV TLTPKAKDGY TTPAAQSTTI
101 SSTNLTPSVN FAYTTVPSTG NGNGNGGTTP TQPFTLNITS PTNGAAATTG
151 TPIRVVFTSS VALSSATCKI GNSAAVNAQV SSTGGYCDVT PTTAGGGLIT
201 VTGTANGQTV SSTVTVDVKA PVVDNRYGTV TPAGDQELTL TNEGIVKDAD
251 NGWRRLGQGV STPSDPNGNV DIYVKGTVNF SVNAAAGSKV EVFLARTTGS
301 DVPTNDDVQA GDVLRSVAST SGTETFSLDS RRLAEFDGVR KWIVVRINGT
351 QVTYQPVIAD NKGPQQPDPE LNGVQNAYSN ILNNYNNSGL TYVRGDVNVF
401 TGNPSLQDRE FGQAPLGSSF VQRRPSGFES IRYYLVPETA FGNKALQESD
451 EMLRAKAIKS VATVVSAPVL EPGTVKATSF SRVIGSGATS TVTPKAQDNV
501 TYRVYAISRD QLGNETASAT YELVRFDNVG PTITGSVIRD TSDLPFASQE
551 PERCLSDIAT ITLGGITDNA GGVGLNPGQG LTFTLGGRQI QAGQFDTNQL
601 ADGEYTIGFN SLTDALGNPV VSAPTNAKVY IDNTDPTVNF NRAVMQGTFA
651 SGERVSVESD ASDGGCGVYE TRLFWDTDNG VVDDATTTPA IGHPVQFARQ
701 RVTDGAKADS LNAGWNALQL PNGAGAVYLR ALVVDRAGNA TISTTPIVVN
751 AKITNQARPL LGGFDAFKRN ASAQFMSNSN AISGVNGTAV TPNTTANSAL
801 DNILSLDSVG TLTTNAYLPR GATETAITEK IRNVGAYGRF DATQWNRIRD
851 YQLNTDPTLR SAYVNAGNLA NQRGNNWRIR TPWVELGSSD TANTQQKFDF
901 NSDLLNDFYF GRTFGNNDNV NLFSYDQFNG IVSGTAGAYS FYGETVQK
```

Fig. 3.7. MASCOT search results for mass spectra of 58 kDa band CS5 shown in Fig. 3.39a and its peptide coverage.

Attempts at over-expressing Hpi protein in *E. coli* were unsuccessful perhaps because the Deinococcal protein could not localize to the *E. coli* membrane. Therefore, Hpi layer was isolated from *D. radiodurans* cells and used for raising antibodies. Bands corresponding to CS2 and CS3 **(Fig. 3.3)** were excised and directly submitted for raising antibodies in rabbit since they could not be easily eluted from the gel. Such antibodies were tested using wild type *Deinococcus* cells and mutant cells lacking the Hpi protein, HMR202. Immunodetection revealed bands of molecular weight 100 kDa, 91 kDa and 61 kDa in wild type cells, while no

band appeared in mutant cells **(Fig. 3.8)**, thus confirming the efficacy of the antibody and the absence of the Hpi protein in mutant cells.

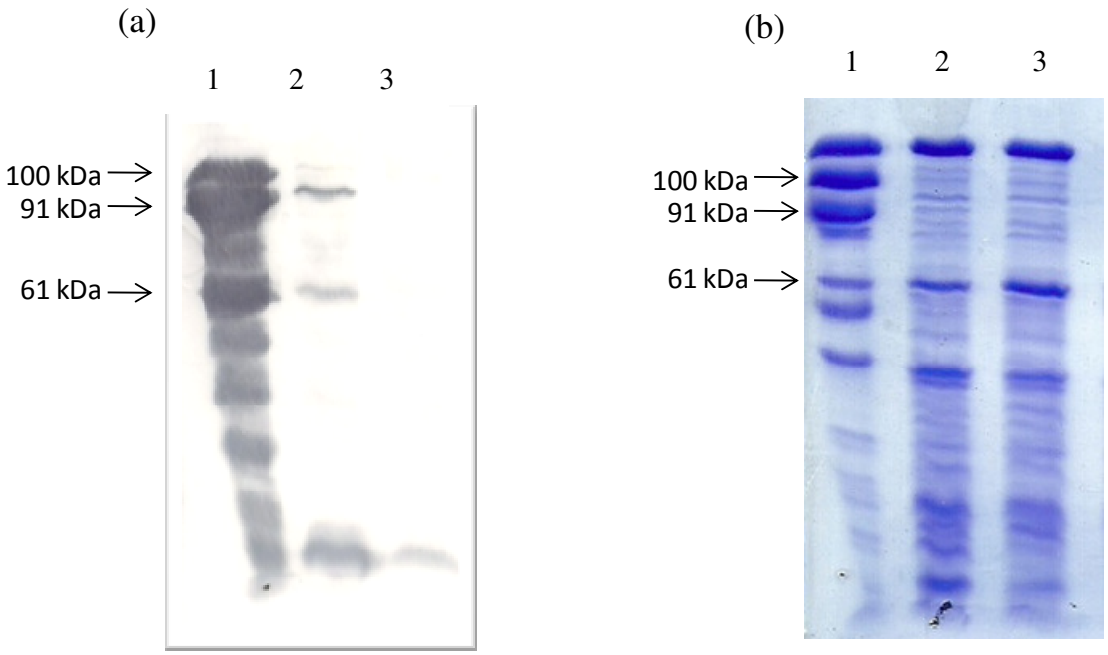

Fig. 3.8. Detection of the Hpi protein by Western Blotting and Immunodetection. About 30 µg each of the Hpi protein isolated from *D. radiodurans* cells (Lane 1) and whole cell extracts from wild type (Lane 2) or Hpi mutant *D. radiodurans* cells (Lane 3) were resolved by 10% SDS-PAGE. The proteins were electroblotted on nitrocellulose membrane. Hpi protein was immunodetected with anti-Hpi serum at 1:1000 dilution, followed by alkaline phosphatase conjugated anti-rabbit IgG. The blot was developed using NBT (nitro-blue tetrazolium chloride) - BCIP (5-bromo-4-chloro-3'-indolyphosphate p-toluidine salt) as substrate. The electroblot after immuno-detection with anti-Hpi (a) and the corresponding gel after CBB staining (b) are shown.

3.2 Cloning, over-expression and localization of SmtA, Hpi-SmtA and SLH-SmtA proteins in recombinant bacteria

The *smtA* gene from *Synechococcus elongatus* codes for a 6 kDa metal binding peptide, metallothionein (MT). The entire gene was cloned as such or as a fusion gene with Deinococcal *hpi* ORF, or with the nucleotide sequence coding for the SLH domain of SlpA in *D. radiodurans*. All constructs were expressed from the deinococcal *PgroESL* promoter.

3.2.1 Cloning of *smtA* gene

In order to clone *smtA* gene downstream to *PgroESL* in pRAD1 **(Table 2.3),** an earlier construct harbouring the *smtA* ORF in pET16b, pS1 was utilized. Primers Smt-f and Smt-r **(Table 2.2)** were used to PCR amplify the *smtA* gene from pS1 as a 176 bp DNA fragment as shown in **Fig. 3.9**. The plasmid pPN1 (Table 2.3) carrying *phoN* gene downstream of the *groESL* promoter was digested with NdeI and BamHI to release the *phoN* ORF. The PCR amplified *smtA* ORF was restriction digested with NdeI and BamHI and ligated to identical sites in the cut pPN1 plasmid, downstream to the *PgroESL* promoter to obtain the plasmid, pPS1 **(Fig. 3.9)**. *E. coli* strain JM109 was transformed with the plasmid and Ap^r transformants selected.

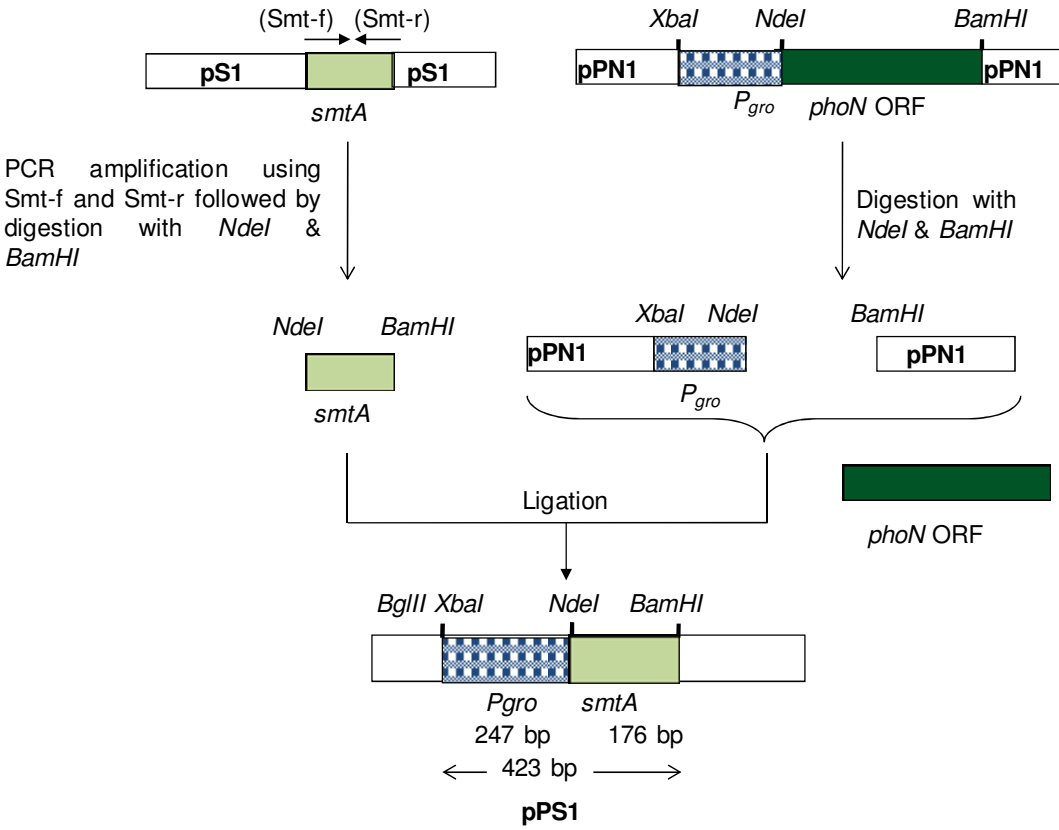

Fig 3.9. Construction and cloning of pPS1. The *smtA* ORF was PCR amplified from an earlier construct pS1 using primers, Smt-f and Smt-r. The 176 bp fragment was restriction digested with NdeI and BamHI. The pPN1 plasmid was prepared by digestion with NdeI and BamHI and ligated to the cut *smtA* ORF to generate plasmid, pPS1.

Colony PCR of putative transformants using primers Smt-f and the pRAD1 vector specific primer, P6 was conducted. A typical result is shown in **Fig. 3.10a,** wherein a 234 bp DNA fragment was obtained, constituting the 176 bp *smtA* ORF along with ~58 bases of the downstream vector sequence. Restriction digestion to confirm correctness of construct is shown in **Fig. 3.10b**. Digestion of the pPS1 plasmid with XbaI-BamHI released a 423 bp *Pgro-smtA* fragment while with BglII (for which a recognition site was present upstream of the XbaI site), and BamHI, a fragment of 463 bp was released as expected. The construct was

also confirmed by DNA sequencing. The plasmid was transformed into *D. radiodurans* cells and the transformants were confirmed by Cm^r and colony PCR.

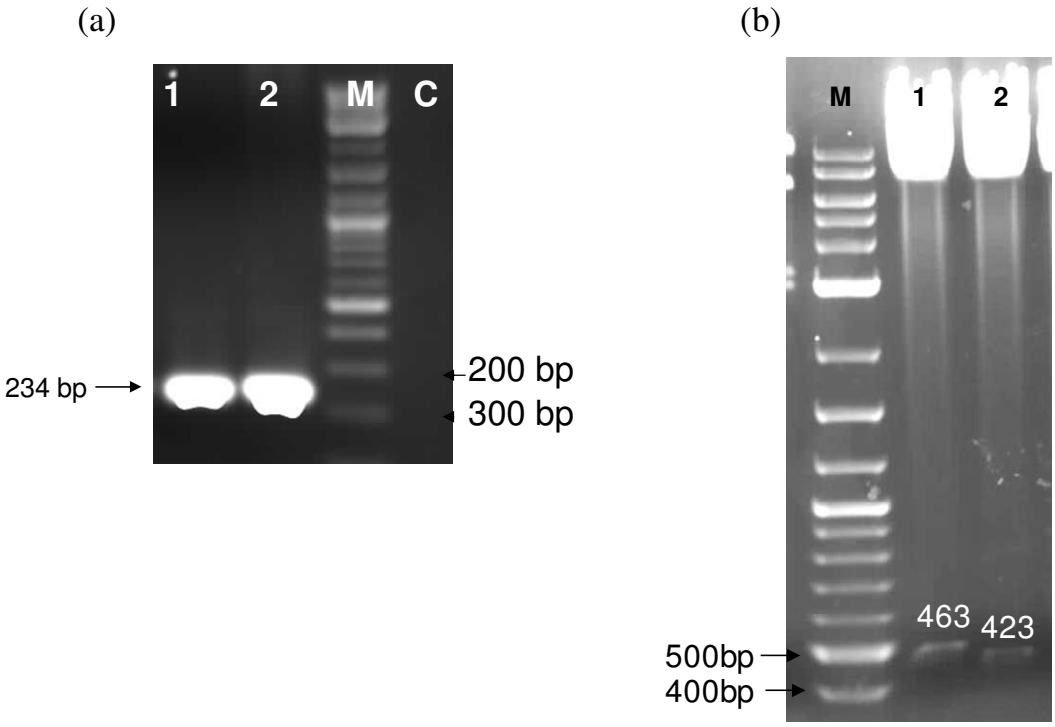

Fig. 3.10. Cloning and confirmation of pPS1. Agarose gel electrophoresis of DNA fragments. (a) Lanes 1 and 2 display products obtained on carrying out colony PCR of two pPS1 transformants with primers, Smt-f and P6. A negative control, pRAD1 (Lane C) was also included in the colony PCR to rule out non-specific products. (b) Restriction digestion of the pPS1 plasmid isolated from one of the transformants tested positive by colony PCR, with BglII - BamHI (Lane 1) or XbaI - BamHI (Lane 2). Lane M contains the 0.1-10 kb DNA ladder.

3.2.2 Cloning of the *hpi-smtA* fusion gene

In order to obtain the *hpi-smtA* fusion, an earlier construct made in the lab, pGDRF4 **(Table 2.3)** was used. This plasmid contains the *smtA* gene, fused to the signal peptide encoding

sequence of the FliY protein in *D. radiodurans* and both cloned downstream to the *PgroESL* in pRAD1 vector **(Table 2.3).** The *hpi* ORF was PCR amplified from *D. radiodurans* genome using primers, Cd-gro and Cd-r **(Table 2.2)** as a 2.8 kb DNA fragment. The pGRDF4 plasmid was restriction digested with XbaI and NdeI to release the sequence coding for the FliY signal peptide. The PCR amplified *hpi* ORF was digested with XbaI and NdeI and ligated to the identical sites in the restriction digested pGDRF4 plasmid between the *PgroESL* and *smtA* ORF. This new construct was named pPHS1 as shown in **Fig. 3.11** and was used to transform *E. coli* JM109 cells.

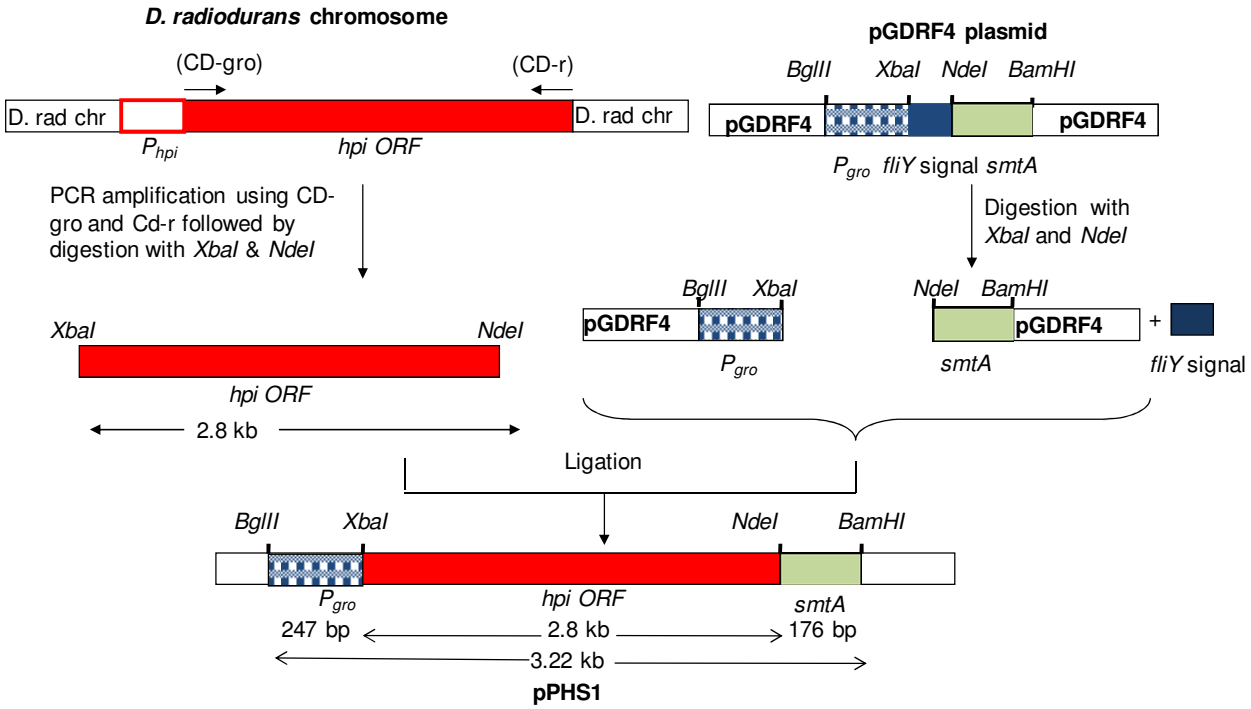

Fig 3.11. Construction and cloning of pPHS1. The *smtA* ORF was PCR amplified from deinococcal chromosome using primers, CD-gro and CD-r. The 2.8 kb fragment was restriction digested with XbaI and NdeI. The pGDRF4 plasmid was prepared by restriction digested with XbaI and NdeI and ligated to the XbaI/NdeI digested *hpi* ORF to generate plasmid, pPHS1.

Colony PCR of Ap^r positive transformants using CD-gro and vector specific primer P6 (**Table 2.2**), yielded a band of ~3.09 kb which consists of the *hpi* ORF (2.8 kb), the *smtA* ORF (176 bp) as well as some of the vector sequence in PCR positive transformants (**Fig. 3.12a**). Restriction digestion of pPHS1 using various enzyme combinations further confirmed correctness of the construct. XbaI-NdeI double digestion released the 2.8 kb *hpi* ORF. BglII-BamHI released two bands due to incomplete digestion and presence of an additional internal BamHI site in the *hpi* ORF, one for the *hpi-smtA* ORF fusion and one for the *PgroESL-hpi-smtA* construct of 3.2 kb size (**Fig. 3.12b**). Partial DNA sequencing was carried out to further confirm the correctness of the sequence. The plasmid was transformed into *D. radiodurans* cells and the Cm^r transformants were again confirmed by colony PCR.

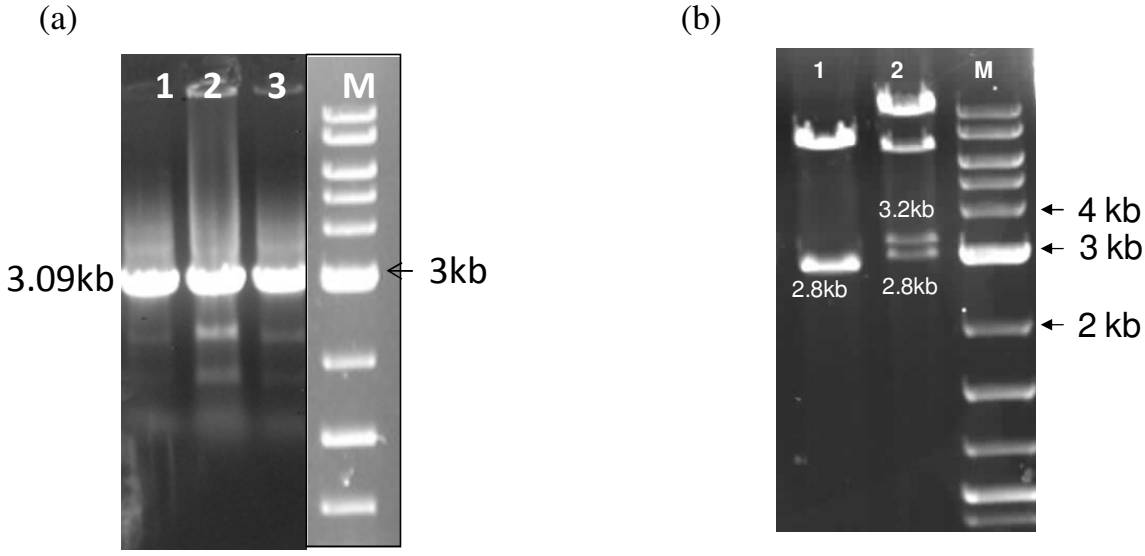

Fig. 3.12. Cloning and confirmation of pPHS1. Agarose gel electrophoresis of DNA fragments. (a) Lanes 1 to 3 display products obtained on carrying out colony PCR of six transformants with primers, CD-gro and P6. (b) Restriction digestion of the plasmid isolated from one of the transformants tested positive by colony PCR, with XbaI-NdeI (Lane 1) and BglII-BamHI (Lane 2). Lane M contains the 1 kb DNA ladder.

3.2.3 Cloning of the *SLH-smtA* fusion gene

The region of the DR_2577 ORF of *D. radiodurans* constituting the SLH domain was determined by the conserved sequence generated in literature by aligning sequences across 557 proteins [83] **(Fig. 3.13 a)**.

(a)

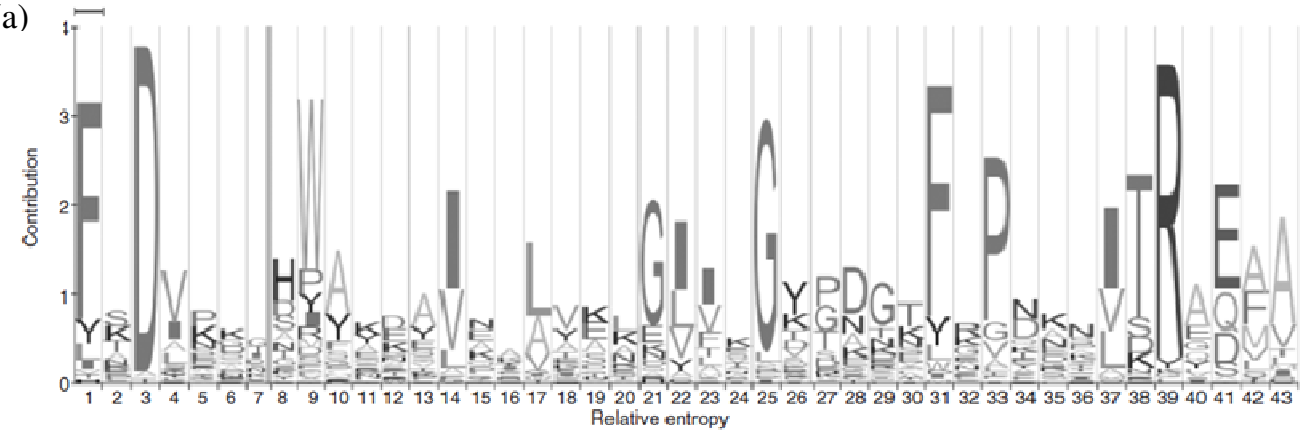

(b)

```
DR_2577                          MKKSLIALTTALSFGLAAAQTAAPVSAPQVPALTDVPAGHWAKDAIDRLV
NTL03TT1893_ T.thermophilus HB   MKKRLVTLLAGLLTVLSMG--------FGLAQFSDVPAGHWAKEAVEALA
                                 *** *::* :.*   *: .          :. ::*********:*:: *.

DR_2577                          SRGVILGYPDGTFRGTQNLTRYEAAIIIARLLDQMRDGETPAG-------
NTL03TT1893_ T.thermophilus HB   AKGIILGFPDGTFRGNENLTRYQAALLIYRLLQQIEEELKTQGTSPTMEA
                                 ::*:***:*******.:*****:**::* ***:*:.:  .. *

DR_2577                          MTAEDMTALQNAIQELAADLAALGVRVSDLEANAVSKDDFARLEARIEEV
NTL03TT1893_ T.thermophilus HB   LAPEDLEALKNAVQELAAELASLGVRVSALEDSAATKEDIARLEAMIAEL
                                 ::.**: **:**:*****:**:****** ** .*.:*:*:***** * *:

DR_2577                          AAAGGEQGATEALQGQIDDLTARVDEYDALRADVDDNASSIAALNDLTVL
NTL03TT1893_ T.thermophilus HB   KAQPMPE---------------------------------------PGM
                                  *    :                                        . :

DR_2577                          LNQDILDLQDRVSAVEAAQADFVQRSDFDALGGRVTTVETRVETVNNSLT
NTL03TT1893_ T.thermophilus HB   DQAALKDLMDRVEAASIAADTALAQA--QQLAERLDALAQDVEGVKGDLA
                                  :  : ** ***.*.. *    : ::  : *. *: ::   ** *:..*:
```

Fig 3.13. Identification of the SLH domain in DR_2577 ORF. (a) SLH alignment shown in the HMM-Logos format reproduced from Desvaux et al. 2006. (b) Amino acid sequence alignment of the SlpA protein from *Thermus thermophilus* with protein coded by DR_2577 using web based ClustalW software. The conserved residues for the SLH domain are highlighted. The nucleotide sequence shown in red was cloned to generate SLH fusion proteins

In addition, the homology between the SlpA protein and DR_2577 was determined using the Clustal W web-based software. The alignment of the sequences showed good homology from 35th amino acid of the deinococcal SlpA protein till 150 amino acids from the N terminal region. In this region, however, the signature homology sequence (**Fig. 3.13b)** extended between 36 and 99 amino acids of the SlpA protein. The conserved residues are highlighted in grey **(Fig. 3.13b)**. Therefore the sequence coding for the first 99 amino acids of the SlpA protein inclusive of its signal peptide was used to construct fusion proteins [83].

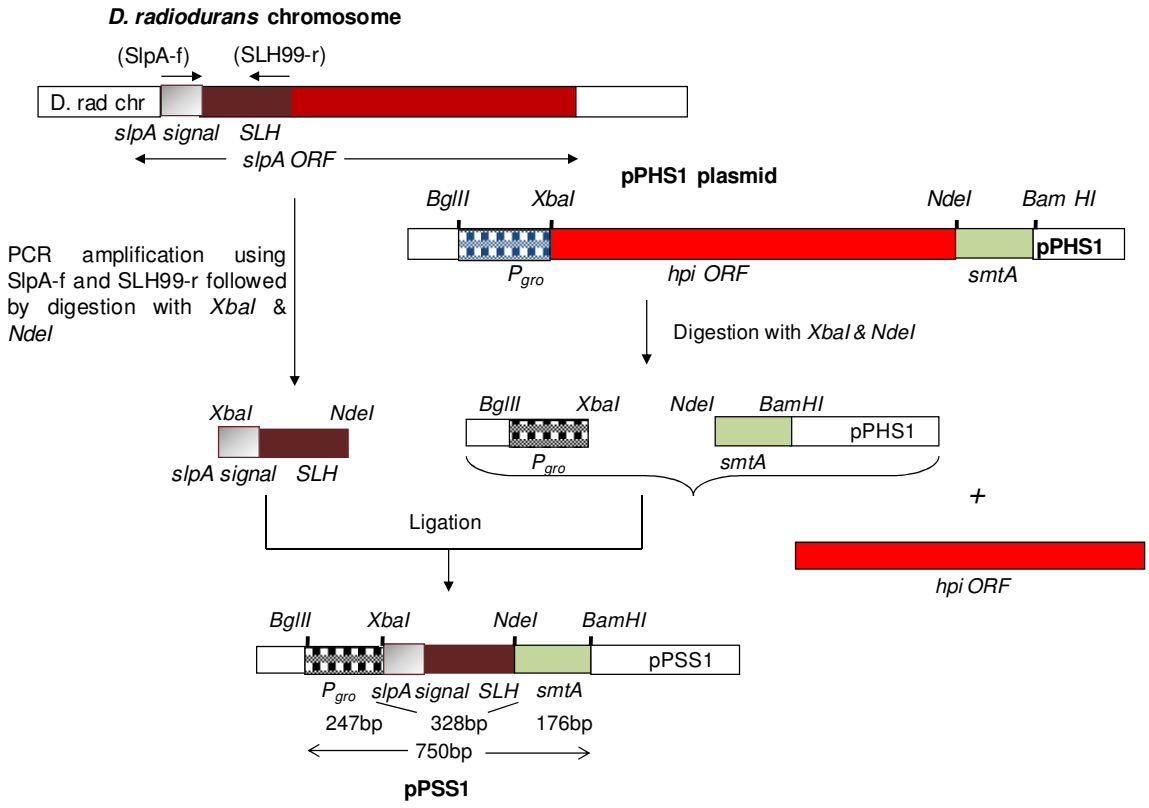

Fig. 3.14. **Construction and cloning of pPSS1.** The sequence coding for the signal peptide and SLH domain of the SlpA protein was PCR amplified from deinococcal chromosome using primers, SlpA-f and SLH99-r. The 328 bp fragment was restriction digested with XbaI and NdeI. The pPHS1 plasmid was restriction digested with XbaI and NdeI and ligated to the cut *smtA* ORF to generate plasmid, pPSS1.

The sequence encoding the SlpA signal peptide along with the SLH domain of SlpA protein was PCR amplified from deinococcal chromosomal DNA using primers SlpA-f and SLH-99r **(Table 2.2)** as a 328 bp DNA fragment. An earlier construct, pPHS1, described above, (**Fig. 3.11**) which carried the *smtA* gene fused to *hpi* was digested with XbaI and NdeI to release the *hpi* ORF. The PCR product constituting the sequence encoding SLH domain was restriction digested with XbaI and NdeI and ligated to the restriction digested pPHS1 plasmid at identical sites, downstream to the *PgroESL* promoter to obtain the plasmid pPSS1 (**Fig. 3.14).** *E. coli* JM109 cells were transformed with pPSS1 plasmid. Colony PCR of Ap^r positive tranformants using SlpA-f and Smt-r **(Table 2.2)** primers yielded a 504 bp fragment constituting the sequence encoding the SLH domain (328 bp) along with the *smtA* ORF (176 bp) (**Fig. 3.15a**).

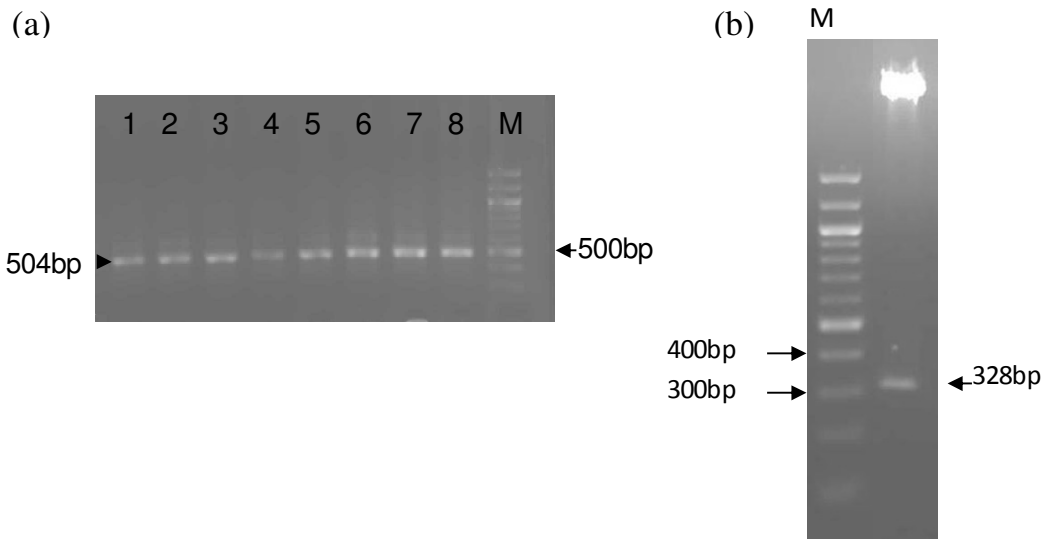

Fig. 3.15. Cloning and confirmation of pPSS1. Agarose gel electrophoresis of DNA fragments to confirm construction of pPSS1. (a) Lanes 1 to 8 display products obtained on carrying out colony PCR of nine Ap^r transformants with primers, SlpA-f and Smt-r. (b) Restriction digestion of the plasmid isolated from one of the Ap^r transformants tested positive by colony PCR, with XbaI-NdeI. Lane M contains the 100 bp DNA ladder.

Restriction digestion of the pPSS1 to confirm correctness of construct, using the enzymes XbaI and NdeI resulted in a 328 bp fragment coding for the SLH domain being released from a positive transformant (**Fig. 3.15b**). Correctness of the construct was further confirmed by DNA sequencing. The plasmid was transformed into *D. radiodurans* cells and the Cm^r transformants were confirmed by colony PCR.

3.2.4 Cloning of the *hpi* gene downstream of *PgroESL* promoter

Cloning of the *hpi* gene downstream of the *PgroESL* promoter was carried out in two steps. In the first step, primers, DG-f and Gro-r **(Table 2.2)** were used to PCR amplify *PgroESL* from deinococcal chromosomal DNA to obtain a DNA fragment of 247 bp. The *PgroESL* fragment was restriction digested with BglII and XbaI and ligated to pRAD1 plasmid **(Table 2.3)** digested with similar enzymes, to generate the pG1 plasmid (**Fig. 3.16**). In the next step, CD-gro and Hpinx-r **(Table 2.2)** were used to PCR amplify the *hpi* ORF to yield a 2.8 kb DNA fragment which was restriction digested with XbaI-NdeI. The pPG1 plasmid was restriction digested with XbaI-NdeI and ligated to the similarly digested *hpi* ORF, to generate the plasmid pPH1. *E. coli* JM109 cells were transformed with pPH1 (**Fig. 3.16**). Positive Ap^r transformants were selected by colony PCR using Hpi5f **(Table 2.2)** (which is an internal primer that binds 210 bases upstream of the stop codon of *hpi* ORF) and a vector specific primer P6 (which binds 170 bp downstream of the NdeI site in pRAD1 vector). As, expected a PCR product of 380 bp was obtained in Ap^r positive transformants (**Fig. 3.17**). Correctness of the construct was further confirmed by restriction digestion of plasmid pPH1 from transformants and partial DNA sequencing. The plasmid was transformed into *D. radiodurans* cells and the Cm^r transformants were confirmed by colony PCR.

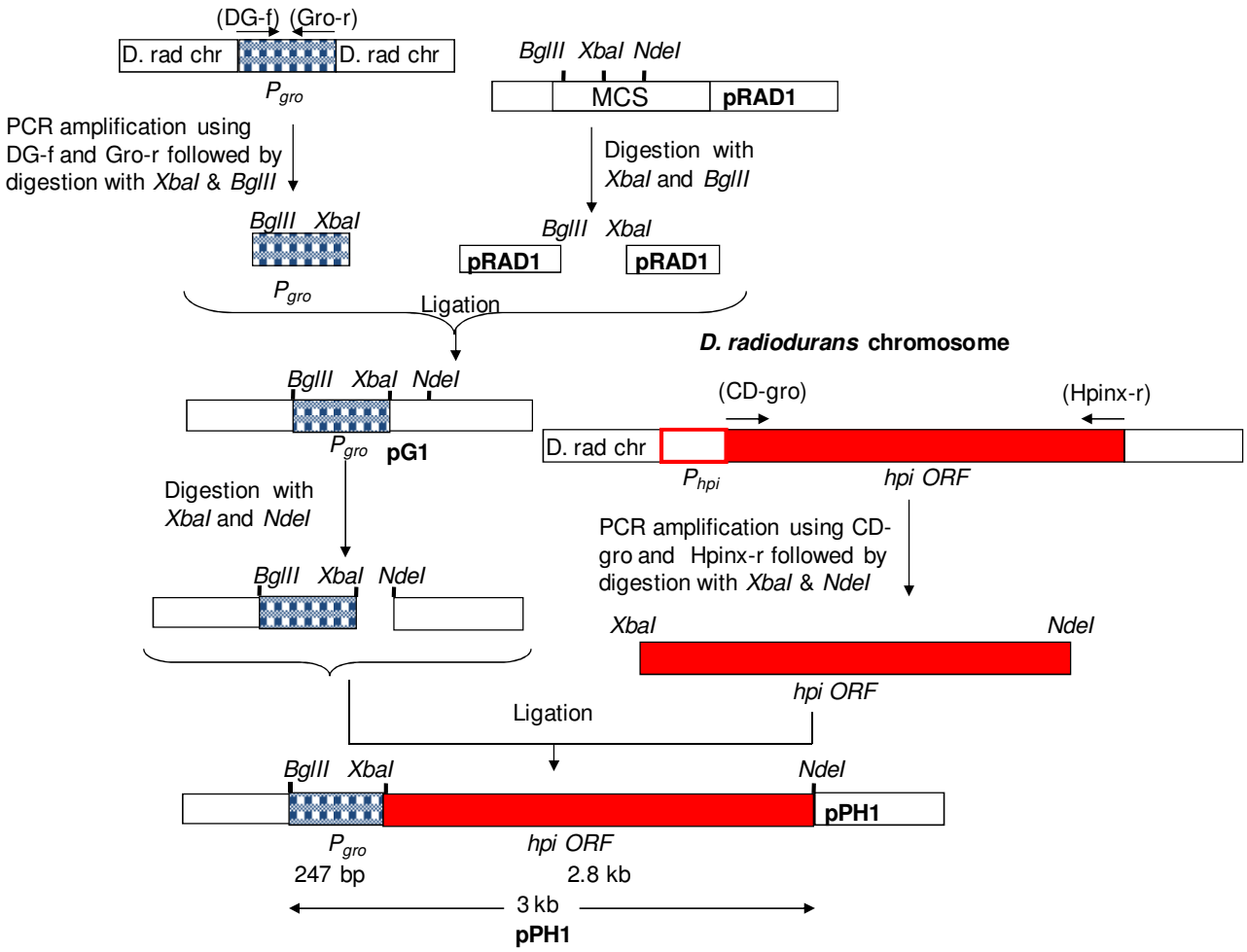

Fig. 3.16. Construction and cloning of pPH1. The *groESL* promoter was PCR amplified using primers DG-f and Gro-r and cloned as a 247 bp fragment into the BglII-NdeI sites of pRAD1 plasmid to generate plasmid pG1. The *hpi* ORF was PCR amplified from deinococcal chromosome using primers, CD-gro and Hpinx-r. The 2.8 kb fragment was restriction digested with XbaI and NdeI and cloned downstream of the *PgroESL* promoter to generate plasmid, pPH1.

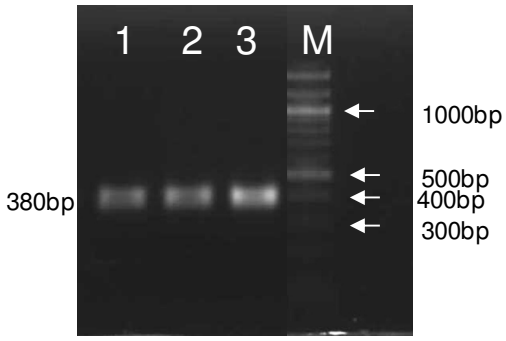

Fig. 3.17. Cloning and confirmation of pPH1. Agarose gel electrophoresis of DNA fragments to confirm construction of pPH1. Lanes 1 to 3 display products obtained on carrying out colony PCR of three Ap^r transformants with primers, Hpi5-f and P6. Lane M contains the 100 bp DNA ladder.

3.2.5 Localization of the Hpi-SmtA and SLH-SmtA fusion proteins in recombinant strains

Fusion of *smtA* gene to S layer proteins was carried out to facilitate its cell surface localization in *D. radiodurans* cells. In order to evaluate whether this was achieved, the localization of these proteins in *D. radiodurans* as well as in *E. coli* cells was studied by immunodetetction with anti-SmtA and anti-Hpi antibodies on Western blots.

Recombinant cells were sonicated to release cytoplasmic proteins. Membrane bound proteins were separated by differential centrifugation. The proteins from each fraction were resolved by 10% denaturing SDS-PAGE and probed with anti-SmtA or anti-Hpi serum to determine localization of SmtA. Results from the blot to detect SmtA protein in cytoplasmic fraction show that in recombinant *D. radiodurans* cells expressing the *hpi-smtA* fusion gene or *SLH-smtA* fusion gene, no unique band appeared in cytosol as compared to recombinant cells expressing only *hpi* gene **(Fig. 3.18)**. In recombinants carrying only *smtA*, a band of ~30 kDa was obtained in the cytosolic fraction. The SmtA is a 6 kDa protein, and the presence of

this larger protein is not a surprise since, multimerization of metallothionein protein is known to occur [84].

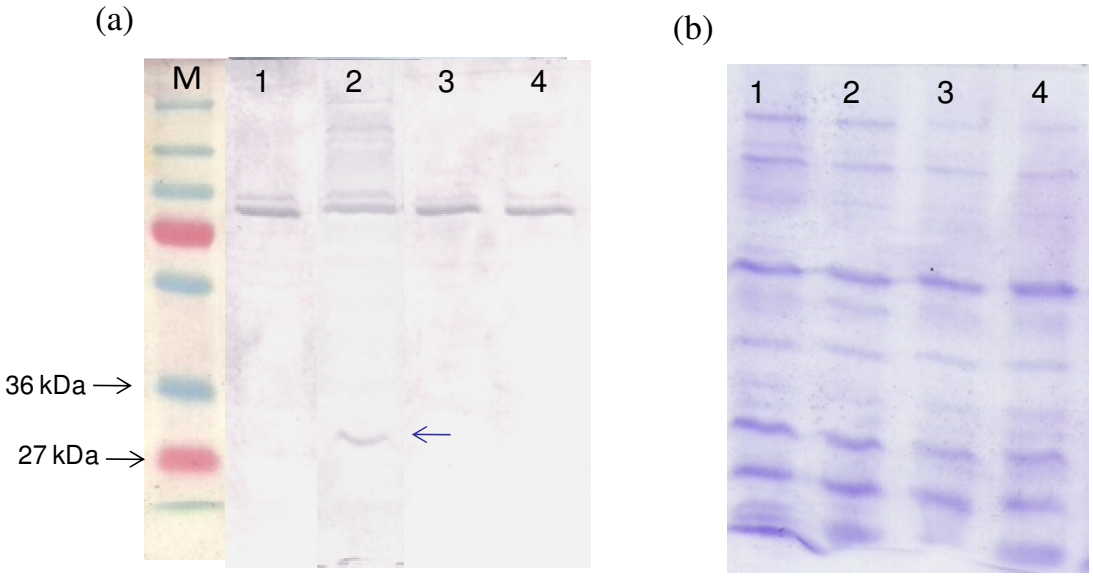

Fig. 3.18. Western Blotting and Immunodetection of SmtA in recombinant *D. radiodurans* cells. About 50 µg cytosolic proteins from recombinant *D. radiodurnas* cells carrying different fusion genes cloned downstream of *PgroESL* in pRAD1 (Lane1-*hpi-smtA*, Lane 2-*smtA*, Lane 3-*hpi*, Lane 4-*SLH-smtA*) were resolved by 10% SDS-PAGE. The proteins were electroblotted and probed with anti-SmtA serum at 1:1000 dilution. Rest of the details are as described in legend to Fig. 3.8. The Western blot (a) and the CBB stained gel (b) are shown. Protein extract were co-electrophoresed with pre-stained molecular mass standards (Lane M).

On probing the membrane fraction from recombinants with anti-Hpi, along with the bands of molecular sizes expected for the Hpi protein, an additional band appeared just above the 100 kDa band, in proteins from *D. radiodurans* cells carrying *hpi-smtA* fusion gene. This band was absent in recombinants carrying *PgroESL-hpi* alone **(Fig. 3.19a)** and band corresponds to the expected size of 106 kDa for the Hpi-SmtA fusion protein (100 kDa Hpi protein and 6 kDa SmtA). Probing of the blot containing membrane bound fractions with

anti-SmtA, immunodetected the same 106 kDa band in recombinants carrying *hpi-smtA* fusion gene, and also a band at around 16 kDa (10 kDa for SLH domain and 6 kDa for the SmtA protein) in recombinants carrying *SLH-smtA* fusion gene **(Fig. 3.19b)**. Interestingly, while the bands corresponding to the S layer fusion proteins appeared exclusively in the membrane bound fraction, the band corresponding to 30 kDa in recombinants carrying the *smtA* gene alone appeared exclusively in the cytosolic fraction. Taken together, these results indicated that the S layer fusion proteins Hpi-SmtA and SLH-SmtA were expressed and localized to the deinococcal cell envelope while the SmtA protein *per se* localized to the cytoplasm.

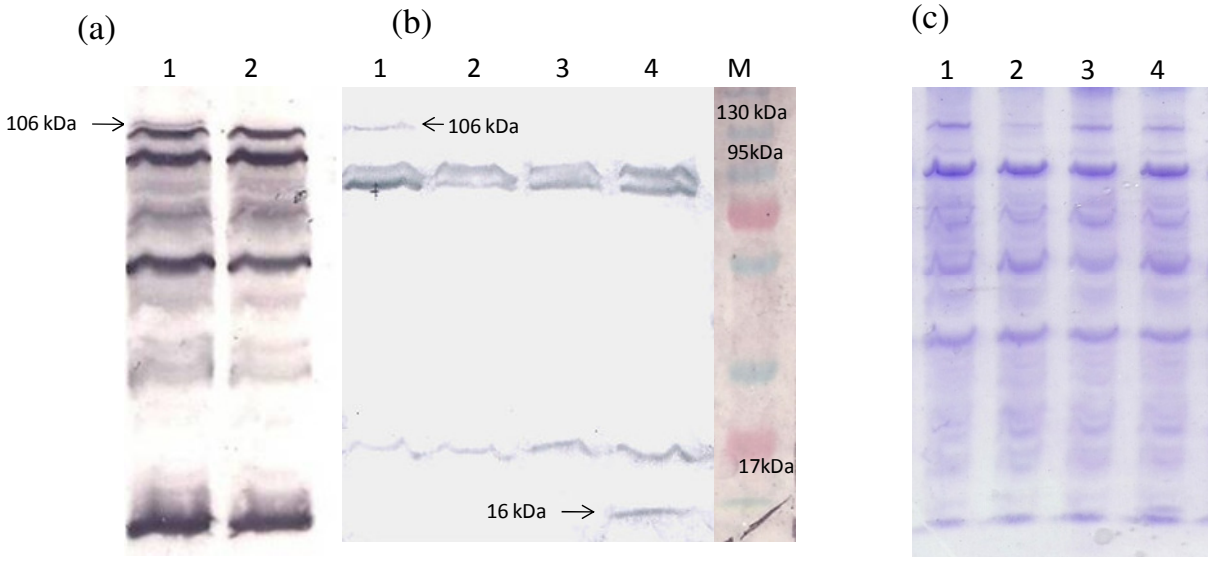

Fig. 3.19. Localization of the S layer fusion proteins by Western Blotting and Immunodetection in recombinant *D. radiodurans* cells. About 50 µg membrane bound proteins from recombinant *D. radiodurnas* cells carrying different fusion genes cloned under *PgroESL* in pRAD1 (Lane1-*hpi-smtA*, Lane 2-*smtA*, Lane 3-*hpi*, Lane 4-*SLH-smtA*) were separated by 10% SDS-PAGE. The proteins were electroblotted and probed with (a) anti-Hpi or (b) anti-SmtA serum at 1:1000 dilution. Rest of the details were as described in the legend to Fig. 3.8. The CBB stained gel (c) is also shown. Protein extract were co-electrophoresed with pre-stained molecular mass standards (Lane M).

Immunodetection using anti-Hpi antibody showed presence of 106 kDa band in membrane bound fraction and to a lesser extent in cytosolic fraction of *E. coli* recombinant cells carrying *hpi-smtA* fusion gene which was absent in recombinants carrying the *smtA* gene alone **(Fig. 3.20).** This indicated that the fusion protein localized to the membrane to a large extent but some also in the cytosol. A lot of non-specific bands were also present in both the blots which may be due to presence of antibodies against *E. coli* proteins in the serum raised in rabbit which may have been exposed to this common gut colonizer.

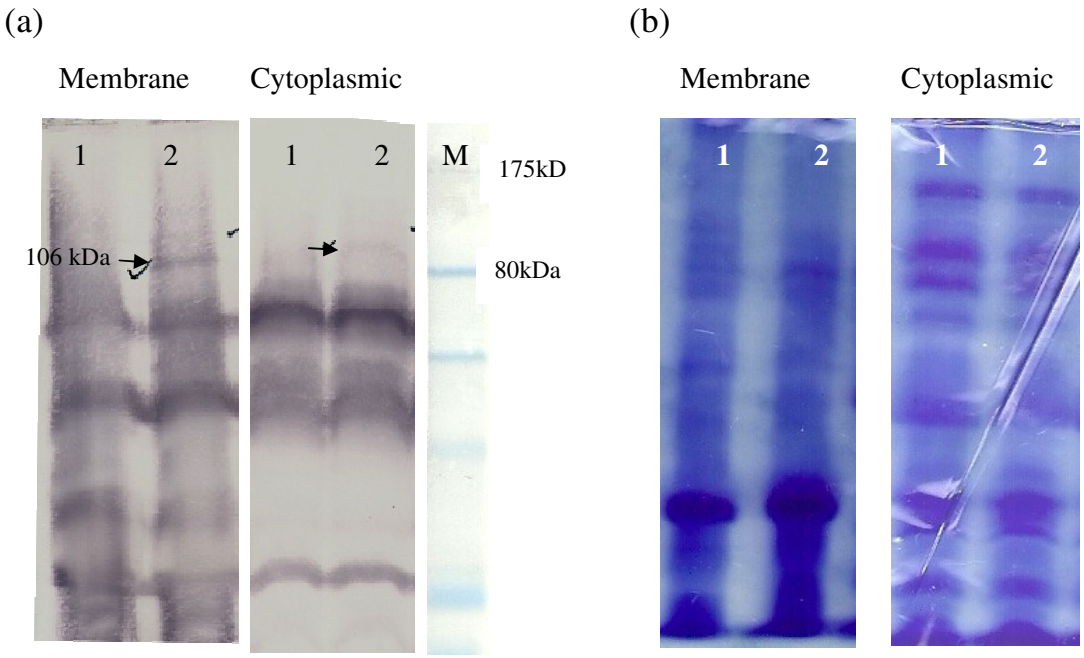

Fig. 3.20: Localization of the Hpi-SmtA fusion protein by Western Blotting and Immunodetection. 50 µg cytosolic or membrane bound proteins from recombinant *E. coli* cells carrying *smtA* gene alone (Lane 1) or the *hpi-smtA* fusion gene (Lane 2) were separated by 10% SDS-PAGE. The proteins were electroblotted and probed with anti-Hpi serum at 1:1000 dilution. Rest of the details were as described in the legend to Fig. 3.8. The Western blot (a) and the CBB stained gel (b) are shown.

3.3 Cloning, over-expression and localization of Hpi-PhoN and SLH-PhoN fusion proteins in recombinant bacteria

The *phoN* gene was fused to the *hpi* ORF as well as to the sequence coding for the SLH domain in *slpA* gene of *D. radiodurans*. The PhoN activity of recombinant cells and the localization of the fusion protein were investigated.

3.3.1 Cloning and expression of the *hpi-phoN* fusion gene

In order to make the *hpi-phoN* fusion, an earlier construct made in the lab, pGDRF2 **(Table 2.3)** was used. This plasmid contains the *phoN* ORF without the sequence coding for its own signal peptide, fused to the signal peptide encoding sequence of the membrane localized FliY protein in *D. radiodurans* and cloned downstream to the *PgroESL* in pRAD1 vector. The *hpi* ORF was PCR amplified using primers, Cd-gro and Cd-r **(Table 2.2)** as a 2.8 kb DNA fragment. The pGRDF2 plasmid was restriction digested with XbaI and NdeI to release the sequence coding for the FliY signal peptide. The *hpi* ORF was digested with XbaI and NdeI and ligated to identical sites in the restriction digested pGDRF2 plasmid between the *PgroESL* and *phoN* ORF. This new construct was named pGDRF3 as shown in **Fig. 3.21** and was used to transform *E. coli* JM109 cells. Colony PCR of Ap^r positive transformants using Cd-gro and Cd-r yielded a band of 2.8 kb which constitutes the *hpi* ORF **(Fig. 3.22a).** Restriction digestion of pGDRF3 using NdeI and BamHI released two inserts due to the presence of an internal BamHI site in *hpi* ORF, 285 bp upstream of the start site. The inserts correspond to the *hpi* ORF without first 285 bp of 2.6 kb and *phoN* ORF without its signal peptide of 0.75 kb **(Fig. 3.22 b)**. Partial DNA sequencing was carried out to further confirm the correctness of the sequence. The plasmid was transformed into *D. radiodurans* cells and the Cm^r transformants were confirmed by colony PCR. This construct was transformed into *D. radiodurans* R1 as well as Hpi mutant, HMR202. The mutant was chosen as a host for

Hpi-PhoN expression to minimize competition in localization of the Hpi-PhoN protein to cell surface with the native Hpi protein.

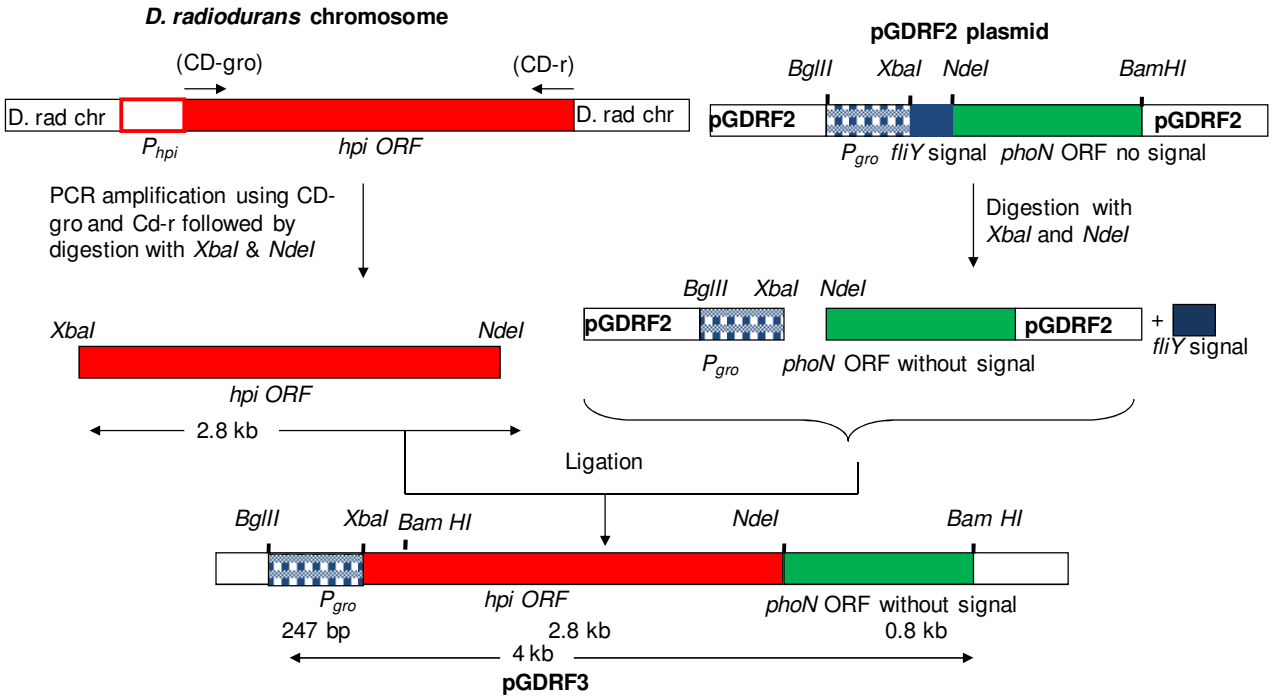

Fig. 3.21. Construction and cloning of pGDRF3. The *hpi* ORF was PCR amplified from deinococcal chromosome using primers, CD-gro and CD-r. The 2.8 kb fragment was restriction digested with XbaI and NdeI. The pGDRF2 plasmid was restriction digested with XbaI and NdeI and ligated to the identically digested *hpi* ORF to generate plasmid, pGDRF3.

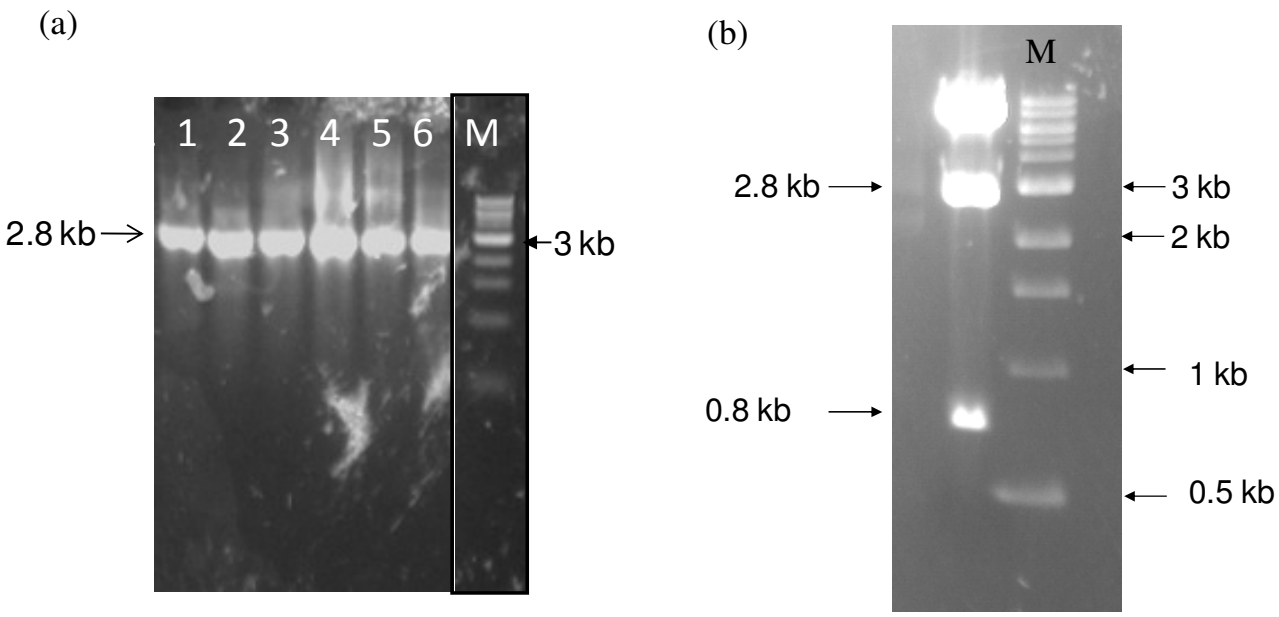

Fig. 3.22. Cloning and confirmation of pGDRF3. Agarose gel electrophoresis of DNA fragments. (a) Lanes 1 to 6 display products obtained on carrying out colony PCR of eight transformants with primers, CD-gro and CD-r. (b) Restriction digestion of the plasmid isolated from one of the Ap^r transformants tested positive by colony PCR, with XbaI-NdeI. Lane M contains the 1 kb DNA ladder.

3.3.2 Expression of the Hpi-PhoN fusion protein

` To ascertain expression of the Hpi-PhoN fusion protein, total cell extracts were made using non-reducing cracking buffer. The proteins were then separated by 10% denaturing gel and developed for phosphatase activity using NBT-BCIP substrate on a zymogram. In both, *E. coli* as well as *D. radiodurans* recombinants bearing the pGRDF3 plasmid, an activity band was obtained at ~127 kDa, as expected for the fusion protein as against 27 kDa band which is normally obtained with *phoN* expressing cells **(Fig. 3.23**). In addition, several discreet activity bands of smaller size were obtained which may be due to degradation of the fusion protein.

(a) (b)

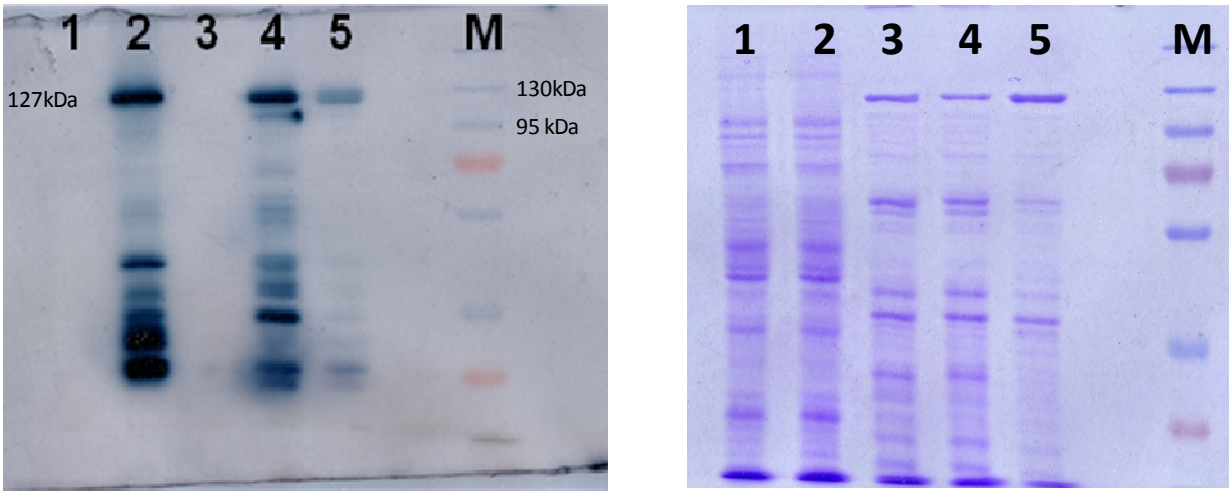

Fig. 3.23. Zymogram showing in-gel PhoN activity. About 20 µg whole cell protein of *E. coli* cells bearing pRAD1 (Lane 1), or expressing Hpi-PhoN fusion protein (Lane 2) or *D. radiodurans* cells bearing pRAD1 (Lane 3), or expressing Hpi-PhoN fusion protein (Lane 4) or HMR202 mutant cell expresssing Hpi-PhoN fusion protein (Lane 5) were separated by 10% SDS-PAGE. The gel was rinsed in water followed by renaturation in 1% Triton X-100 in acetate buffer, pH 5.0. The gel was developed in NBT-BCIP solution. The zymogram (a) and the corresponding CBB stained gel (b) are shown. Protein extract were co-electrophoresed with pre-stained molecular weight standards (Lane M).

Recombinant cells were lysed in Laemmli's buffer and resolved by 10% SDS-PAGE. The proteins were electroblotted on nitrocellulose membrane. Immunodetection using anti-Hpi serum showed presence of a ~127 kDa band in both *E. coli* and *D. radiodurans* recombinants confirming expression of the fusion protein **(Fig. 2.24)**, which was not present in control cells carrying pRAD1 alone.

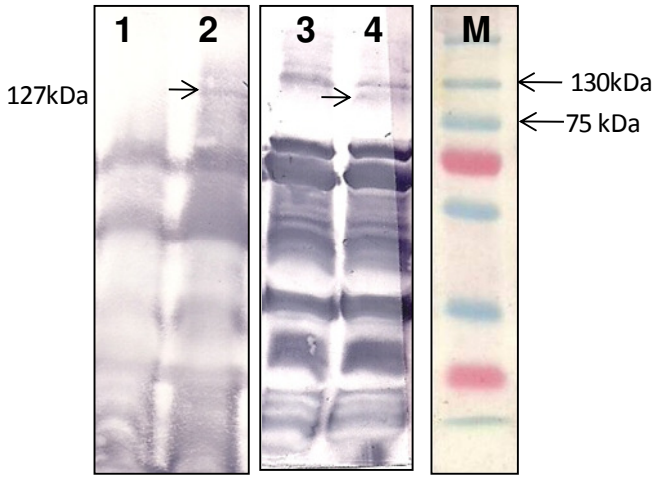

Fig. 3.24. Western blot and immunodetection of Hpi-PhoN fusion protein. About 50 µg whole cell protein of *E. coli* cells bearing pRAD1 (Lane 1), or expressing Hpi-PhoN fusion protein (Lane 2) or *D. radiodurans* cells bearing pRAD1 (Lane 3), or expressing Hpi-PhoN fusion protein (Lane 4) were separated by 10% SDS-PAGE. The proteins were electroblotted and probed with anti-Hpi at 1:1000 dilution. Rest of the details were as described in the legend to Fig. 3.8.

Recombinant *D. radiodurans* cells carrying the *hpi-phoN* construct were patched on histochemical plates containing phenolphthalein diphosphate (PDP) and methyl green (MG). On such medium, cultures over-expressing phosphatases give green color colonies. This is due to precipitation of methyl green under acidic conditions caused by released phosphate ligand (Pi) on the phosphatase positive colonies. *D. radiodurans* cell expressing *hpi-smtA* showed lighter green colonies than those carrying *phoN* alone (**Fig. 3.25**). Assays carried out with whole cells using pNPP as the susbstrate to measure the phosphatase activity per mg of cell protein, showed that recombinant cells carrying the fusion protein (Hpi-PhoN) showed lesser phosphatase activity than those carrying *phoN* gene alone, by a factor of four in *E. coli* cells and a factor of two in *D. radiodurans* cells (**Table 3.1**).

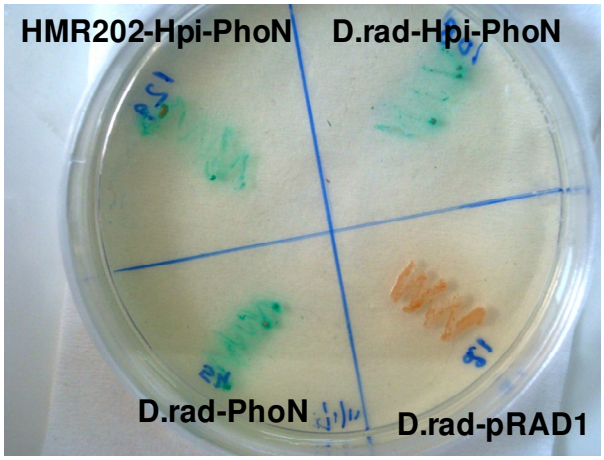

Fig. 3.25. Histochemical screening for whole cell phosphatase activity in recombinant *D. radiodurans* cells. Recombinant *D. radiodurans* were patched on TGY with chloramphenicol (3 µg/ml), phenolphthalein diphosphate (PDP) (1 mg/ml) and methyl green (MG) (100 µg/ml). The PhoN positive clones appeared as green colored colonies due to deposition of MG. In case of *D. radiodurans* harbouring pRAD1 alone, the colony retained its original orange color.

Table 3.1. Specific activity of various recombinants expressing the *phoN* or *hpi-phoN* genes

Clones	**Specific Activity (nmoles pNP released/mg protein/min)**
E. coli-PhoN	1500 ± 200
E. coli-Hpi-PhoN	350 ± 30
D. radiodurans-PhoN	150 ± 20
D. radiodurans-Hpi-PhoN	75 ± 16
HMR202-Hpi-PhoN	50 ± 4

In order to investigate whether fusion to the *hpi* gene facilitates membrane localization of the PhoN protein, fractionation studies were carried out. As seen in **Fig. 3.26a**, in *E. coli* cells carrying *hpi-phoN*, sonication of cells even in the presence of PMSF, resulted in degradation of the protein with bands at ~27 kDa appearing in both cytosolic as well as membrane fractions, but present in much higher amount in the cytosolic fraction. A faint band of ~127 kDa was present in the membrane bound fraction in *E. coli* cells.

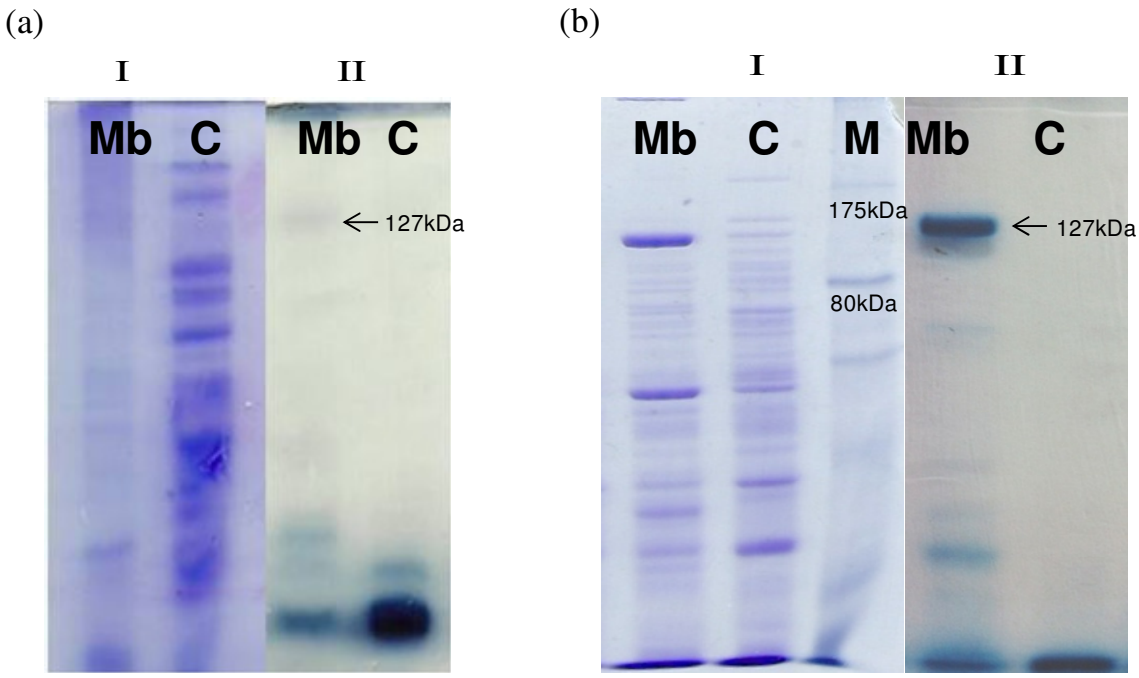

Fig. 3.26. Localization of the Hpi-PhoN fusion protein in recombinant cells. Recombinant *E. coli* (a) and *D. radiodurans* (b) cells expressing *hpi-phoN* fusion protein were sonicated and 20 µg of cytosolic (C) and membrane bound (Mb) fractions were separated by 10% denaturing gel. Rest of the details were as described in legend to Fig. 3.23. CBB stained gel (I) and zymogram (II) have been shown. The standard molecular weight marker is shown in Lane Ma.

On the other hand, in *D. radiodurans* cells carrying *hpi-smtA* fusion gene, phosphatase activity could be detected only in the membrane bound fraction, predominantly as an expected 127 kDa band and to a lesser extent as a 27 kDa band (**Fig. 3.26b**). No phosphatase activity was detected in the cytosolic fraction. The result suggested that Hpi-PhoN accurately localizes as an active fusion protein in deinococcal membrane. In contrast, in *E. coli*, it fails to localize in membrane and gets degraded further in the cytosol.

3.3.3 Cloning and expression of the *SLH-phoN* fusion gene and localization of the SLH-PhoN protein

The sequence encoding the SlpA signal peptide along with its SLH domain was PCR amplified from deinococcal chromosomal DNA using primers SlpA-f and SLH-99r **(Table 2.2)** as a 328 bp DNA fragment. An earlier construct, pGDRF3 **(Table 2.3)**, described above **(Fig. 3.21)**, which carried the *phoN* ORF without its signal peptide fused to *hpi* was digested with XbaI and NdeI to release the *hpi* ORF. The PCR product constituting the sequence encoding SLH domain was restriction digested with XbaI and NdeI and ligated to identical sites in pGDRF3 plasmid, downstream to the *PgroESL* promoter to obtain the plasmid pPSP1 **(Fig. 3.27).** *E. coli* JM109 cells were transformed with pPSP1 plasmid. Colony PCR of Ap^r positive tranformants using SlpA-f and SLH99-r primers yielded a 328 bp fragment constituting the sequence encoding the SLH domain **(Fig. 3.28a)**. The correctness of the plasmid was confirmed by restriction digestion with XbaI-NdeI which released the sequence encoding for SLH domain of 328 bp and with BglII-NdeI to release gene for SLH domain (328 bp) along with the *PgroESL* promoter (247 bp) to yield a product of around 570 bp **(Fig. 3.28b).** The correctness of the construct was further confirmed by sequencing. The plasmid was transformed into *D. radiodurans* cells, and the Cm^r transformants were confirmed by colony PCR.

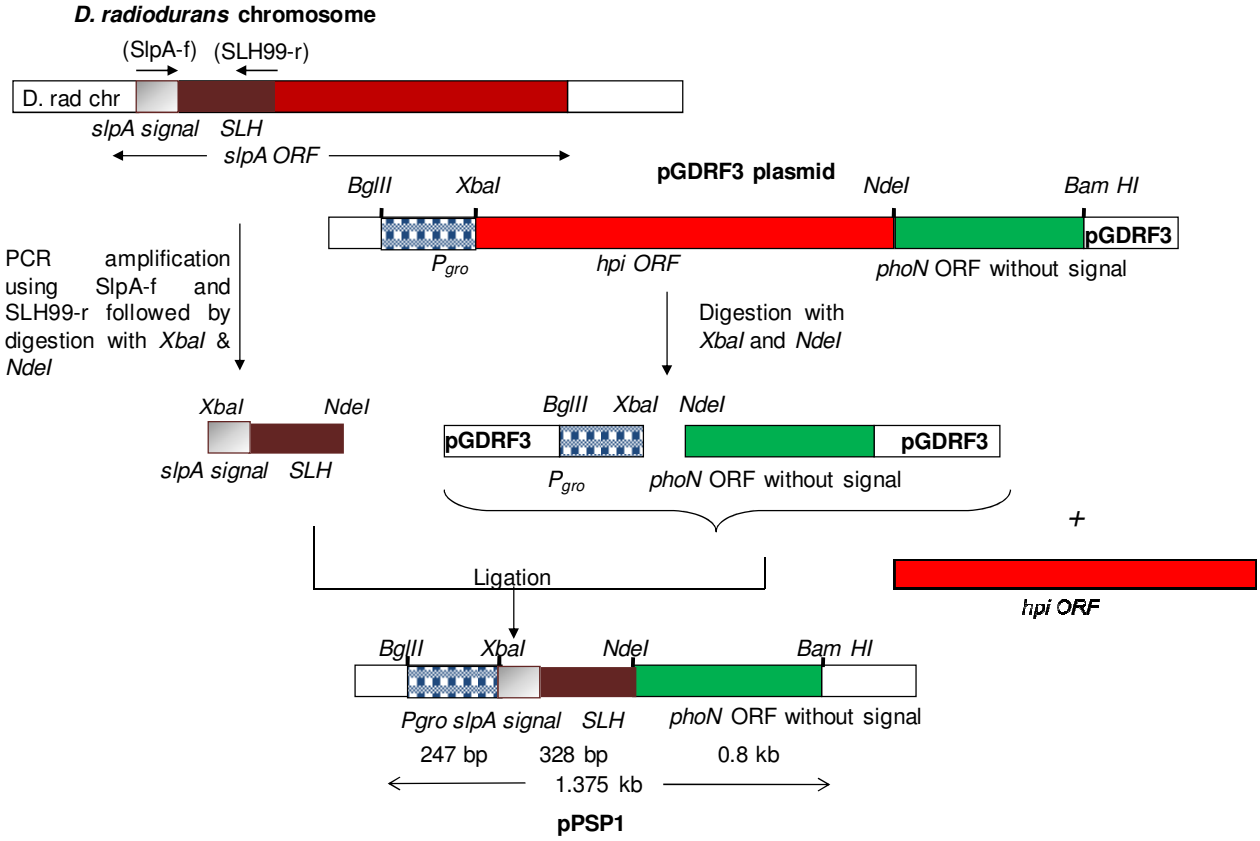

Fig. 3.27. Construction and cloning of pPSP1. The sequence coding for the signal peptide and SLH domain of the SlpA protein was PCR amplified from deinococcal chromosome using primers, SlpA-f and SLH99-r. The 328 bp fragment was restriction digested with XbaI and NdeI. The pGDRF3 plasmid was restriction digested with XbaI and NdeI and ligated to identically digested PCR product to generate plasmid, pPSP1.

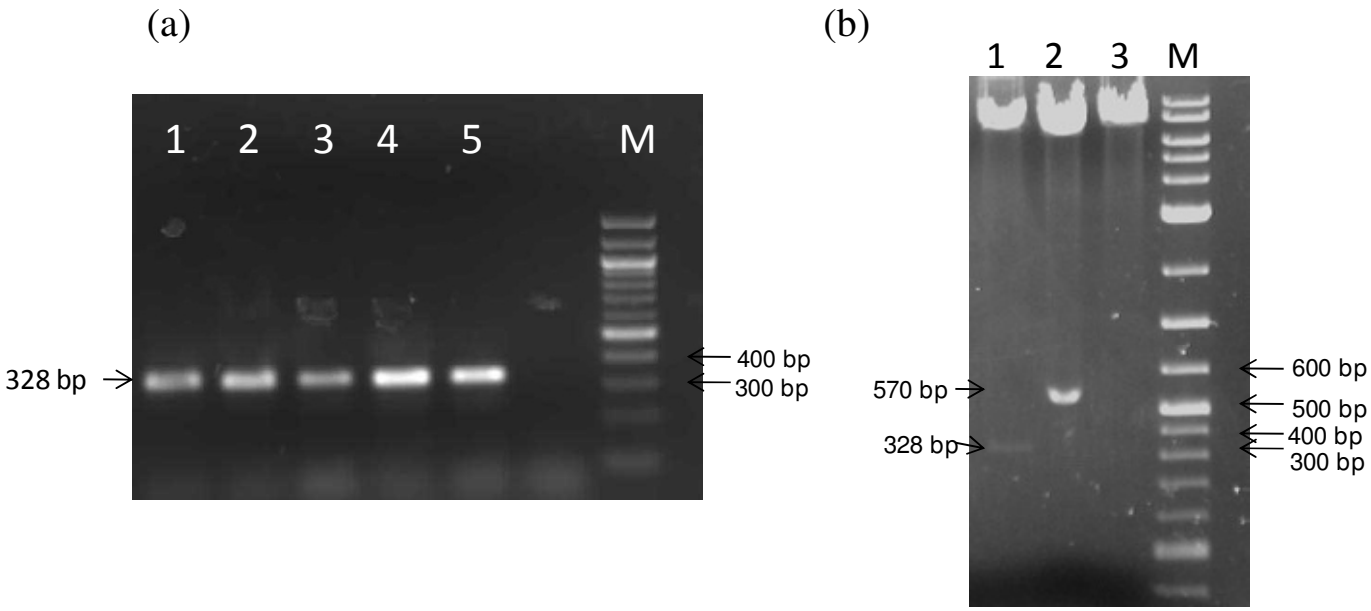

Fig. 3.28. Cloning and confirmation of pPSP1. Agarose gel electrophoresis of DNA fragments. (a) Lanes 1 to 5 display products obtained on carrying out colony PCR of five transformants with primers, SlpA-f and SLH99-r. Lane M contains the 100 bp DNA ladder. (b) Restriction digestion of the plasmid isolated from one of the Ap^r transformants by colony PCR, with XbaI-NdeI (Lane 1), BglII- NdeI (Lane 2) and NdeI (Lane3). Lane M contains the 2-log DNA ladder from New England Biolabs.

E. coli cells carrying the *SLH-phoN* construct yielded green colored colonies on PDP-MG plates indicative of acid phosphatase activity. Zymogram using cell extracts showed an activity band at 37 kDa which is the expected size for the fusion protein **(Fig. 3.29a).** However, *D. radiodurans* cells carrying this construct did not show green colored colonies on PDP-MG plates **(Fig. 3.29b)**. On carrying out a zymogram using protein extracts from recombinant *D. radiodurans* cells however, a band of the expected size was obtained **(Fig. 3.29a)**. This seemed to indicate that the fusion protein though expressed and active was either not folding or localizing appropriately in the deinococcal cell wall.

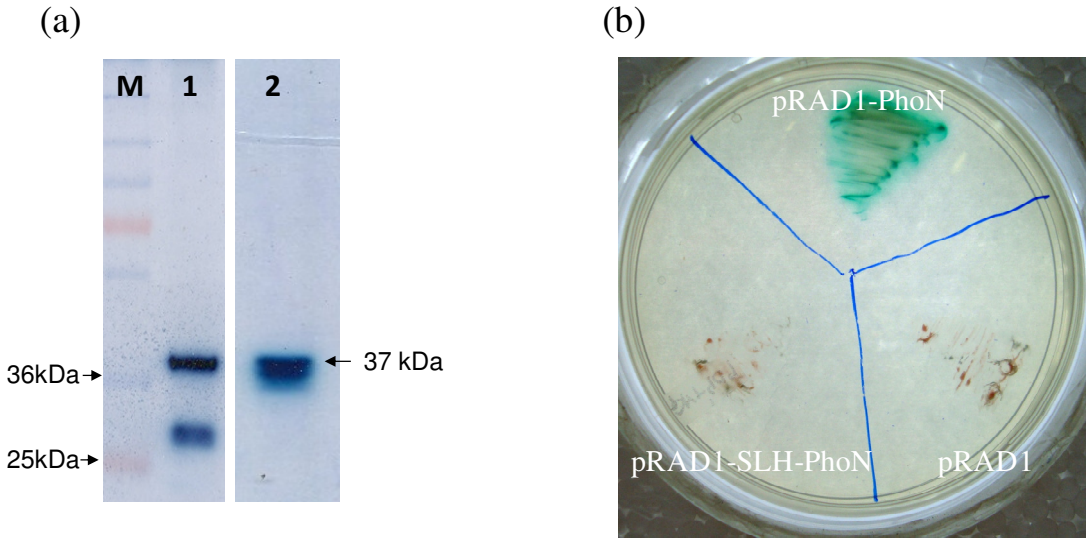

Fig. 3.29. Phosphatase activity of SLH-PhoN fusion protein. (a) Whole cell extracts (30 µg protein) from recombinant *E. coli* (Lane 1) and *D. radiodurans* cells (Lane 2) carrying the *SLH-phoN* fusion gene construct were resolved by 10% SDS-PAGE and developed for phosphatase activity as described in legend to Fig. 3.23. (b) Recombinant *D. radiodurans* were patched on TGY with chloramphenicol (3 µg/ml), phenolphthalein diphosphate (PDP) (1 mg/ml) and methyl green (MG) (100 µg/ml). Rest of the details are as in legend to Fig. 3.25.

Further experiments were carried out to ascertain localization of the SLH-PhoN fusion protein in recombinant *E. coli* and *D. radiodurans* cells. Cells were sonicated and the cell envelope and cytoplasmic fractions were separated. A zymogram carried out with the cell envelope and cytoplasmic fractions showed that in *E. coli* cells, the fusion protein localized to both the cytosolic as well as the membrane bound fraction **(Fig. 3.30a)** equally, while in *D. radiodurans* more than half the fusion protein activity was associated with the cell envelope indicating that the fusion protein was capable of anchoring to the deinococcal cell wall **(Fig. 3.30b)**. A smaller 27 kDa band was also seen in the cytosolic fractions but not in the membrane **(Fig. 3.30b)**. In all probability, this was the C-terminal degradation product of the

SLH-PhoN fusion protein, since it exhibited phosphatase activity. This suggests that in the absence of the SLH domain or signal sequence, PhoN does not localize to the cell envelope.

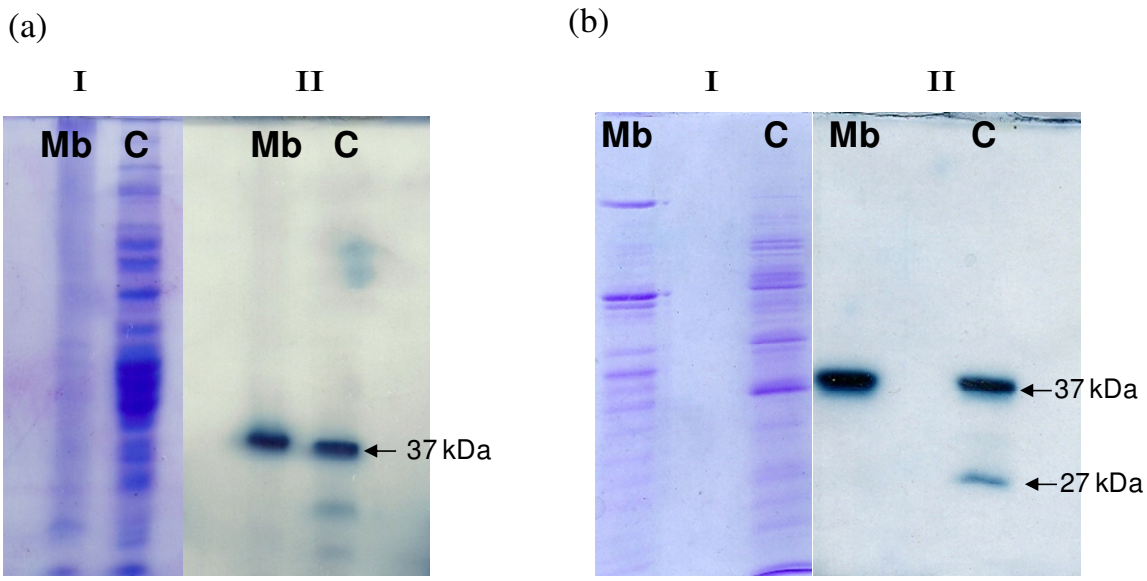

Fig. 3.30. Localization of the SLH-PhoN fusion protein in recombinant cells. Recombinant *E. coli* (a) and *D. radiodurans* (b) cells were sonicated and 30 µg of cytosolic (C) and membrane bound (Mb) proteins were separated by 10% SDS-PAGE. CBB stained gel (I) and zymograms (II) are shown.

3.4 Peptidoglycan based immobilization of SLH-PhoN protein *in vitro*

SLH-PhoN fusion protein did not show whole cell based phosphatase activity in *D. radiodurans*. Therefore, these recombinant organisms would not be useful for cell based metal precipitation. However, the SLH domain is known to interact with SCWP peptidoglycan in other organisms. Therefore, the possibility of over-expressing the SLH-PhoN protein in *E. coli* and exploiting its interaction with Deinococcal peptidoglycan for its immobilization and use in metal precipitation was explored.

3.4.1 Over-expression of SLH-PhoN protein and confirmation of its identity

The PCR amplified gene was first cloned in pET16b and then excised from this vector and re-ligated into pET29b. This had to be done, since an NdeI site was present in the SLH-PhoN fusion protein and an alternative restriction site with the start codon, NcoI was available only in pET16b. However, in pET16b, only N terminal His tagging is possible, which is not the correct option for the SLH-PhoN fusion protein, since it also carries a signal peptide.

The *SLH-phoN* fusion gene was PCR amplified from pPSP1 (described above) **(Fig. 3.27)** using primers SLHo-f and PetC-r **(Table 2.2)** as a 1.012 kb fragment. The PCR product was restriction digested with NcoI and BamHI and cloned into identical sites generated in pET16b, yielding plasmid pPSP2. In the next step, the whole fusion gene, along with a portion of the vector carrying the ribosome binding sequence was excised as an XbaI-XhoI product and ligated into identical sites in pET29b such that the His-tag would be in frame with the fusion gene and lie at the C-terminal end of the translated protein **(Fig. 3.31)**. This plasmid was named pPSP3 and transformed into *E. coli* BL21 (pLysS) cells. Colony PCR of positive tranformants using SlpA-f and SLH99-r primers gave a 328 bp fragment constituting the sequence encoding the SLH domain **(Fig. 3.32a)**. Plasmid was isolated from Ap^r *E. coli* transformants, positive by colony PCR for sequence encoding SLH domain. The plasmid was subjected to restriction digestion with XbaI-XhoI to release a 1.03 kb fragment constituting sequence coding for SLH domain (328 bp) and *phoN* ORF without its signal peptide (684 bp) along with 40 bp of the vector sequence. Plasmid pPSP3 restriction digested with Nco-XhoI released a 990 bp fusion sequence for *SLH-phoN*, or digested with NdeI-XhoI to release a 684 bp *phoN* gene **(Fig. 3.32b).**

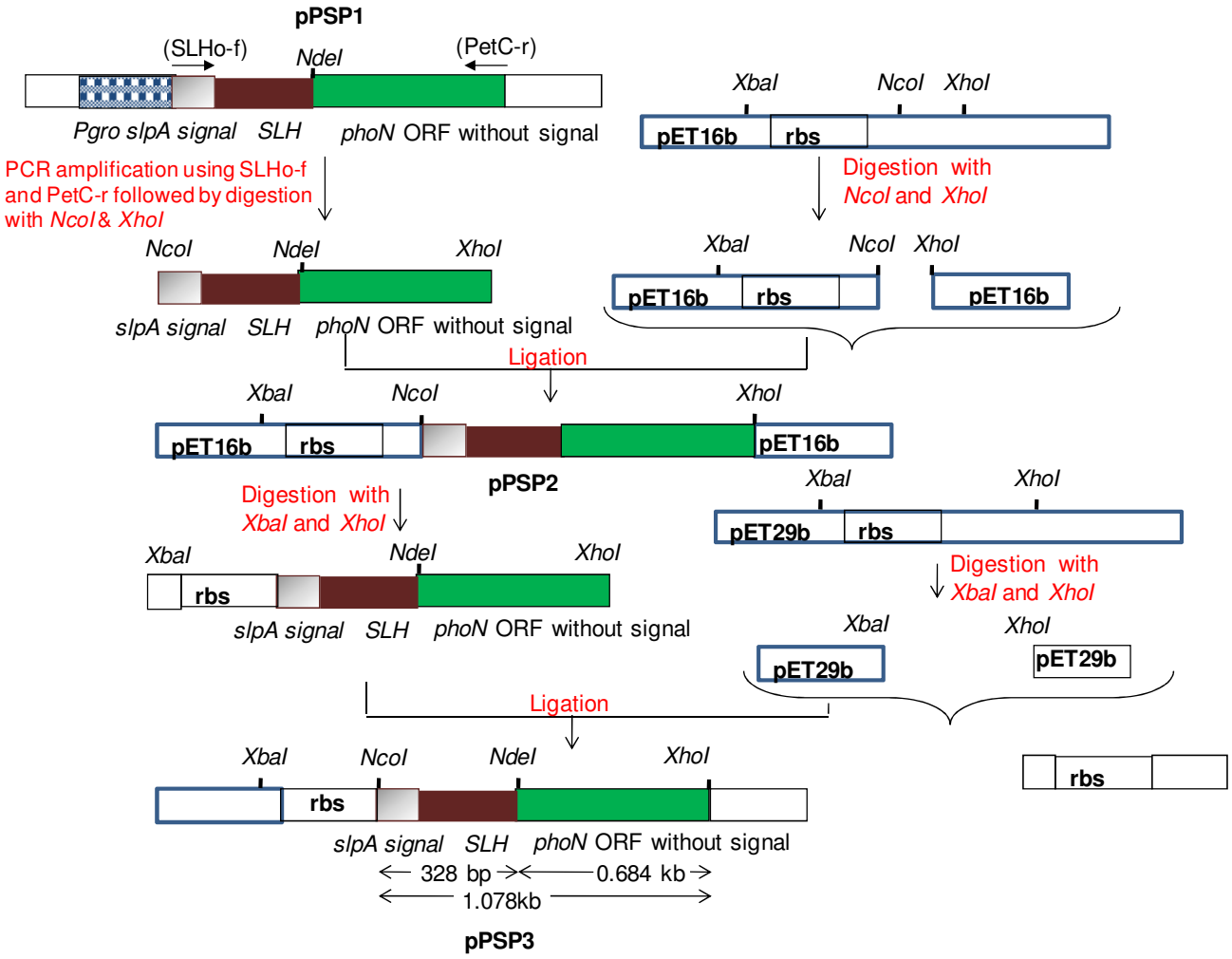

Fig. 3.31. Construction and cloning of pPSP3. The *SLH-phoN* fusion gene was PCR amplified using SLHo-f and PetC-r primers from pPSP1 plasmid. The 1.012 kb fragment was restriction digested with NcoI and XhoI and cloned into identical sites generated in pET16b to generate pPSP2. The pPSP2 plasmid was restricion digested using XbaI and XhoI to release the sequence coding for the *SLH-phoN* fusion gene along with the rbs region of pET16b and ligated into identical sites into pET29b to generate plasmid pPSP3.

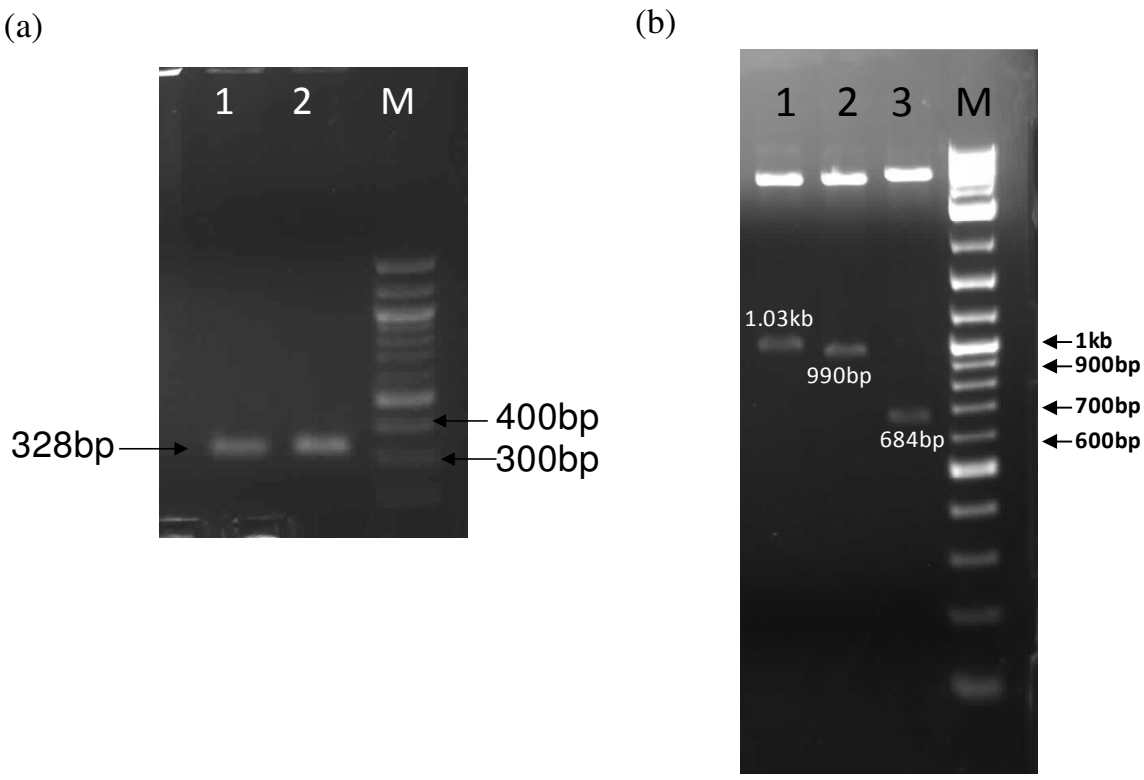

Fig. 3.32. Cloning and confirmation of pPSP3. Agarose gel electrophoresis of DNA fragments. (a) Lanes 1 and 2 display products obtained on carrying out colony PCR of two transformants with primers, SlpA-f and SLH99-r. (b) Restriction digestion of the plasmid isolated from one of the Ap^r transformants positive by colony PCR, with XbaI-Xho (Lane 1), NcoI-XhoI (Lane 2) and NdeI-XhoI (Lane 3). Lane M contains the DNA molecular weight marker.

Over-expression of the SLH-PhoN fusion protein was standardized by varying the time and temperature of incubation of cultures after induction by addition of 1 mM Isopropyl β-D-1-thiogalactopyranoside (IPTG). Maximum induction of the SLH-PhoN fusion protein, visualized as a 38 kDa CBB stained band was obtained when the culture was incubated with IPTG at 30°C for 5 h **(Fig. 3.33a)**. Zymogram of protein extracted from such cells showed that the fusion protein displayed an active phosphatase visible as a 38 kDa band **(Fig. 3.33b)**.

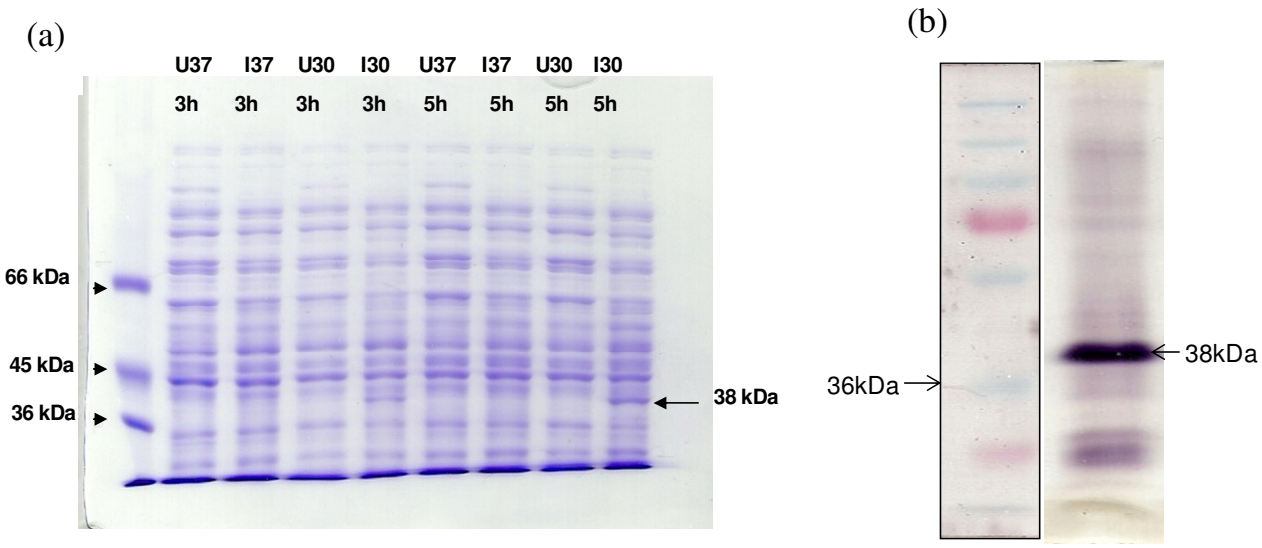

Fig. 3.33. Overexpression of the SLH-PhoN protein in recombinant *E. coli* cells. (a) About 30 µg of protein extracted from cultures grown with IPTG for 3 h or 5 h for induction (I) was resolved by 10% denaturing PAGE and stained with CBB. Following addition of IPTG, the culture was grown at either 37°C or 30°C as indicated. Protein extracted from un-induced culture (U) served as control. (b) Zymogram showing in-gel phosphatase activity of 30 µg of protein extracted from SLH-PhoN expressing cultures induced by addition of IPTG and grown at 30°C for 5 h.

The identity of the band which appeared at 38 kDa was confirmed by peptide mass fingerprinting using MALDI-TOF-MS. The MASCOT based search showed acid phosphatase from *Salmonella* as the first hit **(Fig. 3.34a).** The SLH domain forms only 25% of the mass of the fusion protein and is not likely to generate correct hits in MASCOT search. As a result, in order to confirm the protein identity, theoretical masses for the trypsinized SLH domain were generated and these were identified in the spectra. A MS-MS analysis was performed on the peptides of these particular masses. MASCOT based search for the peptide mass spectra generated for peptide of mass 1294 Da **(Fig. 3.34a)** (which is one of the

peptides that is predicted to be generated due to action of trypsin on the SLH domain), gave SlpA protein as the first hit (**Fig. 3.34b**).

(a)

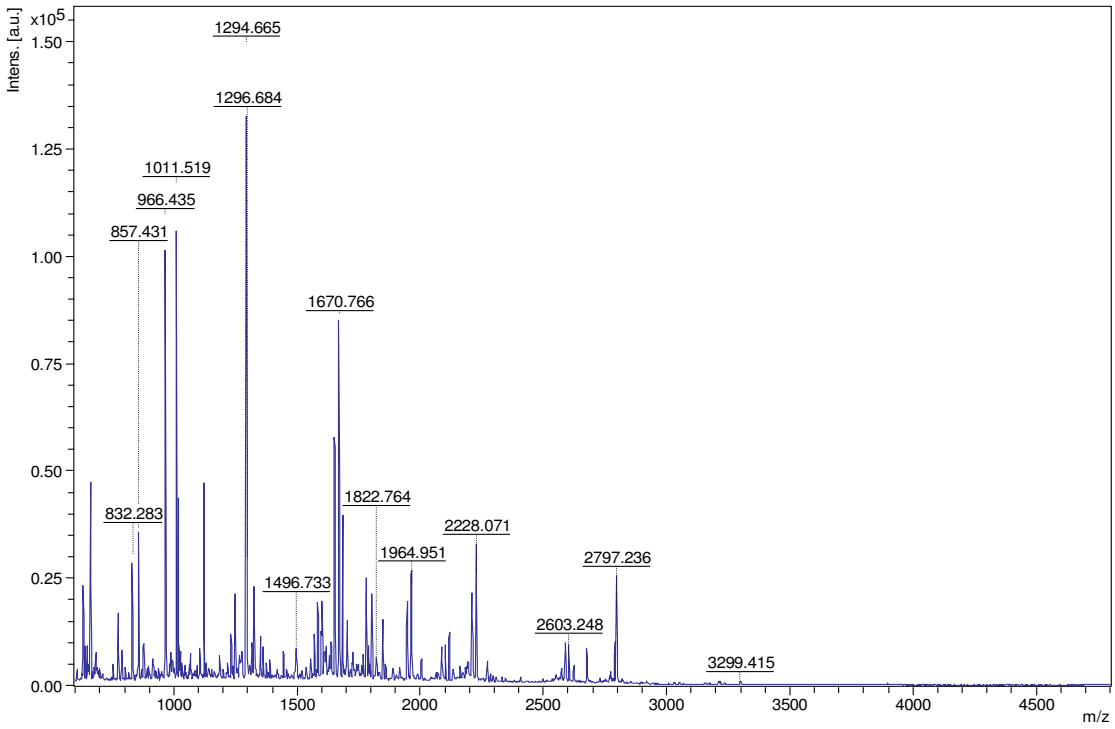

(b)

Database : NCBInr 20140122 (35149712 sequences; 12374887350 residues)
Taxonomy : Bacteria (Eubacteria) (23117317 sequences)
Timestamp : 30 Jan 2014 at 10:57:32 GMT
Top Score : 101 for gi|447104995, acid phosphatase [Salmonella enterica]

1. gi|15807560 **Mass:** 123769 **Score:** 56 **Matches:** 1(0) **Sequences:** 1(0)
S-layer protein [Deinococcus radiodurans R1]
☐ Check to include this hit in error tolerant search

Query	Observed	Mr(expt)	Mr(calc)	ppm	Miss	Score	Expect	Rank	Unique	Peptide
1	1294.6648	1293.6575	1293.6718	-11.00	0	56	0.075	1	U	R.GVILGYPDGTFR.G

Fig. 3.34. MASCOT search result for the mass spectra generated for the 38 kDa protein over-expressed in *E. coli* BL21 cells shown in Fig. 3.32. (a) Mass spectrum and the MASCOT search result for mass spectra of the 38 kDa protein, (b) MASCOT search result for mass spectra generated by MS-MS for peptide of mass 1294 Da.

3.4.2 Isolation of deinococcal peptidoglycan and its interaction with SLH domain

The SLH-PhoN fusion protein provided an easy tool to study peptidoglycan binding in *D. radiodurans*. Peptidoglycan from *D. radiodurans* was isolated by three rounds of 8 h boiling in 4 % SDS, wherein peptidoglycan remained insoluble while the remaining cell components were solubilized and removed through centrifugation. The peptidoglycan fraction was recovered as an insoluble pellet which was washed free of detergent. Ornithine is an amino acid known to be present the Deinococcal peptidoglycan, and was quantified in the preparation by hydrolyzing peptidoglycan in concentrated acid and estimating ornithine by colorimetric method as described (Section 2.11). Around 61 µg ornithine/mg of peptidoglycan was obtained. Thus, ornithine was found to make up around 6.1% of the deinococcal peptidoglycan dry weight, which is in good agreement with the values reported in literature for *Thermus thermophilus* (6.7%). Around 43 µg equivalent of peptidoglycan was used to test peptidoglycan binding by SLH-PhoN in 100 µl reaction volume.

In peptidoglycan binding assays, the insoluble fraction, I represents the protein which bound to the peptidoglycan, while the soluble fraction, S represents protein which did not bind to the peptidoglycan. A zymogram was carried out with the soluble, wash and the insoluble fraction. Most of the activity for SLH-PhoN fusion protein was found in the insoluble fraction while in control, where no peptidoglycan was added, all of the activity was present in the soluble fraction as shown in **Fig. 3.35a**. This indicated that the single copy of the SLH domain was sufficient to bind the deinococcal peptidoglycan. Further, a smaller degradation product of this protein which appeared in zymograms, did not bind the peptidoglycan. In all probability, this degradation product was PhoN lacking the SLH domain since it retained phosphatase activity. When similar binding study was carried out with whole cell extracts containing PhoN (witout SLH domain) as a negative control, it did not bind

peptidoglycan, showing that peptidoglycan binding results exclusively from the SLH domain (**Fig. 3.35b**).

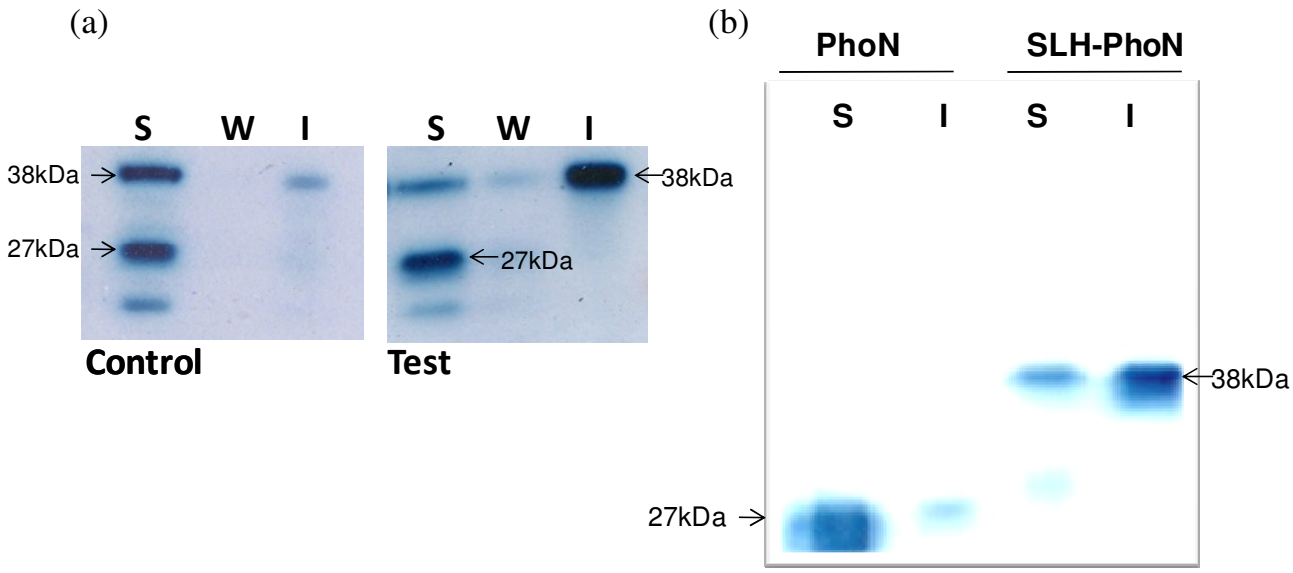

Fig. 3.35. Peptidoglycan binding by SLH-PhoN fusion protein. (a) Cell extract from recombinant *E. coli* cells expressing SLH-PhoN fusion protein was incubated in the absence (Control) or presence (Test) of deinococcal peptidoglycan at 4°C following which soluble fraction (S) was separated by centrifugation. A wash (W) was given and the insoluble fraction (I) was obtained by a 50°C treatment for 15 min in non-reducing Laemmli's buffer. All the fractions were resolved on 10% denaturing gel and developed for phosphatase activity. (b) Peptidoglycan binding by PhoN and SLH-PhoN protein.

3.5 Discussion

Several strategies are in vogue for surface display of proteins for a variety of biotechnological and industrial applications. In Gram negative bacteria, proteins for surface display may be generated by N-terminal, C-terminal, or sandwich fusions to cell wall anchoring proteins [85]. *E. coli* has been a preferred organism for most of the studies owing

to its status as a model organism. Peptidoglycan associated lipoprotein (PAL), *E. coli* adhesion protein AIDA-1, *Shigella* Vir-G protein etc. have been used for display of proteins through N-terminal fusions for vaccine and biosensor development. A popular example for C-terminal fusion is that of Lpp-OmpA hybrid which contains the first nine N-terminal residues of mature *E. coli* lipoprotein and a few residues of the outer membrane porin A protein. Similar system has also been used for display of SmtA protein and the organophosphorous hydrolase for bioremediation of metals and pesticides respectively [86-87].

S layer proteins and outer membrane proteins have been exploited in making sandwich fusions for surface display of proteins [83,85]. The N terminal domain which bound to outer membrane and C terminal secretion signal of S layer protein of *Caulobacter crescentus* were used to display a 12 amino acid peptide from *Pseudomonas aeruginosa* [85]. In Gram positive bacteria, the anchoring domain of Staphylococcal protein A (SpA) constituting the LPXTG box has been used for anchoring proteins to cell surface [83]. Besides this, the SLH domain of S layer proteins of *Bacillus anthracis* and *Bacillus sphaericus* have also been used to display tetanus toxins fragments and allergens for diagnostics [75,80,85].

The status of *D. radiodurans* as a Gram positive organism is somewhat misleading because while it stains violet in Gram reaction, its complex cell wall resembles that of Gram negative organisms [54]. In designing a suitable strategy for surface display in this organism, the Hpi protein seems to be the protein of choice due to its location as a penultimate layer in the multi layered cell wall [45]. Since the crystal structure of the protein is not available, the entire protein was used for generating fusions. Further, since the C terminal of the protein is known to be exposed to the outer surface [58], the PhoN and SmtA protein were fused to C

terminus of the Hpi protein in the present work The other S layer protein, SlpA is a rather large protein (123 kDa) which is poorly characterized. Therefore, the utility of the small SLH domain of SlpA protein in membrane anchoring was studied as has been done in some Gram positive organisms mentioned above. To date, surface display in *D. radiodurans* has not been attempted.

As a prelude to this work, some preliminary work to characterize the S layer proteins of *D. radiodurans* was carried out. The Hpi protein layer has been under study for several years. In *D. radiodurans* Sark strain, isolation of the Hpi layer followed by its electrophoresis on a denaturing gel yields a single band of ~108 kDa, while in *D. radiodurans* R1, a 100 kDa band along with several bands of lower molecular sizes are usually obtained [82]. It has been speculated that these bands appear due to *in vivo* proteolysis of the Hpi layer and is unavoidable even when protease inhibitors are used during its isolation [82]. Two dimensional peptide fingerprinting was used to determine that all the bands indeed belonged to Hpi protein. It was also reported that an exonuclease activity was always found to be present in Hpi preparations [88], and since on SDS gels, a 123 kDa protein was found to co-purify, the exonuclease activity was assigned to this protein. Further, it has been elaborated that the Hpi layer forms a 1:1 complex with this exonuclease, and that the six fold symmetry of Hpi layer subunits is reflected in the exonuclease layer [58], though evidence for the same has not been provided. No further elaboration on the same exists in literature.

The present study provides further confirmation that the various peptide bands obtained on resolving the Hpi layer after total denaturation on a denaturing gel are all indeed discreet degradation products of the Hpi protein as determined by peptide mass fingerprinting using MALDI-TOF-MS. Further, the 123 kDa protein which came up as a contaminant in all Hpi preparations was identified to be the deinococcal S layer protein, SlpA (DR2577) based

on its homology with the S layer protein from *Thermus thermophilus*. This study showed, for the first time that the two S layer proteins, Hpi and SlpA in *D. radiodurans* seem to be intimately associated with each other as part of the architecture of the deinococcal cell envelope. This further supports the popular theory that three-dimensional extension of symmetry into the pink envelope or at least into its outer membrane may be needed in order to satisfy the physiological requirements of cell trafficking [89]. Further, it can be concluded that the nature of the interaction between the Hpi layer and the SlpA protein is non-covalent in nature since it can be disrupted by SDS treatment at high temperature.

All the fusion genes constructed in this study, *hpi-smtA, SLH-smtA, hpi-phoN and SLH-phoN* were actively expressed in *D. radiodurans* as determined by Western Blot and zymograms. Interestingly, both the Hpi constructs made, Hpi-SmtA and Hpi-PhoN fusion proteins were found to be present exclusively in the membrane bound fraction in *D. radiodurans* (**Fig. 3.19 & 3.26**), making this protein an efficient membrane targeting vehicle for any future work requiring cell surface display in *D. radiodurans*. The Hpi protein has been used for patterning of nanoparticles such as gold and CdS/ZnS quantum dots [90], [91]. The results from this work show that the Hpi protein may also be used for surface display of proteins in *D. radiodurans.* In contrast, the SLH-PhoN protein was found both in the cytosol as well as membrane bound fraction of *D. radiodurans* cells, while SLH-SmtA was found exclusively in the membrane bound fraction. Therefore, utility of SLH domain in surface display in this organism is not clear. In many other Gram positive organisms such as *Paenibacillus alvei* [78] *Bacillus anthracis* and *Bacillus spahericus*, with peptidoglycan as the major cell wall component, the SLH domain has been used for surface display of proteins [75]. Broadly, in this study, all the fusion proteins achieved membrane localization as a result of their fusion to S layer proteins.

Attempts at making S layer-PhoN fusions proteins showed that only the Hpi-PhoN fusion protein showed cell based phosphatase activity in *D. radiodurans*, while SLH-PhoN did not display cell-based activity in *D. radiodurans* cells. The whole cell PhoN activity obtained in *D. radiodurans* expressing Hpi-PhoN was only half of that obtained in the earlier recombinants expressing PhoN alone **(Table 3.1)**. This implied that cell surface display did not enhance cell-based phosphatase activity of recombinant *D. radiodurans* ruling out substrate accessibility as a limiting factor for phosphatase activity. Low expression levels of Hpi-PhoN protein compared to PhoN in *D. radiodurans* cells may be a possible reason for lower activity, but is unlikely since both the proteins were expressed from P_{groESL} promoter. Hpi may have interfered with the ability of the enzyme to dimerize effectively or fold appropriately due to the large size of Hpi protein and therefore, result in lower activity. *D. radiodurans* recombinant cells bearing *SLH-phoN* fusion construct, however failed to show cell based PhoN activity on histochemical plates or in pNPP assay in solution. But cell extracts showed activity in zymograms. Perhaps the SLH-PhoN fusion protein is lodged deep into the cell wall or does not fold appropriately in the cell wall, leading to loss of activity.

The SLH domain present in S layer proteins of many organisms bind to the underlying peptidoglycan sacculus by interacting with secondary cell wall polymers (SCWP) attached to the peptidoglycan. Earlier studies carried out in *Thermus thermophilus* had shown that single SLH domain found at the N terminus of the SlpA protein bound a cell wall polymer covalently attached to the peptidoglycan [92]. This polymer was thought to be present as an envelope of thick layer of unstructured material between the peptidoglycan and the S-layer – outer membrane complex. Such an uncharacterized layer has also been visualized in *D. radiodurans* cells by TEM. An antibody raised against S layer-attached cell wall fragments of *T. thermophilus*, αSAC showed cross reactivity with cell walls of *D.*

radiodurans [59]. It was further shown that pyruvylation of the SCWP was an absolute requirement for SLH domain to bind. The function of adding a pyruvyl group to SCWP was assigned to a putative pyruvltransferase, CsaB. Further, all organisms whose genome encoded a SLH domain also harbour *csaB* gene, including *D. radiodurans*. Earlier work showed that SlpA mutants of *T. thermophilus* resulted in the outer membrane peeling off from the peptidoglycan layer suggesting that the SLH domain anchors the outer membrane to the bacterial cell wall [59]. Similar results were reported in SlpA mutant in *D. radiodurans* [54]

The presence of the SLH domain in SlpA protein in *D. radiodurans* was strongly suggestive of a similar mechanism of S layer-cell wall interaction operating in this organism also. S layer proteins from Gram-positive bacteria typically possess three SLH motifs with 10-15 conserved amino acids [93]. The SLH domain occurs in variable numbers in many types of proteins of phylogenetically unrelated bacteria [36]. In *D. radiodurans*, this study showed that the single SLH domain present in a single copy at the N terminus of SlpA is sufficient for binding peptidoglycan. The deinococcal cell wall architecture has been an enigma from the 1980's. The present study has provided the following two insights into the cell wall architecture: (1) Hpi layer interacts non-covalently with SlpA, and (2) in turn the SlpA protein interacts non-covalently with the peptidoglycan, forming continuity in the interactions between different layers of the deinococcal cell wall.

The possibility of using the peptidoglycan as an immobilization matrix for the PhoN enzyme demonstrated here is exciting, especially since peptidoglycan itself is known to adsorb uranium on its functional groups [94]. Further, peptidoglycan is a sturdy biopolymer, resistant to heat and detergents and is hydrolyzed only with concentrated mineral acids at high temperature. These virtues make SLH-peptidoglycan interaction a promising tool for enzyme/protein immobilization.

Chapter 4

Heavy metal bioremediation using recombinant proteins and bacteria

The previous chapter described the characterization of the surface layer proteins, Hpi and SlpA of *D. radiodurans* and the construction of fusion proteins Hpi-PhoN, SLH-PhoN, Hpi-SmtA and SLH-SmtA. The expression of fusion proteins and their localization in the recombinant cells was also assessed to predict their likely utility for metal bioremediation.

This chapter describes the evaluation of the S layer protein, Hpi and recombinant strains expressing various S layer fusion proteins, for their ability to remove metals from solution. Since the SmtA protein localized cytoplasmically while the SLH-SmtA and Hpi-SmtA proteins localized into membrane in recombinant *D. radiodurans* cells, the effect of such differential localization of metallothionein on metal binding ability of recombinant cells has been evaluated. While Hpi-PhoN displayed whole cell phosphatase activity, the SLH-PhoN fusion protein did not show whole cell phosphatase activity. Therefore, as an alternative, its utility in metal precipitation after immobilization on peptidoglycan was assessed. Both the recombinant organisms as well as the fusion proteins isolated from them were tested for their ability to bind/precipitate heavy metals. In addition, biomass bearing the PhoN enzyme was subjected to lyophilisation to see if its shelf life could be enhanced. The cellular localization of precipitated metals was determined by electron microscopy to explore the possibility of recovery of the metal and re-use of biomass. These results are detailed in the following sections:

4.1 Metal binding ability of deinococcal S layer protein

4.1.1 Metal binding by isolated Hpi protein

Hpi layer isolated from *D. radiodurans* was evaluated for its ability to bind uranium and cadmium. The Hpi protein could bind around 37% of 1 mM input uranium, resulting in a loading of around 166 µg uranium/mg Hpi protein, while in a similar set up without any

protein, 6.6% loss of uranium was recorded in the supernatant. In a parallel experiment with cadmium, 7-8% of cadmium was removed from supernatant in the presence or absence of Hpi protein, indicating that the protein did not bind any cadmium **(Table 4.1)**.

Table 4.1. Metal binding by Hpi protein.

Buffer conditions	Per cent U removed[a]	Per cent Cd removed[a]	Per cent uranium desorbed[b]	Re-use efficiency[c]
pH 6.5 Control	6.6 ± 2.2	7.3 ± 3	-	6 ± 1.2
pH 6.5 Hpi	37 ± 5	8.9 ± 0.3	95 ± 7	30 ± 5

[a]200 µg Hpi protein was re-suspended in 20 mM MOPS, pH 7.0 containing 1 mM uranyl nitrate/cadmium nitrate. The final pH of the solution was 6.8. A similar set-up without the Hpi protein served as control. An aliquot was removed after allowing 1 h of binding, subjected to centrifugation and the uranium in supernatant was estimated by Arsenazo-III method.

[b]Per cent uranium recovered from Hpi protein which had biosorbed 37% of uranium from a 1 mM solution.

[c]Per cent uranium removed by desorbed Hpi layer in subsequent round of uranium binding assay.

A time dependent kinetics of uranium biosorption showed that uranium bound to the Hpi protein almost instantaneously and remained associated with the Hpi protein for upto five hours at room temperature **(Fig. 4.1)**. Further, 95% of the uranium bound to Hpi could be recovered by washing the layer in 10 mM acetate buffer pH 5, and the Hpi layer could be used in another round of uranium biosorption effectively **(Table 4.1)**

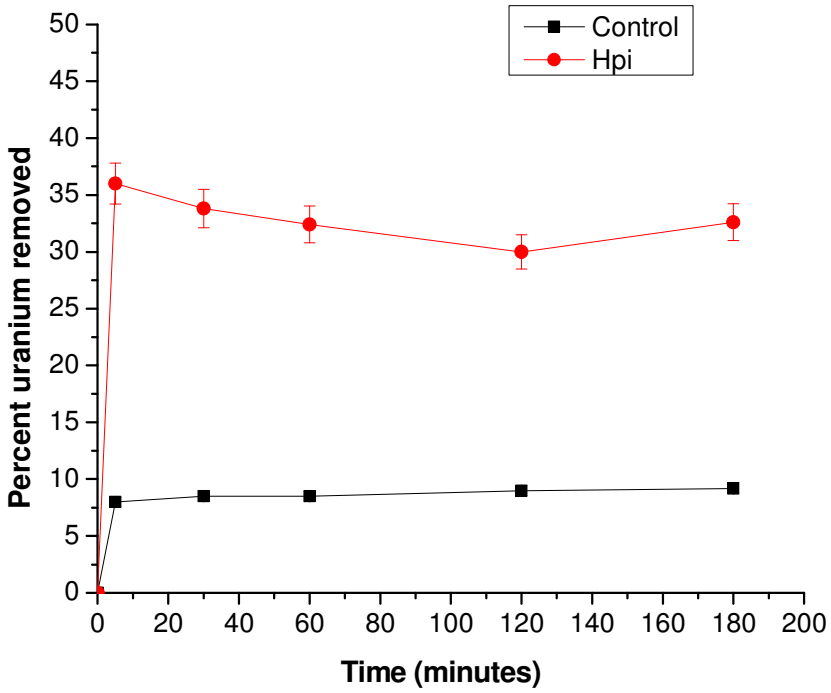

Fig. 4.1. Uranium biosorption by Hpi layer. About 200 µg of Hpi protein was incubated with 1 mM uranyl nitrate solution in 20 mM morpholinosulphonic acid (MOPS) buffer, to attain a final pH of 6.8 in 500 µl reaction volume. Timed aliquots were removed and subjected to centrifugation and uranium remaining in the supernatant was estimated by Arsenazo III reagent. The final uranium loading was 166 µg uranium/mg protein. A similar assay without any protein added served as the control.

4.1.2 Effect of Hpi on uranium binding ability and surface charge of *D. radiodurans* cells

Since the isolated Hpi layer bound uranium, an attempt was made to study its contribution towards uranium binding by whole cells. Cells of wild type *D. radiodurans* and its Hpi mutant, HMR202 cells were incubated in 1 mM uranyl nitrate solution at pH 6.8. The amount of uranium remaining in the supernatant was determined to ascertain amount of uranium biosorbed on the cell surface. The wild type cells bound almost two times more uranium than mutant cells, resulting in a loading of 113 mg uranium/g dry weight cells compared to only 50 mg uranium/g dry weight of cells bound by HMR202 cells **(Fig. 4.2a).**

(a)

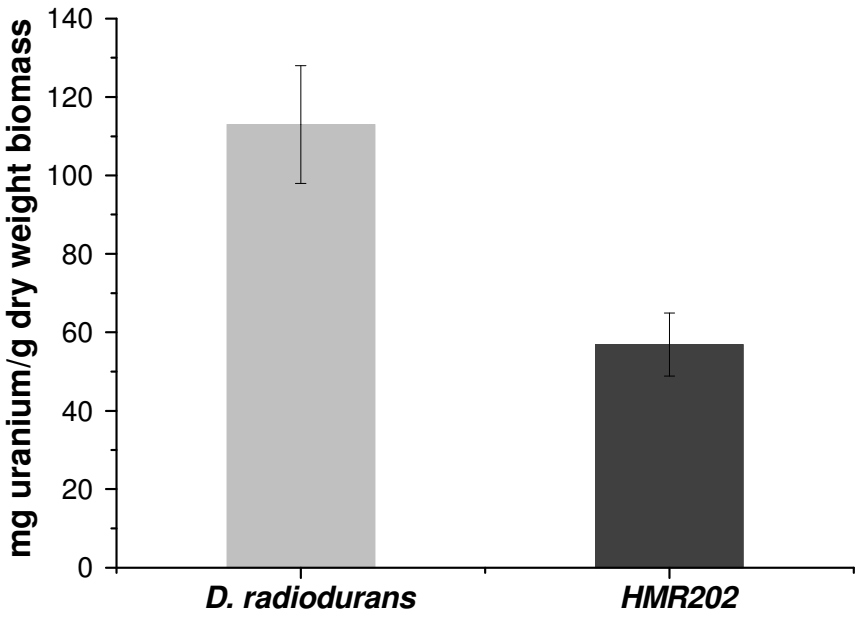

(b)

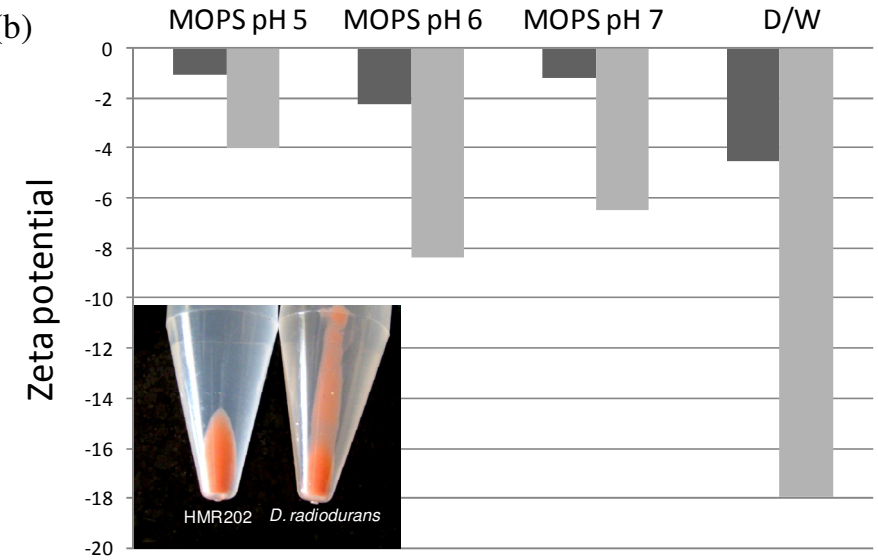

Fig 4.2. Differential uranium biosorption ability and cell surface charge of wild type *D. radiodurnas* (grey) and Hpi mutant cells, HMR202 (dark grey). (a) Uranium binding by the two cell types from a solution containing 1 mM uranium at pH 6.8. (b) Zeta potential of the two cell types recorded by re-suspending the cells at OD_{600nm} 1.0/ml in distilled water (D/W) or in buffer specified. Nature of pellet formed by the two cell types is shown (inset).

Since metal binding is usually a result of electrostatic interactions between functional groups present on cell surface and the metal, the effect of Hpi on cell surface charge was investigated by determining the zeta potential on the cell surface of wild type and HMR202 cells using a Zetameter. In distilled water, the zeta potential values of the two cell types differed widely (wild type cells at -18 mV and HMR202 cells at -4.4 mV). In buffer solutions also, zeta potential of HMR202 cells was always found to be less negative than that of wild type cells **(Fig. 4.2b).** Visually, pellets of HMR202 cells were found to be more compact than those of wild type cells, perhaps due to lesser cell to cell repulsion on account of their reduced surface charge **(Fig. 4.2b inset).** These results indicated that Hpi contributes a net negative cell surface charge which may have a bearing on metal binding by whole cells.

4.2 Metal binding by recombinant S layer-SmtA fusion proteins

4.2.1 Metal binding by recombinant bacteria expressing SmtA, Hpi-SmtA and SLH-SmtA proteins

Metal binding studies were carried out using recombinant strains, expressing various fusion proteins with different metals. The SmtA protein has earlier been shown to bind Cd, Zn and Cu [14]. Typically, concentrations of the metal, at which binding studies are carried out, are at or below the Minimum Inhibitory Concentration (MIC) of that metal for the organism. The MICs of Cd, Zn and Cu for *D. radiodurans* are 1.8 µM, 150 µM and 470 µM respectively [95]. Since, the MIC for cadmium is far too low for studying cadmium biosorption, a concentration of 5 µM was employed for studying Cd biosorption along with 150 µM for Zn and 250 µM for Cu. In subsequent studies, concentration of Cd was raised to 40 µM, though it was known to far exceed the MIC, to test whether even when cells which

are unable to grow at the inhibitory concentrations of metals used, they can still continue to show enhanced metal binding ability.

Cadmium binding studies showed that at 5 μM Cd^{2+} concentration, recombinant *D. radiodurans* cells expressing Hpi-SmtA fusion protein showed marginally higher cadmium binding than other recombinants **(Fig. 4.3a)**. Further, neither of the recombinant *D. radiodurans* cells expressing SLH-SmtA or SmtA showed improved metal binding compared to *D. radiodurans* cells expressing only the native Hpi gene or carrying empty vector pRAD1. At higher cadmium concentration, *D. radiodurans* expressing Hpi-SmtA showed a metal loading of 1.2 mg/g dry weight biomass, while all other recombinants showed metal binding in the range of 0.5 mg/g dry weight biomass **(Fig. 4.3b)**. On the other hand, when recombinant *E. coli* cells were used for cadmium biosorption, recombinants expressing SmtA gene alone showed superior metal binding (1.2 mg/g dry weight biomass) ability compared to other recombinant strains (0.5 mg/g dry weight biomass). Cadmium bound by recombinant *E. coli* cells expressing Hpi-SmtA or SLH-SmtA was in the same range as control cells carrying pRAD1 alone **(Fig. 4.4).**

(a)

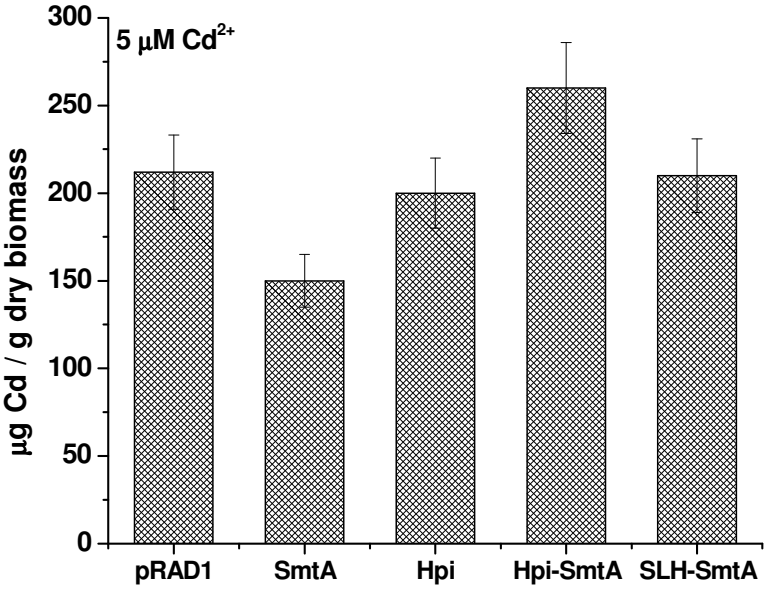

(b)

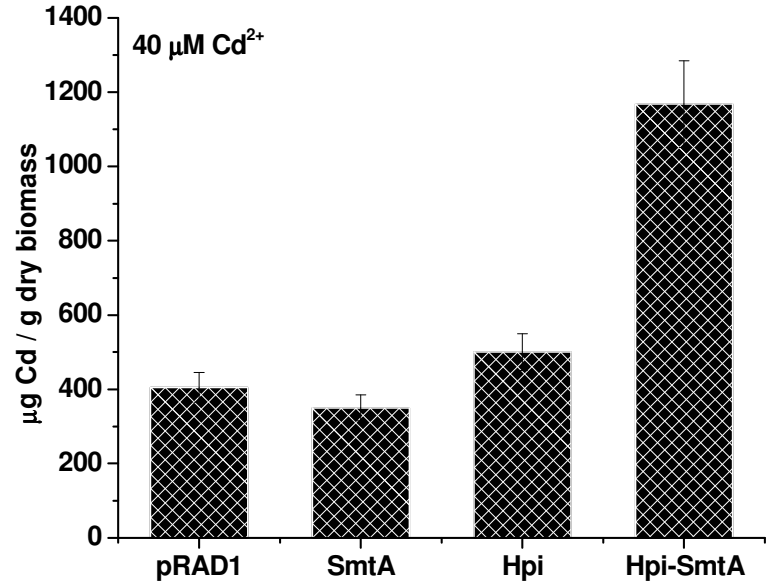

Fig. 4.3. Cadmium binding using recombinant *D. radiodurans* cells at two different concentrations of (a) 5 µM and (b) 40 µM Cd^{2+}. Recombinant *D. radiodurans* cultures were grown to an OD_{600nm} of 0.6/ml or ~3.0/ml, to which cadmium was added at 5 µM or 40 µM, respectively. The cultures were allowed to grow for 16 h after which they were subjected to centrifugation. The cell pellets were washed in medium, dried and digested in conc. HNO_3. Amount of metal in the digested samples was determined by Atomic Absorption Spectrophotometer (AAS).

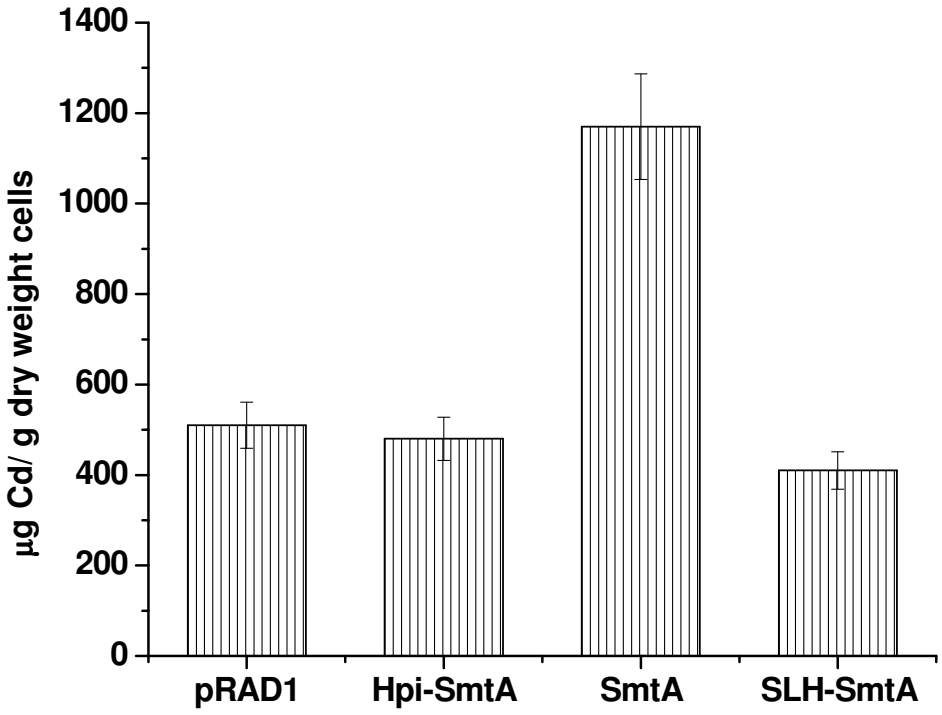

Fig. 4.4. Cadmium binding using recombinant *E. coli* cells. Recombinant cell cultures were grown to an OD_{600nm} of 0.6/ml, to which cadmium was added at 40 µM. Rest of the details were as described in legend to Fig. 4.3.

On using copper and zinc in metal binding experiments employing recombinant *D. radiodurans* cells, a similar trend as that seen for cadmium was observed. Recombinants expressing Hpi-SmtA could bind 225 µg Cu/g dry weight biomass compared to all other recombinants which showed a binding of around 125 µg/g dry weight biomass **(Fig. 4.5a)**. Similarly, *D. radiodurans* cells expressing Hpi-SmtA could bind around 210 µg Zn/g dry weight biomass compared to around 125 µg/g dry weight biomass by all other recombinants **(Fig. 4.5b)**. Also, *D. radiodurans* cells overexpressing Hpi did not show significantly higher metal binding than the other recombinants, though in all experiments they showed marginally higher metal binding than all other recombinants, except *D. radiodurans* expressing Hpi-SmtA.

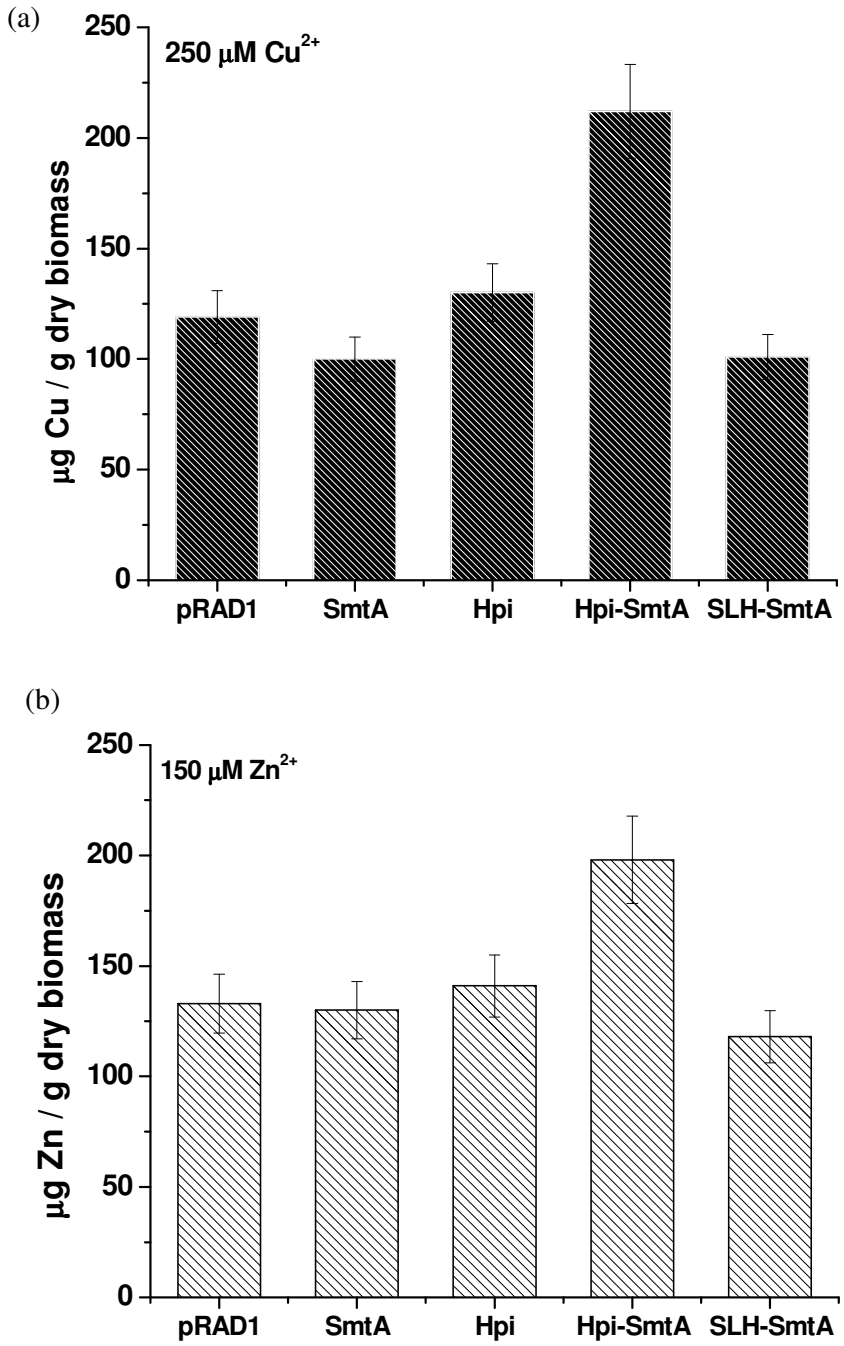

Fig 4.5. Copper (a) and zinc (b) binding using recombinant *D. radiodurans* cells. Recombinant *D. radiodurans* cultures were grown to an OD_{600nm} of 0.6/ml, to which Zn or Cu was added at 150 µM and 250 µM, respectively. Rest of the details were as described in legend to Fig. 4.3.

Independent heterologous expression of *hpi* and *smtA* genes did not result in higher metal binding by *D.radiourans* recombinant cells, but fusion of these two genes did. This implied that surface display of the SmtA on account of its tagging to the Hpi protein enhances the metal binding ability of recombinant cells expressing them. Metal binding by *D. radiodurans* recombinant cells was unaffected as a result of fusion of SmtA to the SLH domain. Among *E. coli* cells, neither fusion of SmtA to Hpi nor SLH domain, increased metal binding by recombinant cells. However, recombinant *E. coli* cells expressing *smtA* gene alone bound two times more cadmium **(Fig. 4.4)** than all other *E. coli* recombinants tested.

4.2.2 Cadmium binding by Hpi layer isolated from recombinant *D. radiodurans*

The Hpi layer was isolated from *D. radiodurans* carrying pRAD1 or *hpi-smtA* fusion construct. When used at equal protein concentration for removing metal from a 1 mM solution, Hpi from both the recombinants removed the metals at comparable efficiencies, of 20 - 25 µg/mg protein of cadmium and 16 - 19 µg/mg protein for zinc **(Table 4.2).** Studies were not carried out for copper, since it spontaneously precipitated out from solution in 20 mM MOPS, pH 7.0.

Table 4.2. Metal binding by isolated Hpi layer.

Metal	Metal bound by Hpi layer isolated from cells carrying pRAD1 alone (µg/mg dry weight protein)	Metal bound by Hpi layer isolated from cells expressing Hpi-SmtA (µg/mg dry weight protein)
Cadmium	21 ± 2.3	25 ± 3
Zinc	16 ± 2	19 ± 1.5

4.3 Metal precipitation by recombinant bacteria over-expressing PhoN

In general, an input metal concentration of 1 mM was used for metal precipitation by recombinants cells or proteins constructed in this study. The main purpose of this study was to investigate if metals can be removed at such low concentrations. Assays at this concentration were used to compare metal precipitation efficiencies of recombinants carrying these constructs with earlier constructs and among themselves. Values for metal removal have been given in per cent for ease of comparison between different recombinants and the loading values have been included in the text.

4.3.1 Cadmium precipitation by recombinant *E. coli* strain expressing *phoN*

All earlier studies involving recombinants expressing *phoN* gene were carried out to precipitate uranium from solution [51]. Since phosphatase based metal precipitation is essentially non-specific in nature, any metal can be precipitated using this approach. As cadmium is a highly toxic metal, the PhoN based approach was evaluated for its precipitation.

The optimum pH for whole cell phosphatase activity as well as for cadmium precipitation was determined in *E. coli* cells bearing *phoN*. While the optimum pH for phosphatase activity was 5.0, optimum pH for cadmium precipitation was 7.0 **(Fig. 4.6).** In addition, the curve for phosphatase activity over various pH was quite broad; in the range of 4-7, with the activity dipping at pH 8 and 9. Cadmium precipitation on the other hand was optimum in the range of 6.5-7.5. This implied that metal precipitation mediated by this phosphatase occurred best in the near-neutral range.

At 1 mM concentration, at pH 7, 83% of the cadmium was precipitated in 3 h using 5 mM β-glycerophosphate as substrate and 0.3 OD_{600nm}/ml cells in 5 ml assay **(Table 4.3).** Nearly all the cadmium removed from the supernatant was recovered in the cell pellet. Spontaneous precipitation of cadmium in assay solution and sorption to the container walls, if

any, accounted for only 8% of precipitated cadmium **(Table 4.3).** In the absence of β-glycerophosphate or the cloned *phoN* gene, cadmium removal from solution was found be to be very low (15%, Table 4.3). Biosorption of cadmium, thus, may account for only 7% of the precipitated cadmium.

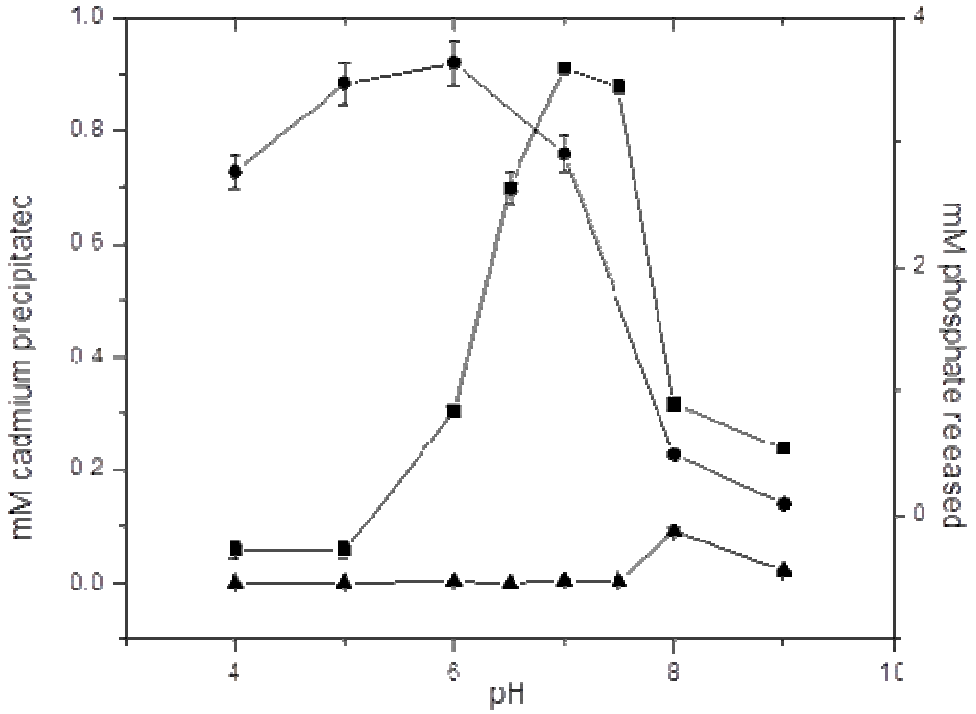

Fig. 4.6. The pH dependence of PhoN phosphatase activity and metal precipitation ability of recombinant *E. coli* cells expressing *phoN*. Amount of phosphate released from β-glycerophosphate (●) and amount of cadmium precipitated (■) from 1 mM cadmium nitrate solution containing 5 mM β-glycerophosphate in 3 h are shown as a function of pH. The different buffers used at 20 mM strength for these assays are acetate buffer for pH 4 & 5; Morpholinosulphonic acid (MOPS) for pH 6 & 7; and Tris-Cl for pH 8 & 9. Amount of cadmium precipitated by *E. coli* cells bearing empty vector alone (▲) served as control.

Table. 4.3. Phosphatase activity and uranium precipitation ability of *E. coli* cells expressing PhoN.

System used	PhoN Activity (nmoles pNP/min / mg cell protein)	Cadmium removed (% removed from a 1 mM solution in 3 h)
E. coli cells bearing *phoN*	932 ± 43	
With 5 mM β-glycerophosphate	-	83 ± 5
Without β- glycerophosphate	-	15 ± 2
E. coli cells carrying vector alone	64.6 ± 10	16 ± 3
No cells	-	8 ± 3

4.3.2 Comparison of uranium and cadmium precipitation by recombinant cells expressing *phoN*

Recombinant *D. radiodurans* and *E. coli* cells expressing PhoN were compared for their ability to precipitate uranium and cadmium. *E. coli* (PhoN) and *D. radiodurans* (PhoN) cells could precipitate 90% of 1 mM cadmium from solution in 3 h **(Fig. 4.7)** compared to uranium which took 6 h. Also, as expected, *D. radiodurans* (PhoN) cells took much longer to precipitate either of the metals than *E. coli* (PhoN) cells, since the specific activity of PhoN in the former was much lower than that in the latter.

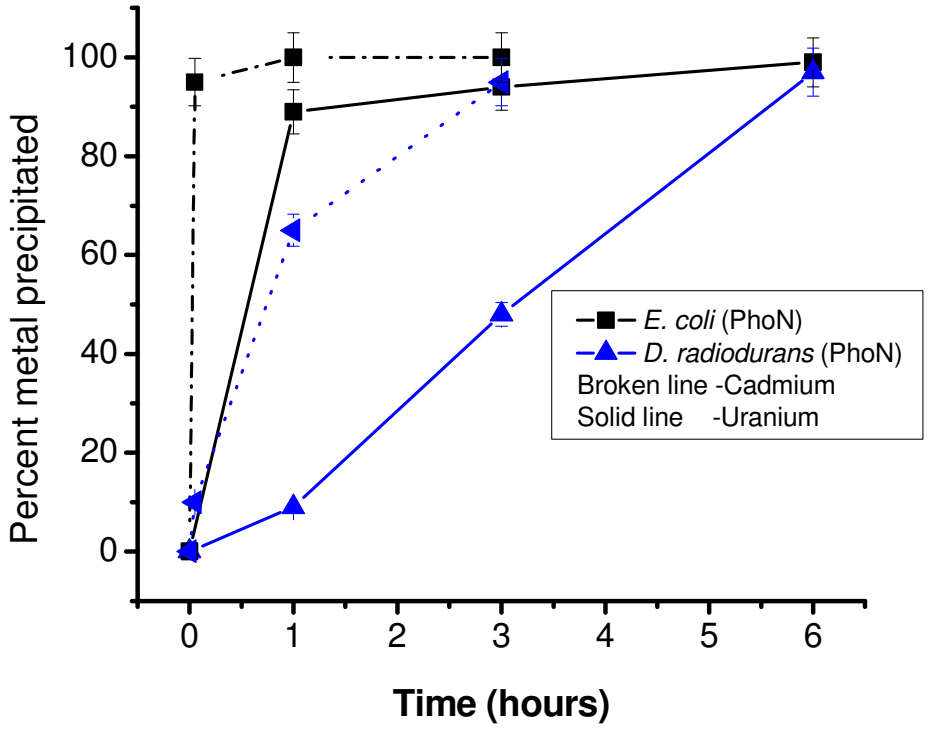

Fig. 4.7. Kinetics of bioprecipitation of uranium and cadmium by *E. coli* (PhoN) and *D. radiodurans* (PhoN) cells. Recombinant cells were used to precipitate 1 mM cadmium nitrate or uranyl nitrate from solution using 5 mM β-glycerophosphate in 2 mM acetate buffer (pH 5.0). The final pH of the solution was 6.8. Timed aliquots were taken, cell suspension was subjected to centrifugation and the metal remaining in the supernatant was determined. Uranium was estimated using Arsenazo III reagent and cadmium was estimated by AAS.

4.4 Uranium precipitation by recombinant S layer-PhoN fusion proteins

4.4.1 Uranium precipitation by *D. radiodurans* cells expressing Hpi-PhoN and Hpi layer isolated from this recombinant

On using recombinant cells in a typical uranium precipitation assay at OD_{600nm} 3.0/ml, *D. radiodurans* (Hpi-PhoN) and HMR202 (Hpi-PhoN) cells could precipitate far less uranium than *D. radiodurans* (PhoN) cells. In 6 h, *D. radiodurans* (PhoN) cells could remove

as much as 83% uranium leading to a loading 310 µg U/mg dry weight cells, while Hpi-PhoN bearing recombinants could remove only 40-50% of input uranium leading to a loading of 136-185 µg U/mg dry weight cells **(Fig. 4.8a).** However, when the cell densities were adjusted to equivalent PhoN specific activities in uranium precipitation assays, the uranium precipitation kinetics were similar. In order to equalize phosphatase activity, higher cell density of OD_{600nm} 6-6.5/ml were used for recombinants expressing Hpi-PhoN. An appropriate control of similar cell density of *D. radiodurans* cells carrying pRAD1 alone was also included. Such control cells at the higher cell density employed, could remove 25% (94 µg U/mg dry weight cells) uranium from solution which appears to be a result of biosorption and presence of native phosphatases which contribute to metal precipitation **(Fig. 4.8b).**

(a)

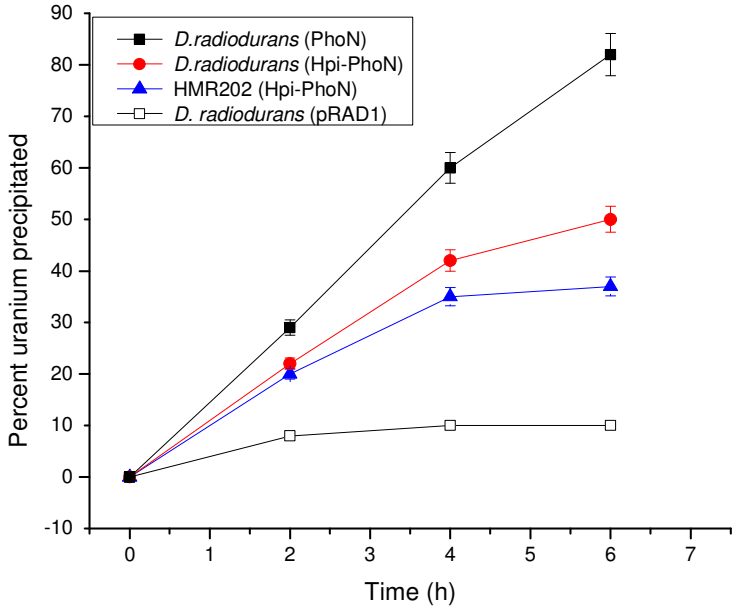

(b)

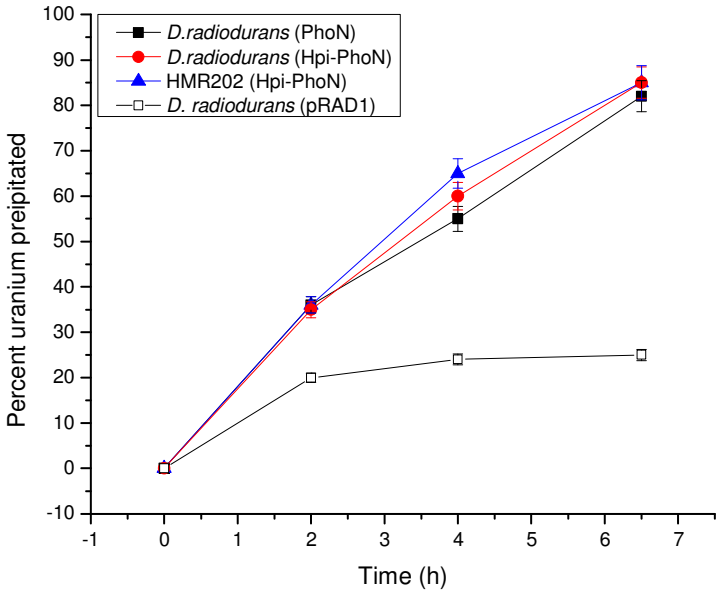

Fig. 4.8. Uranium precipitation by *D. radiodurans* recombinant cells expressing PhoN or Hpi-PhoN. Recombinant cells at OD_{600nm} 3.0/ml (a) or at equal phosphatase activity (b) were used in a uranium precipitation assay comprising 1 mM uranyl nitrate, 5 mM β-glycerophosphate in 2 mM acetate buffer pH 5.0 (final pH 6.8). Suspensions were subjected to centrifugation and the uranium remaining in the supernatant was estimated using Arsenazo III reagent.

To evaluate whether the Hpi layer isolated from recombinants expressing Hpi-PhoN fusion protein could also precipitate uranium from solutions, equal amount of isolated Hpi protein (400 ug/ml) from *D. radiodurans* (pRAD1) and *D. radiodurans* (Hpi-PhoN) cells were used in a typical uranium precipitation assay. As seen, Hpi layer itself from pRAD1 cells could remove around 39% of 1 mM uranium (208 µg U/mg protein), while that from Hpi-PhoN expressing cells could remove 75% of 1 mM uranium in 24 h (446 µg U/mg protein) **(Fig. 4.9).** However, it was observed that when the Hpi layer isolated from Hpi-PhoN expressing cells was extensively washed in water during preparation, it lost phosphatase activity and showed uranium removal comparable to that from cells bearing pRAD1 alone. This seemed to indicate that the Hpi-PhoN was not firmly anchored in the Hpi layer.

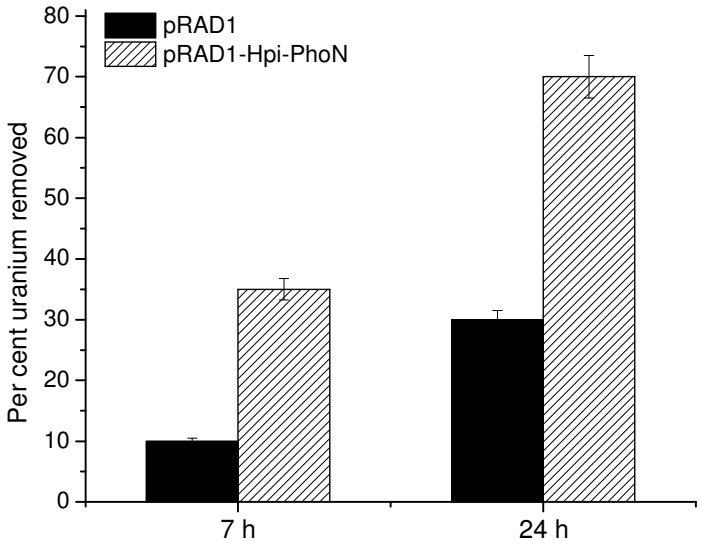

Fig. 4.9. Uranium precipitation by Hpi isolated from recombinant *D. radiodurans* cells. Hpi protein isolated from recombinant *D. radiodurans* cells were re-suspended at 400 µg/ml concentration in a solution containing 1 mM uranyl nitrate, 5 mM β-gycerophosphate and 2 mM acetate buffer, pH 5.0 (final pH 6.8). Suspensions were subjected to centrifugation and the uranium remaining in the supernatant was estimated using Arsenazo III reagent.

4.4.2 Uranium precipitation by SLH-PhoN protein immobilized on peptidoglycan

The utility of SLH-PhoN recombinant protein immobilized on peptidoglycan, for precipitation of uranium was evaluated. Since the interaction between the protein and peptidoglycan is predominantly non-covalent in nature, an attempt to stabilize this interaction was made by treatment with glutaraldehyde.

SLH-PhoN immobilized on peptidoglycan (SPhoNP) was treated with 0.2% glutaraldehyde at 4°C in 100 mM acetate buffer for one hour and washed in acetate buffer twice. Studies on uranium precipitation by glutaraldehyde treated and un-treated SPhoNP were done by re-suspending it in a solution containing 1 mM uranyl nitrate and 5 mM β-glycerophosphate in 2 mM acetate buffer. At the end of 6 h, the peptidoglycan was re-suspended in fresh metal solution and this was repeated for around 6 cycles to evaluate the stability of SPhoNP

SPhoNP could remove 95% uranium from a 1 mM uranyl nitrate solution in ~4 h. SPhoNP which was not treated with glutaraldehyde retained uranium precipitation ability for three cycles, after which the amount of uranium precipitated in 4 h fell to 60% in the fourth cycle and 50% in the fifth cycle. SPhoNP treated with glutaraldehyde, however retained uranium precipitation ability for five cycles to display a total loading of around 160 µg U/mg dry biomass weight **(Fig. 4.10).** However, after the 5^{th} cycle even glutaraldehyde treated SPhoNP showed decreased uranium removal. Peptidoglycan alone, on the other hand, could remove around 20% uranium in the first cycle of metal precipitation assay, after which it did not bind any uranium in subsequent cycles.

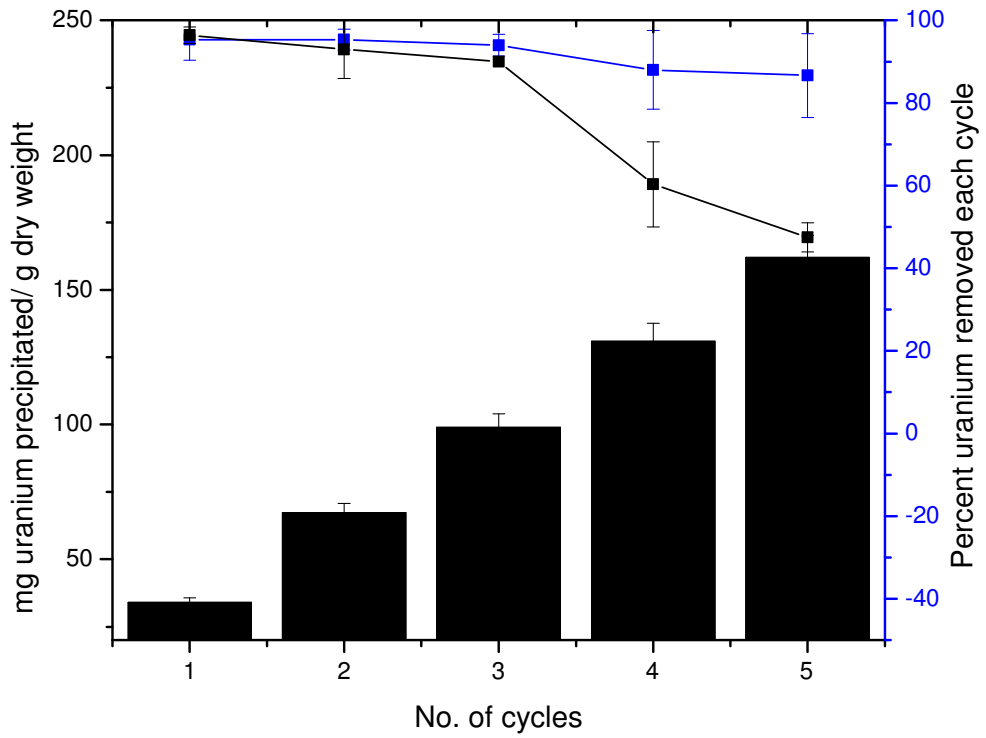

Fig. 4.10. SLH-PhoN immobilized on peptidoglycan for uranium precipitation. Seven mg of SPhoNP was re-suspended in 1 ml of solution containing 1 mM uranyl nitrate, 5 mM β-gycerophosphate and 2 mM acetate buffer, pH 5.0 (final pH 6.8). Rest of the conditions were as specified for legend to Fig. 4.9. Blue (glutaraldehyde treated) and black (glutaraldehyde un-treated) lines represent the per cent uranium removed in each cycle of uranium precipitation, and the bar graph represents the total uranium loading.

4.4.3 Comparative uranium precipitation by different biomass carrying the PhoN protein

In order to evaluate which of the aforesaid biomass is most efficient in precipitating uranium, equal dry weight of *D. radiodurans* (PhoN) cells, *D. radiodurans* (Hpi-PhoN) cells and SPhoNP were used for uranium precipitation in a typical assay. Around 3 mg dry weight biomass was used in a 5 ml assay. It was found that of all the biomass, the SPhoNP could remove uranium from solution more rapidly, followed by *D. radiodurans* (PhoN) and finally *D. radiodurans* (Hpi-PhoN) **(Fig. 4.11).** While SPhoNP removed 317 µg U/mg biomass in 4

h, recombinants expressing PhoN alone and Hpi-PhoN precipitated 230 µg U/mg cells and 138 µg U/mg cells respectively, showing superiority of SPhoNP in precipitating U.

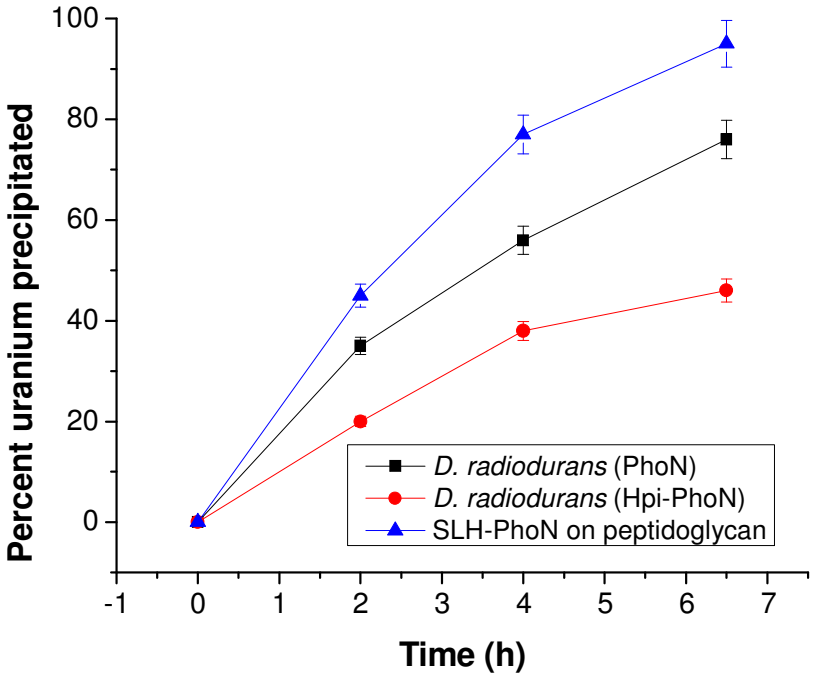

Fig. 4.11. Comparison of PhoN carrying biomass for uranium precipitation. Three mg dry weight of different biomass bearing PhoN were used in 5 ml of a typical uranium precipitation assay. Other details were as given in legend to Fig. 4.9.

4.5 Lyophilisation of PhoN expressing recombinant bacteria for metal precipitation

Both *E. coli* as well as *D. radiodurans* recombinant cells expressing PhoN were subjected to lyophilisation to make the handling of the biomass easy. Its effect on cell integrity, metal precipitation ability and shelf life were studied.

4.5.1 Effect of lyophilisation on cell integrity as observed by Scanning electron Microscopy

Scanning electron microscopy of *E. coli* cells bearing *phoN* indicated that

lyophilisation without lyo/cryoprotectant did not grossly disrupt the cell morphology or result in bursting of cells **(Fig. 4.12a & b).** The treatment, however, resulted in flattening of cells, a noticeable depression in the middle and surface roughness compared to smoother and rounded appearance of fresh cells **(Fig. 4.12a and b).** In case of *D. radiodurans* (PhoN) cells also, electron microscopy **(Fig. 4.12c and d)** showed no gross morphological damage to cells after lyophilisation except that they looked deflated as compared to the plumper appearance of fresh cells. However, in both cases no evidence of rupture or disintegration of cells after lyophilisation could be seen.

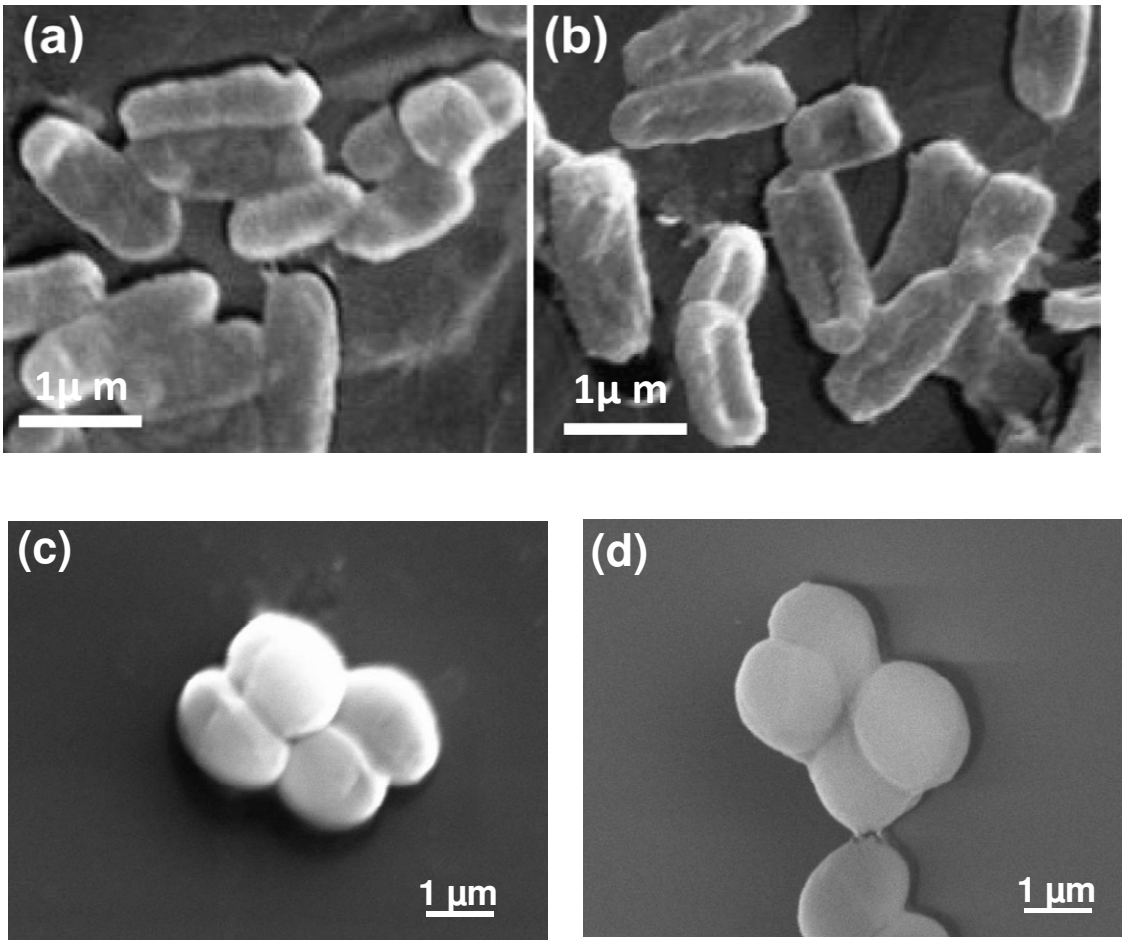

Fig. 4.12. Effect of lyophilisation on cell morphology as observed by scanning electron microscopy. SEM images of *E. coli* (PhoN) [(a) and (b)] and *D. radiodurans* (PhoN) cells [(c) and (d)] before [(a) and (c)] and after [(b) and (d)] lyophilisation.

4.5.2 Cadmium precipitation by lyophilised recombinant *E. coli* cells expressing *phoN*

Lyophilised cells could precipitate 80% of 1 mM cadmium in 3 h at efficiencies identical to those of re-suspended fresh cells **(Table 4.4)**. Lyophilised *E. coli* cells were not viable, but could be stored at room temperature for upto 6 months with only 5% loss in the cadmium precipitation ability **(Table 4.4).**

Table 4.4. Effect of lyophilisation of *E. coli* cells bearing *phoN* on phosphatase activity, cadmium precipitation and cell viability.

System used	PhoN Activity (nmoles pNP / min / mg cell protein)	Cadmium removed (% removed from a 1mM solution in 3 h)	Viability(CFU/ml)[a]
Re-suspended fresh *E. coli* cells bearing *phoN*	932 ± 43		(7.5 ± 0.63) X 10^{10}
Lyophilized cells following storage for			
0 month	989 ± 59	83 ± 7	600 ± 30
1 month	850 ± 89	ND	0
3 months	832 ± 16	ND	0
6 months	781 ± 20	79 ± 4	0

The metal precipitation ability of lyophilised *E. coli* (*phoN*) cells was also tested at higher cadmium concentrations to estimate the extent to which these cells could be loaded with the metal. Total amount of cadmium precipitated increased with increase in cadmium concentration, saturating at 5 mM cadmium **(Fig. 4.13a),** when the concentration of phosphate liberated from 5 mM β-glycerophosphate became limiting. The cells could remove 57–90% of the cadmium present in solution in 24 h at Cd^{2+}concentrations of 0.1-5 mM, respectively.

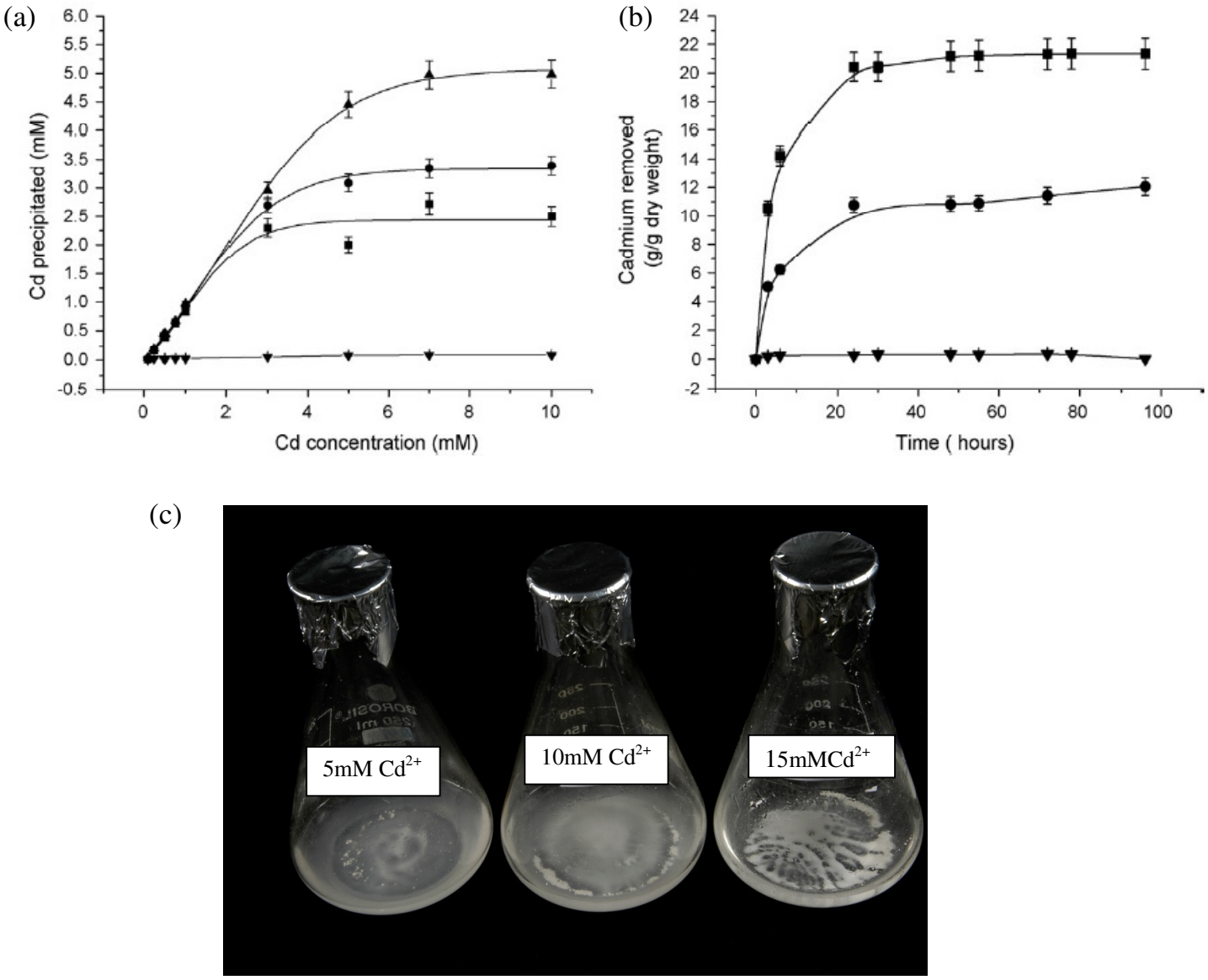

Fig. 4.13. Cadmium bioprecipitation by lyophilised *E. coli* cells bearing PhoN. (a) Effect of cadmium concentrations on metal removal in the presence of 5 mM β-glycerophosphate. Cadmium precipitation was monitored after 3 h (■), 6 h (●), and 24 h (▲) in *E. coli* cells expressing PhoN and 6 h (▼) in *E. coli* cells carrying empty vector alone. (b) Cadmium precipitation using lyophilised *E. coli–phoN* cells (10 mg) in 100 mM MOPS pH 7.0 containing 15 mM cadmium and β-glycerophosphate at 15 mM (●) or 30 mM (■). *E. coli* cells carrying empty vector cells were included as control (▼). (c) Settling down of cells after cadmium precipitation at different metal concentrations.

Depending on the availability of phosphate donor, the lyophilised cells could accumulate nearly 12 g cadmium/g dry weight at 15 mM β-glycerophosphate, which increased to a loading of 21 g/g dry weight at 30 mM β-glycerophosphate over a 4 d period **(Fig. 4.13b).** More than 90% of this precipitation was accomplished in <1d. During this time, the cadmium laden cells became heavy and settled to the bottom of the container as shown in **Fig. 4.13c.**

4.5.3 Lyophilisation of S layer-PhoN fusion protein bearing biomass

D. radiodurans (PhoN), *D. radiodurans* (Hpi-PhoN) and SPhoNP treated with glutaraldehyde were all subjected to lyophilisation as described in Chapter 2. Freshly re-suspended or lyophilised biomass was used in uranium precipitation assays, to evaluate effect of lyophilisation. In lyophilised recombinant *D. radiodurans* strains, at the end of 4 h, around 10-15% lesser uranium was precipitated compared to fresh biomass. However, in case of SPhoNP, uranium precipitation kinetics were unaffected by lyophilisation as shown in **Fig. 4.14.** Here too, lyophilized SPhoNP showed the best performance precipitating 83% of uranium in 4 h leading to loading of 329 µg U/mg dry weight biomass compared to 46% (182 µg U/mg dry weight cells) and only 26% (103 µg U/mg dry weight cells) by *D. radiodurans* (PhoN) and *D. radiodurans* (Hpi-PhoN) respectively **(Table 4.5)**.

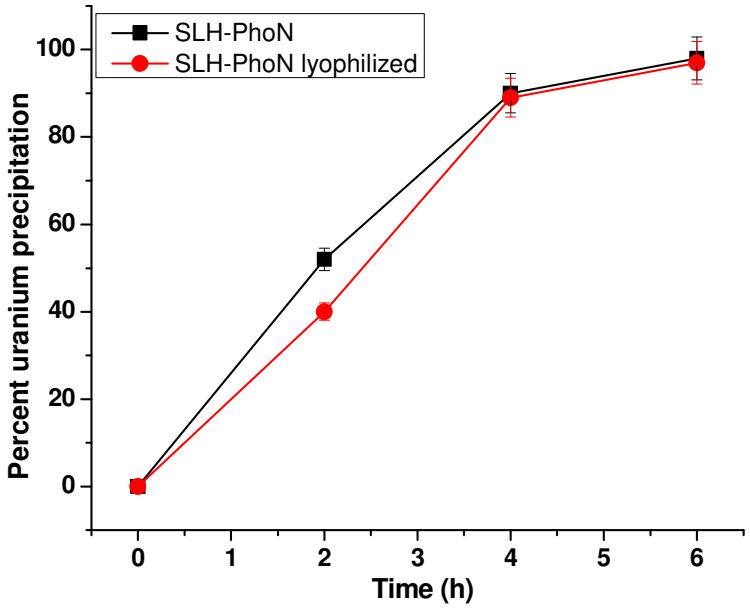

Fig. 4.14. Effect of lyophilisation on uranium precipitation by SPhoNP. Around 7 mg dry weight/ml of SPhoNP was used in a typical uranium precipitation assay containing 1 mM uranyl nitrate and 5 mM β-glycerophosphate in 2 mM acetate buffer before and after lyophilisation. Rest of the details were as described in legend to Fig. 4.9.

Table 4.5. Effect of lyophilisation on uranium precipitation

	D. radiodurans (PhoN)	*D. radiodurans* (Hpi-PhoN)	SPhoNP
U precipitated by fresh biomass	55 ± 4	38 ± 6	85 ± 8
U precipitated by lyophilised biomass	46 ± 2	26 ± 3	83 ± 6

All values refer to the amount of uranium precipitated in 4 h by 3 mg of biomass in a 5 ml typical metal precipitation assay.

4.6 Cell Surface localization of metal phosphate precipitates

4.6.1 Electron microscopy to visualize surface association of metal precipitate

Lyophilized cells, which had precipitated all of 1 mM cadmium did not look markedly different from cells which had not precipitated any cadmium **(Fig. 4.15 a & b)**, but had a

'coated' appearance, with the coating being more concentrated at poles. Cells which had been exposed to 15 mM cadmium and precipitated around 10 g cadmium/g dry weight of cells showed dense precipitate on the cell surface indicating that the precipitate was fully cell associated. The precipitate appeared as clumps attached to the cell surface **(Fig. 4.15c)** and had a general amorphous appearance.

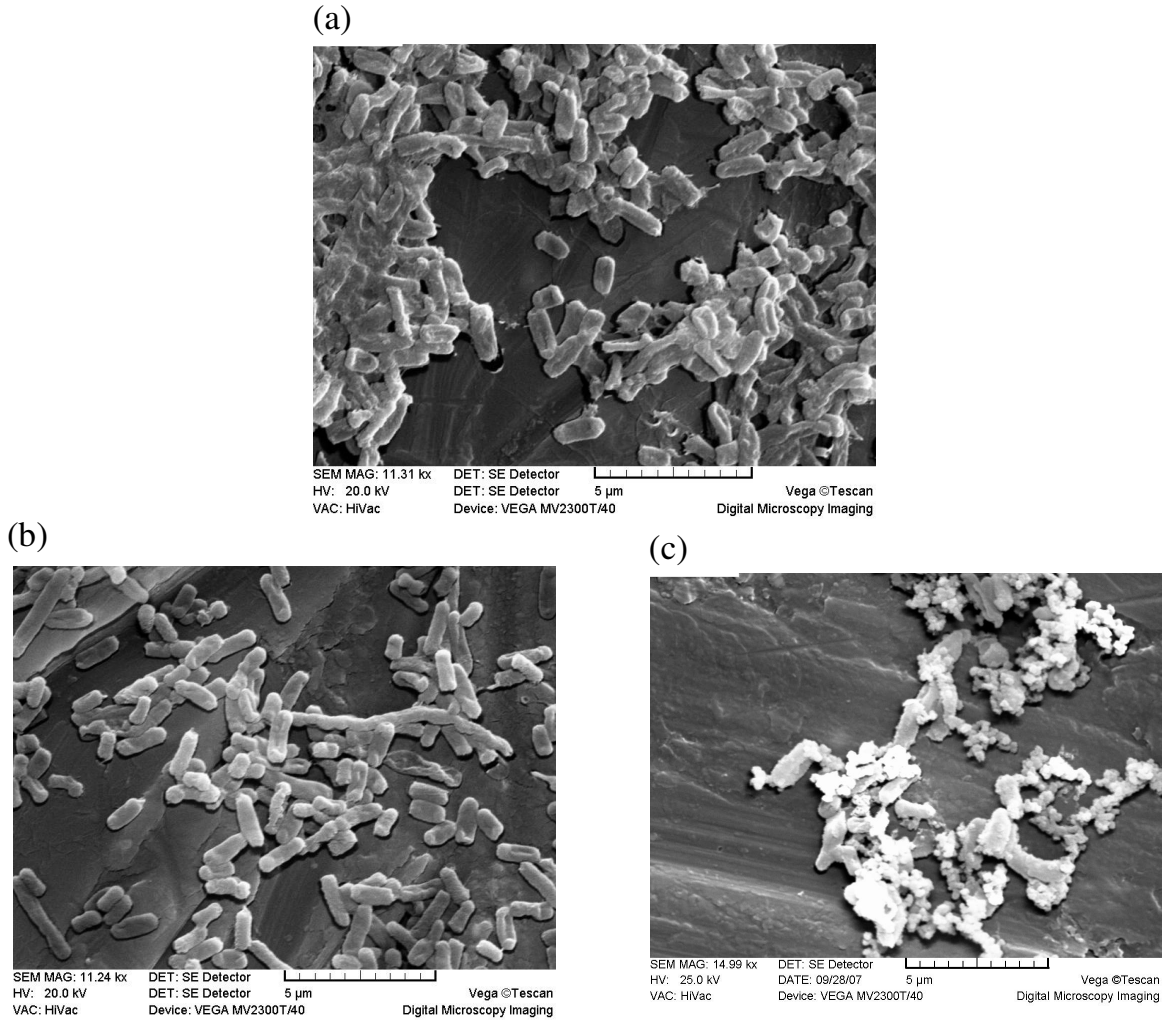

Fig. 4.15. Localization of cadmium phosphate precipitated by *E. coli* cells expressing PhoN. Scanning electron microscopy images of *E. coli* cells expressing PhoN which had been exposed to 1 mM cadmium (b) or 15 mM cadmium (c) with 5 mM and 30 mM β-glycerophosphate respectively, to result in metal loading of 178 µg or 10 g Cd/g dry weight cells. Cells exposed to metal but no phosphate source, were included as control (a).

EDXS data of such cells revealed that the precipitate contained cadmium and phosphorous in a ratio of 1:1 indicating that the precipitate was likely to be $CdHPO_4$ **(Fig.4.16)**. In the absence of β-glycerophosphate, lyophilized cells did not show any deposit on the cell surface **(Fig. 4.16a, inset)**. No cadmium or phosphorous could be detected in such cells **(Fig. 4.16a).**

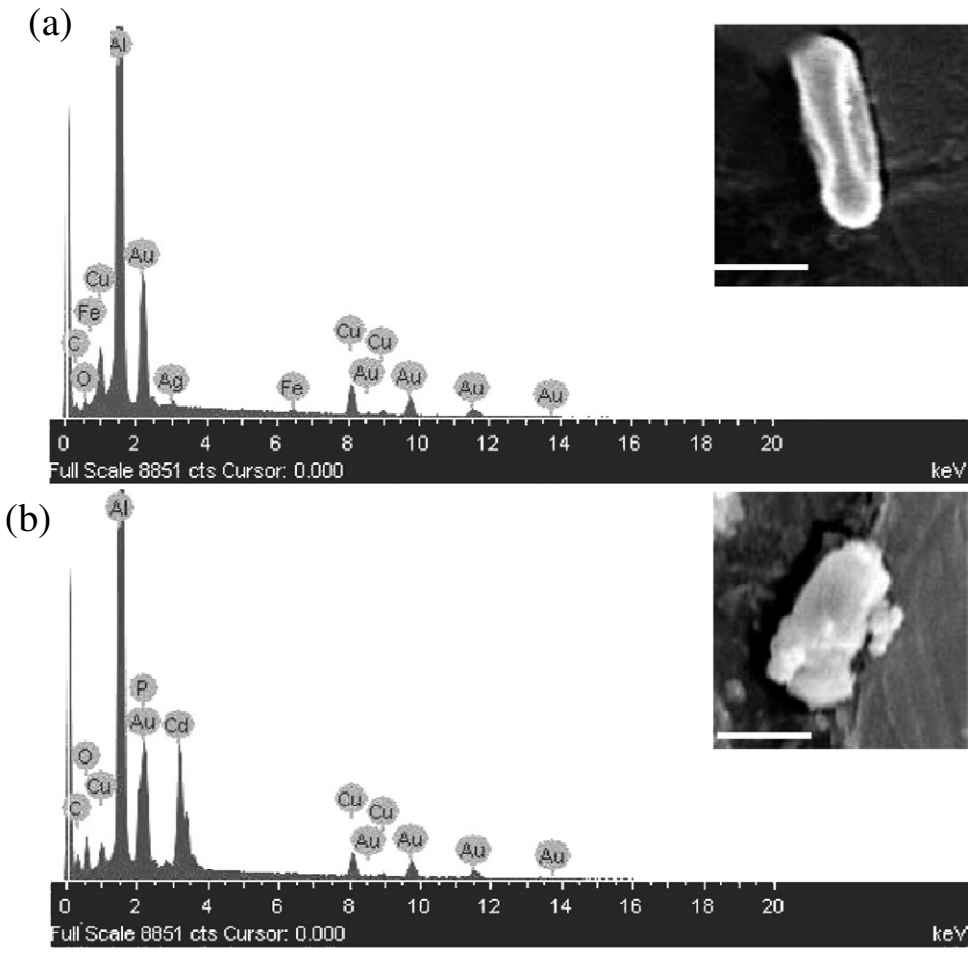

Fig. 4.16. EDX spectra and scanning electron microscopy (insets) of metal laden lyophilized *E. coli* cells expressing *phoN*. Cells were incubated with 15 mM cadmium and with (b) or without (a) 30 mM β-glycerophosphate for 24 h. Cadmium loading in cells shown in (b) was 10 g cadmium/g dry weight of cells while no cadmium or phosphorous was detected in control cells shown in (a). EDXS data from cadmium-laden cells show presence of cadmium:phosphorus in a 1:1 ratio with percent atomic composition of 3.61% and 3.09%, respectively. Aluminium and other metal peaks are due to the studs and gold is from the coating. Bars specify 500 nm.

D.radiodurans (PhoN) cells which had precipitated around 0.3 g uranium/g dry weight of cells exhibited a few uranyl phosphate deposits on the surface **(Fig. 4.17b).** At higher loading of 3.2 g uranium/g dry weight of cells, the entire cell surface was covered with a meshwork of S-shaped (sigmoid) fiber-like precipitate giving the cells a cottony appearance **(Figs. 4.17b** & **4.18a**). At all times, the precipitate remained associated with biomass and no loose precipitate was observed across several SEM fields **(Figs. 4.17a, 4.17b, 4.18a)** or in chemical analysis.

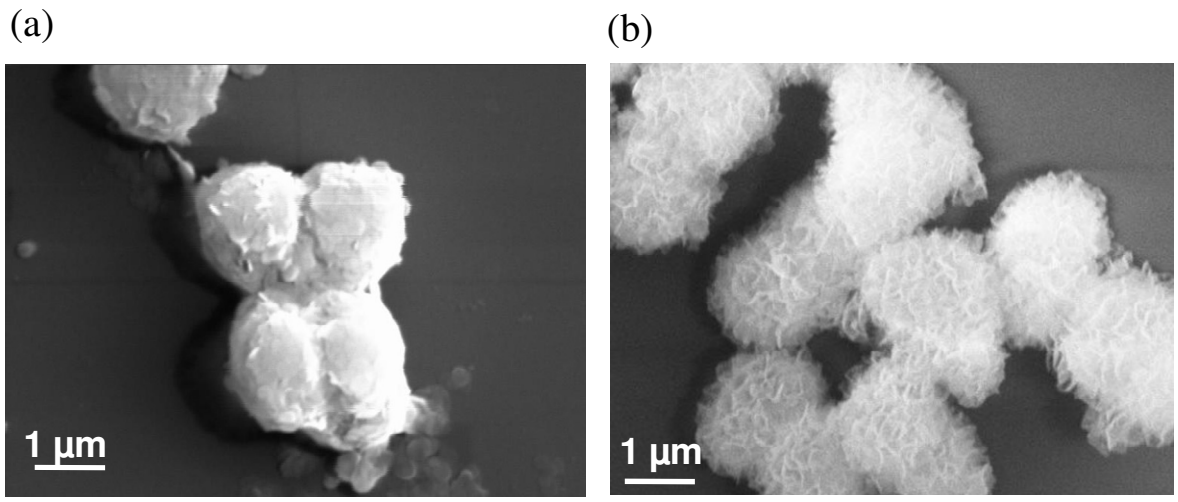

Fig. 4.17. Localization of uranium phosphate precipitated by *D. radiodurans* cells expressing PhoN. Scanning electron micrographs of *D. radiodurans* cells which had been exposed to 1 or 10 mM uranium and 5 mM or 20 mM β-glycerophosphate respectively for 10 d to achieve a loading of (a) 0.3 g uranium/g dry weight cells and (b) 3.2 g uranium/g dry weight respectively.

Energy Dispersive X-ray spectroscopy of *D. radiodurans* (PhoN) cells which had precipitated 95% of uranium from a solution of 10 mM and 20 mM β-glycerophosphate in 7 days (3.2 g uranium/g dry weight of lyophilized cells) showed distinct presence of uranium

and phosphorus peaks **(Fig. 4.18b).** In comparison, in *D. radiodurans* (pRAD1) cells which had been exposed to similar conditions for similar length of time, neither the surface associated structures were visible **(Fig. 4.18c)** nor was uranium and phosphorus detected by EDX **(Fig. 4.18d).**

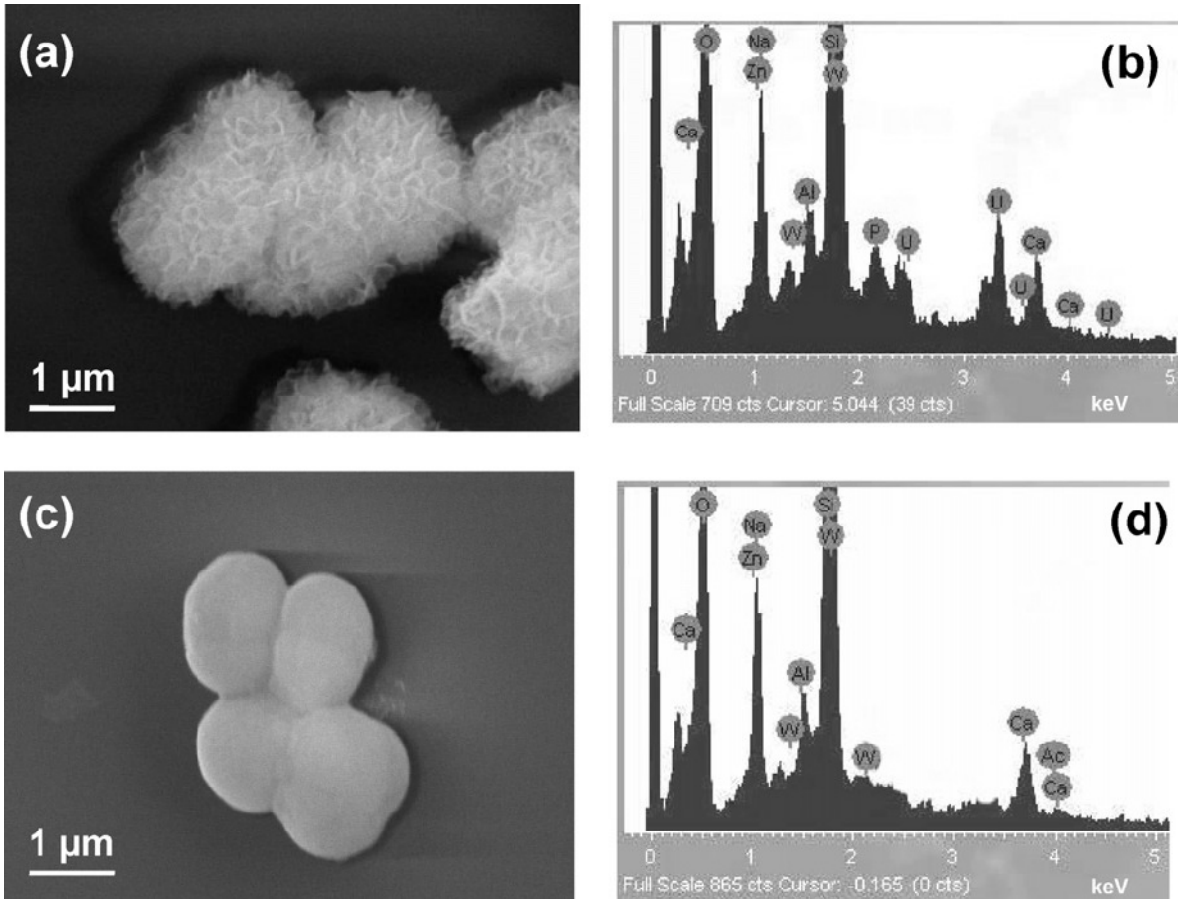

Fig. 4.18. Scanning Electron Microscopy and Energy Dispersive X-ray (EDX) spectra of uranium bioprecipitation by recombinant *Deinococcus* cells. Cells of (a) *D. radiodurans* (PhoN) and (c) *D. radiodurans* (pRAD1) were incubated in a solution containing 10 mM uranium and 20 mM β-glycerophosphate for 7 days and visualized by SEM. Corresponding EDX spectra of uranium challenged cells are shown for (b) *D. radiodurans* (PhoN) or (d) *D. radiodurans* (pRAD1) cells. Silicon peak detected arose from the glass substrate on which the samples were spotted.

Further details of the surface association of the uranyl phosphate precipitate in *D. radiodurans* (PhoN) cells were revealed by TEM. Micrographs obtained after sectioning of samples showed that the precipitate formed spicule-like structures surrounding the entire boundary of the cell surface **(Fig. 4.19).** Here, too, very few fields with loose precipitate were observed. *D. radiodurans* (pRAD1) cells subjected to similar conditions did not show presence of such structures and had smooth cell boundaries.

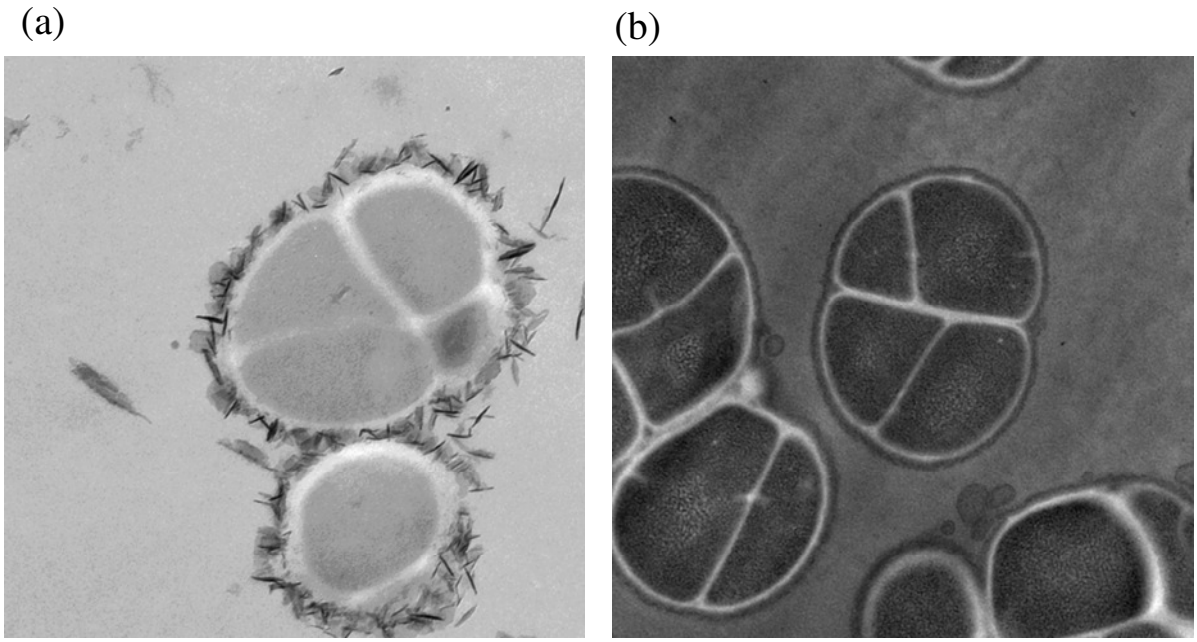

Fig. 4.19. Surface association of uranium phosphate precipitate as observed by Transmission electron Microscope. Cells of (a) *D. radiodurans* (PhoN) and (b) *D. radiodurans* (pRAD1) were incubated in a solution containing 1 mM uranium and 5 mM β-glycerophosphate for 6 h leading to a loading of 0.3 g uranium/g dry weight cells and visualized by TEM.

4.7 Recovery of cadmium precipitated by recombinant strains expressing *phoN* and possible re-use of biomass

Experiments were carried out to evaluate if the precipitated metal could be efficiently desorbed from recombinant cells without affecting the metal precipitation ability of such cells in subsequent cycle. Washing of cadmium laden cells with 0.01N HCl removed 90–100% of the cadmium precipitated on the cell surface **(Table 4.6).** The cells stripped of cadmium still retained 85% of their original ability to precipitate cadmium, in the next cycle **(Table 4.6).** However, only 70% of uranium precipitated could be recovered using 0.01N HCl, which increased to 95% when 0.1 N HCl was used for desorption. Further, cells desorbed with 0.01 N HCl, when used in a second round of uranium precipitation could not precipitate any metal.

Table 4.6. Recovery of precipitated metal from recombinant cells and their reuse.

	Per cent metal precipitated in 1st round	Per cent metal desorbed	Per cent metal removed in 2nd round of metal precipitation
D. radiodurans (PhoN) cadmium	85 ± 7	90 ± 3	50 ± 6
E. coli (PhoN) cadmium	83 ± 5	93 ± 2	72 ± 7
D. radiodurans (PhoN) uranium	69 ± 4	75 ± 5	0
E. coli (PhoN) uranium	70 ± 6	70 ± 7	0

Recombinant cells were used to precipitate metal from a solution containing 1 mM of the metal and then washed in 0.01 N HCl. Desorbed cells were used again in a second round of metal precipitation.

4.8 Discussion

Biosorption is an important phenomenon which has been exploited heavily for bioremediation of heavy metals [8]. Since metal binding by biosorption is essentially a cell

surface phenomenon, the role of S layer proteins in this process assumes considerable importance. Earlier, a surface layer protein from *Bacillus sphaericus* JG-A12 was reported to bind uranium and such cells reversibly and selectively bound U, Al, Cu and Pb [96-97]. The nature of interaction between uranium and S layer protein was thoroughly investigated and found to result from protein phosphorylation. Further sol-gel ceramics were prepared by dispersing *B. sphaericus* JG-A12 vegetative cells, spores, and stabilized surface layer proteins (S-layer) in aqueous silica nanosols and such "biocers" were used for removal of uranium and copper [38,97]. While the S layer protein could remove 20 mg uranium/g proteins, the biocers could remove around 25 mg uranium/g dry weight [98]. In another study, the S layer protein from *Bacillus spahericus* was overexpressed in *E. coli* with a poly-histidine tag. The purified protein was re-assembled and tested for nickel binding ability. While the wild type protein could remove 13.8 mg Ni/g proteins, the recombinant protein removed 31 mg Ni/g protein respectively [41].

In this study, the Hpi protein from *D. radiodurans* was found to possess uranium binding ability. The Hpi protein bound 166 mg uranium/g protein, at pH 6.8. At this pH, uranium is predicted to exist as uranyl-hydroxy species with a net positive charge [99]. The Hpi protein is an acidic protein with a pI of 4.5 [36]. At near neutral pH, the protein is expected to be negatively charged. In addition, the protein has many glutamic and aspartic acid residues, both of which contribute carboxyl groups. A number of studies have reported that the de-protonated carboxyl group of various biomolecules bind uranium with high efficiency [96,100]. It remains to be proven whether these functional groups are the ones involved in interaction of uranium with Hpi. The Hpi protein is one of the most sturdy S layer proteins studied so far and retains its integrity even at 60°C in detergent and urea and at pH as low as 2.0. Its subunits are covalently linked making it a very robust layer [53]. The Deinococcal Hpi layer therefore forms an excellent material for uranium biosorption.

In a number of *Bacillus* species, the S layer protein was found to mask the negative charge of peptidoglycan resulting in cell surface charge neutralization. This was thought to prevent non-specific macromolecule adsorption to prevent pore plugging [101-102]. However, absence of the deinococcal Hpi protein made the overall charge on the cell surface less negative, indicating that the Hpi layer actually enhances the net negative charge on deinococcal cell surface. It should be noted that in the cell wall architecture of the *D. radiodurans* strain R1, Hpi does not form the outermost layer but is overlayed by a carbohydrate layer [54]. The less negative zeta potential of Hpi mutant cells indicates that in spite of an outer carbohydrate coat, the Hpi protein still manages to gain enough surface access to influence cell boundary charge. Wild type cells could bind more uranium than the Hpi mutant, HMR202. Considering that electrostatic interactions play an important role in metal binding, a more negative cell surface charge would be predicted to result in higher binding of uranyl hydroxy complexes.

Since both whole cells, as well as the S layer of *D. radiodurans* show good uranium binding ability, an attempt to extend this ability to other metal ions was made by cloning the metal binding protein, metallothionein in this organism. *D. radiodurans* expressing SmtA alone in cytosol did not show increased metal binding. Similarly, fusion of the SmtA protein with the SLH domain also did not enhance the bioremediation capability of the recombinant cells, in spite of membrane bound localization of the fusion protein. Only fusion with Hpi, increased the metal biosorption capability of recombinant cells **(Fig. 4.3 and 4.5)**. Further, all the Hpi-SmtA fusion protein could be detected in the membrane fraction. The *E. coli* recombinants expressing the Hpi-SmtA fusion protein did not show enhanced metal binding compared to control cells but those carrying the *smtA* gene alone could remove twice as much metal as control cells. In *E. coli* cells deinococcal Hpi protein does not have a designated niche in the cell envelope which appears to impair its surface display, resulting cytosolic

localization and possible degradation and reduced metal binding. However, intracellular metallothionein expression of the recombinant cells did enhance the metal binding capacity of *E. coli* cells as has also been observed with intracellular expression of metallothioneins in this organism earlier [103].

Different approaches have earlier been used for surface display of metal binding peptides/proteins. A similar report of surface display of the SmtA protein by fusion to Lpp-OmpA system in *E. coli* (elaborated in Chapter 3), resulted in a loading of 16 nmoles Cd/mg dry weight cells (1.792 mg Cd/g dry weight cells) [87]. When a eukaryotic metallothionien was fused to Lam B in *E. coli*, recombinant cells could remove 30 nmoles Cd/mg dry cell weight (3.360 mg Cd/g dry weight cells) [104]. In an example of surface display of metallothioniens in organisms other than *E. coli*, when mouse metallothionein (MT) was fused to the β domain of IgA protease of *Neisseria gonorrhoeae* for localization of the MT in outer membrane of *Pseudomonas putida*, it resulted in three fold higher metal binding compared to intracellular expression of the MT, leading to a loading of 27 nmoles Cd/mg dry weight cells (3.024 mg/g dry weight cells) [105]. In *Ralstonia eutropha*, which was engineered using the same approach as *Pseudomonas* to display mouse MT, recombinants could remove a maximum of 42 nmoles Cd/mg dry weight (4.7 mg/g dry weight cells) cells at 300 µM and 16 nmoles Cd/mg dry weight cells (1.7 mg/g dry weight cells) at 30 µM input Cd concentration [32]. A Hexa-histidine peptide was inserted to a permissive site of the surface layer (S-layer) protein RsaA of *Caulobacter crescentus.* The recombinant strain JS4022/p723–6H removed 94.3~99.9% of the Cd(II), leading to a metal loading of 16 mg/g dry cell weight whereas the control strain removed only 11.4~37.0% [40]. The result described in the thesis is the only report of an S-layer-metallothonein fusion protein (Hpi-

SmtA) and resulted in a cadmium loading of 1.2 mg/g dry biomass in recombinant *D. radiodurans* cells exposed to 40 µM Cd^{2+} ions..

While biosorption and complexation of metals are useful mechanisms at nanomolar or lower metal concentrations, they are ineffective when the, metal concentrations are in range of micro or millimolar [25]. At such concentrations, bioremediation by bioprecipitation and bioreduction are much more useful [25]. In earlier studies, the efficiency of PhoN mediated uranium precipitation in the millimolar range has been reported in *D. radiodurans* [51]. Phosphatase mediated metal precipitation is essentially non-specific in nature i.e. any heavy metal present in solution can be precipitated using this approach [17-18]. Therefore, the potential of *phoN* bearing cells in cadmium precipitation was explored since it is a hazardous metal, and widely used in paints and electronic industry.

The rate of cadmium bioprecipitation was found to be significantly higher than uranium bioprecipitation. An important observation was that the toxicity of the metal to the organisms *per se*, did not affect the corresponding precipitation efficiency. *D. radiodurans* is a metal sensitive bacterium with a MIC of 0.018 mM for cadmium compared with 0.5–1 mM for *E. coli* DH5α (Ruggiero et al., 2005). However, both organisms could precipitate out the metal at comparable efficiencies, commensurate with their phosphatase activity. Perhaps extracellular precipitation shields the bacterium from metabolic ill effects of metals.

Efforts to increase uranium precipitation in recombinant cells by fusion of PhoN to surface layer proteins did not *per se* increase metal precipitation ability. As was observed in zymograms, the Hpi-PhoN fusion protein was expressed and displayed phosphatase activity in recombinant *D. radiodurans* cells **(Fig. 3.23 and 3.25).** It was also exclusively cell membrane localized. Since both the PhoN and Hpi-PhoN proteins were expressed from the same promoter, the likelihood of differential expression are low but possible. While, this

could be one of the factors, the low whole cell activity in *hpi-phoN* bearing cells may also be due to low phosphatase activity of the Hpi-PhoN fusion protein *per se*. Hpi being a much larger protein may interfere with correct folding of the fusion protein lowering the phosphatase activity of the protein *per se.* PhoN is an enzyme which is known to function as a dimer. In creating fusion proteins, there is a possibility that the dimerization of the enzyme may be affected and may result in lower activity of the recombinant protein. In contrast, fusion of SmtA to Hpi enhanced metal binding activity because in metallothioneins, metal binding is facilitated by Cys-X-Cys conserved sequence, and only sufficient exposure of this repeating group is required for metal binding.

Both the SLH fusion to SmtA as well as to PhoN failed to enhance metal removal by recombinant cells expressing them. The SLH domain is likely to be present more proximal to peptidoglycan layer than Hpi, and away from the cell surface in *D. radiodurans*. Such cell envelope localization of SLH may not be conducive both to the activity of PhoN enzyme due to low substrate accessibility as well as for the metal binding ability of SmtA. The results show that while surface display of SmtA by fusion to Hpi resulted in superior metal binding by recombinant cells, fusion of PhoN to either of the S layer proteins did not provide value addition.

Isolated Hpi protein from recombinant cells expressing Hpi-PhoN could precipitate uranium more efficiently than that isolated from control pRAD1 cells **(Fig. 4.9)**. However, on washing the Hpi pellet to remove cytoplasmic contamination, this enhanced metal precipitation ability was also lost. Further, the Hpi layer isolated from *hpi-smtA* bearing cells did not show better cadmium/zinc binding compared to the layer isolated from pRAD1 bearing cells. The two results put together seem to indicate that while the fusion to Hpi protein might have conferred membrane localization to the proteins tagged to it, the fusion

protein may not have been properly incorporated covalently into the Hpi layer in the face of competition from native Hpi protein.

Attempt to create S layer-PhoN fusion proteins, however, gave rise to a new possible mode of PhoN exploitation i.e. by immobilization on peptidoglycan using the SLH domain. This was especially relevant considering that peptidoglycan itself is known to adsorb uranium on its functional groups [94]. Further, peptidoglycan is a sturdy biopolymer, resistant to heat and detergents and is hydrolyzed only with concentrated mineral acids at high temperature. SLH-PhoN immobilized on peptidoglycan when stabilized by glutaraldehyde cross linking, showed efficient metal precipitation and excellent re-usability in uranium precipitation assays for upto five cycles **(Fig. 4.10).** PhoN itself proved to be a stable and sturdy enzyme which could withstand glutaraldehyde treatment, prolonged uranium exposure and room temperature incubations.

The usage of interaction between the SLH domain and peptidoglycan for immobilization of enzymes is reported here for the first time. This allows one-step purification of SLH-PhoN from cell extracts and immobilization on peptidoglycan making this a convenient system to implement. Further, of all the systems that were developed in this study using *D. radiodurans* for uranium precipitation, SLH-PhoN immobilized on peptidoglycan (SPhoNP) was found to be the most efficient in precipitating uranium. While SPhoNP removed 376 µg U/mg dry weight in 6 h, recombinants expressing PhoN or Hpi-PhoN alone precipitated only 297 µg U/mg cells and 178 µg U/mg cells respectively, showing superiority of SPhoNP over other biomass in precipitating U. Proteins immobilized on an inert support are far more attractive than using recombinant organisms in the environment, which are associated with risks such as instability, horizontal gene transfer to non-target organisms etc.

While it is important to design organisms with superior bioremediation abilities, it is equally important to make the system appealing by ensuring that using such biomass is non-cumbersome. With this in mind, lyophilisation of recombinant organisms was attempted to achieve volume reduction and ease of handling, storage and transport of such cells. Not only did lyophilisation of PhoN bearing cells reduce volume and convert cell suspensions into a dry easy-to-use-and-disperse-powder, it also achieved the following: (1) preserved the PhoN activity and uranium precipitation ability of cells, (2) retained cellular integrity and surface precipitation property, thereby facilitating easy recovery of precipitated metal with the biomass, (3) significantly extended the shelf life of the product in terms of uranium precipitation capability for up to six months at room temperature.

E. coli is not considered a safe organism for environmental use due to instability, and occurrence of pathogenic strains. Attempts have been made earlier to employ liposomes carrying PhoN for metal removal *in vitro* to avoid direct use of genetically manipulated live bacteria in filtration systems [106]. The present study managed this by using lyophilisation without cryopreservatives to render the recombinant cells non-viable, while preserving their PhoN and metal precipitation activities. Lyophilisation is used as a cell-preservation technique, but is known to cause irreversible damage to *E. coli* cells resulting in death [107]. A number of factors including use of protective excipients during freeze-drying [108], [109] and storage *in vacuo* after lyophilisation [110] are known to maintain viability of microbes. The present study deliberately excluded these from the lyophilisation process to render the cells non-viable. Though lyophilisation is known to cause protein unfolding and denaturation [111], PhoN activity was well preserved after lyophilisation perhaps due to the protection afforded by its periplasmic location in the cell.

D. radiodurans scores over *E. coli* based systems in its utility for bioremediation of radioactive waste solution [49,112]. In the case of *D. radiodurans*, lyophilized cells retained viability which allowed use of such cell powder as inoculum to build-up biomass for *in situ* bioremediation experiments. In addition, no pathogenic strains of this species are known and it is therefore considered safer for environmental use. Lyophilisation was also applied to SPhoNP stabilized by glutaraldehyde, which fully retained its uranium precipitation ability. Uranium precipitation ability of lyophilized SPhoNP was also found to be superior to recombinant *D. radiodurans* cells expressing PhoN or Hpi-PhoN.

Scanning Electron Microscopy revealed that the precipitated metal was firmly lodged on to the surface of recombinant cells. Even at very high loadings, no free precipitate was seen in the fields observed. This has important implications for settling down of precipitated sludge and downstream processing of the effluent as emphasized earlier [18]. Surface precipitation of metal also allowed easy recovery of metal by dilute acid wash.

The two potential candidates for bioremediation of heavy metals from radioactive wastes that emerged from this study as a result of expression of surface layer fusion proteins are as follows: (1) Recombinant *D. radiodurans* expressing Hpi-SmtA for sequestration of metals at micromolar concentrations, and (2) SPhoNP for precipitation of metals from solutions carrying millimolar concentration of metals. In the light of isolated Hpi layer from recombinants not displaying superior metal remediation ability, overexpression of this protein at much higher levels in HMR202 mutant cells, may enable formation of a homogenous Hpi layer comprising of the fusion protein alone, thus increasing metal bioremediation ability of recombinant cells as well as protein. Another important lead from this work is the evaluation of metal precipitation utility of SPhoNP in a flow-through system for superior bioremediation in future.

Chapter 5

Summary and Conclusions

Summary and Conclusions

This study was conceived to develop genetically engineered bacteria expressing S-layer proteins fused either to a non-specific acid phosphatase (PhoN) or a metallothionein (SmtA), aimed at metal bioremediation. The radioresistant organism, *D. radiodurans*, was chosen as a host for expression of constructed fusion proteins, since it is well suited for remediation of radioactive waste. The salient findings of the study are summarized below:

- The two S layer proteins of *D. radiodurans*, Hpi and SlpA, were partially characterized and found to be associated with one another in the deinococcal cell envelope.
- The Hpi layer was isolated and found to undergo *in vivo* degradation, as ascertained by peptide mass fingerprinting of multiple protein bands obtained on resolving the isolated Hpi protein layer on denaturing gels.
- The Hpi protein layer bound (166 µg U/mg protein) U at near neutral pH. Hpi protein was found to confer substantial negative charge to deinococcal cell surface, thereby possibly enhancing its interaction and binding with heavy metals.
- Bioinformatic analysis of the SlpA protein showed presence of a single surface layer homology domain (SLH) at the N terminus, which is known to bind the secondary cell wall polymers (SCWP) attached to peptidoglycan in other organisms, making it a suitable membrane anchoring vehicle.
- The *smtA* gene from the unicellular cyanobacterium, *Synechococcus elongatus,* which codes for a metal binding metallothionein (MT) peptide, was cloned for expression from the strong deinococcal *PgroESL* promoter, or as a fusion gene with *hpi* ORF, or

fused to the nucleotide sequence encoding the SLH domain of SlpA protein in *D. radiodurans.*

- The expressed Hpi-SmtA and SLH-SmtA fusion proteins localized to the deinococcal cell surface as desired, while the SmtA protein *per se* localized to the cytoplasm. Thus tagging SmtA to Hpi/SLH domain facilitated localization of the SmtA protein in the deinococcal cell envelope.

- Recombinant *D. radiodurans* cells expressing the Hpi-SmtA fusion protein removed 1.5-2 times more metals (Cd, Zn and Cu) than those expressing only SmtA or SLH-SmtA fusion protein. Surface display of SmtA by fusion to Hpi enhanced the metal binding ability of recombinants (1.2 mg Cd, 225 µg Cu and 210 µg Zn/g dry weight cells) but its fusion to SLH domain did not. This indicated a more inward localization of SLH closer to peptidoglycan and away from cell surface. Further, intracellular expression of SmtA also did not enhance metal binding ability of recombinant cells (0.35 mg Cd, 100 µg Cu and 125 µg Zn/g dry weight cells).

- The *phoN* gene was fused to *hpi* ORF or sequence encoding the SLH domain of the SlpA protein. Recombinant *D. radiodurans* expressing the Hpi-PhoN and SLH-PhoN proteins showed phosphatase activity bands of 127 kDa and 37 kDa respectively in zymograms, as was expected for the fusion proteins.

- The Hpi-PhoN protein localized exclusively to the cell membrane and showed cell-based phosphatase activity. The SLH-PhoN protein however, localized to both cytoplasm as well as membrane in *D. radiodurans* cells and did not show any cell-based activity.

- Hpi-PhoN fusion protein expression did not enhance cell-based phosphatase activity in *D. radiodurans*. In 6 h, *D. radiodurans* (PhoN) cells could remove as much as 83% uranium leading to a loading 310 µg U/mg dry weight cells, while Hpi-PhoN bearing recombinants could remove only 40-50% of input uranium leading to a loading of 136-185 µg U/mg dry weight cells. But when cells were used at equivalent phosphatase activity, recombinants carrying Hpi-PhoN or PhoN *per se* removed around 90% U in 6 h.

- The Hpi-PhoN protein layer, isolated from recombinant *D. radiodurans* cells could precipitate uranium more efficiently (446 µg U/mg protein) than Hpi layer isolated from *D. radiodurans* (pRAD1) cells (208 µg U/mg protein), but this feature was lost upon extensive washing of the Hpi pellet. The Hpi layer isolated from Hpi-SmtA expressing cells also did not exhibit enhanced cadmium/zinc binding, compared to the Hpi layer isolated from *D. radiodurans* (pRAD1). Thus, while Hpi-SmtA and Hpi-PhoN proteins did localize to membrane, their incorporation into Hpi layer appears to have been hampered in the face of competition from native resident Hpi layer.

- The SLH domain of SlpA protein was shown to bind peptidoglycan *in vitro*. This indicated that the association of SlpA with secondary cell wall polymers of peptidoglycan at one end and Hpi at the other, formed a continuous link in the interactions between different layers of the deinococcal cell wall.

- Utility of peptidoglycan as an immobilization matrix by exploiting its interaction with the SLH domain is an important finding of this study. SLH-PhoN immobilized on peptidoglycan could efficiently remove U from solution (95% in 4 h) and glutaraldehyde stabilized SLH-PhoN-peptidoglycan complex showed excellent

stability and re-usability for upto five cycles of uranium precipitation, leading to a final loading of 160 µg U/mg dry biomass.

- SLH-PhoN immobilized on peptidoglycan (SPhoNP) showed most efficient uranium precipitation (376 µg U/mg dry weight biomass) compared to *D. radiodurans* bearing Hpi-PhoN (178 µg U/mg dry weight cells) or only PhoN (297 µg U/mg dry weight cells).

- Recombinant *Deinococcus* cells expressing PhoN could precipitate cadmium more efficiently (1.59 µmoles/mg dry weight cells) than uranium (0.79 µmoles/mg dry weight cells) from solution.

- Lyophilization of PhoN expressing *E. coli* and *D. radiodurans* reduced the bulk volume and converted the biomass into a dry powdered form. Lyophilized recombinants retained PhoN activity as well as U precipitation ability, while also retaining cellular integrity and surface precipitation property.

- Lyophilisation significantly extended the shelf life of the product in terms of metal precipitation up to six months at ambient temperature.

- Both the uranyl phosphate and cadmium phosphate precipitates were shown to be cell surface associated, leading to easy separation of metal laden cells thereby aiding metal recovery from liquid waste.

To conclude, this study generated the following important results:

1. Hpi emerged as an efficient membrane targeting vehicle in *D. radiodurans*. When used for membrane localization of SmtA, it resulted in enhanced metal binding ability of recombinants expressing the fusion protein.

2. The property of SLH domain to bind SCWP of peptidoglycan could be exploited for one step immobilization of enzymes. SLH-PhoN immobilized on peptidoglycan provided an excellent and efficient biomaterial for metal precipitation.
3. Lyophilization proved to be a good value addition to phosphatase mediated bioremediation by increasing the shelf life of recombinants and making their handling and storage easy.

Generation of S layers, exclusively of fusion proteins, by expressing the protein at high levels in Hpi mutant cells, and evaluation of metal precipitation utility of SPhoNP in a flow-through process may hold promise for superior bioremediation in future.

References

[1] LaGrega, M.D., Buckingham, P.L. and Evans, J.C. (2010) Hazardous waste management, Waveland Press

[2] Mejare, M. and Bulow, L. (2001). Metal-binding proteins and peptides in bioremediation and phytoremediation of heavy metals. Trends Biotechnol 19, 67-73.

[3] Boopathy, R. (2000). Factors limiting bioremediation technologies. Bioresource Technology 74, 63-67.

[4] Malik, A. (2004). Metal bioremediation through growing cells. Environment International 30, 261-278.

[5] Nies, D.H. (1999). Microbial heavy-metal resistance. Applied Microbiology and Biotechnology 51, 730-750.

[6] Lloyd, J.R. and Renshaw, J.C. (2005). Bioremediation of radioactive waste: radionuclide-microbe interactions in laboratory and field-scale studies. Curr Opin Biotechnol 16, 254-60.

[7] Singh, J.S., Abhilash, P.C., Singh, H.B., Singh, R.P. and Singh, D.P. (2011). Genetically engineered bacteria: An emerging tool for environmental remediation and future research perspectives. Gene 480, 1-9.

[8] Barkay, T. and Schaefer, J. (2001). Metal and radionuclide bioremediation: issues, considerations and potentials. Curr Opin Microbiol 4, 318-23.

[9] Gadd, G.M. (2000). Bioremedial potential of microbial mechanisms of metal mobilization and immobilization. Curr Opin Biotechnol 11, 271-9.

[10] Fomina, M. and Gadd, G.M. (2014). Biosorption: current perspectives on concept, definition and application. Bioresource Technology 160, 3-14.

[11] Eccles, H. (1999). Treatment of metal-contaminated wastes: why select a biological process? Trends Biotechnol 17, 462-5.

[12] Cobbett, C. and Goldsbrough, P. (2002). PHYTOCHELATINS AND METALLOTHIONEINS: Roles in Heavy Metal Detoxification and Homeostasis. Annual Review of Plant Biology 53, 159-182.

[13] Turner, J.S. and Robinson, N.J. (1995). Cyanobacterial metallothioneins: biochemistry and molecular genetics. J Ind Microbiol 14, 119-25.

[14] Shi, J., Lindsay, W.P., Huckle, J.W., Morby, A.P. and Robinson, N.J. (1992). Cyanobacterial metallothionein gene expressed in *Escherichia coli*. Metal-binding properties of the expressed protein. FEBS Lett 303, 159-63.

[15] Webb, McGinness and Lappin, S. (1998). Metal removal by sulphate-reducing bacteria from natural and constructed wetlands. Journal of Applied Microbiology 84, 240-248.

[16] Sharma, P.K., Balkwill, D.L., Frenkel, A. and Vairavamurthy, M.A. (2000). A New *Klebsiella planticola* Strain (Cd-1) Grows Anaerobically at High Cadmium Concentrations and Precipitates Cadmium Sulfide. Applied and Environmental Microbiology 66, 3083-3087.

[17] Macaskie, L.E., Wates, J.M. and Dean, A.C. (1987). Cadmium accumulation by a *Citrobacter* sp. immobilized on gel and solid supports: Applicability to the treatment of liquid wastes containing heavy metal cations. Biotechnol Bioeng 30, 66-73.

[18] Macaskie, L.E., Jeong, B.C. and Tolley, M.R. (1994). Enzymically accelerated biomineralization of heavy metals: application to the removal of americium and plutonium from aqueous flows. FEMS Microbiol Rev 14, 351-67.

[19] Basnakova, G., Stephens, E.R., Thaller, M.C., Rossolini, G.M. and Macaskie, L.E. (1998). The use of *Escherichia coli* bearing a phoN gene for the removal of uranium and nickel from aqueous flows. Appl Microbiol Biotechnol 50, 266-72.

[20] Basnakova, G. and Macaskie, L.E. (1997). Microbially enhanced chemisorption of nickel into biologically synthesized hydrogen uranyl phosphate: a novel system for the removal and recovery of metals from aqueous solutions. Biotechnol Bioeng 54, 319-28.

[21] Bonthrone, K.M., Basnakova, G., Lin, F. and Macaskie, L.E. (1996). Bioaccumulation of nickel by intercalation into polycrystalline hydrogen uranyl phosphate deposited via an enzymatic mechanism. Nat Biotechnol 14, 635-8.

[22] Keasling, J.D., Van Dien, S.J. and Pramanik, J. (1998). Engineering polyphosphate metabolism in *Escherichia coli:* implications for bioremediation of inorganic contaminants. Biotechnol Bioeng 58, 231-9.

[23] Renninger, N., Knopp, R., Nitsche, H., Clark, D.S. and Keasling, J.D. (2004). Uranyl precipitation by *Pseudomonas aeruginosa* via controlled polyphosphate metabolism. Appl Environ Microbiol 70, 7404-12.

[24] Macaskie, L.E., Yong, P., Doyle, T.C., Roig, M.G., Diaz, M. and Manzano, T. (1997). Bioremediation of uranium-bearing wastewater: Biochemical and chemical factors influencing bioprocess application. Biotechnology and Bioengineering 53, 100-109.

[25] Valls, M. and Lorenzo, V. (2002). Exploiting the genetic and biochemical capacities of bacteria for the remediation of heavy metal pollution. FEMS Microbiology Reviews 26, 327-338.

[26] Deng, X., Yi, X.E. and Liu, G. (2007). Cadmium removal from aqueous solution by gene-modified *Escherichia coli* JM109. Journal of Hazardous Materials 139, 340-344.

[27] Yuan, C., Lu, X., Qin, J., Rosen, B.P. and Le, X.C. (2008). Volatile Arsenic Species Released from *Escherichia coli* Expressing the AsIII S-adenosylmethionine Methyltransferase Gene. Environmental Science & Technology 42, 3201-3206.

[28] Zhao, X.W., Zhou, M.H., Li, Q.B., Lu, Y.H., He, N., Sun, D.H. and Deng, X. (2005). Simultaneous mercury bioaccumulation and cell propagation by genetically engineered *Escherichia coli.* Process Biochemistry 40, 1611-1616.

[29] Valls, M., de Lorenzo, V., Gonzalez-Duarte, R. and Atrian, S. (2000). Engineering outer-membrane proteins in *Pseudomonas putida* for enhanced heavy-metal bioadsorption. J Inorg Biochem 79, 219-23.

[30] Nilgiriwala, K.S., Alahari, A., Rao, A.S. and Apte, S.K. (2008). Cloning and overexpression of alkaline phosphatase PhoK from *Sphingomonas* sp. strain BSAR-1 for bioprecipitation of uranium from alkaline solutions. Appl Environ Microbiol 74, 5516-23.

[31] Saleem, M., Brim, H., Hussain, S., Arshad, M., Leigh, M.B. and Zia ul, H. (2008). Perspectives on microbial cell surface display in bioremediation. Biotechnol Adv 26, 151-61.

[32] Valls, M., Atrian, S., de Lorenzo, V. and Fernandez, L.A. (2000). Engineering a mouse metallothionein on the cell surface of *Ralstonia eutropha* CH34 for immobilization of heavy metals in soil. Nat Biotechnol 18, 661-5.

[33] Sleytr, U.B., Schuster, B., Egelseer, E.M. and Pum, D. (2014). S-layers: principles and applications. FEMS Microbiol Rev

[34] Engelhardt, H. (2007). Are S-layers exoskeletons? The basic function of protein surface layers revisited. J Struct Biol 160, 115-24.

[35] Fagan, R.P. and Fairweather, N.F. (2014). Biogenesis and functions of bacterial S-layers. Nat Rev Micro 12, 211-222.

[36] Pavkov-Keller, T., Howorka, S. and Keller, W. (2011) Chapter 3 - The Structure of Bacterial S-Layer Proteins. In Progress in Molecular Biology and Translational Science (Stefan, H., ed.^eds), pp. 73-130. Academic Press

[37] Ilk, N., Egelseer, E.M. and Sleytr, U.B. (2011). S-layer fusion proteins--construction principles and applications. Curr Opin Biotechnol 22, 824-31.

[38] Pollmann, K., Raff, J., Merroun, M., Fahmy, K. and Selenska-Pobell, S. (2006). Metal binding by bacteria from uranium mining waste piles and its technological applications. Biotechnol Adv 24, 58-68.

[39] Velasquez, L. and Dussan, J. (2009). Biosorption and bioaccumulation of heavy metals on dead and living biomass of Bacillus sphaericus. J Hazard Mater 167, 713-6.

[40] Patel, J., Zhang, Q., McKay, R.M., Vincent, R. and Xu, Z. (2010). Genetic engineering of *Caulobacter crescentus* for removal of cadmium from water. Appl Biochem Biotechnol 160, 232-43.

[41] Pollmann, K. and Matys, S. (2007). Construction of an S-layer protein exhibiting modified self-assembling properties and enhanced metal binding capacities. Appl Microbiol Biotechnol 75, 1079-85.

[42] Battista, J.R. (1997). Against all odds: the survival strategies of Deinococcus radiodurans. Annu Rev Microbiol 51, 203-24.

[43] Minton, K.W. (1994). DNA repair in the extremely radioresistant bacterium *Deinococcus radiodurans*. Mol Microbiol 13, 9-15.

[44] Minton, K.W. (1996). Repair of ionizing-radiation damage in the radiation resistant bacterium *Deinococcus radiodurans*. Mutat Res 363, 1-7.

[45] Slade, D. and Radman, M. (2011). Oxidative stress resistance in *Deinococcus radiodurans.* Microbiol Mol Biol Rev 75, 133-91.

[46] Venkateswaran, A., McFarlan, S.C., Ghosal, D., Minton, K.W., Vasilenko, A., Makarova, K., Wackett, L.P. and Daly, M.J. (2000). Physiologic determinants of radiation resistance in *Deinococcus radiodurans.* Appl Environ Microbiol 66, 2620-6.

[47] Zahradka, K., Slade, D., Bailone, A., Sommer, S., Averbeck, D., Petranovic, M., Lindner, A.B. and Radman, M. (2006). Reassembly of shattered chromosomes in *Deinococcus radiodurans.* Nature 443, 569-73.

[48] Misra, H.S., Khairnar, N.P., Kota, S., Shrivastava, S., Joshi, V.P. and Apte, S.K. (2006). An exonuclease I-sensitive DNA repair pathway in *Deinococcus radiodurans:* a major determinant of radiation resistance. Molecular Microbiology 59, 1308-1316.

[49] Brim, H., McFarlan, S.C., Fredrickson, J.K., Minton, K.W., Zhai, M., Wackett, L.P. and Daly, M.J. (2000). Engineering *Deinococcus radiodurans* for metal remediation in radioactive mixed waste environments. Nat Biotechnol 18, 85-90.

[50] Lange, C.C., Wackett, L.P., Minton, K.W. and Daly, M.J. (1998). Engineering a recombinant Deinococcus radiodurans for organopollutant degradation in radioactive mixed waste environments. Nat Biotechnol 16, 929-33.

[51] Appukuttan, D., Rao, A.S. and Apte, S.K. (2006). Engineering of Deinococcus radiodurans R1 for bioprecipitation of uranium from dilute nuclear waste. Appl Environ Microbiol 72, 7873-8.

[52] Kulkarni, S., Ballal, A. and Apte, S.K. (2013). Bioprecipitation of uranium from alkaline waste solutions using recombinant Deinococcus radiodurans. J Hazard Mater 262, 853-61.

[53] Baumeister, W., Karrenberg, F., Rachel, R., Engel, A., Ten Heggeler, B. and Saxton, W.O. (1982). The Major Cell Envelope Protein of Micrococcus radiodurans (R1). European Journal of Biochemistry 125, 535-544.

[54] Rothfuss, H., Lara, J.C., Schmid, A.K. and Lidstrom, M.E. (2006). Involvement of the S-layer proteins Hpi and SlpA in the maintenance of cell envelope integrity in Deinococcus radiodurans R1. Microbiology 152, 2779-87.

[55] Mark, S.S., Bergkvist, M., Yang, X., Teixeira, L.M., Bhatnagar, P., Angert, E.R. and Batt, C.A. (2006). Bionanofabrication of metallic and semiconductor nanoparticle arrays using S-layer protein lattices with different lateral spacings and geometries. Langmuir 22, 3763-74.

[56] Thompson, B.G., Murray, R.G.E. and Boyce, J.F. (1982). The association of the surface array and the outer membrane of Deinococcus radiodurans. Canadian Journal of Microbiology 28, 1081-1088.

[57] Müller, D.J., Baumeister, W. and Engel, A. (1996). Conformational change of the hexagonally packed intermediate layer of Deinococcus radiodurans monitored by atomic force microscopy. Journal of Bacteriology 178, 3025-30.

[58] Engelhardt, H. and Peters, J. (1998). Structural Research on Surface Layers: A Focus on Stability, Surface Layer Homology Domains, and Surface Layer–Cell Wall Interactions. Journal of Structural Biology 124, 276-302.

[59] Cava, F., de Pedro, M.A., Schwarz, H., Henne, A. and Berenguer, J. (2004). Binding to pyruvylated compounds as an ancestral mechanism to anchor the outer envelope in primitive bacteria. Mol Microbiol 52, 677-90.

[60] Kapoor, A. and Viraraghavan, T. (1995). Fungal biosorption — an alternative treatment option for heavy metal bearing wastewaters: a review. Bioresource Technology 53, 195-206.

[61] Selatnia, A., Bakhti, M.Z., Madani, A., Kertous, L. and Mansouri, Y. (2004). Biosorption of Cd2+ from aqueous solution by a NaOH-treated bacterial dead Streptomyces rimosus biomass. Hydrometallurgy 75, 11-24.

[62] Riordan, C., Bustard, M., Putt, R. and McHale, A.P. (1997). Removal of uranium from solution using residual brewery yeast: combined biosorption and precipitation. Biotechnology Letters 19, 385-388.

[63] Sar, P., K. Kazy, S. and D'Souza, S.F. (2004). Radionuclide remediation using a bacterial biosorbent. International Biodeterioration & Biodegradation 54, 193-202.

[64] Matsunaga, T., Takeyama, H., Nakao, T. and Yamazawa, A. (1999). Screening of marine microalgae for bioremediation of cadmium-polluted seawater. Journal of Biotechnology 70, 33-38.

[65] Tauriainen, S.M., Virta, M.P.J. and Karp, M.T. (2000). Detecting bioavailable toxic metals and metalloids from natural water samples using luminescent sensor bacteria. Water Research 34, 2661-2666.

[66] Lovley, D.R. and Phillips, E.J.P. (1994). Reduction of Chromate by Desulfovibrio vulgaris and Its c3 Cytochrome. Applied and Environmental Microbiology 60, 726-728.

[67] Riccio, M., Rossolini, G., Lombardi, G., Chiesurin, A. and Satta, G. (1997). Expression cloning of different bacterial phosphataseencoding genes by histochemical screening of genomic libraries onto an indicator medium containing phenolphthalein diphosphate and methyl green. Journal of Applied Microbiology 82, 177-185.

[68] Sambrook, J., Fritsch, E.F. and Maniatis, T. (1989) Molecular cloning, Cold spring harbor laboratory press New York

[69] Lennon, E. and Minton, K.W. (1990). Gene fusions with lacZ by duplication insertion in the radioresistant bacterium Deinococcus radiodurans. Journal of Bacteriology 172, 2955-2961.

[70] Peterson, G.L. (1977). A simplification of the protein assay method of Lowry< i> et al.</i> which is more generally applicable. Analytical biochemistry 83, 346-356.

[71] Laemmli, U.K. (1970). Cleavage of structural proteins during the assembly of the head of bacteriophage T4. Nature 227, 680-685.

[72] Panda, B., Basu, B., Rajaram, H. and Kumar Apte, S. (2014). Methyl viologen responsive proteome dynamics of Anabaena sp. strain PCC7120. Proteomics 14, 1895-1904.

[73] Bolton, P. and Dean, A. (1972). Phosphatase synthesis in< italic> Klebsiella</italic>(< italic> Aerobacter</italic>)< italic> aerogenes</italic> growing in continuous culture. Biochem. J 127, 87-96.

[74] Work, E. (1957). Reaction of ninhydrin in acid solution with straight-chain amino acids containing two amino groups and its application to the estimation of α∈-diaminopimelic acid. Biochemical Journal 67, 416.

[75] Mesnage, S., Tosi-Couture, E. and Fouet, A. (1999). Production and cell surface anchoring of functional fusions between the SLH motifs of the Bacillus anthracis S-layer proteins and the Bacillus subtilis levansucrase. Molecular Microbiology 31, 927-936.

[76] Fritz, J. and Bradford, E. (1958). Detection of thorium and uranium. Analytical Chemistry 30, 1021-1022.

[77] Karnovsky, M.J. (1965). A formaldehyde-glutaraldehyde fixative of high osmolarity for use in electron microscopy. J. cell Biol 27

[78] Janesch, B., Messner, P. and Schäffer, C. (2013). Are the Surface Layer Homology Domains Essential for Cell Surface Display and Glycosylation of the S-Layer Protein from Paenibacillus alvei CCM 2051T? Journal of Bacteriology 195, 565-575.

[79] Lemaire, M., Ohayon, H., Gounon, P., Fujino, T. and Béguin, P. (1995). OlpB, a new outer layer protein of Clostridium thermocellum, and binding of its S-layer-like domains to components of the cell envelope. Journal of Bacteriology 177, 2451-9.

[80] Mesnage, S., Tosi-Couture, E., Mock, M. and Fouet, A. (1999). The S-layer homology domain as a means for anchoring heterologous proteins on the cell surface of Bacillus anthracis. Journal of Applied Microbiology 87, 256-260.

[81] Meima, R. and Lidstrom, M.E. (2000). Characterization of the minimal replicon of a cryptic Deinococcus radiodurans SARK plasmid and development of versatile Escherichia coli-D. radiodurans shuttle vectors. Appl Environ Microbiol 66, 3856-67.

[82] Rachel, R., Engel, A. and Baumeister, W. (1983). Proteolysis of the major cell envelope protein of Deinococcus radiodurans remains morphologically latent. FEMS Microbiology Letters 17, 115-119.

[83] Desvaux, M., Dumas, E., Chafsey, I. and Hébraud, M. (2006). Protein cell surface display in Gram-positive bacteria: from single protein to macromolecular protein structure. FEMS Microbiology Letters 256, 1-15.

[84] Vergani, L., Grattarola, M., Dondero, F. and Viarengo, A. (2003). Expression, purification, and characterization of metallothionein-A from rainbow trout. Protein Expression and Purification 27, 338-345.

[85] Lee, S.Y., Choi, J.H. and Xu, Z. (2003). Microbial cell-surface display. TRENDS in Biotechnology 21, 45-52.

[86] Richins, R.D., Kaneva, I., Mulchandani, A. and Chen, W. (1997). Biodegradation of organophosphorus pesticides by surface-expressed organophosphorus hydrolase. Nature biotechnology 15, 984-987.

[87] Tafakori, V., Ahmadian, G. and Amoozegar, M.A. (2012). Surface display of bacterial metallothioneins and a chitin binding domain on Escherichia coli increase cadmium adsorption and cell immobilization. Applied biochemistry and biotechnology 167, 462-473.

[88] Mitchel, R.E. (1980). Micrococcus radiodurans surface exonuclease. Dimer to monomer conversion by ionizing radiation-generated aqueous free radicals. Biochim Biophys Acta 621, 138-46.

[89] Farci, D., Bowler, M.W., Kirkpatrick, J., McSweeney, S., Tramontano, E. and Piano, D. (2014). New features of the cell wall of the radio-resistant bacterium Deinococcus radiodurans. Biochimica et Biophysica Acta (BBA) - Biomembranes 1838, 1978-1984.

[90] Bergkvist, M., Mark, S.S., Yang, X., Angert, E.R. and Batt, C.A. (2004). Bionanofabrication of Ordered Nanoparticle Arrays: Effect of Particle Properties and Adsorption Conditions. The Journal of Physical Chemistry B 108, 8241-8248.

[91] Mark, S.S., Bergkvist, M., Yang, X., Teixeira, L.M., Bhatnagar, P., Angert, E.R. and Batt, C.A. (2006). Bionanofabrication of Metallic and Semiconductor Nanoparticle Arrays Using S-Layer Protein Lattices with Different Lateral Spacings and Geometries. Langmuir 22, 3763-3774.

[92] Olabarria, G., Carrascosa, J.L., de Pedro, M.A. and Berenguer, J. (1996). A conserved motif in S-layer proteins is involved in peptidoglycan binding in Thermus thermophilus. J Bacteriol 178, 4765-72.

[93] Sára, M. (2001). Conserved anchoring mechanisms between crystalline cell surface S-layer proteins and secondary cell wall polymers in Gram-positive bacteria? Trends in Microbiology 9, 47-49.

[94] Barkleit, A., Moll, H. and Bernhard, G. (2009). Complexation of uranium (VI) with peptidoglycan. Dalton Transactions, 5379-5385.

[95] Ruggiero, C.E., Boukhalfa, H., Forsythe, J.H., Lack, J.G., Hersman, L.E. and Neu, M.P. (2005). Actinide and metal toxicity to prospective bioremediation bacteria. Environmental Microbiology 7, 88-97.

[96] Merroun, M.L., Raff, J., Rossberg, A., Hennig, C., Reich, T. and Selenska-Pobell, S. (2005). Complexation of uranium by cells and S-layer sheets of Bacillus sphaericus JG-A12. Appl Environ Microbiol 71, 5532-43.

[97] Raff, J., Soltmann, U., Matys, S., Selenska-Pobell, S., Böttcher, H. and Pompe, W. (2002). Biosorption of Uranium and Copper by Biocers. Chemistry of Materials 15, 240-244.

[98] Raff, J., Soltmann, U., Matys, S., Selenska-Pobell, S., Böttcher, H. and Pompe, W. (2003). Biosorption of uranium and copper by biocers. Chemistry of Materials 15, 240-244.

[99] Prikryl, J.D., Jain, A., Turner, D.R. and Pabalan, R.T. (2001). UraniumVI sorption behavior on silicate mineral mixtures. Journal of Contaminant Hydrology 47, 241-253.

[100] Merroun, M.L. and Selenska-Pobell, S. (2008). Bacterial interactions with uranium: An environmental perspective. Journal of Contaminant Hydrology 102, 285-295.

[101] Sára, M., Pum, D. and Sleytr, U.B. (1992). Permeability and charge-dependent adsorption properties of the S-layer lattice from Bacillus coagulans E38-66. Journal of Bacteriology 174, 3487-3493.

[102] Sára, M. and Sleytr, U.B. (1987). Charge distribution on the S layer of Bacillus stearothermophilus NRS 1536/3c and importance of charged groups for morphogenesis and function. Journal of Bacteriology 169, 2804-2809.

[103] Odawara, F., Kurasaki, M., Suzuki-Kurasaki, M., Oikawa, S., Emoto, T., Yamasaki, F., Arias, A.R.L. and Kojima, Y. (1995). Expression of Human Metallothionein-2 in Escherichia coli: Cadmium Tolerance of Transformed Cells. Journal of Biochemistry 118, 1131-1137.

[104] Valls, M., González-Duarte, R., Atrian, S. and De Lorenzo, V. (1998). Bioaccumulation of heavy metals with protein fusions of metallothionein to bacteriol OMPs. Biochimie 80, 855-861.

[105] Valls, M., de Lorenzo, V.c., Gonzàlez-Duarte, R. and Atrian, S.l. (2000). Engineering outer-membrane proteins in< i> Pseudomonas putida</i> for enhanced heavy-metal bioadsorption. Journal of inorganic biochemistry 79, 219-223.

[106] Jeong, B.C., Hawes, C., Bonthrone, K.M. and Macaskie, L.E. (1997). Localization of enzymically enhanced heavy metal accumulation by Citrobacter sp. and metal accumulation in vitro by liposomes containing entrapped enzyme. Microbiology 143 (Pt 7), 2497-507.

[107] Israeli, E., Kohn, A. and Gitelman, J. (1975). The molecular nature of damage by oxygen to freeze-dried Escherichia coli. Cryobiology 12, 15-25.

[108] Tessema, D.A., Rosen, R., Pedazur, R., Belkin, S., Gun, J., Ekeltchik, I. and Lev, O. (2006). Freeze-drying of sol–gel encapsulated recombinant bioluminescent E. coli by using lyo-protectants. Sensors and Actuators B: Chemical 113, 768-773.

[109] Zárate, G. and Nader-Macias, M.E. (2006). Viability and biological properties of probiotic vaginal lactobacilli after lyophilization and refrigerated storage into gelatin capsules. Process Biochemistry 41, 1779-1785.

[110] Morgan, C.A., Herman, N., White, P.A. and Vesey, G. (2006). Preservation of micro-organisms by drying; A review. Journal of Microbiological Methods 66, 183-193.

[111] Arakawa, T., Prestrelski, S.J., Kenney, W.C. and Carpenter, J.F. (2001). Factors affecting short-term and long-term stabilities of proteins. Advanced Drug Delivery Reviews 46, 307-326.

[112] Appukuttan, D., Seetharam, C., Padma, N., Rao, A.S. and Apte, S.K. (2011). PhoN-expressing, lyophilized, recombinant Deinococcus radiodurans cells for uranium bioprecipitation. J Biotechnol 154, 285-90.

Publications from this work

Process Biochemistry 44 (2009) 246–250

Contents lists available at ScienceDirect

Process Biochemistry

journal homepage: www.elsevier.com/locate/procbio

Short communication

Lyophilized, non-viable, recombinant *E. coli* cells for cadmium bioprecipitation and recovery

Chitra Seetharam [a], Suvarna Soundarajan [b], Ambuja C. Udas [b], Amara Sambasiva Rao [a], Shree Kumar Apte [a,*]

[a] Molecular Biology Division, Bhabha Atomic Research Centre, Trombay, Mumbai 400085, India
[b] Analytical Chemistry Division, Bhabha Atomic Research Centre, Trombay, Mumbai 400085, India

ARTICLE INFO

Article history:
Received 7 March 2008
Received in revised form 13 October 2008
Accepted 22 October 2008

Keywords:
Lyophilization
Non-viable
Recombinant
E. coli
phoN
Cadmium

ABSTRACT

The *phoN* gene, encoding a non-specific acid phosphatase from *Salmonella enterica* sv. Typhi, was cloned and overexpressed into *Escherichia coli*. The *E. coli* cells bearing *phoN* showed high acid phosphatase activity and removed 83% of cadmium from a 1 mM solution in 3 h, when provided with 5 mM β-glycerophosphate as a source of phosphate. Such cells, when lyophilized without any lyo/cryoprotectant, were rendered non-viable but fully retained cadmium precipitation ability. Lyophilized recombinant cells could be stored at room temperature, without significant loss of activity for up to 6 months, and removed upto 21 g cadmium/g dry weight. The precipitated cadmium could be easily recovered from the cells by dilute acid wash, following which the cells retained their cadmium precipitation ability, facilitating their reuse. The use of genetically engineered, non-viable *E. coli* cells offers an environmentally safe biotechnology for bioremediation of cadmium from contaminated sites.

1. Introduction

Microbe-mediated removal of heavy metals [1] holds promise since it spans a wide range of concentrations and is eco-friendly and less expensive compared to physico-chemical methods such as ion exchange, adsorption, precipitation, solvent extraction, etc. [2]. *Citrobacter* cells harboring a periplasmic non-specific acid phosphatase (PhoN) have been earlier shown to precipitate cadmium and uranium [3]. PhoN hydrolyzes organo-phosphates like β-glycerophosphate to release inorganic phosphate, which interacts with the metal to form insoluble metal phosphate, $CdHPO_4$ which is deposited on the cell surface [4].

Microbes have been genetically modified to enhance their inherent bioremediation capacity or to introduce new abilities. However, undesirable mutagenesis, uncontrolled survival or dispersal of genetically engineered microbes (GEM) into the environment and the possibility of lateral or horizontal gene transfer to non-target organisms in the vicinity are major concerns associated with the use of GEM in the field [5]. We have explored the possibilities of (a) engineering *E. coli* to overexpress the PhoN non-specific acid phosphatase, from *S. enterica* sv. Typhi MB2 for improved bioprecipitation of cadmium, followed by (b) lyophilization under conditions, which did not affect the high acid phosphatase activity of PhoN enzyme, but rendered the cells non-viable making their usage environmentally safe. Our data show that lyophilized, non-viable cells of the genetically modified *E. coli* strain overexpressing *phoN* could bioprecipitate up to 21 g cadmium/g biomass dry weight from aqueous solutions, exhibited a 6-month long shelf life and could be reused after desorption of precipitated cadmium.

2. Materials and methods

2.1. Bacterial strains and growth conditions

The *E. coli* strain DH5α (φ80 d *lacZΔ* M15, *recA*1, *gyrA*96, *thi*-1 *hsdR*17 ($r_k^- m_k^+$), *supE*44, *relA*1, *deoR*, Δ(*lacZYA-argF*) U169) and a local isolate of *S. enterica* sv. Typhi MB2 were grown aerobically in Luria–Bertani (LB) growth medium at 37 °C with shaking (180 rpm). For PhoN activity assay and cadmium precipitation experiments, recombinant *E. coli* cells were grown to $OD_{600\ nm}$ of 1.0–1.5, re-inoculated in fresh growth medium at a $OD_{600\ nm}$ of 0.05 and grown overnight under normal growth conditions. The culture was then harvested, washed twice with saline and stored at 4 °C until further use.

2.2. Cloning of PhoN gene

The *phoN* gene was PCR amplified from *S. enterica* sv. Typhi MB2 chromosome, using the following gene specific primers: 5′-CCG GTA TGG ACA GAC GAT TT-3′ (forward) and 5′-CCT ACG CAG TTG CAC TTC CT-3′ (reverse) (GenBank accession No: X59036) [6]. The amplified 0.94 kb product, which included the *phoN* gene along

* Corresponding author. Tel.: +91 22 25595342; fax: +91 22 25505189.
E-mail addresses: sksmbd@barc.gov.in, aptesk@barc.gov.in (S.K. Apte).

1359-5113/$ – see front matter © 2008 Elsevier Ltd. All rights reserved.
doi:10.1016/j.procbio.2008.10.015

with its native promoter, was blunt ended with T4 DNA polymerase, and ligated to the *SmaI* digested multicopy plasmid vector, pUC18 [7]. The resulting plasmid, pASK1 was used to transform *E. coli* DH5α cells. The transformants were selected on LB agar plates containing ampicillin (100 μg/mL). The identity of the cloned insert was confirmed by nucleotide sequencing.

2.3. Acid phosphatase expression: screening, zymogram and PhoN activity assay

Cultures were screened for PhoN activity on LB agar containing phenolphthalein diphosphate (PDP) (1 mg/mL) and methyl green (MG) (50 μg/mL) [8] wherein PhoN positive colonies displayed a dark green coloration. Zymogram analysis for acid phosphatase activity was carried out as described earlier [8] with some modifications [9]. Protein extracts were electrophoretically resolved on sodium dodecyl sulfate polyacrylamide gel (10%, w/v). The gel was washed, renatured and developed using nitroblue tetrazolium (NBT) and 5-bromo-4-chloro-3-indolylphosphate (BCIP) mix in 100 mM acetate buffer at pH 5.0, to visualize phosphatase activity bands.

The cell bound (periplasmic) PhoN acid phosphatase activity was assayed by estimating the *p*-nitrophenol (*p*-NP) liberated from *p*-nitrophenylphosphate (*p*-NPP) by whole cells in 2-morpholinoethanesulfonic acid (MES) buffer (pH 5.0) as described earlier [10]. Protein concentration was estimated by Lowry's method [11].

2.4. Cadmium precipitation studies

Cells were resuspended in normal saline at $OD_{600\ nm}$ of 0.3 which corresponds to 89 ± 4 μg dry weight/mL. Precipitation assays contained β-glycerophosphate (5 mM) and cadmium (0–10 mM) in a total volume of 10 mL. The reaction was carried out in 100 mM 3-(*N*-morpholino)propanesulfonic acid (MOPS), pH 7 under shaking (50 rpm) at 30 °C. At specified time intervals, aliquots were centrifuged at 15,000 × *g* for 4 min to pellet cells. Cadmium was estimated in the supernatant and also in the cell lysate, obtained from acid (Conc. HNO_3) digestion of cell pellet as described earlier, followed by Flame/Graphite Atomic Absorption Spectrophotometry (Model 906AA FAAS, GBC Scientific Equipment Pvt. Ltd., Australia) [12]. Appropriate controls were included to ascertain (a) spontaneous chemical precipitation of cadmium (b) cadmium sorption to the container surface, and (c) biosorption of cadmium on the cell surface.

2.5. Lyophilization of cells

A thick saline-based suspension of recombinant *E. coli* cells, was placed in Petri plates, frozen in liquid nitrogen for 5 min and lyophilized without any lyo/cryoprotectant overnight in a Lyophilizer (Lyospeed, Genevac, United Kingdom) at 0.07 mbar for 18 h and stored in vials, at room temperature without applying vacuum, until further use. Viability of lyophilized cells was determined before and after lyophilization by resuspending (1 mg/mL) in saline/Luria–Bertani medium and plating the appropriate dilution(s) on LB agar to determine CFU/mL. Equivalence between the $OD_{600\ nm}$ of the suspension submitted for lyophilization and the weight of the lyophilized powder obtained was determined to calculate the total number of viable cells in the lyophilized powder and to equalize cell numbers used in cadmium precipitation studies. For cadmium precipitation studies, a 100 μg/mL suspension of lyophilized cells was prepared in 100 mM MOPS buffer and used immediately.

2.6. Scanning electron microscopy and energy dispersive X-ray spectroscopy of cells

Cell samples were washed in normal saline and fixed in 2.5% glutaraldehyde for 2 h. The cells were then dehydrated in a graded ethanol series, spotted on aluminum studs and dried at 37 °C for 1 h. The dried samples were gold coated by thermal evaporation technique and analyzed by scanning electron microscopy (SEM) and energy dispersive X-ray spectroscopy (EDXS) using a Tescan VEGA 40 Microscope and INCA energy 250, Oxford Instrument EDXS system.

2.7. Recovery of precipitated cadmium

Cells which had precipitated ~83% of input cadmium (1 mM) were washed with equal volume of acetate or MOPS (100 mM, pH 5.0) buffer, or distilled water or 0.01N HCl for 5 min to remove the precipitated cadmium. The metal released from the cells was estimated as described above. The ability of the cells, freed from the metal phosphate, to re-precipitate cadmium further was also evaluated.

2.8. Statistical analyses

All reported values were obtained from experiments repeated at least three times, wherein variation between the experiments was less than 15%. Each treatment was carried out with three replicates and the values reported are means with standard error.

3. Results

3.1. Acid phosphatase (PhoN) activity in recombinant strain

A recombinant *E. coli* strain harboring cloned *phoN*, was constructed for overexpression using the multicopy pUC18 plasmid. The 938 bps *phoN* cloned with its native promoter was completely sequenced and the sequence has been submitted to GenBank (accession no. AF366353). *In-gel* zymogram analysis of *E. coli* cells bearing pASK1 showed an intense 27 kDa acid phosphatase activity band corresponding to PhoN (data not shown). This band corresponded to an acid phosphatase activity of 946 ± 69 *p*-NP released/mg protein/min in the cells, which was at least 12-fold higher than the PhoN activity (75 ± 6 units) seen in parent, *S. enterica* sv. Typhi strain thus confirming overexpression and high activity of PhoN in the engineered *E. coli* strain.

3.2. Cadmium precipitation by recombinant E. coli strain

Spontaneous precipitation of cadmium in assay solution and sorption to the container walls, if any, accounted for only 8% of precipitated cadmium (Table 1). In the absence of β-glycerophosphate or the cloned *phoN* gene, cadmium removal from solution was found be to be very low (15%, Table 1). Biosorption of cadmium, thus may account for only 8% of precipitated cadmium. At 1 mM concentration, 83% of the cadmium was precipitated in 3 h using 5 mM β-glycerophosphate as substrate and 0.3 $OD_{600\ nm}$ cells. Nearly all the cadmium removed from the supernatant was recovered in the cell pellet (data not included).

3.3. Cadmium precipitation by lyophilized E. coli cells

Lyophilized cells could precipitate ~80% of 1 mM cadmium in 3 h at efficiencies identical to those of resuspended fresh cells (Table 1). The lyophilized cells were not viable but could be stored at room temperature for upto 6 months with only a minor loss in

Table 1
Comparison of PhoN activity and cadmium precipitation ability of recombinant *E. coli* cells after various treatments.

System used	PhoN activity (nmoles pNP/min/mg cell protein)	Cadmium removed (% removed from a 1 mM solution in 3 h)	Viability (CFU/mL)
Resuspended fresh *E. coli* cells bearing *phoN* cells	932 ± 43		(7.5 ± 0.63) × 10^{10}
1. With 5 mM β-glycerophosphate	–	83 ± 5	–
2. Without β-glycerophosphate	–	15 ± 2	–
Resuspended fresh *E coli* cells carrying pUC 18 vector alone	64.6 ± 10	16 ± 3	–
No cells	–	8 ± 3	–
Lyophilized cells following storage for			
0 month	989 ± 59	83 ± 7	600 ± 30
1 month	850 ± 89	Not determined	0
3 months	832 ± 16	Not determined	0
6 months	781 ± 20	79 ± 4	0

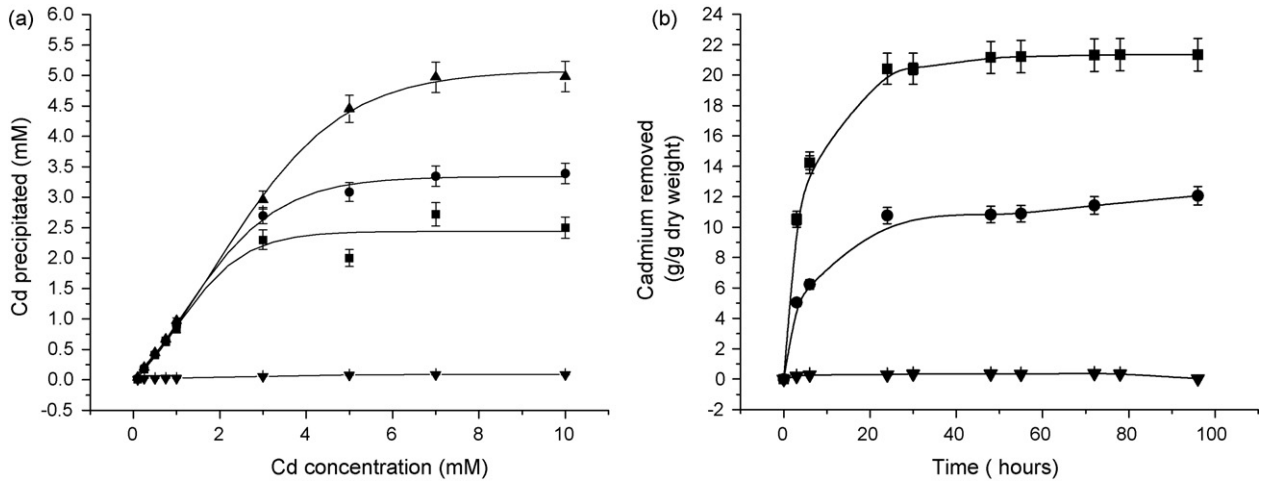

Fig. 1. Cadmium bioprecipitation by lyophilized *E. coli* cells bearing PhoN. (a) Effect of cadmium concentrations on metal removal in the presence of 5 mM β-glycerophosphate. Cadmium precipitation was monitored after 3 h (■), 6 h (●), and 24 h (▲) in *E. coli* cells bearing *phoN* and 6 h (▼) in *E. coli* cells carrying empty pUC vector alone. (b) Cadmium precipitation using lyophilized *E. coli–phoN* cells (10 mg) in 100 mM MOPS solution containing 15 mM cadmium and β-glycerophosphate at 15 mM (●) or 30 mM (■). *E. coli* cells carrying empty vector cells were included as control (▼).

the cadmium precipitation ability (Table 1). Total amount of cadmium precipitated increased with increase in cadmium concentration, saturating at 5 mM cadmium (Fig. 1a), when the concentration of phosphate liberated from 5 mM β-glycerophosphate became limiting. The cells could remove 57–90% of the cadmium present in solution in 24 h at concentrations of 0.1–5 mM, respectively.

The cadmium bioprecipitation capability of recombinant cells was tested at very high concentrations of 15 mM cadmium. Depending on the availability of phosphate donor, the lyophilized cells could accumulate nearly 12 g cadmium/g dry weight at 15 mM β-glycerophosphate, which increased to a loading of 21 g/g dry weight at 30 mM β-glycerophosphate over a 4 d period (Fig. 1b). More than 90% of this precipitation was accomplished in <1 d.

3.4. SEM and EDX of lyophilized cells

Scanning electron microscopy of *E. coli* cells bearing *phoN* indicated that lyophilization without lyo/cryoprotectant did not grossly disrupt the cell morphology or result in bursting of cells (Fig. 2). The treatment, however, resulted in flattening of cells causing depression of the cell around the middle (Fig. 2b) as compared to the rounded appearance of fresh live cells (Fig. 2a, inset). Lyophilized cells, which had precipitated 10 g cadmium/g dry weight of cells showed dense precipitate on the cell surface indicating that the precipitate was cell associated (Fig. 3b, inset). EDXS data of such cells revealed that the precipitate contained cadmium and phosphorous in a ratio of 1:1 indicating that the precipitate was likely to be $CdHPO_4$.(Fig. 3b) In the absence of β-glycerophosphate, lyophilized cells did not show any deposit on the cell surface (Fig. 3a, inset). No cadmium or phosphorous could be detected in such cells (Fig. 3a).

3.5. Cadmium precipitation and recovery using recombinant E. coli strain

Washing of cadmium laden cells with 100 mM MOPS or acetate buffer (pH 5.0) or 0.01N HCl could remove 90–100% of the cadmium precipitated on the cell surface, while washing with distilled water failed to do so (Table 2). The cells stripped of cadmium still retained 85% of their original ability to precipitate cadmium, in the next cycle (Table 2).

4. Discussion

Enzymatic bioprecipitation of heavy metals offers an economic and eco-friendly approach for bioremediation of metal contaminated

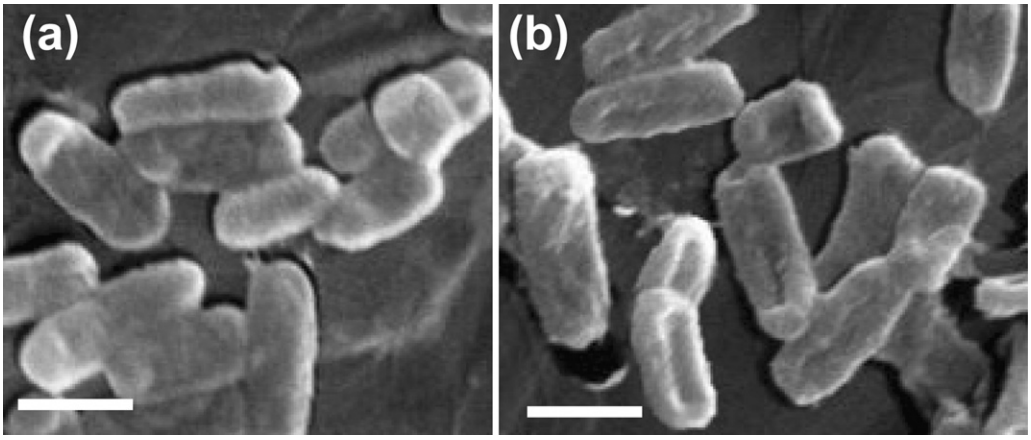

Fig. 2. Scanning electron microscopy of *E. coli* cells bearing *phoN* before (a) and after (b) lyophilization. Bars, 1 μm.

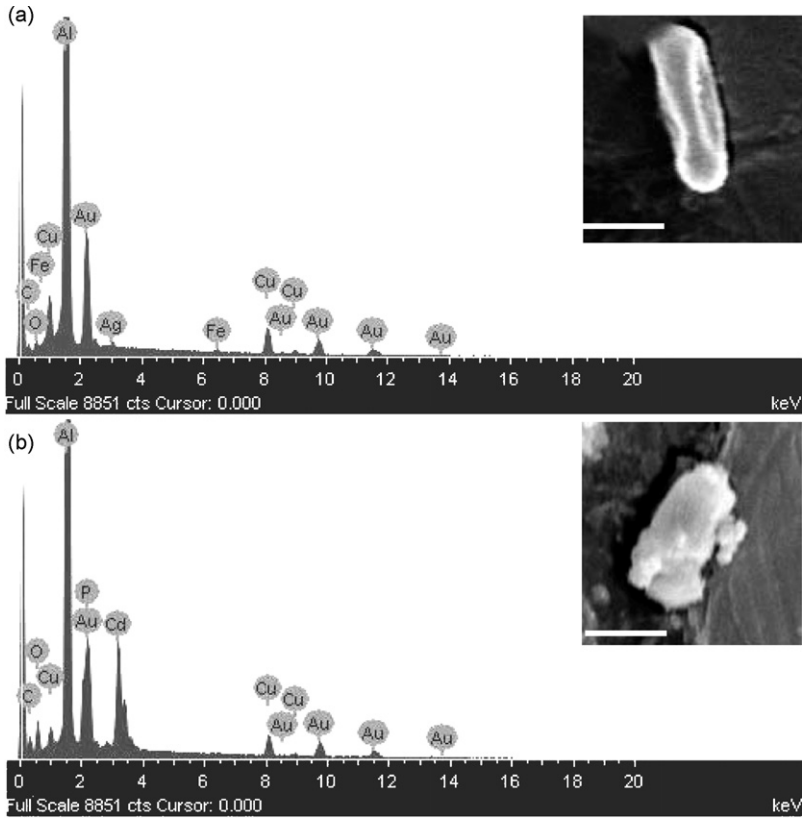

Fig. 3. EDX spectra and scanning electron microscopy (insets) of lyophilized *E. coli* cells bearing *phoN* incubated with 15 mM cadmium and with (b) or without (a) 15 mM β-glycerophosphate for 24 h. Cadmium loading in cells shown in (b) was 10 g cadmium/g dry weight of cells while no cadmium or phosphorous could be detected in cells shown in (a). EDXS data from cadmium-laden cells show presence of cadmium:phosphorus in a 1:1 ratio with percent atomic composition of 3.61% and 3.09%, respectively. Aluminum and other metal peaks are due to the studs and gold is from the coating. Bars, 500 nm.

environments. C*itrobacter* possessing PhoN has earlier been used for bioprecipitation of cadmium as $CdHPO_4$ [5,13]. The cloned *S. typhi* PhoN enzyme used in this study exhibited much higher PhoN activity (~1000 U) in recombinant *E. coli* as compared to an earlier *E. coli* clone (100 U) [14] and showed a higher tolerance to cadmium (50% inhibition at 190 mM cadmium, data not included) compared to *Citrobacter* (50% inhibition at 95 mM cadmium) [15]. In a batch process, the recombinant *E. coli* bearing *phoN* rapidly bioprecipitated cadmium only in the presence of β-glycerophosphate as $CdHPO_4$ as revealed by SEM and EDXS analysis.

The introduction of genetically modified organisms into the environment is wrought with considerations regarding their potential to displace resident species in the receiving community or their dispersal to other locations, as also possible horizontal gene transfer to other organisms. Also, *E. coli* is not considered a safe organism for environmental use. Attempts have been made earlier to employ liposomes carrying PhoN for metal removal *in vitro* to avoid direct use of genetically manipulated live bacteria in filtration systems [16]. The present study managed this by rendering the recombinant cells non-viable, while preserving their PhoN and cadmium precipitation activities. Lyophilization is used as a cell-preservation technique, but is known to cause irreversible damage to *E. coli* cells resulting in death [17]. A number of factors including use of protective excipients during freeze-drying [18–20] and storage *in vacuo* after lyophilization [21] are known to maintain viability of microbes. We deliberately excluded both of these from the lyophilization process to render the cells non-viable. Though lyophilization is known to cause protein unfolding and denaturation [22], PhoN activity was well preserved after lyophilization perhaps due to the protection afforded by its periplasmic location in the cell.

Table 2
Recovery of precipitated cadmium from recombinant cells and their reuse.

Treatment	Cadmium recovery[a]	Reuse efficiency[b]
Distilled water	14 ± 5.0	72.28 ± 4.7
0.01N HCl	90 ± 6.3	74.04 ± 0.6
100 mM acetate, pH 5.0	88 ± 9.2	71.24 ± 1.8
100 mM MOPS, pH 5.0	100 ± 2.8	72.31 ± 2.0

[a] Percent cadmium recovered from cells which had precipitated 83% cadmium phosphate from a 1 mM cadmium solution.
[b] Percent of input cadmium precipitated by desorbed cells in the next cycle of precipitation.

Lyophilization, without the use of any lyo/cryoprotectant and storage of cells under ambient conditions without vacuum achieved the desired goal. SEM pictures showed that the aforesaid treatments preserved cell integrity, which is essential for maintaining the nucleation sites, which are required for cell, associated precipitation of metal on the cell surface [16]. The lyophilized non-viable *E. coli* cells bearing *phoN* are much more robust and circumvent the problems associated with the environmental safety of genetically modified microbes. Lyophilization also facilitated (a) easy handling and storage of cells at room temperature, (b) extended shelf life upto 6 months without activity loss and (c) resulted in impressively high cadmium loadings provided unlimited organic phosphate was available.

Cadmium levels reported from highly contaminated sites lie in the range of ~60–1150 ppm (0.5–10 mM) (www.atsdr.cdc.gov/toxprofiles/tp5-p.pdf, pp. 118 and http://www.atsdr.cdc.gov/HAC/PHA/murraysmel/musm_p4.html# _1_85-table). The data presented in

this study show that PhoN bearing *E. coli* can effectively remove cadmium from this concentration range. In addition, the ease of recovery of precipitated cadmium and the possibility of reuse of the recombinant cells makes this system very attractive, since the metal-laden cells settle down as a compact mass and facilitate easy separation from the clear solution. This is in contrast to chemical precipitation by direct addition of phosphate, which may result in a colloidal suspension requiring extensive settling out [23]. Efforts are on to employ alternate substrates cheaper than β-glycerophosphate, to make the process more economical.

Acknowledgement

The authors wish to thank Ms. N. Padma for SEM and EDX analyses.

References

[1] Valls M, de Lorenzo V. Exploiting the genetic and biochemical capabilities of bacteria for the remediation of heavy metal pollution. FEMS Microbiol Rev 2002;26:327–38.
[2] Eccles H. Treatment of metal-contaminated wastes: why select a biological process? Biotopic 1999;17:462–5.
[3] Macaskie LE. An immobilized cell bioprocess for the removal of heavy metals from aqueous flows. J Chem Technol Biotechnol 1990;49:357–79.
[4] Macaskie LE, Dean ACR, Cheetham AK, Jakeman RJB, Skarnulis AJ. Cadmium accumulation by a *Citrobacter* sp., the chemical nature of the accumulated metal precipitate and its location on the bacterial cells. J Gen Microbiol 1987;133:539–44.
[5] Pandey G, Paul D, Jain RK. Conceptualizing suicidal engineered microorganisms for bioremediation applications. Biochem Biophys Res Commun 2005; 327:637–9.
[6] Kasahara M, Nakata A, Shingagawa H. Molecular analysis of the *Salmonella typhimurium phoN* gene, which encodes nonspecific acid phosphatase. J Bacteriol 1991;173:6760–5.
[7] Yanisch-Perron C, Vieira J, Messing J. Improved M13 phage cloning vectors and host strains: nucleotide sequences of the M13mp18 and pUC19 vectors. Gene 1985;33:103–19.
[8] Riccio ML, Rossolini GM, Lombardi G, Chiesurin A, Satta G. Expression cloning of different bacterial phosphatase-encoding genes by histochemical screening of genomic libraries onto an indicator medium containing phenolphthalein diphosphate and methyl green. J Appl Microbiol 1997;82:177–85.
[9] Appukuttan D, Rao AS, Apte SK. Engineering of *Deinococcus radiodurans* R1 for bioremediation of uranium from dilute nuclear waste. Appl Environ Microbiol 2006;72:7873–8.
[10] Bolton PG, Dean ACR. Phosphatase synthesis in *Klebsiella* (*Aerobacter*) *aerogenes* growing in continuous cultures. J Biochem 1972;127:87–96.
[11] Lowry OH, Rosebrough NJ, Farr AL, Randall RJ. Protein measurement with the Folin phenol reagent. J Biol Chem 1951;193:265–75.
[12] Cordero B, Lodiero P, Herrero R, de Vicente MES. Biosorption of cadmium by *Fucus spiralis*. Environ Chem 2004;1:180–7.
[13] Michel LJ, Macaskie LE, Dean ACR. Cadmium accumulation by immobilized cells of a *Citrobacter* sp. using various phosphate donors. Biotechnol Bioeng 1986;28:1358–65.
[14] Basnakova G, Stephens ER, Thaller MC, Rossolini GM, Macaskie LE. The use of *Escherichia coli* bearing a *phoN* gene for the removal of uranium and nickel from aqueous flows. Appl Microbiol Biotechnol 1998;50:266–72.
[15] Hambling SG, Macaskie LE, Dean ACR. Phosphatase synthesis in a *Citrobacter* sp. growing in continuous culture. J Gen Microbiol 1987;133:2743–9.
[16] Jeong BC, Hawes C, Bonthrone KM, Macaskie LE. Localization of enzymically enhanced heavy metal accumulation by *Citrobacter* sp. and metal accumulation in vitro by liposomes containing entrapped enzyme. Microbiology 1997;143:2497–507.
[17] Israeli E, Kohn A, Gitelman J. The molecular nature of damage by oxygen to freeze-dried *Escherichia coli*. Cryobiology 1975;12(1):15–25.
[18] Dejene AT, Rosen R, Pedazur R, Belkin S, Gunb J, Ekeltchik I, et al. Freeze-drying of sol–gel encapsulated recombinant bioluminescent *E. coli* by using lyoprotectants. Sens Actuator B 2006;113:768–73.
[19] Zarate G, Nader-Macias ME. Viability and biological properties of probiotic vaginal Lactobacilli after lyophilization and refrigerated storage into gelatin capsules. Process Biochem 2006;41:1779–85.
[20] Oterio ML, Espeche MC, Nader-Macias ME. Optimization of the freeze-drying media and survival throughout storage of freeze-dried *Lactobacillus gasseri* and *Lactobacillus delbrueckii* subsp. *dellbrueckii* for veterinarian probiotic applications. Process Biochem 2007;42:1406–11.
[21] Morgan CA, Herman N, White PA, Vesey G. Preservation of micro-organisms by drying; a review. J Microbiol Methods 2006;66:183–93.
[22] Tsutomu A, Steven JP, William CK, John FC. Factors affecting short-term and long-term stabilities of proteins. Adv Drug Deliv Rev 2001;46:307–26.
[23] Macaskie LE, Jeong BC, Tolley MR. Enzymically accelerated biomineralization of heavy metals: application to the removal of americium and plutonium from aqueous flows. FEMS Microbiol Rev 1994;14:351–68.

Journal of Biotechnology 154 (2011) 285–290

Contents lists available at ScienceDirect

Journal of Biotechnology

journal homepage: www.elsevier.com/locate/jbiotec

PhoN-expressing, lyophilized, recombinant *Deinococcus radiodurans* cells for uranium bioprecipitation

Deepti Appukuttan[a,1], Chitra Seetharam[a,1], N. Padma[b], Amara Sambasiva Rao[a], Shree Kumar Apte[a,*]

[a] *Molecular Biology Division, Bhabha Atomic Research Centre, Trombay, Mumbai 400085, India*
[b] *Technical Physics Division, Bhabha Atomic Research Centre, Trombay, Mumbai 400085, India*

ARTICLE INFO

Article history:
Received 18 November 2010
Received in revised form 1 April 2011
Accepted 9 May 2011
Available online 14 May 2011

Keywords:
Lyophilized
Recombinant
Deinococcus radiodurans
Uranium

ABSTRACT

Employment of genetically engineered radiation resistant organisms to recover radionuclides/heavy metals from radioactive wastes is an attractive proposition. Cells of recombinant *Deinococcus radiodurans* strain expressing, a non-specific acid phosphatase encoding *phoN* gene, were lyophilized. Lyophilized recombinant *Deinococcus* cells retained viability and PhoN activity and could efficiently precipitate uranium from aqueous solutions for up to six months of storage at room temperature. Batch process for uranium removal using lyophilized cells was more efficient compared to a flow through system, in terms of percent uranium removed, substrate conservation and time taken. Lyophilized recombinant *Deinococcus* cells exhibited high loading of up to 5.7 g uranium/g dry weight of cells in a batch process at 20 mM input uranium concentration. Lyophilization deflated the cells but did not alter gross cell morphology or surface nucleation capability of cells for uranium precipitation. The precipitated uranyl phosphate remained tightly associated with the cell surface, thus facilitating easy recovery.

1. Introduction

Nuclear waste management has been a contentious aspect of nuclear power programs around the world. Radionuclide-containing wastes are produced at all steps in the nuclear fuel cycle from milling and mining of uranium ores to fuel fabrication, reactor operation and fuel reprocessing. Biological treatment strategies of waste have evoked considerable interest (Gadd, 2000) as viable and eco-friendly alternatives, especially at low concentrations of the radionuclide and for *in situ* bioremediation. Naturally occurring organisms such as *Citrobacter* harboring a non-specific periplasmic acid phosphatase PhoN, have been considered suitable for bioremediation of heavy metals (Macaskie et al., 1994). PhoN hydrolyses organic phosphates and the inorganic phosphate, thus released, brings about metal precipitation as insoluble metal phosphate on the cell surface (Kier et al., 1977; Macaskie et al., 1994). In the past, efficient bioprecipitation of uranium with *Citrobacter* strains (Macaskie, 1990; Jeong et al., 1997; Macaskie et al., 1994) and recombinant *Escherichia coli* strains expressing PhoN (Basnakova et al., 1998) have been reported. However, radioactivity restricts the survival, cellular integrity and functionality of such microbes in nuclear wastes (Daly, 2000; Appukuttan et al., 2006).

The bacteria belonging to *Deinococcaceae* family have the extraordinary ability to withstand radiation doses up to 10–15 kGy (Battista, 1997; Daly, 2000). Recently our laboratory genetically engineered *Deinococcus radiodurans* R1 to express *phoN* (Appukuttan et al., 2006). The recombinant strain, DrPhoN survived extreme radiation stress, unlike recombinant *E. coli*-PhoN clones and precipitated uranium from dilute aqueous solutions in high radiation environment. In order to extend the use of the recombinant *Deinococcus* strain for application in nuclear waste, the following factors need to be suitably addressed: (a) the ease of handling and transportation of biomass, (b) shelf-life and storage of cells, (c) mode of application, and (d) substrate conservation. Biological materials often must be dried to reduce bulk volume and to stabilize them for storage or distribution. Drying causes significant loss of activity and viability. But, freeze-drying, significantly reduces such damage (Snowman, 1988; Seetharam et al., 2009).

The present study investigated the utility of lyophilization to achieve aforesaid desirable features for PhoN expressing *D. radiodurans* strains. Our results show that lyophilized recombinant *Deinococcus* cells retained viability, PhoN activity as well as uranium precipitation ability up to 6 months of storage at room

* Corresponding author. Tel.: +91 22 25595342; fax: +91 22 25505189.
E-mail address: sksmbd@barc.gov.in (S.K. Apte).
[1] These authors contributed equally to this work.

0168-1656/$ – see front matter © 2011 Elsevier B.V. All rights reserved.
doi:10.1016/j.jbiotec.2011.05.002

temperature. Lyophilized cells also retained surface localization property of the precipitate, and facilitated, loading of 5.7 g/g dry weight of biomass in a batch process.

2. Materials and methods

2.1. Bacterial strains and growth conditions

Cells of recombinant *D. radiodurans* strains, DrEV (carrying the shuttle vector pRAD1) (Meima and Lidstrom, 2000) and DrPhoN (carrying *phoN* gene from *Salmonella enterica* serovar *Typhi* cloned downstream of *Deinococcal groESL* promoter) (Appukuttan et al., 2006) were grown aerobically in TGY (1% Bacto Tryptone, 0.1% glucose, and 0.5% yeast extract) liquid medium with 3 μg/ml of chloramphenicol at 32 °C ± 1 °C under agitation (180 ± 5 rpm). Growth was assessed by measuring turbidity (OD_{600nm}) or by determining colony forming units (CFUs) on TGY agar plates (1.5% Bacto Agar) after 48 h incubation at 32 °C ± 1 °C.

2.2. Lyophilization

Overnight grown cells were washed twice with distilled water and re-suspended in distilled water to form a thick suspension which was taken in a Petri plate and frozen in liquid nitrogen. The frozen cells were lyophilized overnight in a Lyospeed (Genevac, United Kingdom, Model Refrigerant R502) at 0.07 mbar for 18 h. The lyophilized cells were scraped off from the Petri plate and stored in Eppendorf vials at room temperature until used for uranium recovery. The survival of cells was measured in terms of the colony forming units (CFUs) before lyophilization or after re-wetting of the lyophilized powder. Fresh and lyophilized cells, equivalent in terms of their protein content were plated onto TGY agar plates containing chloramphenicol for determination of CFUs. The protein content of 0.33 mg lyophilized cells re-suspended in 1 ml distilled water was equivalent to 1 ml of 1.0 OD_{600nm} fresh cells. The lyophilized cells when re-suspended rapidly formed a uniform suspension in acetate buffer and were allowed to equilibrate for 5 min before the PhoN activity and uranium precipitation assays were carried out.

2.3. Acid phosphatase activity assays

The cell-bound PhoN activity was estimated by the liberation of *p*-nitrophenol from di-sodium *p*-nitrophenyl phosphate (*p*NPP), as described earlier (Bolton and Dean, 1972), and expressed as nmol of *p*-nitrophenol (*p*NP) liberated min^{-1} mg^{-1} bacterial protein. Protein concentration was determined by Lowry's method (Lowry et al., 1951) using a protein estimation kit (Bangalore Genei Pvt. Ltd., India).

2.4. Batch precipitation of uranium

Uranium precipitation assays were performed as described previously (Macaskie et al., 2000) with certain modifications (Appukuttan et al., 2006). About 80 mg lyophilized cells were re-suspended in 100 ml (equivalent to $O.D_{600nm}$ of 2.4) of 2 mM acetate buffer (pH 5.0) for 5 min followed by addition of uranyl nitrate and β-glycerophosphate at concentrations specified for each experiment. At different time intervals, aliquots were subjected to centrifugation and the uranium in the supernatant was estimated by Arsenazo method as described previously (Appukuttan et al., 2006). Appropriate controls were included to determine (a) spontaneous chemical precipitation of the metal (assays without any cells), (b) biosorption of uranium on the surface of the lyophilized cells (assays with DrEV cells) and (c) uranium sorption to the surface of the container (assays carried out in different containers which were washed post assay extensively to ascertain that no uranium bound to the surface).

Table 1
Viability and PhoN activity of lyophilized DrPhoN cells. Fresh and lyophilized cells equivalent in terms of their protein content were suitably diluted and plated onto TGY agar plates containing 3 μg/ml chloramphenicol. The viable counts reported are the average values from three independent lyophilization experiments. PhoN activity is expressed as nmol of *p*-NP liberated min^{-1} mg^{-1} protein.

Treatment	cfu/ml	PhoN activity
Before lyophilization	$(1.1 \pm 0.07) \times 10^8$	190 ± 10
After lyophilization	$(1.0 \pm 0.056) \times 10^8$ (90%)	167 ± 5 (87.8%)

Values in parentheses indicate percent of fresh cells.

2.5. Column-based uranium precipitation

About 5 ml of 15% polyacrylamide gel was prepared in distilled water (2.4 ml of distilled water, 2.5 ml of 30% Acrylamide–bisacrylamide solution, 50 μl of 10% APS and 50 μl of TEMED) with 150 mg of lyophilized cells and allowed to set at 4 °C for 45 min. The gel containing the cells was washed four times in 10 ml distilled water and then shredded into small pieces using a sieve (8 pores cm^{-1}). The shredded gel pieces were allowed to swell in distilled water for 5 min, following which they were mixed with 2.5 ml of acid washed sand and packed into a plastic column (1.4 cm inner diameter × 9 cm). The column was equilibrated and allowed to stand overnight. Following this, the input solution containing 1 mM uranyl nitrate and 5 mM β-glycerophosphate in 2 mM acetate buffer (pH 5.0) was allowed to continuously flow through the system at a flow rate of 5 ml h^{-1}. The uranium concentration in the flow through was recorded at different time intervals. A similar column set-up with no added cells served as a negative control where no change in uranium concentration was recorded in the flow-through.

2.6. Scanning Electron Microscopy (SEM) and Energy Dispersive X-ray spectroscopy (EDX) of lyophilized cells

Deinococcus cells were processed for electron microscopy as described earlier (Heather et al., 2006). Briefly, cells were washed in cacodylate buffer (100 mM, pH 7.4) and fixed in Karnovskys fixative (Karnovsky, 1965) for 2 h at 4 °C. Samples were then washed in 100 mM cacodylate buffer, dehydrated in a graded series of 20–100% ethanol, spotted on glass slides and dried at 37 °C for 1 h. The dried samples were gold coated by thermal evaporation technique and analyzed by SEM and EDX using a VEGA 40, Tescan Microscope, Czechoslovakia and INCA energy 250 EDX System, Oxford Instrument, United Kingdom.

3. Results

3.1. Effect of lyophilization on survival, cell morphology, PhoN activity and uranium precipitation ability of recombinant D. radiodurans cells

Lyophilization of recombinant DrPhoN cells converted them into a fine powder which could be more easily handled and stored in vials at room temperature. The lyophilized powder was weighed and directly used, after 5 min of wetting in 2 mM acetate buffer, in all experiments to compare their performance against equivalent fresh cells.

Lyophilized DrPhoN cells retained 90% viability and 88% PhoN activity (Table 1) of fresh cells. Scanning Electron Microscopy (Fig. 1a and b) showed no gross morphological damage to cells except that they looked deflated as compared to fresh cells. Lyophilized DrPhoN cells were introduced into a typical reaction

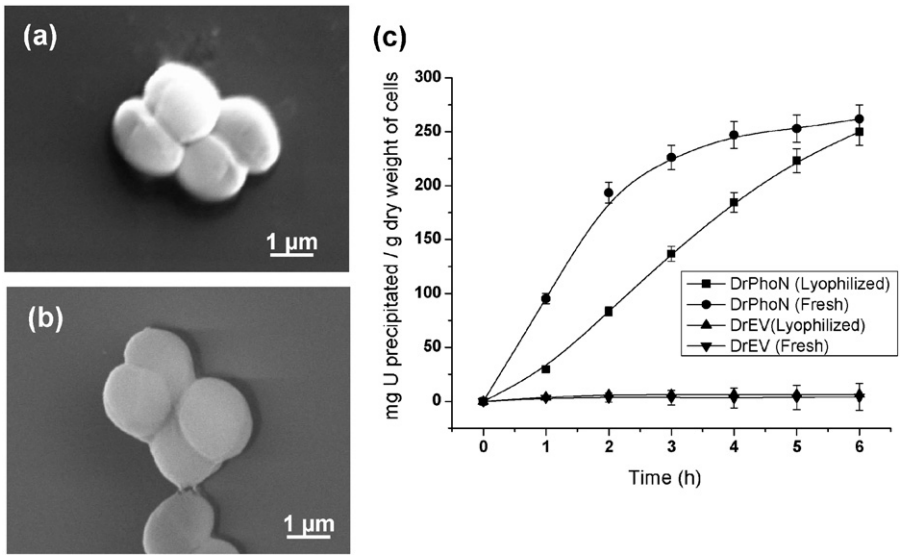

Fig. 1. Effect of lyophilization on cell morphology and uranium precipitation ability of recombinant DrPhoN cells. Scanning Electron micrographs of DrPhoN cells before (a) and after (b) lyophilization. (c) Kinetics of uranium precipitation by fresh (●) or lyophilized (■) DrPhoN cells. Lyophilized cell mass (equivalent to OD_{600} 3.0 of fresh cells) was tested in 3 ml assays containing 1 mM uranyl nitrate and 5 mM β-glycerophosphate. Timed aliquots of the cell suspension were subjected to centrifugation and the uranium in the supernatant was estimated. Lyophilized (▲) or fresh (▼) DrEV cells were included as negative controls.

mix containing 1 mM uranyl nitrate and 5 mM β-glycerophosphate. The uranium precipitation by lyophilized cells was found to be considerably lower than in fresh cells initially but improved with time (Fig. 1c). Approximately 90% (~240 mg U/g dry weight cells) precipitation was achieved by lyophilized DrPhoN cells in 6 h and by fresh cells in 4 h, while fresh or lyophilized DrEV cells failed to precipitate uranium.

3.2. Shelf-life of lyophilized recombinant cells

The PhoN activity as well as the uranium precipitation ability of lyophilized cells remained largely unaffected even after six months of storage at room temperature (Table 2). In contrast, in fresh cells these activities were severely inhibited after 8–10 days of storage even at 4 °C. Lyophilization, thus, significantly extended the shelf-life of the recombinant DrPhoN clones. No uranium precipitation was observed in the absence of DrPhoN cells, while controls lacking β-glycerophosphate or DrEV cells displayed negligible precipitation (<3%) of input uranium in 6 h (Table 2).

3.3. Immobilization of lyophilized, recombinant cells for column-based uranium precipitation

Lyophilized cells of DrPhoN or DrEV were immobilized into polyacrylamide gels and tested in a continuous gravity based flow-through system as described in Section 2. The uranium metal concentration in the flow through was reduced by 50–60% of the input uranium concentration on an average. The rate of uranium precipitation was similar for 5–6 days, following which the rate started to decrease due to clogging of the column. At the end of 8 days, around 1 L of the uranyl nitrate solution had passed through the column resulting in uranium loading of 0.73 g/g dry weight (Fig. 2a). At the end of the experiment the column packed with recombinant cells turned distinctly yellow due to substantial deposition

Table 2
PhoN activity and uranium precipitation ability of fresh and lyophilized DrPhoN cells during storage. PhoN activity is expressed in nmol of *p*-NP liberated min^{-1} mg^{-1} protein. For uranium precipitation, fresh cells (OD_{600} of 3.0) or lyophilized cells (3 mg) were employed in 3 ml assays containing 1 mM uranyl nitrate and 5 mM β-glycerophosphate in 2 mM acetate buffer pH 5.0. Data from controls are also included.

Time (days)	PhoN activity	Amount of U precipitated in 6 h	mg uranium precipitated/g dry weight cells
Time (in days)	Fresh DrPhoN cells		
0	190 ± 10	90 ± 2%	214.20 ± 4.7
2	175 ± 5	84 ± 5%	199.90 ± 1.19
4	150 ±10	73 ± 5%	173.74 ± 1.19
8	120 ± 8	31 ± 3%	73.78 ± 0.07
10	110 ± 5	28 ± 5%	66.60 ± 1.19
Time (months)	Lyophilized DrPhoN cells		
0	167 ± 5	85 ± 5%	202.30 ± 1.19
1	165 ± 4	84 ± 6%	199.92 ± 1.43
2	166 ± 6	86 ± 4%	204.60 ± 0.09
4	160 ± 5	83 ± 6%	197.54 ± 1.42
6	157 ± 4	76 ± 5%	180.88 ± 1.19

Control data for uranium precipitation

Assay conditions	Amount of U precipitated in 6h	mg uranium precipitated/g dry weight cells
Without cells	n.d.	n.d.
Without β-glycerophosphate	2.2 ± 0.3%	5.22 ± 0.5
DrEV	2.8 ± 0.3%	6.65 ± 0.45
DrPhoN	85 ± 5%	202.3 ± 1.19

n.d.: not detectable.

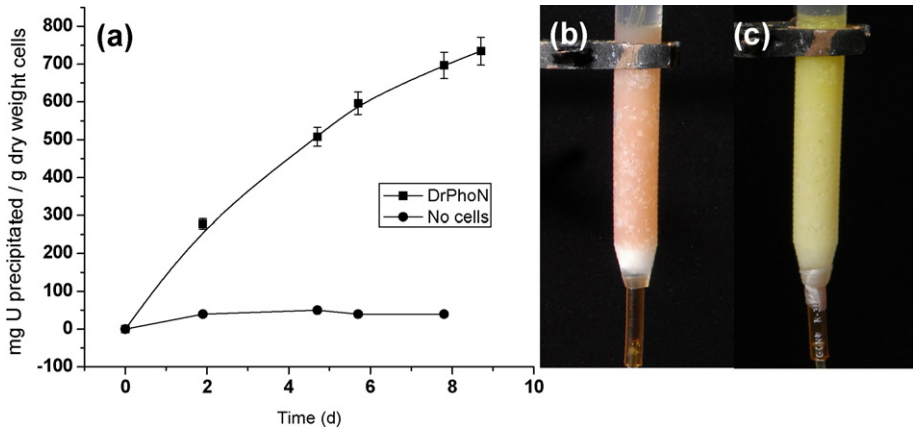

Fig. 2. Uranium precipitation by immobilized recombinant *D. radiodurans* cells. Lyophilized DrPhoN (■) cells (150 mg) immobilized in polyacrylamide gel were filled into a column. A similar column without any immobilized cells (●) served as a negative control. One litre of feed solution containing 1 mM uranyl nitrate and 5 mM β-glycerophosphate was passed through the column over a period of 8 days at an average flow rate of 5 ml h^{-1}. (a) Uranium was estimated in the flow through at regular intervals and the loading on the column was calculated accordingly. (b and c) Column of DrPhoN cells, immobilized in polyacrylamide gel, before the start of the experiment (b) and at the end of the experiment (c).

of uranyl phosphate (Fig. 2b and c). In column without cells, no uranium removal was observed in the flow-through effluent.

3.4. Metal precipitation by DrPhoN cells at high uranium concentrations

In a batch process, the lyophilized cells were used to precipitate higher concentrations of uranyl nitrate (10–20 mM) with twice the corresponding concentration of β-glycerophosphate. The precipitation kinetics is shown in Fig. 3a. At 10 mM uranyl ion concentration, DrPhoN clones took 8 days to reach 80% (2.4 g/g dry weight cells) precipitation of uranium and 13 d to achieve 100% precipitation (2.7 g/g dry weight cells). At higher concentrations of 15 and 20 mM, the cells took 13 days to obtain ~85% (3.7 and 4.85 g/g dry weight cells) precipitation, with complete precipitation occurring in 17 days. The maximum uranium loading obtained was 5.7 g uranium/g dry weight at 20 mM uranium concentration. No metal precipitation occurred in assays without cells, at all the concentrations of the metal tested.

3.5. Scanning Electron Microscopy and Energy Dispersive X-ray spectroscopy of uranium loaded cells

DrPhoN cells which had precipitated around 0.3 g uranium/g dry weight of cells exhibited a few uranyl phosphate deposits on the surface (Fig. 3b). At higher loading of 3.2 g uranium/g dry weight of cells, the entire cell surface was covered with a meshwork of S-shaped (sigmoid) fiber-like precipitate giving the cells a cottony appearance (Figs. 3c and 4a). At all times, the precipitate remained associated with biomass and no loose precipitate was observed either in several SEM fields (Figs. 3b, 3c and 4a) or in chemical analysis (Table 2 and Fig. 1). Energy Dispersive X-ray spectroscopy of DrPhoN cells which had precipitated 95% of uranium from a solution of 10 mM and 20 mM β-glycerophosphate in 7 days (3.2 g uranium/g dry weight of lyophilized cells) showed

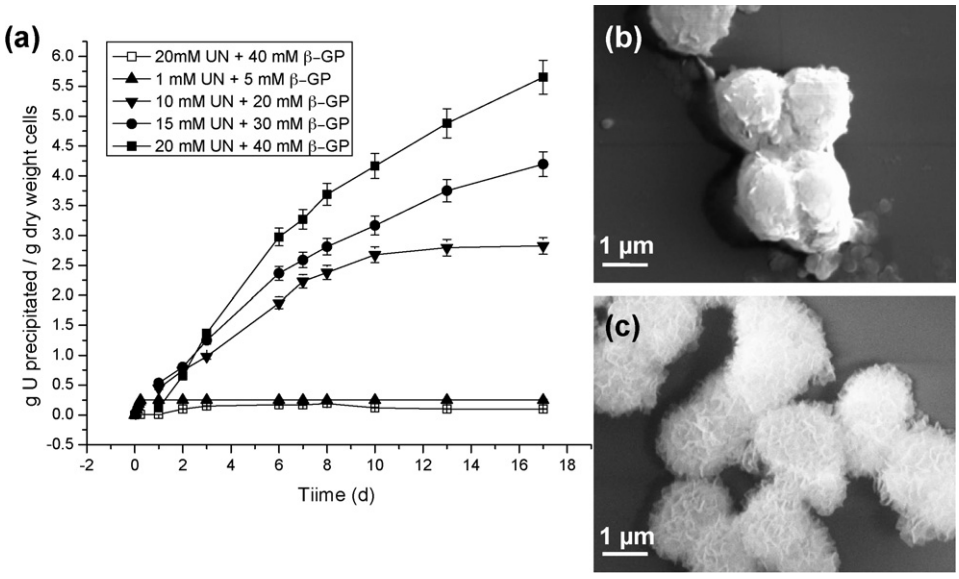

Fig. 3. Uranium precipitation by lyophilized DrPhoN cells at different concentrations of uranyl nitrate (UN). (a) About 80 mg of lyophilized cells were used to precipitate 1, 10, 15 and 20 mM uranyl nitrate with 5, 20, 30 and 40 mM of β-glycerophosphate (β-GP) respectively in 100 ml reaction volume. Timed aliquots of the cell suspension were subjected to centrifugation and uranium in the supernatant was estimated to calculate the metal loading on the biomass. Data from control, without any added cells are also shown (□). (b, c), Scanning electron micrographs of cells which had been exposed to 1 and 10 mM uranium for 10 d to achieve a loading of (b) 0.3 g uranium/g dry weight cells and (c) 3.2 g uranium/g dry weight respectively.

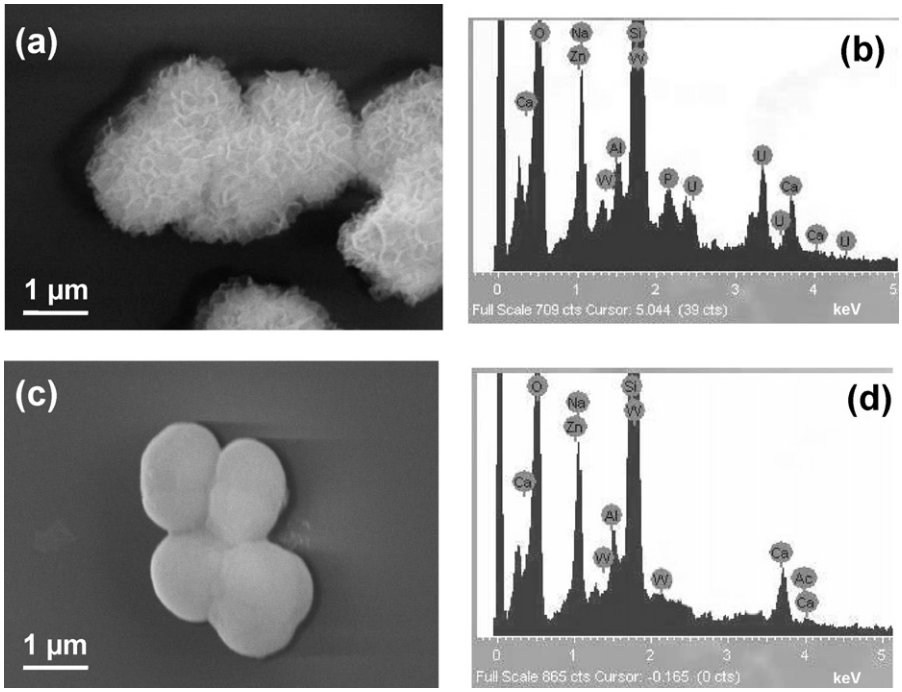

Fig. 4. Scanning Electron Microscopy and Energy Dispersive X-ray (EDX) spectra of uranium bioprecipitation by recombinant *Deinococcus* strains. Cells of (a) DrPhoN and (c) DrEV were incubated in a solution containing 10 mM uranium and 20 mM β-glycerophosphate for 7 days and visualized by SEM. Corresponding EDX spectra of uranium challenged cells are shown for (b) DrPhoN or (d) DrEV cells. Silicon peak detected arose from the glass substrate on which the samples were spotted.

distinct presence of uranium and phosphorus peaks (Fig. 4b). In comparison, in DrEV cells which had been exposed to similar conditions for similar length of time, neither the surface associated structures were visible (Fig. 4c) nor was uranium and phosphorus detected by EDX (Fig. 4d).

4. Discussion

The radioresistant bacterium, *D. radiodurans* offers a potential system for genetic manipulation for application in bioremediation of radioactive nuclear waste (Daly, 2000). However, the microbe suffers from inherent sensitivity to many metals (Ruggiero et al., 2005). Surface bioprecipitation of metals from wastes using a periplasmic enzyme such as PhoN is a mechanism which is essentially de-coupled from growth and cellular toxicity of the metal involved. The inherent metal sensitivity of *D. radiodurans* (Ruggiero et al., 2005) can therefore be circumvented by introducing cell surface associated metal bioremediation capabilities. Accordingly, we constructed a PhoN expressing recombinant *D. radiodurans* strain, DrPhoN, reported earlier (Appukuttan et al., 2006). The DrPhoN strain showed lower PhoN activity than the recombinant *E. coli* cells expressing *phoN* (Appukuttan et al., 2006; Basnakova et al., 1998) or the *Citrobacter* cells reported earlier (Macaskie, 1990; Macaskie et al., 1994), but could efficiently precipitate >90% uranium from dilute (0.8 mM) metal solutions in 6 h if higher cell densities were employed (Appukuttan et al., 2006). Inclusion of appropriately designed controls in such assays (a) clearly ruled out spontaneous precipitation of uranium or its non-specific sorption to container or cells, and (b) established that the uranium precipitated was entirely a consequence of enzymatic (PhoN) activity of recombinant DrPhoN cells.

High efficiency of uranium precipitation have been reported for *Citrobacter* strain or PhoN expressing recombinant *E. coli* strains in optimized column/pump based flow-through systems resulting in high loading of ~9 g U/g dry weight biomass weight (Basnakova et al., 1998). The major advantage DrPhoN cells score over the aforesaid bacteria is in their utility for bioremediation of radioactive waste solution. As reported earlier, DrPhoN cells continued to precipitate uranium under high radiation conditions (6 kGy) of Co-60 γ-rays (Appukuttan et al., 2006). In contrast, PhoN over-expressing *E. coli* strain failed to do so and disintegrated above a dose of 1 kGy.

Further improvement of the recombinant cells aimed at their application in bioremediation of uranium from nuclear waste was achieved through lyophilization. Lyophilization of DrPhoN cells without cryopreservatives had the following beneficial consequences: (1) reduced the bulk volume and converted the biomass into a dry powdered form, thereby increasing the ease of handling, storage, transport and application, (2) preserved the PhoN activity and uranium precipitation ability of cells for application in a batch process or in a flow through system, (3) retained cellular integrity and surface precipitation property, thereby facilitating easy recovery of precipitated metal with the biomass, (4) retained cell viability and allowed use of such cell powder as inoculum to build-up biomass for *in situ* bioremediation experiments, and (5) significantly extended the shelf life of the product in terms of viability and uranium precipitation capability for up to six months at room temperature.

Assessment of the suitable mode of application of lyophilized cells revealed the superiority of batch process over a column-based flow-through system in terms of (a) time required, (b) extent of uranium removal, and (c) substrate conservation. In a batch process, lyophilized cells could remove 100% of 1 mM input uranium in 6 h with 15 μmol of substrate (β-glycerophosphate) resulting in a loading of 260 mg U/g dry weight cells. To achieve equivalent loading in a flow-through system, containing lyophilized cells immobilized in polyacrylamide gel, required two days and 1200 μmol of substrate. The potential of flow-through system appeared to be limited due to clogging of the column by the precipitate formed. In a batch process, the uranium loaded cells settled down rapidly enabling easy removal of metal free supernatant. Thus, a simple set-up, easy downstream processing, rapid uranium precipitation, and substrate economy clearly make the batch process the preferred mode of operation for PhoN mediated uranium precipitation.

Further, for radioactive waste, a continuous flow-through operation would require setting up an additional independent facility with columns, pumps, etc. which may pose additional containment requirement and thereby contribute to cost. In contrast, in batch process, the already existing facility of delay tanks/waste tank farms can be utilized for easy application of the lyophilized powder. Additionally, batch operation provides better process control over the system which is a priority while handling radioactive waste.

Scanning Electron Microscopy revealed that precipitated uranium was firmly lodged on to the surface of DrPhoN cells. Even at very high loadings of 3.2 g/g dry weight of cells, no free precipitate was seen in the fields observed. This has important implications for settling down of precipitated sludge and downstream processing of the effluent as emphasized earlier (Macaskie et al., 1994). It has been postulated that formation of nucleation sites on the cell surface is important for initiation of metal precipitate formation and membrane phospholipids may function as sites for uranyl phosphate crystallization (Macaskie et al., 1996; Jeong et al., 1997). The high density of uranyl phosphate precipitate on the surface of DrPhoN cells is a clear indication that abundant sites are available on such cells. This makes the system capable of not only biorecovery of traces of uranium from dilute nuclear wastes but also of precipitating much higher amounts of uranium.

In the environment, uranium concentrations range from 1 to 10 mg/L in contaminated ground water sources to up to 20 g/L (~10 mM) in high-level waste generated from reprocessing of spent nuclear fuel (Joshi et al., 2005). In oxygenated aqueous systems, uranyl nitrate is highly soluble, while uranyl phosphate is insoluble (Finch and Murakami, 1999). The insolubility and stability of uranyl phosphate provides a long term sink for uranium. Therefore, bio-mineralization as phosphates is an effective mechanism for metal immobilization, especially from radioactive waste.

This study has demonstrated important capabilities of recombinant DrPhoN cells: (a) to precipitate uranium efficiently, as a dehydrated powder with a shelf life of up to six months without refrigeration or vacuum, (b) to precipitate uranium over a wide range of concentrations without any noticeable poisoning of the enzyme by the metal, and (c) to retain the entire precipitated uranium cell surface bound. When combined with the already well known non-pathogenicity, ubiquitous distribution and high radioresistance of *D. radiodurans*, the attributes elucidated in the present study make recombinant DrPhoN strain an appropriate choice for environmental application in metal removal from nuclear waste.

References

Appukuttan, D., Rao, A.S., Apte, S.K., 2006. Engineering of *Deinococcus radiodurans* R1 for bioprecipitation of uranium from dilute nuclear waste. Appl. Environ. Microbiol. 72, 7873–7878.

Basnakova, G., Stephens, E.R., Thaller, M.C., Rossolini, G.M., Macaskie, L.E., 1998. The use of *Escherichia coli* bearing a *phoN* gene for the removal of uranium and nickel from aqueous flows. Appl. Microbiol. Biotechnol. 50, 266–272.

Battista, J.R., 1997. Against all odds: the survival strategies of *Deinococcus radiodurans*. Annu. Rev. Microbiol. 51, 203–224.

Bolton, P.G., Dean, A.C.R., 1972. Phosphatase synthesis in *Klebsiella (Aerobacter) aerogenes* growing in continuous cultures. Biochem. J. 127, 87–96.

Daly, M.J., 2000. Engineering radiation-resistant bacteria for environmental biotechnology. Curr. Opin. Biotechnol. 11, 280–285.

Finch, R., Murakami, T., 1999. Systematics and paragenesis of uranium minerals. In: Burns, P.C., Finch, R. (Eds.), Uranium: Mineralogy, Geochemistry and the Environment. Mineralogical Society of America, Washington, DC.

Gadd, G.M., 2000. Bioremedial potential of microbial mechanisms of metal mobilization and immobilization. Curr. Opin. Biotechnol. 11, 271–279.

Jeong, B.C., Hawes, C., Bonthrone, K.M., Macaskie, L.E., 1997. Localization of enzymically enhanced heavy metal accumulation by *Citrobacter* sp. and metal accumulation in vitro by liposomes containing entrapped enzyme. Microbiology 143, 2497–2507.

Joshi, J.M., Pathak, P.N., Manchanda, V.K., 2005. Selective removal of uranium from high-level waste solution employing Tri-n-Butyl phosphate as the extractant. Solvent extraction and ion exchange 23, 663–675.

Karnovsky, M.J., 1965. A formaldehyde-glutaraldehyde fixative of high osmolality for use in electron microscopy. J. Cell Biol. 27, 137A–138A (Abst).

Kier, L.D., Weppelman, R.M., Ames, B.N., 1977. Resolution and purification of three periplasmic phosphatases of *Salmonella typhimurium*. J. Bacteriol. 130, 399–410.

Lowry, O.H., Rosebrough, N.J., Farr, A.L., Randall, R.J., 1951. Protein measurement with the Folin phenol reagent. J. Biol. Chem. 193, 265–275.

Macaskie, L.E., 1990. An immobilized Cell Bioprocess for the Removal of Heavy Metals from Aqueous Flows. J. Chem. Technol. Biotechnol. 49, 357–379.

Macaskie, L.E., Jeong, B.C., Tolley, M.R., 1994. Enzymically accelerated biomineralization of heavy metals: application to the removal of americium and plutonium from aqueous flows. FEMS Microbiol. Rev. 14, 351–368.

Macaskie, L.E., Lloyd, J.R., Thomas, R.A.P., Tolley, M.R., 1996. The use of microorganisms for the remediation of solutions contaminated with actinide elements, other radionuclides, and other organic contaminants generated by nuclear fuel activities. Nucl. Energy 35 (4), 257–271.

Macaskie, L.E., Bonthrone, K.M., Yong, P., Goddard, D.T., 2000. Enzymically mediated bioprecipitation of uranium by a *Citrobacter* sp.: a concerted role for exocellular lipopolysaccharide and associated phosphatase in biomineral formation. Microbiology 146, 1855–1867.

Meima, R., Lidstrom, M.E., 2000. Characterization of the minimal replicon of a cryptic *Deinococcus radiodurans* SARK plasmid and development of versatile *Escherichia coli–D. radiodurans* shuttle vectors. Appl. Environ. Microbiol. 66, 3856–3867.

Heather, R., Lara, J.C., Schmid, A.K., Lidstrom, M.E., 2006. Involvement of the S-layer proteins Hpi and SlpA in the maintenance of cell envelope integrity in *Deinococcus radiodurans* R1. Microbiology 152, 2779–2787.

Ruggiero, C.E., Boukhalfa, H., Forsythe, J.H., Lack, J.G., Hersman, L.E., Neu, M.P., 2005. Actinide and metal toxicity to prospective bioremediation bacteria. Environ. Microbiol. 7, 88–97.

Seetharam, C., Soundarajan, S., Udas, A.C., Rao, A.S., Apte, S.K., 2009. Lyophilized, non-viable, recombinant *E. coli* cells for cadmium bioprecipitation and recovery. Process Biochem. 44, 246–250.

Snowman, J.W., 1988. Downstream Processes: Equipment and Techniques. Alan R. Liss, Inc., New York, pp. 315–351.

Bioengineered Bugs 3:1, 44–48; January/February 2012; © 2012 Landes Bioscience

Recombinant *D. radiodurans* cells for bioremediation of heavy metals from acidic/neutral aqueous wastes

Chitra Seetharam Misra,[1,†] Deepti Appukuttan,[1,†] Venkata Siva Satyanarayana Kantamreddi,[2] Amara S. Rao[1] and Shree Kumar Apte[1,*]
[1]Molecular Biology Division, Bhabha Atomic Research Centre; Mumbai, India; [2]Department of Chemistry, GITAM University; Hyderabad, India

[†]These authors contributed equally to the work.

The stability and superior metal bioremediation ability of genetically engineered *Deinococcus radiodurans* cells, expressing a non-specific acid phosphatase, PhoN in high radiation environment has already been established. The lyophilized recombinant DrPhoN cells retained PhoN activity and uranium precipitation ability. Such cells also displayed an extended shelf life of 6 months during storage at room temperature and showed surface associated precipitation of uranium as well as other metals like cadmium. Lyophilized cells, immobilized in polyacrylamide gels could be used for uranium bioprecipitation in a flow through system resulting in 70% removal from 1mM input uranium solution and a loading of 1 g uranium/g dry weight cells. Compared with a batch process which achieved a loading of 5.7 g uranium/g biomass, the efficiency of the column process was low due to clogging of the column by the precipitate.

Keywords: *D. radiodurans*, heavy metals, bioremediation, radioactive waste, lyophilized, PhoN

Submitted: 08/31/11

Revised: 11/26/11

Accepted: 11/28/11

http://dx.doi.org/10.4161/bbug.3.1.18878

*Correspondence to: Shree Kumar Apte;
Email: sksmbd@barc.gov.in

Introduction

Bacteria like *Citrobacter* and *Pseudomonas* sp. have the ability to transform, detoxify or immobilize a variety of metallic and organic pollutants.[1,2] However, like most organisms, these bacteria are very sensitive to ionizing radiation, and their use for bioremediation in high radiation environments is very limited. Aqueous liquid nuclear waste generated during the reprocessing of spent fuel rods contains high levels of radioactivity.[3] Actinides present in this waste along with other fission products emit highly damaging beta and gamma radiation. Use of radio-resistant microbes is an essential prerequisite for bioremediation in such an environment.

In recent years, the extremely radioresistant Gram positive bacterium, *Deinococcus radiodurans*, has become an organism of choice for engineering a number of strategies for bioremediation of radioactive waste.[4-6] The genus, *Deinococcus* comprises of a large number of radioresistant species, many of which also display dessication, temperature and metal tolerance (*D. deserti, D. geothermalis* and *D. indicus*).[7-9] The most studied, *D. radiodurans* strain R1 has a small 3.28 Mb genome comprised of two chromosomes (2.64 Mb and 0.41 Mb), a megaplasmid (0.18 Mb) and plasmid (0.045 Mb) and can withstand exposure to 5–6 kGy of ionizing radiation without significant loss of viability.[10] Such extreme radioresistance of the strain stems from its phenomenal DNA repair proficiency. Multiplicity of genome organized in a torroid ring-like structure, possession of novel genes for repair of damaged DNA (Extended Synthesis-Dependent Strand Annealing, PprA etc.), Mn(II) complexes which protect cellular enzymes from oxidative stress damage and efficient damage cleaning systems that restore homeostasis post-irradiation, all contribute to radioresistance.[11-15] Comparative genomes of at least three deinococcal strains has revealed commonality of genes, molecular mechanisms underlying radioresistance across the species.[16]

Attempts to introduce novel bioremediation capabilities into *D. radiodurans*

have been successful. Strategies involving both chromosomal integration as well as vector based expression of foreign genes in trans have proved effective in this organism.[4-6] Explorations on the possibility of using *D. radiodurans* in high radiation environments also revealed the inherent organic solvent tolerance[4] and metal reduction ability[17] of this organism. Taken together, *D. radiodurans* has emerged as an organism which is easy to genetically manipulate and is also radiation resistant with reasonable inherent pollutant tolerance. These traits make this organism ideally suited for remediation of nuclear waste sites.

Recombinant strains of *D. radiodurans* expressing toluene dioxygenase (TDO) from *Pseudomonas putida F1* could oxidize a variety of organic substrates, while strains carrying the *merA* operon could reduce toxic ionic Hg(II) to the less toxic elemental mercury Hg(0).[4,5] Importantly, the recombinant strains could grow in the presence of both the pollutant and γ-radiation at 60Gy/h. Improvements in the bioremediation capabilities of *D. radiodurans* were brought about by pyramiding different genes into a single strain to bring about complete, simultaneous degradation of organic pollutant (complete oxidation of toluene by expression of *tod* and *xyl* genes)[18] as well as to impart metal detoxification and organic pollutant degradation ability (toluene and mercury detoxification by expression of *tod* and *mer* operons)[5] for mixed waste.

We have earlier reported uranium bioprecipitation by genetically engineered *D. radiodurans* expressing a nonspecific acid phosphatase, PhoN. In *E. coli*, the enzyme resides in periplasm and cleaves a phosphomonoester to generate high, local concentrations of inorganic phosphate which can precipitate uranium (**Fig. 1**). The corresponding gene, *phoN* was cloned from *Salmonella enterica* serovar Typhi and expressed under the influence of a strong deinococcal *groESL* promoter (P_{groESL}) in both *E. coli* and *D. radiodurans*.[19,20] The PhoN expression in recombinant bacteria was qualitatively ascertained on histochemical plates containing phenolphthalein diphosphate (PDP) and methyl green (MG). On such plates, colonies which are positive for acid phosphatase appear dark green due to precipitation of methyl green at acidic pH caused by the release of inorganic phosphate ions (**Fig. 1**).[21] The liberated inorganic phosphate from a suitable substrate molecule like β-glycerophosphate, causes precipitation of metals as cell-bound metal phosphates and facilitates their easy removal from aqueous solution. Similar approach was also designed for uranium precipitation from alkaline solutions by cloning a novel, high specific activity alkaline phosphatase (PhoK) from Sphingomonas and overexpressing it in *E. coli*.[22] The recombinant *E. coli* overexpressing 55 times higher levels of PhoK, very efficiently precipitated uranyl carbonate from dilute solutions at pH 9.0. PhoK gene is currently being engineered into *D. radiodurans*. The mechanism for metal precipitation is essentially extracellular and de-coupled from growth. Therefore, the chemical toxicity of waste is not a deterrent in use of the recombinant strain.

Application of DrPhoN Cells for Metal Removal

Our earlier studies using the recombinant *E. coli* (EcPhoN) and *D. radiodurans* (DrPhoN) cells expressing the *phoN* gene from the deinococcal P_{groESL} promoter showed that both the in-gel as well as the cell bound PhoN activities were higher in recombinant cells of *E. coli* than in Deinococcus. A possible explanation for this may lie in the six layered cell wall which *D. radiodurans* is known to possess.[23] The precise localization of the PhoN enzyme among these six layers is not known since the periplasm is poorly defined in Deinococcus. But, this may limit access of substrate and its availability and result in lower activities.

The lower PhoN activity of the recombinant Deinococcus clones was compensated by using higher cell density to obtain the required activity.[19] When uranium precipitation was performed with EcPhoN and DrPhoN cells carrying equal PhoN activity (~2000 U as determined by *p*-nitrophenyl phosphate assays), the kinetics of uranium precipitation was nearly identical in both strains with >90% uranium precipitated in approximately 3h (**Fig. 2A**). Appropriate controls were included to ensure that the observed precipitate was due to β-glycerophosphate dependent PhoN activity and not a result of spontaneous chemical precipitation under the experimental conditions used.[19] Controls were also included to correct for possible uranium loss due to non-specific binding to cells and to the container. Notwithstanding the difference between *E. coli* and Deinococcus *phoN* clones, equivalent PhoN activities from both the recombinant clones exhibited efficient and equal uranium precipitation capabilities (**Fig. 2A**). The chemical nature of the precipitate

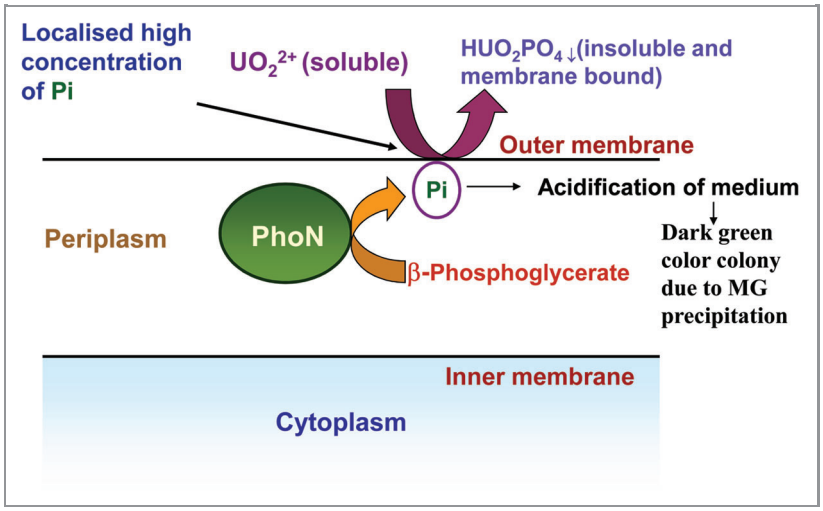

Figure 1. Schematic representation of a periplasm-located phosphatase-mediated bioprecipitation of uranium and the histochemical approach for detection of phosphatase-expressing bacteria.

was revealed by powder X-ray diffraction (XRD) studies to be uranyl hydrogen phosphate (HUO_2PO_4) (**Fig. 2B**). Further, when recombinant EcPhoN and DrPhoN strains were subjected to very high doses of ionizing ^{60}Co-gamma radiation (1 to 6 kGy), followed by challenge with 1mM uranyl nitrate, DrPhoN cells far outperformed the corresponding EcPhoN cells. The recombinant DrPhoN strain retained its uranium precipitation ability even after 6 kGy of ^{60}Co-gamma irradiation. In contrast, EcPhoN cells showed severe inhibition of uranium precipitating ability at doses greater than 1 kGy.[19]

Surface Bioprecipitation of Metals Circumvents Metabolic Toxicity of Metals

Cell surface association of the bioprecipitated uranium was confirmed in DrPhoN cells by scanning electron microscopy wherein the uranyl phosphate precipitate appeared as small needle like structures covering the entire cell surface.[24] It has been hypothesized that cell associated metal precipitation is initiated at nucleation sites present on the cell surface.[25] In Citrobacter, the high content of phosphates in extracellular polysaccharide acts as complexation sites for the incoming metal ion and the initial nucleation site is consolidated by continuous addition of phosphate ligand generated by the enzymatic process.[25,26] The fact that a variety of organisms tested so far, including *E. coli*,[27] *D. radiodurans*[19] and Sphingomonas[22] could bring about cell bound metal precipitation indicates that the cell surface structures required for metal precipitation are not very specific but are of a more general character, across different bacteria and sufficient for efficient metal precipitation and loading.

Phosphatase mediated bioprecipitation can be applied to a wide range of metals which form insoluble phosphates. Compared with uranium, EcPhoN and DrPhoN cells could precipitate 90% of 1 mM cadmium from solution much more rapidly; in 3 h (**Fig. 3**). This is probably because of the lower solubility product of cadmium phosphate compared with uranyl phosphate. An important observation of this experiment was that the toxicity of the metal to the organisms per se, did not affect their corresponding precipitation efficiency. *D. radiodurans* is a metal sensitive bacterium with a MIC of 0.018 mM for cadmium compared with 0.5–1 mM for *E. coli DH5α*.[28] However, both organisms could precipitate out the metal at comparable efficiencies, commensurate with their phosphatase activity. This is an indication that in spite of the high metal sensitivity of *D. radiodurans*, its potential for phosphatase mediated bioprecipitation of metals is not affected. Perhaps extracellular precipitation shields the bacterium from metabolic ill effects of metals.

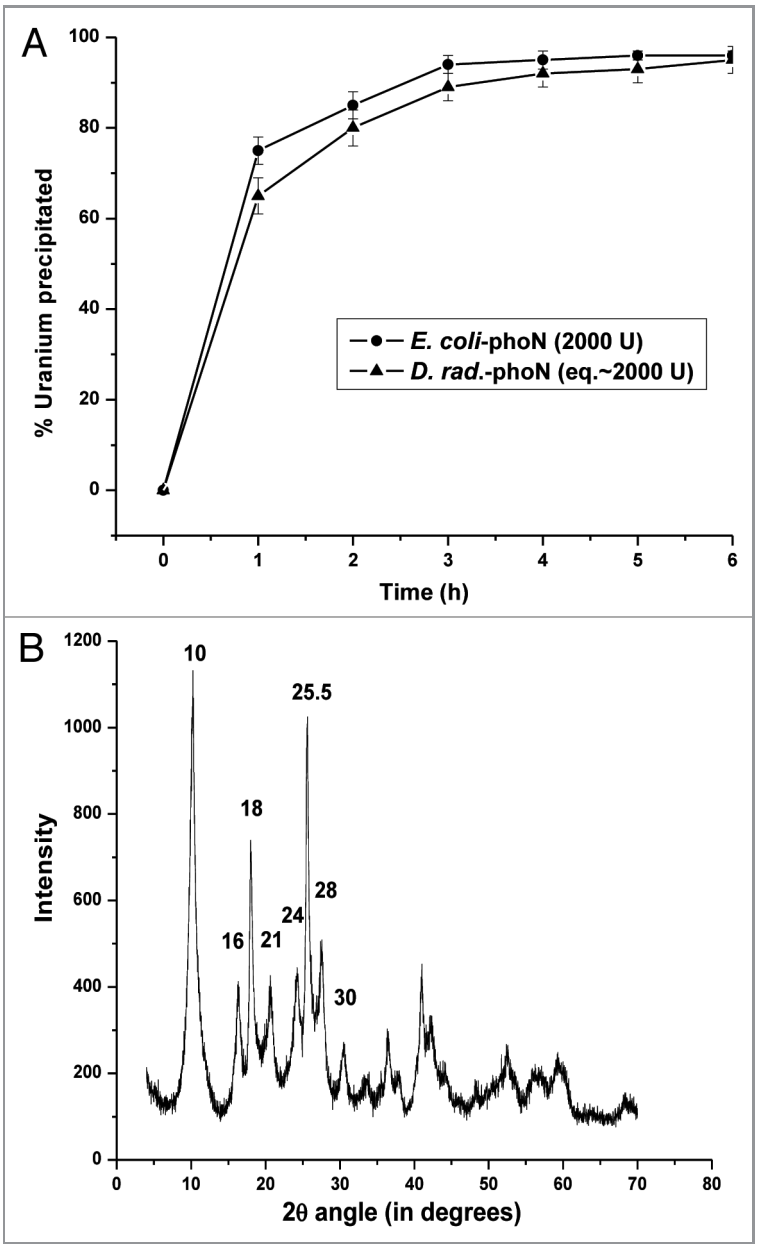

Figure 2. Uranium precipitation by PhoN expressing recombinant bacterial strains. (A) Comparison of uranium precipitation by EcPhoN and DrPhoN cells possessing equivalent PhoN activities. Cells possessing equivalent activity were incubated with 1 mM uranyl nitrate and 5 mM β-glycerophosphate in 2 mM acetate buffer (pH 5.0) at room temperature under static condition and loss of uranium from test solution was determined by Arsenazo-III reagent. (B) X-ray diffraction (XRD) analysis of the precipitate obtained in the cell pellet fraction after uranium precipitation assay with DrPhoN cells. The precipitate formed was identified as uranyl hydrogen phosphate (HUO_2PO_4) by comparison with standard database.

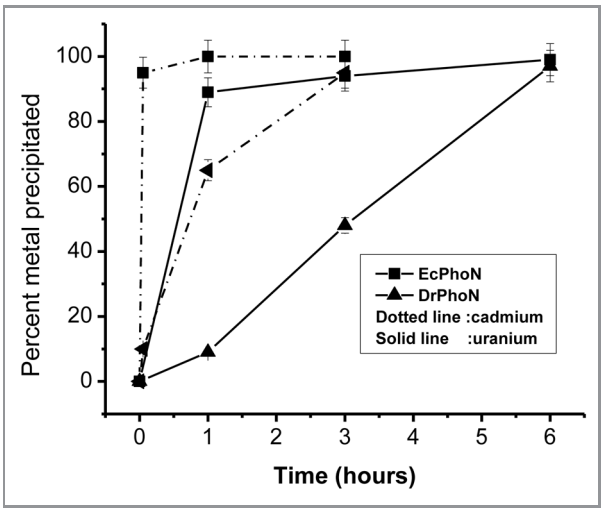

Figure 3. Kinetics of bioprecipitation of uranium and cadmium by EcPhoN and DrPhoN cells. DrPhoN and EcPhoN cells (O.D $_{600nm}$ 1.0) were used to precipitate 1 mM cadmium chloride or uranyl nitrate from solution using 5 mM β-glycerophosphate in 2mM acetate buffer (pH 5.0). Timed aliquots were taken, cell suspension was subjected to centrifugation and the metal remaining in the supernatant was determined. Arsenazo-III reagent was used for estimation of uranium, while cadmium was estimated using Atomic Absorption Spectrophotometer.

Uranium Precipitation: Batch vs. Flow-Through Process

With the objective of simplifying environmental application of recombinant PhoN expressing bacteria for metal bioremediation, cells were subjected to lyophilization. Lyophilized EcPhoN and DrPhoN cells retained phosphatase activity as well as uranium precipitation ability for up to six months of storage at room temperature.[24,27] Further, such lyophilized cells could be immobilized in polyacrylamide gels and packed into columns to construct a flow-through system for uranium precipitation. When gravity based flow-through column was used for uranium precipitation, a loading of 0.73 g uranium/g dry weight of biomass was achieved. An improvement in operation of the column was attempted by using a bigger column (2.5 cm I.D × 50 cm H, 90 ml void volume) and passing the assay solution upwards using a peristaltic pump. The results indicated that lyophilized cells (immobilized in acrylamide) remained stable throughout the operation of the column and over a long period of time. Nearly 70% removal of the input uranium concentration could be achieved when the column was operated at a flow rate of 38 ml/h. With time, the uranium removal efficiency decreased since the column started to clog and resist flow of solution (**Fig. 4**). A maximum loading of 1 g uranium/g dry weight biomass could be achieved in the flow through process.

Our studies showed that batch operation was more suitable than column operation of this system, especially since over a period of time the column was clogged by the precipitated uranium. Compared with a loading of 5.7 g uranium/g dry weight biomass achieved in a batch process, this may not seem attractive, however, the flow-through system has the advantages of continuous operation and ease of handling. More porous matrices are being explored to circumvent problems related to clogging of the column.

Conclusion

The superior uranium precipitation ability of DrPhoN cells in high radiation environments had already been established. The ability to precipitate other toxic metals like cadmium, amenability for use in batch and continuous process and improved shelf life and ease of application achieved through lyophilization have been recent value additions to this strain. A number of further improvements are desirable to bring PhoN based metal precipitation technology to its full potential. These include (a) alternative, cheap substrate for phosphatase in place of β-glycerophosphate in order to make the process economically viable, (b) engineering

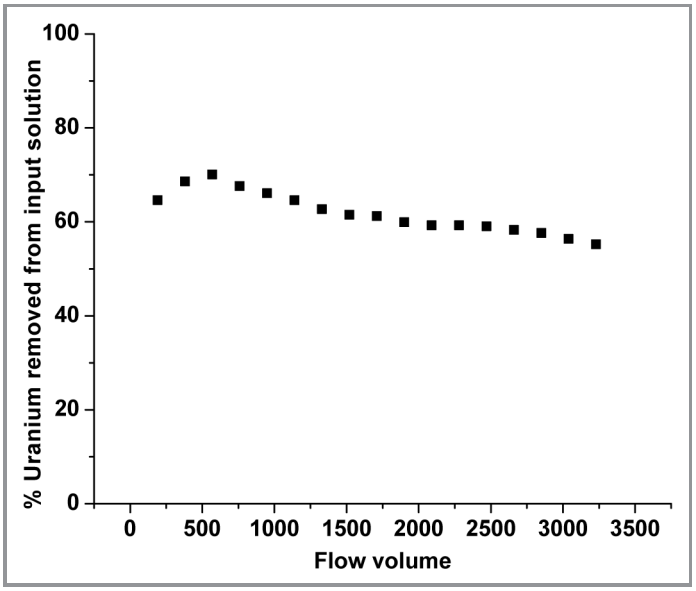

Figure 4. Column-based uranium removal from aqueous flow by immobilized DrPhoN cells. DrPhoN cells were immobilized in polyacrylamide gel and loaded into a column of bed volume, 90 ml. A solution containing 1 mM uranyl nitrate and 5 mM β-glycerophosphate in 2 mM acetate buffer was passed upwards through the column using a peristaltic pump at a flow rate of 38 ml/h. The uranium remaining in the flow through was estimated to determine percent uranium removed.

the phosphatase to localize closer to the cell surface especially in an organism like *D. radiodurans* where multi-layered cell walls may seriously limit the substrate availability and metal access to the enzyme and (c) recombinant Deinococcus cells also need to be tested for a wide array of metals for even non-nuclear applications, such as in nickel cadmium battery waste clean-up. These possibilities are currently being investigated.

Application of metal bio-precipitating Deinococcus strains for in situ bioremediation would require investigation on (a) survival and stability of such strains in actual waste sites, (b) better insight into the precise metal-microbe interaction in cells, (c) scaling up of such cells for large scale use and (d) improvements in their bioprecipitation efficiency. Although *D. radiodurans* is not a human pathogen, the concerns related to use of genetically engineered microbe are relevant and will need to be adequately addressed by ensuring its environmental biosafety and ecological safety for application.

References

1. Lovley DR, Coates JD. Bioremediation of metal contamination. Curr Opin Biotechnol 1997; 8:285-9; PMID:9206008; http://dx.doi.org/10.1016/S0958-1669(97)80005-5
2. Macaskie LE, Empson RM, Cheetham AK, Grey CP, Skarnulis AJ. Uranium bioaccumulation by a *Citrobacter* sp. as a result of enzymically mediated growth of polycrystalline HUO_2PO_4. Science 1992; 257:782-4; PMID:1496397; http://dx.doi.org/10.1126/science.1496397
3. Yeotikar RG. High level liquid radioactive waste, their characterization and quality assurance. Indian Association of Nuclear Chemists and Allied Scientists (IANCAS).Bulletin. 2007; 6:204-17.
4. Lange CC, Wackett LP, Minton KW, Daly MJ. Engineering a recombinant *Deinococcus radiodurans* for organopollutant degradation in radioactive mixed waste environments. Nat Biotechnol 1998; 16:929-33; PMID:9788348; http://dx.doi.org/10.1038/nbt1098-929
5. Brim H, McFarlan SC, Fredrickson JK, Minton KW, Zhai M, Wackett LP, et al. Engineering *Deinococcus radiodurans* for metal remediation in radioactive mixed waste environments. Nat Biotechnol 2000; 18:85-90; PMID:10625398; http://dx.doi.org/10.1038/71986
6. Brim H, Venkateshwaran A, Kostandarithes HM, Fredrickson JK, Daly MJ. Engineering *Deinococcus geothermalis* for bioremediation of high-temperature radioactive waste environments. Appl Environ Microbiol 2003; 69:4575-82; PMID:12902245; http://dx.doi.org/10.1128/AEM.69.8.4575-4582.2003
7. de Groot AD, Chapon V, Servant P, Christin R, Saux MF, Sommer S, et al. *Deinococcus deserti* sp. nov. a gamma-radiation tolerant bacterium isolated from the Sahara desert. Int J Syst Evol Microbiol 2005; 55:2441-6; PMID:16280508; http://dx.doi.org/10.1099/ijs.0.63717-0
8. Ferreira AC, Nobre MF, Rainey FA, Silva MT, Wait R, Burghardt J, et al. *Deinococcus geothermalis* sp. nov. and *Deinococcus murrayi* sp. nov., two extremely radiation-resistant and slightly thermophilic species from hot springs. Int J Syst Bacteriol 1997; 47:939-47; PMID:9336890; http://dx.doi.org/10.1099/00207713-47-4-939
9. Suresh K, Reddy GSN, Sengupta S, Shivaji S. *Deinococcus indicus* sp. nov., an arsenic-resistant bacterium from an aquifer in West Bengal, India. Int J Syst Evol Microbiol 2004; 54:457-61; PMID:15023960; http://dx.doi.org/10.1099/ijs.0.02758-0
10. White O, Eisen JA, Heidelberg JF, Hickey EK, Peterson JD, Dodson RJ, et al. Genome sequence of the radioresistant bacterium *Deinococcus radiodurans* R1. Science 1999; 286:1571-7; PMID:10567266; http://dx.doi.org/10.1126/science.286.5444.1571
11. Levin-Zaidman S, Englander J, Shimoni E, Sharma AK, Minton KW, Minsky A. Ringlike structure of the *D. radiodurans* genome: a key to radioresistance?. Science 2003; 299:254-6; PMID:12522252; http://dx.doi.org/10.1126/science.1077865
12. Zahradka K, Slade D, Bailone A, Sommer S, Averbeck D, Petranovic M, et al. Reassembly of shattered chromosomes in *D. radiodurans*. Nature 2006; 443:569-73; PMID:17006450
13. Narumi I, Satoh K, Cui S, Funayama T, Kitayama S, Watanabe H. PprA: a novel protein from *Deinococcus radiodurans* that stimulates DNA ligation. Mol Microbiol 2004; 54:278-85; PMID:15458422; http://dx.doi.org/10.1111/j.1365-2958.2004.04272.x
14. Daly MJ, Gaidamakova EK, Matrosova VY, Vasilenko A, Zhai M, Venkateswaran A, et al. Accumulation of Mn(II) in *Deinococcus radiodurans* facilitates gamma-radiation resistance. Science 2004; 306:1025-8; PMID:15459345; http://dx.doi.org/10.1126/science.1103185
15. Basu B, Apte SK. Gamma radiation induced proteome of *D. radiodurans* primarily targets DNA repair and oxidative stress alleviation. Mol Cell Prot 2011 doi:10.1074/mcp.M111.011734.
16. de Groot A, Dulermo R, Ortet P, Blanchard L, Guérin P, Fernandez B, et al. Alliance of Proteomics and Genomics to Unravel the Specificities of Sahara Bacterium *Deinococcus deserti*.. PLoS Genet 2009; 5:e1000434; PMID:19370165; http://dx.doi.org/10.1371/journal.pgen.1000434
17. Fredrickson JK, Kostandarithes HM, Li SW, Plymale AE, Daly MJ. Reduction of Fe(III), Cr(VI), U(VI) and Tc(VII) by *D. radiodurans* R1. Appl Environ Microbiol 2000; 66:2006-11; PMID:10788374; http://dx.doi.org/10.1128/AEM.66.5.2006-2011.2000
18. Brim H, Osborne JP, Kostandarithes M, Fredrickson JK, Wackett LP, Daly MJ. *D. radiodurans* engineered for complete toluene degradation facilitates Cr(VI) reduction. Microbiology 2006; 152:2469-77; PMID:16849809; http://dx.doi.org/10.1099/mic.0.29009-0
19. Appukuttan D, Rao AS, Apte SK. Engineering of *Deinococcus radiodurans* R1 for bioprecipitation of uranium from dilute nuclear waste. Appl Environ Microbiol 2006; 72:7873-8; PMID:17056698; http://dx.doi.org/10.1128/AEM.01362-06
20. Meima R, Lidstrom ME. Characterization of the Minimal Replicon of a Cryptic *Deinococcus radiodurans* SARK Plasmid and Development of Versatile *Escherichia coli-D. radiodurans* Shuttle Vectors. Appl Environ Microbiol 2000; 66:3856-67; PMID:10966401; http://dx.doi.org/10.1128/AEM.66.9.3856-3867.2000
21. Riccio ML, Rossolini GM, Lombardi G, Chiesurin A, Satta G. Expression cloning of different bacterial phosphatase-encoding genes by histochemical screening of genomic libraries onto an indicator medium containing phenolphthalein diphosphate and methyl green. J Appl Microbiol 1997; 82:177-85; PMID:12452591
22. Nilgiriwala KS, Alahari A, Rao AS, Apte SK. Cloning and overexpression of alkaline phosphatase PhoK from *Sphingomonas* sp. strain BSAR-1 for bioprecipitation of uranium from alkaline solutions. Appl Environ Microbiol 2008; 74:5516-23; PMID:18641147; http://dx.doi.org/10.1128/AEM.00107-08
23. Makarova KS, Aravind L, Wolf YI, Tatusov RL, Minton KW, Koonin EV, et al. Genome of the extremely radiation-resistant bacterium *Deinococcus radiodurans* viewed from the perspective of comparative genomics. Microbiol Mol Biol Rev 2001; 65:44-79; PMID:11238985; http://dx.doi.org/10.1128/MMBR.65.1.44-79.2001
24. Appukuttan D, Seetharam C, Padma N, Rao AS, Apte SK. PhoN-expressing, lyophilized, recombinant *Deinococcus radiodurans* cells for uranium bioprecipitation. [REMOVED HYPERLINK FIELD]. J Biotechnol 2011; 154:285-90; PMID:21616102; http://dx.doi.org/10.1016/j.jbiotec.2011.05.002
25. Jeong BC, Hawes C, Bonthrone KM, Macaskie LE. Localization of enzymically heavy metal accumulation by *Citrobacter* sp. and metal accumulation *in vitro* by liposomes containing entrapped enzyme. Microbiology 1997; 143:2497-507; PMID:9245830; http://dx.doi.org/10.1099/00221287-143-7-2497
26. Macaskie LE, Lloyd JR, Thomas RAP, Tolley MR. The use of micro-organisms for the remediation of solutions contaminated with actinide elements, other radionuclides, and other organic contaminants generated by nuclear fuel activities. Nuclear energy 1996; 35:257-271.
27. Seetharam C, Soundarajan S, Udas AC, Rao AS, Apte SK. Lyophilized, non-viable, recombinant *E. coli* cells for cadmium bioprecipitation and recovery. Process Biochem 2009; 44:246-50; http://dx.doi.org/10.1016/j.procbio.2008.10.015
28. Ruggiero CE, Boukhalfa H, Forsythe JH, Lack JG, Hersman LE, Neu MP. Actinide and metal toxicity to prospective bioremediation bacteria. Environ Microbiol 2005; 7:88-97; PMID:15643939; http://dx.doi.org/10.1111/j.1462-2920.2004.00666.x